

**DEVELOPING A BIM-BASED LCA APPROACH FOR COST-EFFECTIVE  
LIFECYCLE OPTIMIZATION OF BUILDING ENERGY AND CARBON  
EMISSIONS**

**MARK KYEREDEY ANSAH**

**PhD**

**The Hong Kong Polytechnic University**

**2022**

The Hong Kong Polytechnic University

Department of Building Environment and Energy Engineering

**Developing a BIM-Based LCA Approach for Cost-Effective Lifecycle Optimization of  
Building Energy and Carbon Emissions**

**Mark Kyeredey Ansah**

A thesis submitted in partial fulfillment of the requirements for the degree of

Doctor of Philosophy

June 2022

## **CERTIFICATE OF ORIGINALITY**

I hereby declare that this thesis is my own work and that, to the best of my knowledge and belief, it reproduces no material previously published or written, nor material that has been accepted for the award of any other degree or diploma, except where due acknowledgement has been made in the text.



(Signed)

Mark Kyeredey Ansah (Name of student)

Department of Building Environment and Energy Engineering

The Hong Kong Polytechnic University

Hong Kong SAR, China

**June 2022**

## **ABSTRACT**

Abstract of thesis entitled:

Developing a BIM-Based LCA Approach for Cost-Effective Lifecycle Optimization  
of Building Energy and Carbon Emissions

Submitted by: Mark Kyeredey Ansah

For the degree of: Doctor of Philosophy

at The Hong Kong Polytechnic University in June 2022

This thesis aims to develop a Building information Modelling (BIM)-based design assessment approach with an application to the whole lifecycle design and optimization of the energy use, carbon emission, and economic performances of buildings. Current life cycle assessment (LCA) tools are criticized for complex assessment methods, intricate data requirements and incompatibility with conventional whole building energy simulation tools. Therefore, an LCA approach based on the BIM and optimization framework is proposed to improve the integration of a holistic life cycle assessment with the whole building energy simulation which can address the intrinsic synergy between energy, carbon, and economic performances throughout the entire lifecycle of buildings. This comprehensive design approach can account for the interactive effects between different design strategies in different life cycle phases of a building (i.e. material production, transportation, building construction, building operation, building maintenance, and end-of-life cycle phases) and enable decision-makers to comprehend the relative importance of each design strategy in order to deploy them for achieving the optimum energy, carbon and cost performance.

The functional database, BIM module, and impact estimation module were determined as the fundamental components to develop the detailed whole lifecycle design assessment model. After designing the data structure and repository, impact estimation module and BIM module, BIM models were developed at various assessment levels specific to prefabricated and non-prefabricated buildings to assess its robustness for evaluating the energy and carbon performance of buildings using various energy and environmental indicators. The accuracy and robustness of the model was validated through a comparison with lifecycle assessment results of the same buildings with conventional tools. The results showed high levels of consistency and accuracy for various energy use and carbon emission indicators. Prediction accuracy and swiftness were improved through parametric modelling and data structure.

On top of the BIM-based model, a tier-hybrid uncertainty assessment method was developed to evaluate the uncertainties specific to the embodied impacts (i.e. material production, transportation, building construction, building maintenance, and end-of-life phases) of buildings. The parameter, model, and scenario uncertainties intrinsic to these lifecycle phases were determined through a comprehensive literature review and characterized using quantitative and qualitative analyses. LCA parameters with sufficient data from literature and manufactures were characterized using pure statistical distributions and Monte Carlo simulations whereas Data Quality Indicator (DQI) method was applied to LCA parameters without sufficient datasets. The tier-hybrid model was proved reliable given its consistency with a deterministic LCA. After uncertainty characterization, a propagation model was applied to understand the relative uncertainties specific to various lifecycle stages and building materials. After determining the parameter uncertainties, alternative statistical distributions (lognormal, triangular, normal and uniform) were explored to show the impacts of model uncertainties. The results of the model/analytical uncertainty imply that the final output uncertainty is highly correlated with defined probability distributions rather than the uncertainty

characterization method. Hence integrating the pure statistical approach based on adequate data with the DQI method can reflect uncertainties more precisely. However, the proposed tier-hybrid approach can increase dispersion of LCA results as pure statistical distributions are collected from a wide range of sources.

Succeeding the above statistical analysis, a staged design optimization approach was proposed integrating embodied and operational impacts through the whole building energy simulation and LCA of passive design parameters as well as building materials and constructions with a multi-objective optimization. The NSGA-II optimization was conducted to obtain the Pareto front which demonstrates a trade-off between embodied and operational impacts. Following the post-optimization analysis and comparison of optimal solution selection methods, the optimal solution showed energy savings of up to 36.93% when compared with the baseline building. The BIM-based optimization method was further applied to three other tropical and subtropical climate cities.

Finally, a novel comprehensive BIM-based energy use, carbon emission and economic assessment and optimization model as a better alternative to the traditional whole building energy simulation and conventional lifecycle assessment was established and applied to a holistic lifecycle building design and assessment. The optimization approach is a single tiered integrated optimization process with an extensive evaluation of the embodied and operational impacts of buildings. The operational assessment includes energy use, carbon emission and economic implications of the building orientation, shape coefficient, window to wall ratio, external wall, roof and floor thermal resistance, windows U-value, infiltration rate, photovoltaic configuration. The embodied assessment also includes the corresponding implications of materials, constructions and energy systems. With the comprehensive BIM-based design model finalized, different optimization settings were examined to identify the most suitable settings that balance computational efficiency and optimization productivity. The most suitable settings

showed up to 50% reduction in computational time. After a post evaluation of the optimization results, the final optimum BIM-based lifecycle design achieved 42%, 58% and 32% energy, carbon and cost reductions, respectively.

A post-optimization exploration is then conducted on confounding factors such as the lighting density, equipment load, ventilation rate, occupancy gains and occupancy density. In comparison to the optimized base case design, a low-level internal load scenario can reduce energy use, carbon emission and cost by 53%, 75% and 59%, respectively whereas a high-level internal load scenario can increase energy use, carbon emission by 63%, 91% and 68%, respectively. The BIM-based lifecycle optimization model was further applied to explore the influence of climate change representative concentration pathways (RCPs) in four scenarios: RCP 2.6, RCP 4.5, RCP 6.0 and RCP 8.5. It is shown that global warming will lead to higher energy use and carbon emissions in tropical regions within the near future, while stringent mitigation strategies aligned with RCP 2.6 can reverse the trend after two decades. A further exploration of end-of-life strategies indicates that demolishing, transportation and sorting processes increase the energy use, carbon emission and cost, while recycling strategies can reduce such impact especially when extensively adopted. The BIM-based optimization model has been successfully applied to both typical mid-rise and high-rise residential buildings and its modularity allows for applications to other building archetypes.

The proposed BIM-based optimization model can be used by researchers, developers, consultants and engineers to improve the overall lifecycle energy use, carbon emission and economic performance of buildings. The model bridges the segmentation between operational and embodied impacts of buildings and provides opportunities to explore the trade-off between design parameters from a lifecycle perspective. This comprehensive design approach curbs the surge in embodied impacts during the early design stage when it can be minimized. Furthermore, the design approach provides great opportunities for low carbon designs in a cost-

effective approach and is therefore a pertinent step towards reducing the impact of the climate change. The proposed BIM-based optimization model can be further adapted and extended to other applications such as retrofitting of existing buildings.

## PUBLICATIONS DURING PHD STUDY

### Journal Papers:

- 1) Ansah, M. K., Chen, X., & Yang, H. (2021). Two-Stage Lifecycle Energy Optimization of Mid-Rise Residential Buildings with Building-Integrated Photovoltaic and Alternative Composite Facade Materials. *Buildings*, 11(12).  
<https://doi.org/10.3390/buildings11120642>
- 2) Ansah, M. K., Chen, X., & Yang, H. (2022). A holistic environmental and economic design optimization of low carbon buildings considering climate change and confounding factors. *Science of The Total Environment*, 821, 153442.  
<https://doi.org/https://doi.org/10.1016/j.scitotenv.2022.153442>
- 3) Ansah, M. K., Chen, X., Yang, H., Lu, L., & Lam, P. T. I. (2019). A review and outlook for integrated BIM application in green building assessment. *Sustainable Cities and Society*, 48, 101576.  
<https://doi.org/https://doi.org/10.1016/j.scs.2019.101576>
- 4) Ansah, M. K., Chen, X., Yang, H., Lu, L., & Lam, P. T. I. (2020). An integrated life cycle assessment of different façade systems for a typical residential building in Ghana. *Sustainable Cities and Society*, 53, 101974.  
<https://doi.org/https://doi.org/10.1016/j.scs.2019.101974>
- 5) Ansah, M. K., Chen, X., Yang, H., Lu, L., & Lam, P. T. I. (2021a). Developing an automated BIM-based life cycle assessment approach for modularly designed high-rise buildings. *Environmental Impact Assessment Review*, 90, 106618.  
<https://doi.org/https://doi.org/10.1016/j.eiar.2021.106618>
- 6) Ansah, M. K., Chen, X., Yang, H., Lu, L., & Li, H. (2021b). Developing a tier-hybrid uncertainty analysis approach for lifecycle impact assessment of a typical high-rise residential building. *Resources, Conservation and Recycling*, 167, 105424.

**Conference Papers:**

- 1) Ansah, M. K., Chen, X., & Yang, H. Lifecycle performance of high-rise buildings with maximized Integrated Photovoltaic Façades. The 11<sup>th</sup> International Conference on Applied Energy, August 12-15, 2019, Västerås, Sweden.
- 2) Ansah, M. K., Chen, X., & Yang, H. An integrated uncertainty analysis approach for prefabricated high-rise buildings. The 12<sup>th</sup> International Conference on Applied Energy, December 1-10, 2020, Bangkok (Virtual).
- 3) Mark Kyeredey Ansah, Xi Chen and Hongxing Yang. An integrated environmental and cost optimization approach for low carbon buildings. The 14<sup>th</sup> International Conference on Applied Energy, Bochum, Germany, 8-11, August, 2022. (Virtual)

## ACKNOWLEDGEMENT

I would like to express profound gratitude to my Chief supervisor Professor Yang Hongxing for mentoring me through this PhD study. I am always overwhelmed with joy for his endless support and encouragement and excellent guidance in my research work. I also appreciate his numerous invitations to participate in extra-curriculum activities including badminton and hiking. It has indeed been an amazing PhD journey with you. I could not have imagined a better supervisor and mentor for my PhD study.

I would also like to express my utmost appreciation to Dr Chen Xi who has been fundamental from the very conceptualization to completion of my PhD study. Your insightful ideas, comments, feedback and encouragement have broadened and incentivized me to be a better researcher.

My sincere thanks also go to Prof. Lu Lin and Prof. Patrick T. I. Lam, my co-supervisors. Your support and feedback are very much appreciated.

I would also like to thank all members and teachers of Renewable Energy Research Group (RERG) for your valuable inputs into my research and social life. I appreciate your warm companionships, feedback, and comments.

I especially appreciate the financial support from the Research Institute for Sustainable Urban Development (RISUD) for providing me a 4-year studentship.

Special thanks go to my friends, family and church fellowship for your kind thoughts, prayers and well wishes. You have all been a shoulder to lean on.

Most importantly, I give thanks to God almighty for His grace and mercies throughout my PhD study. I am forever grateful for all the amazing people and opportunities that He has positioned in my life. I stand in awe for His glory and light over my path.

## TABLE OF CONTENT

ABSTRACT .....	II
PUBLICATIONS DURING PHD STUDY .....	VII
ACKNOWLEDGEMENT .....	IX
TABLE OF CONTENT .....	X
LIST OF FIGURES .....	XVI
LIST OF TABLES .....	XIX
LIST OF APPENDICES .....	XXI
NOMENCLATURE.....	XXII
CHAPTER 1 INTRODUCTION .....	1
1.1 Research background.....	1
1.2 Research aim and objectives.....	6
1.3 Organization of the thesis .....	8
CHAPTER 2 LITERATURE REVIEW .....	12
2.1 Integration of BIM and LCA for buildings .....	12
2.2 Design optimization of whole building lifecycle using BIM-based methods. ....	18
2.3 Uncertainties in the buildings LCA .....	23
2.3.1 Uncertainties in the material production phase .....	24
2.3.2 Uncertainties in the maintenance phase .....	24
2.3.3 Uncertainties in the construction phase.....	26

2.3.4	Uncertainties in the end-of-life phase .....	26
2.3.5	Evaluating uncertainties in building LCA.....	27
2.4	Reducing embodied energy in building.....	29
2.5	Life cycle assessment of façade systems .....	31
2.6	Research gaps on BIM-based life cycle assessment and design optimization of buildings .....	35
<b>CHAPTER 3 RESEARCH DESIGN AND METHODOLOGY FOR BIM-BASED LCA.....</b>		<b>37</b>
3.1	Integrating BIM for automated building LCA .....	37
3.1.1	Data repository .....	38
3.1.2	BIM module.....	39
3.1.3	Impact estimation module .....	40
3.2	Evaluating uncertainties in the life cycle of buildings .....	47
3.2.1	Tier-hybrid stochastic analysis.....	48
3.2.2	Scenario and model analysis .....	54
3.3	Multi-objective lifecycle optimization of building.....	57
3.3.1	Energy evaluation.....	58
3.3.2	Environment evaluation .....	58
3.3.3	Economic evaluation .....	59
3.3.4	Multi-objective optimization.....	60
3.3.5	Optimization algorithm .....	60
3.3.6	Scenario analysis for confounding factors and climate change .....	61
3.4	Summary.....	65

CHAPTER 4 SYSTEMATIC BIM-BASED LCA OF A TYPICAL PREFABRICATED	
HIGH-RISE BUILDING..... 66	
4.1	Modelling the embodied impacts of a prefabricated high-rise building..... 66
4.2	Profile of inventory..... 70
4.3	Embodied impacts at the whole building level..... 71
4.4	Embodied impacts at flat level ..... 74
4.5	Embodied impacts at assembly levels ..... 76
4.6	Embodied impacts at component level..... 77
4.7	Summary..... 80
CHAPTER 5 A COMPARATIVE INTEGRATED LIFE CYCLE ASSESSMENT OF	
DIFFERENT FAÇADE SYSTEMS FOR A TYPICAL LOW-RISE RESIDENTIAL	
BUILDING..... 83	
5.1	Case descriptions ..... 83
5.1.1	Concrete block and mortar façade..... 84
5.1.2	Stabilized earth block façade..... 85
5.1.3	Galvanised steel insulated composite façade ..... 86
5.1.4	Shotcrete insulated composite façade ..... 86
5.2	Life cycle inventory ..... 88
5.3	Life cycle impact assessment ..... 91
5.4	Scenario analysis for each façade ..... 93
5.5	Model validation..... 94
5.6	Comparative analysis of façade types ..... 96

5.6.2	Stabilized Earth Block Façade .....	98
5.6.3	Galvanised Steel Insulated Composite Façade .....	100
5.6.4	Shotcrete Insulated Composite Façade .....	102
5.6.5	Life Cycle Cost.....	104
5.7	Scenario analysis .....	105
5.8	Summary.....	107
CHAPTER 6 TIER-HYBRID UNCERTAINTY ANALYSIS APPROACH FOR		
LIFECYCLE IMPACT ASSESSMENT.....		109
6.1	Assessment of embodied impacts.....	109
6.2	Scenario uncertainties.....	114
6.2.1	End-of-life cycle strategies.....	114
6.2.2	Alternative materials .....	116
6.3	Model uncertainties .....	118
6.4	Summary.....	122
CHAPTER 7 STAGED WHOLE LIFECYCLE ENERGY OPTIMIZATION		
ALTERNATIVE COMPOSITE FAÇADE SYSTEMS FOR MID-RISE RESIDENTIAL		
BUILDINGS .....		125
7.1	Case study building model .....	125
7.2	Energy analysis.....	131
7.3	Optimization settings.....	132
7.4	Validation .....	138
7.5	Stage one optimization results.....	141

7.6	Stage two optimization results.....	143
7.7	Summary.....	150
CHAPTER 8 HOLISTIC ENVIRONMENTAL AND ECONOMIC DESIGN		
OPTIMIZATION TOWARDS LOW CARBON BUILDINGS CONSIDERING CLIMATE		
CHANGE AND CONFOUNDING FACTORS ..... 153		
8.1	Case study description.....	153
8.2	Multi-objective optimization.....	155
8.3	Impacts of confounding factors.....	166
8.4	Impacts of climate change.....	167
8.4.1	RCP 2.6.....	167
8.4.2	RCP 4.5.....	169
8.4.3	RCP 6.0.....	170
8.4.4	RCP 8.5.....	171
8.5	Summary.....	176
CHAPTER 9 CONCLUSION AND RECOMMENDATION FOR FUTURE WORK ..... 178		
9.1	Development of the BIM-based LCA method for the embodied phases of buildings 179	
9.2	Comparative assessment of the energy and carbon performance of alternative façade systems.....	180
9.3	Uncertainty in the embodied impacts of buildings.....	181
9.4	Staged optimization of mid-rise residential buildings with alternative composite façade systems.....	182

9.5	Holistic environmental and economic design optimization of buildings .....	183
9.6	Recommendations for future research .....	185
REFERENCES .....		186
APPENDIX .....		219

## LIST OF FIGURES

Fig. 1. 1 Life cycle phases of building [5] .....	2
Fig. 1. 2 Projection of embodied vs operational energy [19].....	3
Fig. 1. 3 Overall study framework on BIM-based LCA methodology and optimization framework for buildings.....	9
Fig. 3. 1 Framework on BIM-based LCA methodology.....	37
Fig. 3. 2 Developed database and naming convention in the BIM model .....	38
Fig. 3. 3 Logic flow diagram for LCA implementation .....	42
Fig. 3. 4 Methodological framework for uncertainty analysis .....	48
Fig. 3. 5 Flow chart for uncertainty analysis.....	48
Fig. 4.1 Modular flats and samples of prefabricated components used in Hong Kong public residential buildings.....	67
Fig. 4. 2 Floor plan and 3D BIM Model of case building	69
Fig. 4.3 Life cycle impacts at the whole building level	74
Fig. 4.4 Embodied impacts at flat levels	75
Fig. 4.5 Embodied impacts at assembly levels	76
Fig. 4.6 Embodied impacts at component levels	78
Fig. 5.1 Floor plan and 3D BIM simulation model .....	85
Fig. 5.2 Schematic diagrams of the four façades .....	87
Fig. 5.3 Materials inventory of four façades .....	89
Fig. 5.4 Comparison of energy end-use data and simulation data of case building.....	95
Fig. 5.5 CED and GWP for CBMF per unit GFA and across the building lifespan .....	98
Fig. 5.6 CED and GWP for SEBF per unit GFA and across the building lifespan.....	99
Fig. 5.7 CED and GWP for per unit GFA and across the building lifespan .....	101
Fig. 5.8 CED and GWP per unit GFA and across the building lifespan .....	103

Fig. 5.9 Life Cycle Cost for all façades per floor area .....	105
Fig. 6.1 BIM model and a typical floor plan of the case building .....	110
Fig. 6.2 Contribution analysis of material production phase (CED).....	112
Fig. 6.3 Contribution analysis of material production phase (GWP).....	112
Fig. 6.4 Contribution analysis of building maintenance phase .....	113
Fig. 6.5 Comparison of end-of-life management strategy 1 and 2.....	115
Fig. 6.6 Scenario analysis of end-of-life management strategy 1 .....	115
Fig. 6.7 Scenario analysis of end-of-life management strategy 2 .....	116
Fig. 6.8 Impact reduction from the use of recycled aggregates. ....	117
Fig. 6.9 Impact reduction from the use of alternative cementitious materials. ....	118
Fig. 7.1 Framework for two-stage optimization of residential building .....	126
Fig. 7.2 Floor plan and 3D BIM model of the case study building.....	127
Fig. 7.3 Weekday building schedules.....	128
Fig. 7.4 Weekend building schedules.....	129
Fig. 7.5 Illustration of passive and active parameters two-stage optimization [217].....	137
Fig. 7.6 Estimated CV(RMSE) and NMBE of calibrated simulation model for operational energy uses .....	139
Fig. 7.7 Validation of base model building loads .....	140
Fig. 7.8 Scatterplot of Energy use intensity against PV energy supply .....	142
Fig. 7.9 Total operational energy use against PV energy supply .....	142
Fig. 7. 10 Scatterplot of WWR, infiltration rate, orientation and BIPV window ratio against energy use intensity .....	145
Fig. 7.11 Scatterplot of operational energy use against embodied energy use (Accra, Ghana) .....	145

Fig. 7. 12 Scatterplot of operational energy use against embodied energy use (Abuja, Nigeria)	149
Fig. 7. 13 Scatterplot of operational energy use against embodied energy use (Ouagadougou, Burkina Faso)	149
Fig. 8. 1 Framework for cost effective optimization of energy and carbon of residential building	154
Fig. 8. 2 Parametric model of case study building	156
Fig. 8.3 Single and multiobjective convergence over generations	159
Fig. 8. 4 Validating the developed model	160
Fig. 8. 5 3D Scatter plot of CED, GWP and Cost of the optimized base model	161
Fig. 8. 6 Contribution of embodied and operational impacts of the baseline and optimized solutions	163
Fig. 8. 7 Monthly profile of operational energy use of the optimized solution	164
Fig. 8. 8 Contribution of building elements to the total CED, GWP and Cost	165
Fig. 8.9 3D Scatter plot of CED, GWP and Cost for optimization under confounding factors	166
Fig. 8.10 Trajectory of CED, GWP and cost under RCP 2.6	169
Fig. 8.11 Trajectory of CED, GWP and cost under RCP 4.5	170
Fig. 8.12 Trajectory of CED, GWP and cost under RCP 6.0	171
Fig. 8.13 Trajectory of CED, GWP and cost under RCP 8.5	172
Fig. 8.14 Trajectory of CED and GWP for RCPs from 2030 to 2069	172

## LIST OF TABLES

Table 2. 1 Comparison of characteristics of previous BIM-based LCA studies.....	15
Table 3. 1 Uncertainty parameters and assessment methods .....	50
Table 3. 2 Data quality pedigree matrix .....	51
Table 3. 3 Variance of additional uncertainties.....	52
Table 3. 4 Summary of scenarios analysis .....	56
Table 3. 5 Optimization settings .....	61
Table 3. 6 Scenarios for confounding factors .....	62
Table 3. 7 Scenarios for climate change .....	64
Table 4.1 Characteristics of case building .....	67
Table 4. 2 Assessment level, system boundary and functional units used in this study .....	68
Table 4. 3 Inventory of materials/elements .....	70
Table 4.4 Comparative analysis of residential buildings in Hong Kong .....	79
Table 5.1 Material replacement and waste factors .....	90
Table 5.2 The energy use, emission factor and transportation distance for the transport mode .....	91
Table 5.3 Equipment energy use and emission factors for the construction stage.....	92
Table 5.4 Input parameter for building energy simulations .....	93
Table 5.5 Main assumptions for scenario analysis.....	95
Table 5.6 Breakdown of simulated annual energy demands during use phase of buildings....	95
Table 5.7 Embodied energy and global warming potential of concrete block and mortar façade .....	97
Table 5.8 Embodied energy and global warming potential of stabilised earth block façade...	99
Table 5.9 Embodied energy and global warming potential of Galvanised Steel Insulated Composite Façade .....	102

Table 5.10 Embodied energy and global warming potential of Shotcrete Insulated Composite Façade.....	103
Table 5.11 Percentage reductions after scenario analysis .....	106
Table 5. 12 Ranking of four façade before and after scenario analysis .....	106
Table 6.1 Comparison of the stochastic and deterministic cumulative energy demands	110
Table 6.2 Comparison of the stochastic and deterministic global warming potential. ....	111
Table 6.3 Comparison of overall mean lifecycle impacts, standard deviation and coefficient of variation from different probability distributions.....	120
Table 7. 1 Variable for the two-staged optimizations [8,217.....	133
Table 7. 2 Building parameter settings.....	134
Table 7. 3 Configuration of Pareto optimal solutions of stage one.....	143
Table 7. 4 Configuration of Pareto optimal solutions of stage two.....	147
Table 8. 1 Setting for the baseline model	155
Table 8. 2 Design optimization variables .....	157

## LIST OF APPENDICES

Appendix 1 Uncertainty characterization for DQI-based parameters .....	219
Appendix 2 Uncertainty characterization for pure statistical parameters .....	222
Appendix 3 Windows types, U-value, GWP, CED and Cost .....	223
Appendix 4 Roof types, U-value, GWP, CED and Cost.....	224
Appendix 5 Windows types, U-value, GWP, CED and Cost .....	225
Appendix 6 GWP, CED and Cost of PV modules .....	225
Appendix 7 Windows types, U-value, GWP, CED and Cost .....	226

## NOMENCLATURE

### ABBREVIATIONS

AAC	Autoclaved Aerated Concrete
ADP-f	Abiotic Depletion (kg Sb-eq)
ANN	Artificial neural network
AP	Acidification Potential (kg SO <sub>2</sub> -eq)
AR5	IPCC fifth Assessment Report
ASHRAE	American Society of Heating, Refrigerating and Air Conditioning Engineers
BIM	Building Information Modelling
BIPV	Building integrated photovoltaics
BO	Building orientation
BOQ	Bill of Quantity
BWMF	Block wall and mortar façade
CBMF	Concrete Block and Mortar Façade
CDD	Cooling Degree Days
CED	Cumulative energy demand
CMA-ES	Covariance Matrix Adaptation Evolution Strategy
CMBF	Compressed mud block façade
CV	Coefficient of variation
CV(RMSE)	Coefficient of variation of root mean square error
d.PC	Net present value of periodic costs
DQI	Data quality indicators
EPD	environmental product declarations
EPDM	Ethylene propylene diene terpolymer

ETICS:	External Thermal Insulation Composite Systems
EUI <sub>ao</sub>	Annual energy use intensity
FAETP	Fresh Water Aquatic ecotoxicity (kg 14-DB-eq)
G. Steel ICF	Galvanised Steel Insulated Composite Façade
GBFS	Granulated Blast furnace Slag
GFA	Gross floor area
GHG	Greenhouse gas
GS. ICF	Galvanized steel insulated composite façade
GWP	Global Warming potential (kg CO <sub>2</sub> -eq)
HDD:	Heating Degree Days
HDE	Hybrid Differential Evolution
HGPSO	Hybrid generalized particle search particle swarm optimization
HTP	Human Toxicity Potential (kg 14-DB-eq)
HVAC:	Heating Ventilation and Air Conditioning
HypE	Hypervolume Estimation algorithm
IC	Initial investment cost
IEA	International Energy Agency
IES-VE:	Integrated Environmental Solutions Virtual Environment
IPCC	Intergovernmental Panel on Climate Change
ISO	International Organization for Standardization
LCA	Lifecycle Assessment
LCC	Life cycle cost assessment
LCI	Life cycle Inventory
LCIA	Lifecycle Impact Assessment
MAEP	Marine Aquatic Ecotoxicity (kg 14-DB-eq)

MC	Periodic maintenance cost
MOO	Multi-objective optimization
MOPSO	Multi-objective particle swarm optimization
MOPSO	multi-objective particle swarm optimization
NMBE	Normalized mean bias error
NSGA-II	Non-dominated sorting genetic algorithm
NV	Normalized values
OC	Operational carbon emission
OC <sub>ao</sub>	Annual operational carbon intensity
ODP	Ozone depletion potential
OE	Operational energy
OPC	Ordinary Portland Cement
PFA	Pulverized Fly Ash
PFA	Pulverized Fly Ash
POCP	Photochemical ozone creation potential
PUR	Polyurethane rigid foam insulation
PV	Photovoltaics
RCP	Representative concentration pathways
$R_f$	Replacement factor
SD	Standard deviation
SEBF	Stabilized Earth Block Façade
SHGC	Solar heat gain coefficient
Shotcrete ICF	Shotcrete Insulated Composite Façade
SPEA-2	Strength Pareto Evolutionary Algorithm
SQL	Structured Query Language

TETP	Terrestrial Ecotoxicity (kg 14-DB-eq)
WWR	Window to wall ratio

## SYMBOLS

$\sigma_{a,i}^2$	Additional uncertainties
$\sigma_b^2$	Basic uncertainties
$\sigma_t^2$	Total uncertainties
$\sigma$	Standard deviation
$\mu'$	Mean
1B	1-bedroom flat
2B	2-bedroom flat
2P3P	2-person-3-person flat
$e$	energy type
EC	Embodied carbon emission
ECa	Initial embodied carbon
ECz	Recurring embodied carbon
EE	Embodied energy
EEa	Initial embodied energy
EEc	Construction Embodied Energy
$E_{ee}$	impact coefficient of the material
EE <sub>m</sub>	Materials Embodied Energy
EE <sub>t</sub> :	Transportation Embodied Energy
EEz	Recurring embodied energy
EI <sub>C</sub>	Onsite construction

$EI_E$	End-of-life
$EI_P$	Material production
$EI_T$	Transportation
EP	Eutrophication Potential
EP	Eutrophication Potential (kg PO4-eq)
EP	total lifecycle impacts
$E_{p,e}$	mass of energy used by equipment type
$EP_c$	Embodied impact of construction
$EP_e$	Embodied impact of end-of-life phase
$EP_m$	Embodied impacts of material production
$EP_{mc}$	Embodied impacts from production of insitu elements
$EP_{mp}$	Embodied impacts from production precast elements
$EP_{mp1}$	Embodied impacts from materials extraction for precast elements
$EP_{mp2}$	Embodied impacts from materials transport to prefabrication factory
$EP_{mp3}$	Embodied impacts from manufacturing of precast elements
EPS	Expanded polystyrene
$EP_t$	Embodied impacts of transportation
$EP_u$	Embodied impact of use phase
$E_{re}$	Impacts incurred in demolishing process
$E_t$	Impacts from transporting materials
$f$	Total number of energy types
$g$	Total number of materials to be demolished
$GWP_c$ :	Construction Embodied GWP
$GWP_{EE}$ :	Embodied GWP
$GWP_m$ :	Materials Embodied GWP

$GWP_{OE}$ :	Total Operational GWP
$GWP_t$ :	Transportation Embodied GWP
$IC_{c,e}$	Impact coefficient of the equipment
ICE	Inventory of carbon and energy
ICF	Insulated composite façades
$IC_p$	Impact coefficient of material production
$IC_{p,e}$	Impact coefficient of energy type
$IC_t$	impact coefficient for transport mode
$IC_{t,m}$	Impact coefficient for the transport mode
$l$	Equipment/activity
$l_f$	Load factor
$L_s$	Building lifespan
$m$	Total number of precast components to be transported
$n$	Year of assessment
$n$	Number of different materials
$p$	Transport mode
$Q$	Activity quantity
$q$	Equipment type
$Q_{bo}$	Quantity of equipment/activity
$Q_c$	Amount of work
$Q_c$	Quantity of construction activity
$Q_d$	Quantity of building material or components (tonnes/GFA) to be Demolished/sorted/recycled
$Q_p$	Quantity of material
$Q_{p,c}$	Production volume of prefabricated component

$Q_r$	Percentage of total materials to be recycled or landfilled
$Q_t$	Quantity of material or component to transported
$Q_t$	Quantity of materials to be transported
$r$	Interest rate
$T_t$	Time spent on construction activity
$u$	Total number of activities in operation phase
$w$	Work type to be accomplished
$wf$	Waste factor
$Z$	Value of CED, GWP, or cost in the Pareto front to be normalized
$x$	Total number of transport mode
$Z_{max}$	Maximum value of CED, GWP or cost of the Pareto front
$Z_{min}$	Minimum value of CED, GWP or cost of the Pareto front
$y$	Total number materials/components
$z$	Total number of equipment

## CHAPTER 1 INTRODUCTION

A holistic environmental performance assessment is underscored globally as an effective approach to decarbonize building stock towards a carbon neutral future. Hence increasing efforts are being made to bridge the gap between building energy simulation and conventional life cycle assessment (LCA). This thesis presents a study on developing a building information modelling (BIM) based life cycle assessment method for buildings. Its main aim is to develop a unified method to evaluate the whole lifecycle impacts of buildings in order to promote holistic lifecycle-based design optimization of buildings. This first chapter introduces the background to the research which illustrates the setbacks of traditional building LCA, complexities in integrating with building design process and the significance of developing new approaches to bridge the gap between building design and LCA. Then, the status of BIM and prospects of integration with LCA for the advancement of holistic lifecycle performance assessment of buildings is introduced. Finally, the aim, objectives, framework, and organization of this thesis are presented.

### 1.1 Research background

Buildings generate multiple environmental impacts during their various lifecycle phases as illustrated in Fig. 1.1. On one hand, the manufacture of materials, transportation, construction, maintenance, demolition, disposal, and recycling often known as the embodied impacts requires large amounts of energy with catastrophic implications for carbon emissions [1]. On the other hand, large amount of energy is used for cooling, lighting, equipment and ventilation during the use phase often known as operational impacts with corresponding greenhouse gas (GHG) emissions [2]. LCA and building energy simulation can be used by architects, engineers, and researchers to evaluate and mitigate the environmental impacts of the former and latter, respectively to decarbonize building stock globally [3,4].

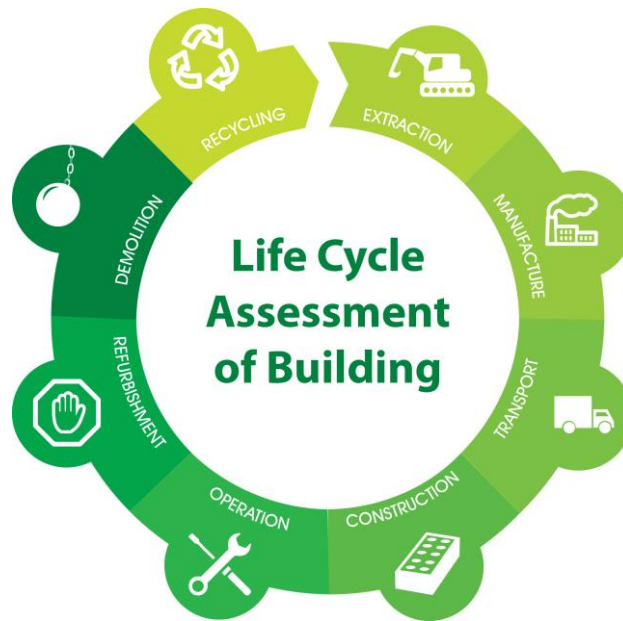


Fig. 1. 1 Life cycle phases of building [5]

In the past decades, building energy simulation has been a global focus supported by a boom in energy efficiency initiatives, policies and regulations which were based on the notion that operational impacts contribute up to 80% of the total lifecycle impacts of buildings [6]. Many building stakeholders resorted to the application of passive design techniques to reduce energy use and carbon emissions during the operational phase of buildings [7–12]. However, this inadvertently increases the embodied impacts of buildings. For instance, some studies reported that the embodied impacts in low energy/passive buildings contribute to as high as 50% of the overall lifecycle impacts which is very significant in comparison with up to 20% in conventional buildings. The distribution of embodied and operational impacts for conventional and low energy buildings which illustrates the increasing share of embodied energy in passive/low energy buildings [13–16].

Governments and other agencies around the world have expressed renewed interest in new building construction given the steadily increasing housing deficits [17,18]. Thus, more

residential buildings are expected to be constructed with critical impacts on the environment. In the absence of stringent mitigation strategies, the embodied impacts of buildings are expected to exceed operational impacts as projected in Fig. 1.2. To reduce the environmental impacts of buildings throughout all lifecycle phases, a steady increase in the use of whole building LCA is observed globally.

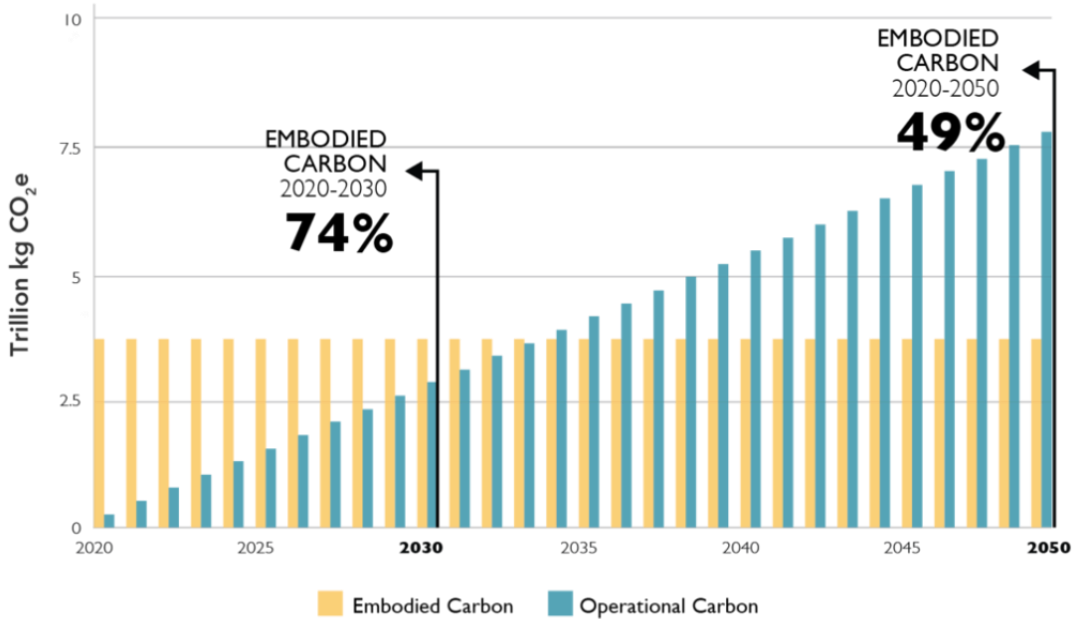


Fig. 1. 2 Projection of embodied vs operational energy [19]

Although LCA is promising to mitigate the environmental impacts of buildings, it is seldom performed by building stakeholders such as architects, designer, and engineers during the design process. Quite often, conventional LCA methods which are complicated by their intricacy, numerous parameters, and data requirement for the various life cycle phases of buildings are used [20–22]. Hence, it is often performed in hindsight to satisfy or gain green building accreditation but without any potentials for environmental performance improvement. The challenges of conventional LCA is multi-faceted and spotlighted as limitations to

integration of LCA into an iterative design process. For instance, most conventional LCA tools such as GaBi and SimaPro are not interoperable with building design tools. To import data from the design tools to LCA tools, there is the need for semi-automated methods or manual input of data which requires significant amount of data and often leads to errors [4]. Even in the case of semi-automated transfer of data using quasi-methods, there is often loss of data which is a deterrent to most architect and designers. A couple of iteration between tools will lead to huge data loss and require manual corrections if recognized, otherwise lead to huge errors, and make the results of the analysis unreliable [16,23].

The transitioning to sustainable buildings has been accompanied by the emergence and application of digital technologies. One such technology is BIM, which has been widely explored in sustainability assessment [24,25]. BIM is a digital representation of a physical facility which serves as a repository for multidisciplinary data. It also has inherent capabilities to manipulate and generate data required for a wide range of building assessments [26–28]. In this context, the integration of BIM and LCA provides many opportunities to improve whole lifecycle assessment of buildings [4]. BIM-based LCA can mitigate challenges of conventional LCA process, which is time-consuming, costly and involves manual data entry [29]. It is therefore important to leverage this opportunity to promote different approaches for BIM-based LCA.

Recently, there has been some attempts to integrate BIM with LCA. However, they have mostly been limited to the use of BIM tools for quantity takeoffs, and semi-automated transfer of data. There are limitations to assessment within BIM tools such as lack of integration methods, prolonged computation time, and impractical assessments due to the structure of database and assessment models. Besides the assessment of embodied impacts, there are also limitations to joint evaluation of operational impacts within BIM tools. Most LCA are performed separately from the building energy simulation. Since the operational and embodied

impacts are correlated, a nonparallel assessment may limit the opportunities to optimize the whole lifecycle performance of buildings. Thus, it has become necessary to develop methods for parallel assessment of both operational and embodied impacts in a joint workflow. Conceivably, such methods will provide opportunities for fast real-time automated workflows required by architects, engineers, and designers to improve the whole lifecycle performance of buildings.

Beside the challenges of integrating LCA within building design process, LCA in itself is further complicated by the wide range of archetypes such as residential, office, scientific, and educational buildings. Even within each archetype, buildings might vary in design components, and therefore construction processes [30]. Furthermore, every component has different performance requirements and customizable materials [21,31]. Accordingly, the material production phase of a building is deemed a complex process. In the construction phase, each material transported to the site has different assumptions in transportation modes, loading factors, and energy requirements. Also, onsite construction involves numerous construction processes and workflows with different equipment and amount of time based on the complexity of works to be accomplished [32,33]. During the use phase, each material has varying technical performances, requiring different replacement schedules, based on their service life [34]. At the end-of-life phase, different management strategies can be applied, assuming unique demolishing or deconstruction processes and recycling, landfill, or reuse [35]. These complexities in each lifecycle phase increase assumptions for processes in building LCA. The results obtained are largely inaccurate due to uncertainties caused by lack of data and assumptions. Uncertainties introduced in LCA process involve parameter uncertainties, scenario uncertainties and model uncertainties which are being spotlighted owing to the inaccuracies induced in building LCA results.

## 1.2 Research aim and objectives

Life cycle assessment is increasingly promoted as a method to improve the environmental performance of buildings towards the global goal of achieving carbon neutrality. A major concern among architect, designers, and engineers in performing building LCA is the limitation of integrating conventional LCA within the building design process. Conventional LCA has been introduced to facilitate the implementation of sustainable construction building practices. However, the introduced methodologies are criticized for their non-interoperability with existing building design tools, unparallel evaluation of embodied and operational impacts, slow assessment process, errors due to manual entries of large amounts of data, and uncertainties induced by the lack of data, evaluation model and scenarios. In view of these flaws, a robust BIM-based method founded on automated assessment of the embodied impacts of buildings in BIM tools, parallel whole lifecycle assessment, comprehensive design optimization and uncertainty analysis is proposed in this research. The main research objectives are outlined as follows:

- 1) To develop an automated BIM-based LCA method within a comprehensive assessment framework for the embodied impacts of buildings. A structured approach integrating various lifecycle phases and systematic zoning of buildings according to different assessment levels including components, assemblies, and whole buildings is proposed. A data repository structure, BIM module, impact estimation module is determined to optimize performance and minimize computational resource requirement within the BIM framework.
- 2) To construct a generic building model with different assumptions of building levels and systematic configurations, life cycle phases, environmental impact assessment methods in a BIM environment to generate life cycle impacts when design parameters are varied in real time. High-rise and mid-rise residential buildings in Ghana and Hong Kong are adopted as

target buildings for the systematic evaluation of the developed BIM-based lifecycle assessment.

- 3) To develop a tier-hybrid uncertainty assessment approach to evaluate parameter, model, and scenario uncertainties in the life cycle of buildings. The integration of pure quantitative/statistical and qualitative/data quality indicator (DQI) approaches is proposed to characterize parameters uncertainties in the embodied impacts of buildings. Proper assumptions are also modelled to assess the influence of model and scenario uncertainties. Monte Carlo approach will be adopted to propagate parameter, model, and scenario uncertainties in the embodied impacts of buildings.
- 4) To conduct a robust whole lifecycle optimization approach for the embodied and operational lifecycle phases of buildings. Multi-objective optimization will be integrated with building energy simulation and LCA to explore the optimal building configuration process in an iterative design process. The optimization of whole life cycle performance will integrate passive design strategies and renewable energy integration to explore the trade-off between embodied and operational impacts.
- 5) To propose a BIM-based parametric technical and economic lifecycle optimization framework to achieve optimal environmental performance of buildings in a cost-effective approach. Multi-objective optimization will be performed from an energy, environmental and economic approach. A detailed technical and economic assessment with application to the passive design and renewable energy integration will be performed for a mid-rise building in Ghana. The holistic optimization process will also account for the impacts of confounding factors and climate change in the whole lifecycle design and optimization process.

This comprehensive BIM-based LCA study on whole lifecycle design in buildings can help stakeholders such as architects, designers, engineers and researchers to evaluate the

environmental performance of buildings in a cost-effective approach while considering passive design strategies and renewable energy applications. This systematic approach can also provide the basis for the integration of further assessment criteria and analyses to accelerate the development of buildings towards carbon neutrality.

### **1.3 Organization of the thesis**

Following the above introduction and research objectives, Chapter 2 presents a comprehensive literature review of existing BIM-based LCA studies, uncertainty characterization and analysis methods, BIM-based LCA design optimization, low energy and low carbon design strategies and novel façade systems used in Ghana. Specific research gaps are identified in the concluding subsection. The overall framework of the thesis on BIM-based lifecycle design optimization for low carbon buildings is illustrated in Fig. 1.4. It includes the BIM-based LCA design methodology, uncertainty assessment method and optimization method (Chapter 3), automated assessment and validation on a prefabricated high-rise building in Hong Kong and a comparative assessment of different façade systems in Ghana (Chapters 4-5), tier-hybrid uncertainty analysis for a high-rise residential building in Hong Kong (Chapter 6), and multi-objective optimization of energy, carbon and cost of buildings in Ghana (Chapters 7-8).

Chapter 3 details the various aspects of the modelling approach to develop a comprehensive BIM-based LCA and optimization framework. This approach begins with the framework for the BIM-based LCA which comprises of a data repository, BIM module and impact estimation module. The assessment method is realized in a computational tool with systematic assessment levels and multiple impact assessment methods. Furthermore, a tier-hybrid uncertainty analysis method which incorporates quantitative and qualitative analysis prior to uncertainty propagation is illustrated.

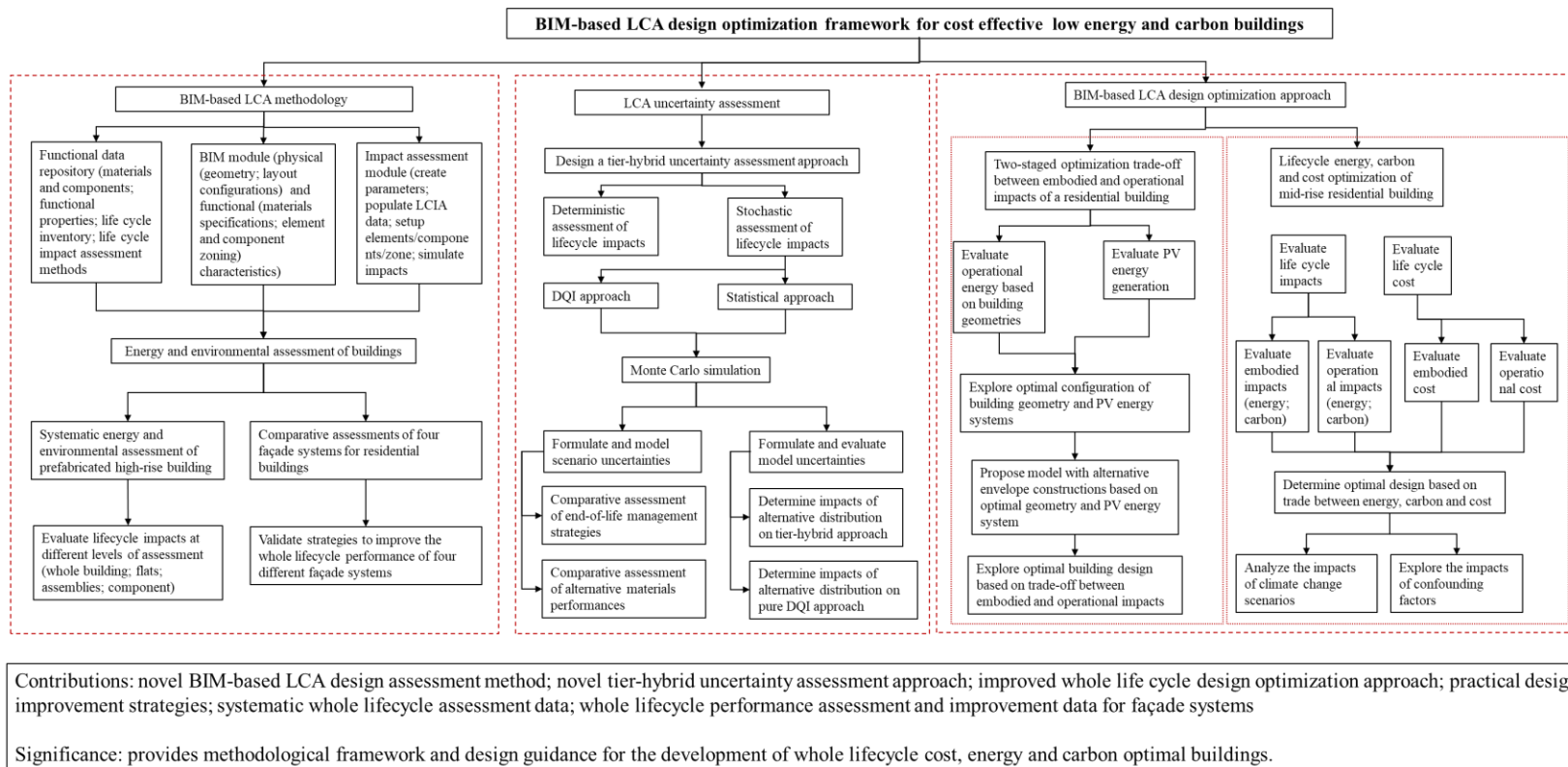


Fig. 1. 3 Overall study framework on BIM-based LCA methodology and optimization framework for buildings

Finally, an optimization framework incorporating LCA, and life cycle costing (LCC), multi-objective optimization, passive design strategies and renewable energy systems is presented.

Chapter 4 focuses on operationalizing the developed BIM-based LCA methodology for the embodied impacts of a prefabricated high-rise building. Detailed simulation assessments are performed at various levels of assessment including whole building levels, flats, assemblies, and components. The embodied impacts are also evaluated according to the various lifecycle phases and different environmental impact categories.

To further validate the robustness of the developed model, Chapter 5 details a comparative assessment of novel façade systems with reference to a conventional façade system used in Ghanaian residential buildings. Simulation assessments are performed to evaluate the embodied and operational performances of the various façade systems in terms of energy and carbon criteria. Further scenarios analyses are also performed to improve the performance of all façades including economic assessment.

Chapter 6 presents the results of a tier-hybrid uncertainty analysis of a high-rise building in Hong Kong. Uncertainties in the various life cycle phases and materials are characterized using quantitative and qualitative approaches followed by uncertainty propagation. A deterministic LCA is first performed to validate stochastic propagation of parameter, scenario, and model uncertainties. Parameter uncertainties due to lack of data or variations in LCA data are quantified. In addition, uncertainties which occur due to scenario assumption and the uncertainty evaluation model are also quantified. Furthermore, potential for performance improvement is also evaluated through alternative materials and end-of-life cycle processes of the case building.

By incorporating an optimization process into the developed BIM-based LCA method, a two-staged multi-objective optimization with considerations for embodied and operational impacts is performed on a mid-rise Ghanaian residential building in Chapter 7. The first stage entails the optimization of geometry and renewable energy systems followed by an optimization of the trade-off between embodied and operational impacts with reference to the thermophysical properties of building envelope materials.

Based on the previous optimization incorporated into the BIM-based LCA, chapter 8 proposes a robust computational multi-objective optimization to identify cost effective low energy and carbon building design solutions to mitigate environmental impact and climate change. Lifecycle assessment is integrated with life cycle cost assessment and multi-objective optimization to optimize passive design parameters and renewable energy systems throughout the lifecycle of buildings. Post-analysis including confounding factors such as building occupancy loads and climate change representative concentration pathways are also performed.

In conclusion, Chapter 9, highlights the main findings and limitations of this thesis while making suggestions for future work.

## CHAPTER 2 LITERATURE REVIEW

This chapter presents a comprehensive literature review on developing BIM-based LCA methods for buildings which include integration frameworks, optimization methods, and LCA uncertainty research. Research gaps are outlined based on the literature review.

### 2.1 Integration of BIM and LCA for buildings

The integration of BIM and LCA of buildings has been explored in recent studies [36]. BIM-based LCA can mitigate challenges of conventional LCA process, which is time-consuming, costly and involves manual data entry [37]. Previous studies have leveraged this opportunity to promote different approaches for BIM-based LCA. One group of studies has simplified lifecycle inventory (LCI) by extracting bill of quantity (BOQ) from BIM tools. Basbagill et al. [38] integrated BIM and LCA to evaluate the embodied impacts of building components. The study exported data from a conceptual level building modeler (DProfiler) and conventional LCA tool (SimaPro) to perform LCA manually in Excel. Although the study provided a method to visualize the embodied impacts of building components, the proposed tools were not computationally integrated. Furthermore, the conceptual level builder provides very limited design exploration other than type of materials and thicknesses. Georges et al. [39] integrated Revit and SimaPro to investigate the operational and embodied emissions of materials for a net-zero emission building. The length, area and volume of materials and components were exported from Revit to Excel for LCA computations using SimaPro. Likewise, the study did not achieve any computational integration of LCA within BIM. Hao et al. [40] proposed a BIM-based approach to evaluate the carbon emissions during the material manufacturing stage of prefabricated buildings. However, BIM tools (GGJ2013 and GCL2013) were primarily used to generate Bill of quantities for structural and steel works of the buildings. The study did not illustrate any integration of BIM and LCA to evaluate carbon emission of prefabricated buildings. Peng [41] proposed carbon accounting method for the buildings using

Revit BIM and Ecotect LCA tool. The study only leveraged BIM to generate Bill of Quantities (BoQs) for LCA whereas Ecotect was used to simulate the energy consumption of the air-condition system. Shin et al. [42] detailed the data requirements and integration processes for BIM-based LCA using ArchiCAD BIM, EcoDesigner and Excel. Although the study provided a detailed integration process compared to previous study, it still required manual entry of large LCA data.

Another group of studies defined workflows combining BIM, LCA and other auxiliary tools to eliminate the manual entry of data. Najjar et al. [43] proposed an automated framework integrating BIM, LCA and mathematical optimization to improve the selection of energy efficient building envelopes. The study leveraged Tally and Autodesk Green Building Studio to evaluate the embodied and operational impacts, respectively. Tally plug-in generated an inventory of materials which was linked to Gabi LCA database to evaluate the embodied impacts of construction materials whereas Autodesk Green building studio estimated the operational impact of different assemblies. Despite, the improved BIM-LCA integration for the selection of energy efficient materials, it is impractical to evaluate energy envelopes without considerations for the functionality of the building. Nizam et al. [44] proposed a BIM-based LCA framework to estimate the embodied impacts from material production, transportation, and construction of buildings. The study developed an Application Programming Interface (API) for Revit and used the Inventory of Carbon and Energy (ICE) database to evaluate the impacts of a case study building. Although the API bridged the disconnect between the BIM tool and LCA database (MS Access), its development and application is complex which limits a wide application among industrial professionals. Rezaei et al. [45] developed a BIM-based LCA framework for both early and detailed design stages of buildings considering material production, construction, operation and maintenance and demolition phases. The study developed a functional database of building elements from common materials used in Canadian

residential buildings and matched them with a related dataset in Ecoinvent LCI manually. After designing the BIM model, a BOQ is generated and matched with LCI data from the functional database. The results are then used to perform the LCA in OpenLCA. While the study simplified the LCA process through a functional data, the execution of LCA outside the BIM framework limits the usefulness of the integration process especially for an automated optimization process. Yang et al. [46] developed a BIM-enabled LCA method to evaluate the whole lifecycle of low carbon building design in China. Revit and Glodon BIM5D tools were used to develop a BIM model and generate BOQ while eBalance, Ecoinvent and European Life Cycle Database provided life cycle inventory (LCI) for the study. The BIM model was exported to Design builder to generate a model for operational energy simulation in EnergyPlus. The developed BIM-LCA framework involved export of data which might lead to data loss, hence not ideal for an iterative design process. Zhang et al. [47] proposed a BIM-based LCA method to evaluate and optimize the embodied energy of building construction in China. The study developed an API which connected Revit BIM model to a functional database to evaluate the impacts of the material production, transportation, and construction phases with ICE and other supplementary data. The proposed model to optimize transportation and construction processes are not intrinsic to the BIM process, which limits its usefulness in a BIM-based optimization process.

A third group of researchers argues that the inclusion and manipulation of LCA data within BIM environment is a more effective approach to harness the power of BIM such as real time LCA during design changes. In this regard, more recent approaches have used visual programming plug-ins with BIM tools such as Dynamo and Grasshopper. Cavalliere et al. [48] proposed an approach to structure BIM parameters for LCA of buildings. The proposed parameters were tested on the materials and component production, construction, maintenance, and end-of-life phases of the exterior wall of a residential building in Italy. The results showed that the parameters are sufficient to perform and LCA within the BIM environment in an

effective way. Hollberg et al. [49] developed a BIM-based LCA tool to evaluate the embodied emissions of a building through the whole design process. The study linked Swiss LCA database Ökobilanzdaten im Baubereich to Revit using unique identifiers. The LCI data for each material is then written automatically to the Revit file using Dynamo. Thereafter, a BOQ is extracted to compute the embodied emissions of the building elements. Santos et al. [50] identified the information necessary to propose a BIM-LCA framework for the product, construction, use and end-of-life stages of buildings. The framework implemented using a prototype tool and a case study building developed in Revit. The prototype tool identifies various materials in the building and evaluates their impacts by matching an appropriate LCI data from Belgium environmental product declarations (EPDs) or Ecoinvent database to the materials. Although the study provided a detail background knowledge to develop BIM-based LCA tool, the required processes are complex and may deter widespread application among practitioners. Shadram et al. [51] developed a BIM-based optimization framework to reduce the embodied and operational energy of buildings. The study developed an input-output interface using Dynamo to extract building element and properties, write information and estimate embodied energy using Inventory of Carbon and Energy (ICE) LCI data. On the other hand, Grasshopper was used to simulate the operational energy performance.

Table 2. 1 Comparison of characteristics of previous BIM-based LCA studies

<b>Level of integration</b>	<b>LCA stages</b>	<b>BIM Tool and LCA tools</b>	<b>LCA Tool</b>	<b>LCI Database</b>	<b>Applica-tion site</b>	<b>Reference</b>
	Materials production, construction, maintenance repair and	DProfiler ,	SimaPro & EQuest		Norway	[38]

<b>Level of integration</b>	<b>LCA stages</b>	<b>BIM Tool and LCA tools</b>	<b>LCA Tool</b>	<b>LCI Database</b>	<b>Application site</b>	<b>Reference</b>
	replacement, demolition.					
	Materials production & building operation	Revit	Excel, SimaPro	Ecoinvent, Environmental Product Declarations		[39]
	Materials production, transportation, construction	GGJ2013 & GCL2013		National Greenhouse Gas Inventory Guidelines	China	[40]
	Material production, transportation, construction, operational & demolition	Revit	Ecotect	National Greenhouse Gas Inventory Guidelines, Literature	China	[41]
	Materials production, transportation, construction, operation, maintenance and repair, disposal	ArchiCAD	EcoDesigner, Excel		Korea	[42]
	Materials production, transportation, operation, maintenance and repair and disposal	Revit	Autodesk Green Building Studio, Tally	GaBi database	Brazil	[43]
	Materials production, transportation, construction,	Revit	Revit API	ICE database	China	[44]
	Materials production, transportation, operation, maintenance and end-of-life	Revit	OpenLCA	Ecoinvent	Canada	[45]

<b>Level of integration</b>	<b>LCA stages</b>	<b>BIM Tool and LCA tools</b>	<b>LCA Tool</b>	<b>LCI Database</b>	<b>Application site</b>	<b>Reference</b>
	Material production, transportation, construction, operation, refurbishment, demolition and disposal	Revit and Glondon BIM5D	eBalance	Ecoinvent and European Life Cycle Database	China	[46]
	Material production, transportation, and construction phases	Revit	API	ICE	China	[47]
	product, construction, use and end-of-life stages of buildings	Revit	API	EPDs & Ecoinvent database	Belgium	[50]
	Materials and component production, construction, maintenance, and end-of-life phases	Revit		Ecoinvent	Italy	[48]
	Materials production, waste processing, disposal	Revit	Dynamo	Ökobilanzdaten im Baubereich	Switzerland	[49]
	Materials production, construction, operation, maintenance, refurbishment & end-of-life phases	Revit & Rhinoceros	Dynamo & Grasshopper	ICE	Sweden	[51]

These studies on developing a BIM-based method for building LCA are summarized in Table 2.1. Despite these developments, there are several limitations. It is observed that most studies use BIM to improve the accuracy of materials inventory for LCA but miss the potential of BIM to store and perform automated LCA. Furthermore, there is the lack of a comprehensive localized embodied coefficient database for many regions such as Hong Kong and Ghana which often leads to assumptions in the impact coefficients of different materials used in building construction and consequently uncertainties in the LCA results. The use of auxiliary tools often leads to interoperability issues and consequent loss of data which is counteractive to iterative optimization processes. Most studies which focus on specific components or life cycle phases also limit the feasibility of improving the overall lifecycle performance of buildings. Numerous opportunities exist to develop simple and practical approaches to enhance databases and repositories, retain data within the BIM process and automate data exchange and computations.

## **2.2 Design optimization of whole building lifecycle using BIM-based methods.**

Design optimization is an effective approach to improve building performance criteria such as energy use, carbon emission and cost. Over the years, many studies proposed extensive optimization methods to reduce any or combinations of these criteria during the operational stage of buildings [52]. Quite often, passive design is a first step to reduce energy use before the integrating renewable energy systems [53–59]. However, a mere application of passive design for energy efficiency during the operational phase of buildings is not sufficient to curb the energy use and carbon emissions from buildings. Recent studies indicate that passive strategies such as highly insulated envelopes in new construction and retrofits can even increase embodied energy and carbon related emissions beyond levels which are beneficial [60]. Quite often, the embodied carbon emission of passive buildings is increased to levels that jeopardize the transitioning towards improved whole lifecycle performance [61]. This therefore requires rethinking of building design problems as it has become essential to consider the interaction

between all passive design strategies on the whole lifecycle energy consumption and carbon emission of buildings. Also, the implementation of passive design strategies to improve the energy and carbon performance of buildings affects their economic performance, and therefore it is necessary to evaluate the economic implications of pathways towards carbon neutrality [62].

Most passive design optimization studies focus on passive design strategies under fixed building shapes. A residential building was optimized with non-dominated sorting genetic algorithm (NSGA-II) by varying the building orientation, envelope insulation, window type, window-to-wall ratio (WWR), air infiltration rate and renewable energy generation system for energy use, life cycle cost and thermal comfort criteria [63]. The results showed that WWR, air infiltration and insulation thickness are the most influential parameters for building energy consumption. Overall, more than 21% energy saving was achieved for different regions in Morocco and about 40% of the case building energy consumption can be covered by renewable energy generation. The cost-effectiveness of the renewable energy systems however depended largely on the climatic condition. This study did not evaluate the cost of the building envelope in the economic analysis. A similar study evaluated the glazing types, wall types, WWR and shading devices for an educational building considering thermal comfort, energy use and daylight criteria [64]. The optimal results with minimal energy use and maximum visual and thermal comfort were characterized by a 60% WWR with double or triple glazing. Vettorazzi et al. [65] optimized the passive house concept for residential buildings in Brazil using a hybrid evolutionary algorithm based on the Covariance Matrix Adaptation Evolution Strategy (CMA-ES) and Hybrid Differential Evolution (HDE) considering energy use and thermal comfort criteria. The study compared the passive house with a reference building stipulated by the Brazilian national thermal code which showed up to 83% and 86% improvement in energy use and thermal comfort, respectively. The optimization results indicated preference for high

thermal insulation in roofs, envelope walls, ground slabs and the mechanical ventilation system in a decreasing order. Wang et al. [66] proposed a method to optimize the energy demand and comfort levels of passive buildings in China. The study explored the thermo-physical properties of the building envelope, orientation, WWR and external shading devices. A highly reliable energy and comfort level improvement model integrating the NSGA-II, sensitivity analysis, redundancy analysis and gradient boosted decision tree was achieved in reducing energy use and discomfort by 88% and 63% respectively. However, the economic analysis performed was not integrated into the optimization. Another study optimized a residential building with NSGA-II by varying the external wall thermal resistance and specific heat, window to ground ratio and U-value of windows, overhang projection fraction, infiltration air mass flow coefficient and building orientation for thermal comfort, daylighting, and natural ventilation criteria [67]. Lapisa et al. [68] optimized a low-rise commercial building for different climate zones with NSGA-II by varying the building orientation, solar reflectivity, skylight surface area, envelope thermal insulation and natural ventilation strategies for energy and thermal comfort criteria. The results showed that for northern regions of France, the optimal design solutions have considerably insulated envelopes, standard roofs with high solar absorption and small skylight areas whereas those for southern regions of France have non-insulated ground slabs, large skylight areas and reflective cool roofs. The study explored the cost as a selection criterion for the optimal results rather than integrating it with the optimization. Furthermore, this was performed for a cold region and results are not representative of buildings in warm/hot region. Vukadinovic et al. [69] optimized the energy use and thermal comfort of a residential building in Serbia by varying the WWR, glazing type, wall construction and window shading using NSGA-II. The results showed that for the cold region of Serbia, the WWR influenced energy use the most. The optimal configuration of the building required triple-glazed window units, highly insulated external walls and minimal or no external shading devices.

There are other studies which consider the impact of building shapes and layouts. D'Agostino et al. [70] proposed a computational workflow to optimise the energy use, cost, and useful daylight of educational buildings by varying the orientation of the central and lateral block, WWR, skylight to roof ratio, shading and thermo-physical properties of the building envelope with NSGA-II. The results of the optimization indicated a strongest influence of the WWR on the useful daylight illuminance and energy use among all objectives. The study also proposed a visualization platform to improve the usefulness of the results to stakeholders and decision makers. Building shapes were optimized to improve the primary energy consumption, the passive volume ratio and best oriented surfaces in an urban context using a parametric approach [71]. The results of this approach produced an optimal result at the early design stage but may be suboptimal when evaluating the whole lifecycle performance. Chen et al. [72] integrated conventional passive design parameters with photovoltaic facades to explore the energy conservation potential of a high-rise commercial building using the hybrid generalized particle search particle swarm optimization (HGPPSO). The study explored design parameters including the building orientation, infiltration rate, WWR, shading and the thermo-physical properties of the building envelope. Furthermore, the study explored some building archetypes and confounding factors such as the building size and shape, urban context and internal heat gain. Zhu et al. [73] optimized the energy use and useful daylight of rural tourism buildings by varying the shape and WWR of three archetypes using the Strength Pareto Evolutionary Algorithm (SPEA-2) and the Hypervolume Estimation algorithm (HypE).

Other studies have also attempted to address the environmental performance of building. For instance, Jung et al. [55] focused on a method to optimize the thermal comfort, energy use and lifecycle economic-environmental impacts of a high-rise residential building in Korea by varying the WWR, airtightness, occupancy, window U-value and solar heat gain coefficient (SHGC), wall insulation, thermal inertia and surface solar absorptance. The study

identified the airtightness, number of occupants and WWR ratio as the most influential parameters to all three evaluated criteria. Using NSGA– II, the results showed a decrease in energy use and cost by 52.7% and 39.5%, respectively compared to the reference building. For the environmental impacts, GWP, AP and POCP were decreased whereas ODP and EP were increased. An uncertainty analysis of the optimal solutions revealed that the optimal energy and economic design solutions are less sensitive to variations in the future utility cost and improvement in the energy system efficiency whereas the environmental impacts are more sensitive to variations in these two. Therefore, more studies are needed to explore the impacts of the future energy systems, materials production efficiency and climate modelling on carbon neutrality of buildings. Another study performed a seasonal analysis of the impacts of the window type, heating/cooling system setpoint and ventilation/window opening type on the thermal comfort, energy use, environmental and economic performance of buildings [74]. The results revealed that from spring to summer, building design scenarios with higher setpoint temperatures and lower U-values improved the energy use and environmental impacts however it decreased the thermal comfort of occupants. Furthermore, highly insulated windows were more beneficial in terms of initial investment costs. Kiss et al. [75] optimized the building envelope, building geometry, and building service components under six environmental impact categories. Ciardiello et al. [76] developed a two-phase method for the design of residential buildings in Italy. The first phase involved a geometry optimization by varying parameters such as the building shape, shape proportion, WWR and orientation, followed by the thermo-physical properties of the building envelope (glazing systems, insulation, and envelope optics) and PV and solar thermal panels. The study explored three objectives including energy use, investment costs and environmental impacts, however, the environmental impacts resulting from variations in the thermo-physical properties of the building envelope were not studied. Moreover, the staged optimization can limit the interactive effects of various parameters on the objectives. Xu

et al. [77] couple the artificial neural network (ANN), NSGA-II and multi-objective particle swarm optimization (MOPSO) to optimize the daylighting, thermal comfort, energy use and economic performance of educational buildings in China. The study applied a two-stage process in which shading devices and thermo-physical properties of the building envelope were optimized prior to the optimization of the photovoltaic generation system. The results showed that the NSGA-II generated better performing solutions in its Pareto front in comparison to the MOPSO.

From the literature review, it can be observed studies seldom focus on joint optimization of the embodied and operational impacts of building. Also, most studies focus on energy use and thermal comfort while very few studies have focused on the environmental performance of buildings. Even though a few studies attempted to address the environmental performance of buildings, most of them evaluated the carbon emissions from electricity use during the operational phase without considering building construction related emissions. Also, while the impacts of climate change are profound on the carbon performance of buildings, none of these studies performed a comprehensive evaluation on the impacts of extreme weather conditions towards achieving carbon neutrality in buildings. Likewise, the economic aspects have been largely segmented and there is a lack of studies that perform an exhaustive economic evaluation of buildings towards carbon neutrality. It is also observed that only few studies have jointly optimized renewable energy generation systems (e.g. solar photovoltaic (PV)) as building integrated systems together with the passive parameters. Finally, none of these studies modelled other confounding factors such as varying internal loads due to occupancy behaviors and variations in building construction related emissions.

### **2.3 Uncertainties in the buildings LCA**

While many studies have focused on the identification of major sources of embodied impacts, development of new materials, and minimization of building impacts, few studies

address the uncertainties in the building LCA process [78]. However, it is necessary to address the reliability and uncertainties of building LCAs from the perspective of the whole building lifecycle, individual components/materials or a particular lifecycle phase.

### **2.3.1 Uncertainties in the material production phase**

Many studies have either investigated the material production phase or the entire building life cycle phase but with a focus on the former due to its high contribution to the embodied impacts of buildings [79]. Building LCA studies focusing on the material production have addressed major uncertainty sources including material quantities, embodied coefficients, materials waste rates, technical densities and system boundaries [80–85]. These studies indicate that despite the higher contribution of the material production to the total embodied impacts in buildings, uncertainties are lower compared to other life cycle stages due to the availability of LCA data. In the context of transportation, assumptions about the sources of materials or components as well as transportation modes when such data is lacking may lead to large uncertainties in the transportation stage of building lifecycle analysis [82]. The overall accuracy of the environmental impact of the transportation phase is contingent on the accuracy of input data which is hard to achieve due to massive components and materials used in each building [86]. Given the simplifications applied to the transportation phase, a rigorous uncertainty analysis should be applied to improve the accuracy of LCA results.

### **2.3.2 Uncertainties in the maintenance phase**

Addressing maintenance issues has become urgent due to the increasing demand of meeting building performance requirements, new maintenance techniques and complex maintenance cultures of building operators [87]. However, studies have indicated that there are high uncertainties associated with the maintenance phase in building LCA due to the complexities in evaluating the service life of building components [88]. Recent studies have shown that many factors can influence the service life building components such as the material

and quality of workmanship, maintenance level, internal and external climate of the building, building design, technological change, availability of replacement components, legal requirements, residual value of building and energy efficient renovations [89]. Given the need to reduce such uncertainties, some studies have tried to improve the accuracy of service life modelling. For instance, Ferreira et al. [90] developed a method to quantify the impact of maintenance actions on the components of building envelopes. A probabilistic approach through stochastic maintenance modelling reveals that a combination of maintenance activities such as cleaning and minor interventions with total replacement ensures the high performance of a building component through its service life. Marques et al. [91] applied a factor method to predict the service life of ETICS through the visual inspection of case buildings and modelling of the characteristics and degradation of patterns. Shohet et al. [92] developed a framework for a performance-based maintenance of public facilities which showed consistent improvement in the performance of facilities during implementation. Mousavi et al. [93] developed a model for predicting the service life of natural stone cladding with direct fastening systems to aid the definition of maintenance strategies and rational management systems for heritage buildings. Another study presents a fuzzy inference system based on the expert knowledge for the prognosis of the functional service life of buildings [94]. Among these studies for maintenance uncertainties, two distinct themes are addressed: (i) approaches to predicting the service life of materials; and (ii) maintenance strategies. Three main approaches are identified in predicting the service life of building components: (i) accelerated life test in laboratories; (ii) factorial methods; and (iii) the reference service life based on the documented service life. Also, two maintenance approaches are identified: (i) planned and unplanned maintenance. Planned maintenance can be further categorized into preventive, corrective and improvement types. In order to achieve a realistic maintenance modelling, data accumulated from historical cases are required. In the absence of such information, most researchers apply the reference service life

approach. Although the application of service life databases for building components is proven reliable, some of these databases may be outdated or based on different calculation methods. To overcome these challenges, the variations in the service life of building components and materials should be included as uncertainty parameters.

### **2.3.3 Uncertainties in the construction phase**

The construction phase usually receives less attention due to its low contribution to the total embodied impacts [95]. Researchers often apply simplified approaches when quantifying the impacts of the construction phase [96]. One example of such simplification is the use of construction data from previous building projects which induce large uncertainties given the lack of standardization in construction processes. Hence, interest in uncertainty characterization of construction phases has been growing because unrepresentative data is often applied to its impact assessment.

### **2.3.4 Uncertainties in the end-of-life phase**

The end-of-life phase is frequently overlooked when modelling building LCAs since it contributes least to the total embodied impacts. However, the large amount of demolition and recyclable materials from high-rise buildings provide numerous opportunities to improve the environmental performance of buildings. The uncertainties induced in the end-of-life stages often come from assumptions in end-of-life modelling such as recycling, and demolition strategies. Chau et al., 2017 and Hossain and Ng, 2020 [97,98] defined scenarios to evaluate the impact of end-of-life stages but failed to address intrinsic uncertainties of parameters and assumptions in modelling the end-of-life stages. Given the lack of reliable input data, rigorous statistical approaches are required for quantifying these uncertainties and increasing the reliability of LCA results.

Generally, researchers have identified uncertainty sources including variability of data and characterization models (spatial and temporal), imperfect measurements, incompleteness

of data, unrepresentativeness of inventory data, normative choices, selected scenarios, technical performance, functional units, estimation of uncertainties and mathematical relationships [99–102]. In summary, uncertainty sources can be classified into parameter, scenario and model uncertainties among which parameter uncertainty is the most commonly addressed.

### **2.3.5 Evaluating uncertainties in building LCA**

To evaluate uncertainties in LCA, it is important to identify the methods to characterize uncertainties. Uncertainties can be generally characterized statistically using probability distributions although qualitative descriptions may be applied when historic data are insufficient. Hence, both quantitative and qualitative methods have been explored in previous studies. Clavreul et al. [103] identified the fuzzy theory, Tylor series expansion, data quality indicators (DQI), stochastic modelling, possibility theory, expert judgement and hybrid of two or more methods in their study. Although the performance of each method can vary depending on the nature of uncertainties, the positive review of DQI and stochastic modelling has identified its wide application in building LCA and is therefore incorporated in this research. In the DQI method, a pedigree matrix is applied to model the underlying uncertainties in a semi-qualitative fashion, and then propagated quantitatively through stochastic modelling such as the Monte Carlo simulation [104]. The advantages of this approach include easy implementation, little computational resource requirements and applicability to a wide range of problems. However, the solution may be low quality due to human biases in the DQI method.

There has been ample research integrating DQI and stochastic methods. For instance, Teng and Pan [105] applied a semi-quantitative method which combined the DQI and stochastic simulation to propagate uncertainties in the LCA of a prefabricated high-rise building. Morales et al. [88] investigated uncertainties in the maintenance phase of a building using several scenarios of repairs or replacements. Similarly, DQI is applied to describe input data uncertainties while Monte Carlo simulation is used to calculate the model output uncertainties.

Giuseppe et al. [106] analyzed the implication of data availability and quality on LCA of five insulation systems for historic buildings in Italy. Su et al. [107] performed a probabilistic LCA of eight insulation materials to evaluate the uncertainties induced by variability of data such as in the density using the data quality analysis and Monte Carlo simulation. The study also implemented a sensitivity analysis which reveals that the variability and uncertainty of parameters can significantly affect LCA results. Robati et al. [108] collected data to determine the probability distribution of the lifespan, embodied emission and transport distances of 16 materials. A Monte Carlo simulation is then applied to perform a global sensitivity analysis which reveals uncertainties in the studied materials. Heijungs et al. [109] compared two uncertainty propagation methods: sampling and analytical methods. Although the sampling method requires more input data such as the probability distribution and parameters, a detail output can be generated and subject to rigorous statistical analyses. On the contrary the analytical method only requires variances but yields very limited results. Nonetheless, the sampling method requires a huge computational time due to the generation of a huge number of random variables.

In general, most researchers have adopted semi-quantitative methods in which qualitative techniques are applied for uncertainty characterization while quantitative techniques are used for stochastic modelling of uncertainties. This is a progressing research domain due to the large number of parameters, scenarios and models available. Also, very few studies have considered using quantitative techniques alone or jointly with qualitative techniques to characterize uncertainties prior to stochastic modelling. With the significant increase in LCA data from case studies, it has become possible to adopt rigorous statistical techniques to provide highly accurate results.

## **2.4 Reducing embodied energy in building**

Researchers have investigated the field of embodied impacts of buildings to identify strategies to reduce the energy use and carbon emissions. Orsini et al. [110] reviewed literature and summarized the pros and cons of low carbon building strategies such as reusable materials, alternative materials, local materials, renewable energy sources, increased performances, correct applications and innovation of production processes. In this regard, some studies have explored these strategies to reduce the energy use and carbon performance of buildings. For instance, Robatti et al. [111] and Teng and Pan [112] conducted case studies to explore measures for reducing embodied carbon such as adopting low carbon concrete, optimizing the prefabrication rate, and changing the thickness of walls. The results underscore that replacing ordinary Portland cement with blast furnace slag cement yields the highest carbon savings. Hossain and Ng [98] compared deviations between building construction emissions using a localized and generic database. Two emission reduction measures namely alternative concrete materials and end-of-life processes are explored and proven to effectively reduce carbon emissions. Gan et al. [113] presented a method to explore the carbon reduction potential of procurement strategies including the steel manufacturing process, recycling scrap, alternative cement materials and transportation distances. The results underscore the use of fly ash or slag for cement in ready-mix concrete, and also the production of steel with high amounts of recycled scrap in an electric arc furnace.

Xiao et al. [114] evaluated the potential embodied impact reduction by replacing natural aggregate concrete with recycled aggregate concrete in case study approach showing significant reductions in both the energy use and carbon emission. AzariJafari et al. [115] investigated the potential environmental impacts of alternative concrete mixtures when exposed to high temperatures, where a reduction in environmental impacts was achieved by using pozzolanic materials. Kurda et al. [116] presented an approach to optimize concrete mixes containing

various recycled concrete aggregates and fly ash for different building architypes. Mavrokapnidis et al. [117] assessed the impacts of structural systems on the environmental performance of tall buildings and proposed the use of recycled materials as a potential approach to improve building sustainability. Other studies have also utilized waste materials to reduce the energy and carbon emission of cement and concrete significantly [118–120]. Hossain et al. [121] identified that an on-site sorting system could reduce energy use and carbon emissions significantly due to the higher recyclability of materials, with a comparison between onsite and offsite waste sorting strategies. Previous studies primarily focus on alternative materials for cement production. The achievable amount of carbon emission reduction is still limited to the practicality of strategies and availability of these alternative materials. For instance, the use of alternative materials may reduce energy and environmental impacts during material production, but their transportation over long distances may decrease the overall net benefit. Hence, exploring the impact of transportation is strongly recommended.

Improvement in the energy efficiency of the operational phase often leads to a surge in embodied carbon emissions. Therefore, low carbon solutions are essential to keep the embodied impacts within beneficial levels. Researchers have evaluated strategies to reduce the embodied energy and carbon emissions. It is established that the embodied impacts of construction processes largely depend on the manufacturing process of materials, haulage distances, efficiency of production and construction processes. For instance, Cabeza et al. [122] concluded that substituting carbon intensive materials like aluminum with timber can reduce the embodied impacts of building significantly. In other studies, non-cementitious materials such as rammed earth are recommended as sustainable façade constructions [123]. The use of recycled aggregates in place of natural aggregates as a carbon reduction measure has been illustrated in case studies which show significant reduction in carbon emissions [124–126]. Another study also recommended the use of local materials to reduce energy use and carbon emissions from

long haulage distances [127]. Zhang et al. [128] highlighted the role of innovative construction processes in reducing the embodied impacts of buildings. This study highlighted geopolymerization as a more sustainable way to produce brick instead of firing or cement and lime-based methods. Salas et al. [129] also emphasized that the use of renewable energy sources such as hydroelectricity can improve the embodied impacts of geopolymer concrete significantly. Natural and recycled insulation materials such as sheep wool and recycled cork have also been found as a more sustainable solution instead of other carbon intensive insulation materials [130, 131].

## **2.5 Life cycle assessment of façade systems**

In addition to the general approaches used to reduce the embodied impacts of buildings, façade systems have been a primary focus to reduce embodied and operation impacts besides their economic benefit. Using Ghana as a case study, new façade systems besides the conventional ones are being widely used. However, there are very limited studies that investigate their environmental and economic impacts. The use of concrete frames infilled with sandcrete blocks is very popular in Ghana. A survey indicated that about 64% and 35% of residential buildings are composed of sandcrete blocks and mud/burnt bricks respectively [132]. Other alternative materials have also been researched in the recent past [133]. According to Oppong & Badu [134] interactions between concerns such as the construction duration, environmental and economic performance have motivated the use of alternative materials in Ghana. Some alternative materials include soil-based façades: Stabilized Earth Block Façade (SEBF) and two other composite façades: Galvanised Steel Insulated Composite Façade (G. Steel ICF) and Shotcrete Insulated Composite Façade (Shotcrete ICF). While these alternative façades are gaining attention in Ghana, their sustainability has not been studied. Mostly the operational performance of façades is prioritised by designers and researchers whereas their effectiveness on reducing life cycle impacts is debatable [135].

Christoforou et al. [136] evaluated different production scenarios of adobe bricks in Cyprus and found that using sawdust instead of wheat straw and the transport distances significantly vary the result. LCA was used to compare the environmental performance of naturally stabilized earth blocks and three conventional load-bearing walls in Spain [137]. The study suggests that stabilized earth blocks perform better in terms of the span, but the concrete block masonry has less wall mass. Joglekar et al. [138] conducted a comparative LCA of five bricks incorporating different industrial and agro wastes in India and argued that these bricks outperform the conventional clay bricks. Guo et al. [139] evaluated the mechanical and environmental impacts of recycled concrete aggregates in concrete building blocks. Their study shows that environmental impacts of normal concrete blocks are much higher due to longer transportation distances. Ben-Alon et al. [140] evaluated the environmental impacts of cob wall materials used in USA and showed that the impacts of cob are highly dependent on the wall thickness and material source. An assessment of energy embodied in cement stabilized rammed earth wall construction suggests an optimization of the cement content and compaction due to clay content [141]. The embodied energy of a cement stabilised rammed earth building in India was found to be approximately 60% lower than a burnt clay brick alternative [142]. Sandanayake et al. [143] compared the environmental impacts of a concrete and timber building in Australia which revealed that recycling and the use of regional materials make the most significant impacts. Autoclaved Aerated Concrete (AAC) and fired brick exterior walls were subject to environmental, economic and thermal assessment which indicates that the impact of the former wall system is less owing to the cement content [144]. Arrigoni et al. [145] assessed the environmental impact of hempcrete blocks in Italy and identified the binder production as the most significant source of environmental impacts. Further investigation revealed that hempcrete blocks have a favourable environmental impact due to the uptake of CO<sub>2</sub> during hemp growth and carbonation. The environmental impact of an alkali-activated block and

stabilized soil block were compared against a conventional concrete block and an architectural concrete block [146]. The results suggest both emergent masonry blocks reduce embodied carbons by over 40% when compared with conventional blocks. Environmental impacts of mud concrete block and other industrious walling materials in Sri Lanka were compared based on a fixed area of walls [147]. This study indicates the mud concrete block has the lowest environmental impact which can be further reduced using renewable energy.

On top of cement-based and soil-based façades, there are a few studies noteworthy on the environmental performances of insulated composite façades (ICF). Only Yılmaz et al. [148] conducted a comparative LCA on rockwool or polyurethane filled galvanised insulated composite façade panels in Turkey. The study concludes that for the same functional requirement, polyurethane filled panels are more environment friendly due to the less use of galvanised steel. Potrč et al. [149] analysed the life cycle impact of External Thermal Insulation Composite Systems (ETICS) with expanded polystyrene (EPS), mineral wool and wood fibre board insulation filling. The study proves that insulation materials cause the major environmental impacts among which EPS contributes the least. [150] evaluated the environmental performance of ETICS, ventilated façade and internal insulation façade for different climate zones of Spain and revealed that ETICS with glass wool filling has the least environmental impact. The study also focused on auxiliary materials used for each façade given their critical impacts. A multi-criteria decision-making process was developed to select the optimal façade system between the AAC panel, aluminium composite panel, ceramic cladding, concrete block and double brickwork in Australia [151]. The study identified embodied energy/carbon of materials as the most critical factor and AAC panel is found to have the worst performance. Densley Tingley et al. [152] evaluated the life cycle impact of EPS, phenolic foam and mineral wool insulation for UK homes and concluded that EPS had the least environmental impact in most categories. However, considering the embodied carbon alone, phenolic foam is

the least impactful insulation material. Schmidt et al. [153] evaluated the environmental performance of stone wool, paper wool and flax and concluded paper wool has the least environmental impacts whereas flax insulation has the largest impacts. Schiavoni et al. [154] reviewed commercialized insulation materials and found that existing LCA studies lack a common boundary and calculation process which makes a direct comparison across studies very difficult. Hill et al. [155] also presented an extensive review of insulation materials and emphasized the need for scenario specific LCA data when comparing insulation materials.

From the above literature review, it can be observed that the environmental impacts of ICFs strongly depend on their composition while the impact of G. Steel ICF has not been sufficiently evaluated. Also, no LCA study on Shotcrete ICF has been identified in existing literatures. Although LCA of similar soil-based façades has been conducted in regions such as India, Sri Lanka, Cyprus and Spain, their conclusions might not be applicable to Ghana due to variations in materials compositions, construction technology, energy/carbon database and other supporting structures of the façade. Thus, the environmental impacts of façade systems should be analysed within a context specific approach. Also, it is necessary to consider the impact of other facade supporting components as they may vary LCA results significantly. Given the steadily increasing demand for housing, more residential units are expected to be constructed with critical impacts on the environment. LCA is therefore required to select façades with the least environmental impacts while fulfilling economic targets. Thus a detailed comparative assessment of the environmental and economic impacts of G. Steel ICF, Shotcrete ICF and SEBF with the conventional Concrete Block and Mortar Façade (CBMF) used in Ghana is necessary. Furthermore, scenario analysis and optimization are also needed to improve the performances of these façade systems. This will contribute significantly to the Ghanaian housing sector as well as regions with similar realities by providing a comprehensive guidance to selecting a sustainable façade to cope with the growing housing demand.

## **2.6 Research gaps on BIM-based life cycle assessment and design optimization of buildings**

This chapter reviewed literature on BIM-based LCA for buildings with regards to integration methodologies and design optimization approaches, uncertainty in the lifecycle phases of buildings, approaches to reducing the lifecycle impacts of buildings and sustainable façade systems as alternative to the conventional façade systems. Based on the literature reviewed, the following research gaps were identified:

1. Automated BIM-based LCA studies on buildings were seldom conducted to evaluate the embodied impacts of buildings in a seamless and iterative design assessment workflow. The existing approaches are fragmented leading loss of data, poor assessment results, and inability to retain and use LCA results within the BIM-based design workflow.
2. Few BIM-based design optimization studies have been limited to the operational impacts of buildings without considerations for the embodied impacts. The trade-off between embodied and operational impacts in low energy building remains unexplored. Few design optimization studies have integrated passive design strategies and renewable energy systems while exploring both operational and embodied impacts in an integrated framework.
3. Limited studies have considered cost and environmental criteria when evaluating the whole lifecycle impacts of low energy buildings. Design optimization studies have been limited to performance criteria of the operational stages while the embodied energy, environmental and economic impacts have been ignored. Further few studies have considered the trade-offs between energy, environmental and economic criteria in the whole lifecycle of buildings.

4. Limited building LCA studies have considered uncertainties in the various lifecycle phases of buildings. Moreover, there are limitation in existing uncertainty assessment methods. The existing quantitative uncertainty assessment methods require large amounts of data which is a challenge in building LCA while qualitative methods are likely to errors due to their subjectiveness. While these have their strengths and weakness under various scenarios, no study has developed a hybrid approach to improve the robustness of uncertainty analysis in building LCA. Moreover, limited studies have explored uncertainties due to the assessment models applied.
5. Few LCA studies have focused on buildings in Ghana and sub-Saharan Africa region. While a few of studies exist, most focus on conventional envelope systems without considerations of novel and suitable envelope systems. Multi-objective optimization approaches are seldom addressed in this research studies.

## CHAPTER 3 RESEARCH DESIGN AND METHODOLOGY FOR BIM-BASED LCA

This chapter details the development of the BIM-based LCA assessment methodology, tier-hybrid uncertainty assessment and BIM-based lifecycle performance optimization approach for buildings.

### 3.1 Integrating BIM for automated building LCA

A BIM-based LCA framework is developed through LCA framework conceptualization, mathematical model formulation, and BIM-based simulation to support an automated LCA of buildings. The methodology design focuses on both conceptualizing and operationalizing the BIM-based method for a systematic whole life cycle which is applicable to a wide range of building architypes. The framework of the proposed BIM-based LCA is illustrated in Fig. 3.1, while details are described in subsections below.

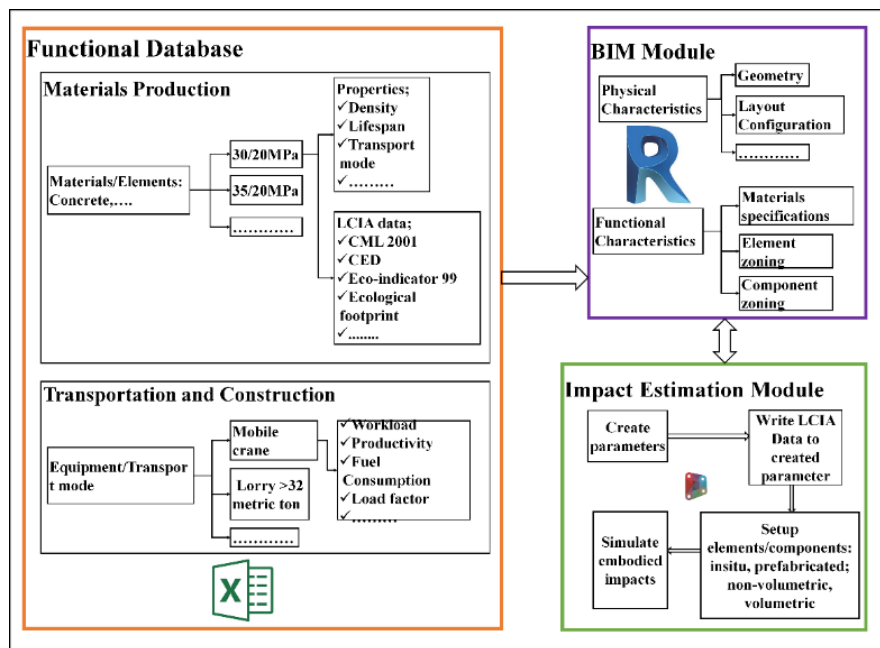


Fig. 3. 1 Framework on BIM-based LCA methodology

Autodesk Revit is selected as the main BIM tool, however, the method is applicable to other BIM tools such as Rhinoceros/Grasshopper and is implemented in other sections.

### 3.1.1 Data repository

The fundamental component of the method is a functional database since LCA implementation is impossible without pertinent data. The functional database includes all a comprehensive material/component library for the scope of study which is Hong Kong and Ghana. The first step is to develop a comprehensive material/component list, followed by the establishment of properties relevant to the assessment of all lifecycle phases. This includes material's density, lifespan, construction/demolition equipment, transportation modalities and lifecycle impact coefficients/factors for various materials or activities. These data are catalogued in relationships (i.e., each material/component with a set of parameters in Excel) so that their retrieval is simplified for subsequent stages. Fig. 3.2 shows a section of the developed database.

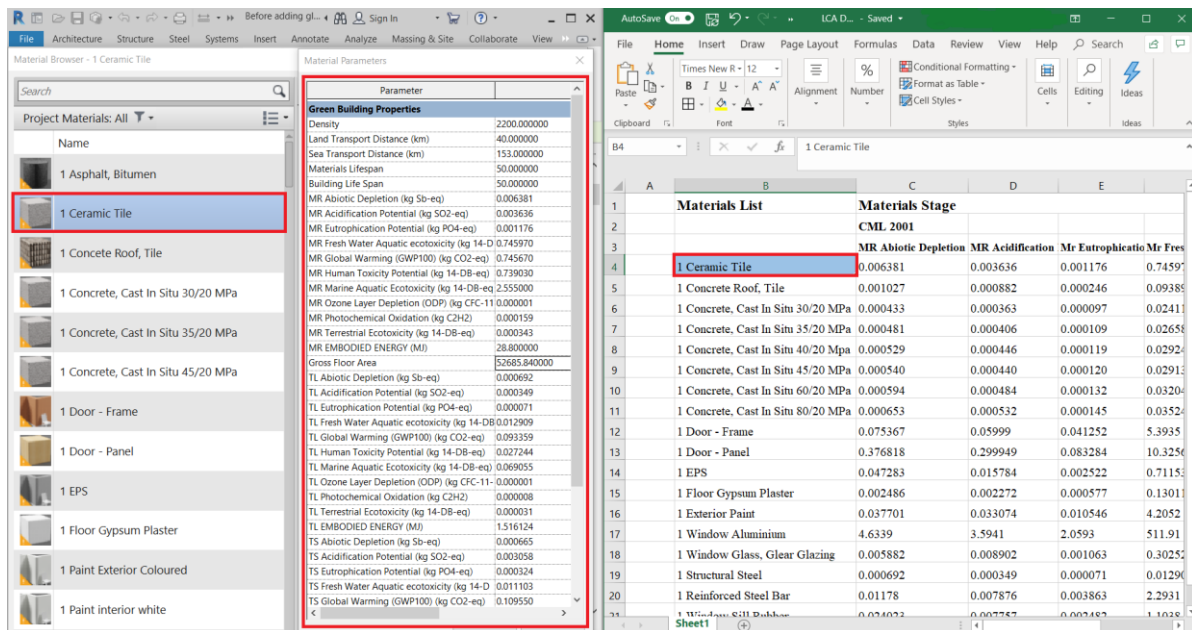


Fig. 3. 2 Developed database and naming convention in the BIM model

LCIA data are sourced from Ecoinvent [156] while supplementary information such as material wastage, and lifespan are sourced from literature. The emission factors were adapted to reflect the particularities of Hong Kong and Ghana by adjusting the transportation distances

and transportation mode with available local data from experts. Furthermore, the fuel mix for electricity production was also adjusted to reflect the electricity production in Hong Kong /Mainland China and Ghana. The established impact assessment data are based on the CML 2001 and CED method.

The material production phase includes the impact of producing materials/components from the extraction of raw materials to the end of manufacturing. For some materials such as concrete and steel, several subcategories are included to account for different strengths or grades. The functional units vary in Ecoinvent so that the database is designed to support conversions between units. Environmental performance data on the transportation phase include three modes of transport (i.e. sea vessels, trucks, and rails) with different loading capacities and distances sourced from [157]. Especially, different loading factors are considered for prefabricated and insitu components. The productivity, workload, fuel consumption of equipment for different work items are also included in this functional database to evaluate the construction phase as sourced from [44]. For the end-of-life phase, the developed database includes the productivity, fuel efficiency, energy conversion factors and environmental impacts of equipment used for the demolishing and transportation to recycling or landfill sites sourced from [158].

A naming convention is adopted to assign a unique ID to each item in the database to facilitate automated matching of data. The database is developed manually in Microsoft Excel. New materials can be easily added using the predefined naming convention.

### **3.1.2 BIM module**

A BIM model is developed which includes physical and functional characteristics [159]. Physical characteristics comprise geometries and layout configurations while functional characteristics include material specifications, element, and component zoning. It is important to establish a consistent modelling workflow to produce an accurate LCA result. The BIM

model must be developed using the same naming conventions in the developed material database as illustrated in Fig. 3.2. It is critical to populating the BIM model with LCA data. Also, all elements must be tagged prefabricated or insitu through a parameter at the instance level. Since the native BIM element classification is not favorable for a prefabricated inventory analysis, a zoning technique is introduced to group composite elements. This technique can be applied to group for instance, concrete and reinforcement bars of a reinforced concrete column. Similarly, the zoning technique can group prefabricated components at volumetric (kitchen/washroom pods) or non-volumetric (façade) levels so that their impacts can be assessed appropriately. This technique is also applied at the flat level with standardized flat designs.

### **3.1.3 Impact estimation module**

The impact estimation module is a computational script using nodes and codes to write the required LCA data to the BIM model, process the data and provide the lifecycle impacts of prefabricated buildings. It is realized in Dynamo/Grasshopper, a built-in computational tool of Autodesk Revit/Rhinoceros, respectively whose unlimited nodes provide endless opportunities to customize tasks and generate desired results. Moreover, support for Python and C# facilitates the development of custom scripts or packages to optimize the workflow. The script is split into parts and executed in chains to increase the computational efficiency and track errors quickly. The steps involved in the impact estimation module are discussed as follows.

The first step is to create parameters for all materials/components to write LCA data from the functional database to the building model. As the database comprises numerous impact assessment methods, this step enables users to select parameters suited to their desired LCIA method. Thereafter, a second interface writes the impact assessment data to the created parameters. Fig. 3.2 also shows a sample of data written to a ceramic material in the Revit library. The naming conventions used in the database is kept for an automatic execution. An

intelligent match of the impact assessment data with the method selected in the previous step is achieved with Structured Query Language (SQL), which queries data such as the impact coefficient from the functional database and writes automatically to created parameters.

The next step involves setting up materials/components and is critical to producing an appropriate prefabricated/insitu inventory. Here, the parameter assigned at the instance level during modelling is used to determine whether an element/component is insitu or prefabricated. A set of constraints is then applied to each element/component, such as transportation modalities including partial loads, types of vehicles or vessels and types of construction equipment. Wastage factors depending on the type of materials and mode of construction are also assigned in this step.

After setting up elements/components, a customized quantity takeoff and impact factors for each lifecycle phase is extracted into Dynamo/Grasshopper. For most parts, the volume of each material is derived from multiplying its area by its thickness while the mass is obtained as a product of its volume and density. For some materials/elements such as rebars and windows, the estimation method is adapted as geometric information extracted from these elements cannot produce an accurate result. The impact assessment is then performed by intelligently matching each material with the appropriate LCA data. Finally, a report containing the embodied impacts of the model is generated in accordance with the various levels of assessments.

The automation process is a major contribution of the developed method which expedites the assessment process in Dynamo/Grasshopper. Originally, many nodes in the designed scripts resulted in longer computational time especially when combined with large number of elements in a high-rise building. To reduce the number of nodes, this study first utilized list management functions and extracted similar parameters with a single node. However, it yielded limited improvement. An effective solution was then proposed to convert nodes into codes and simplify

them in Python wherever possible. This approach reduced the number of nodes and computational time significantly. To track errors, the entire script is first split into stages discussed above and run consecutively in Dynamo Player. At the final stage of the impact assessment, a unique script is run for each level of assessment, reducing the computational time required. Fig. 3.3 illustrates a logic flow diagram for LCA computation.

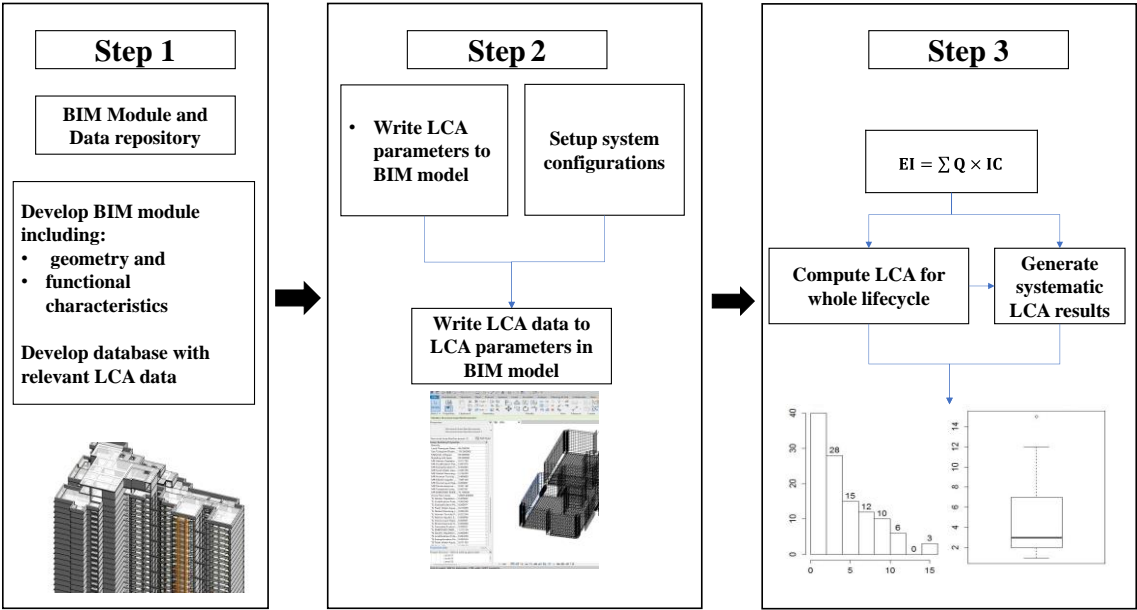


Fig. 3. 3 Logic flow diagram for LCA implementation

**3.1.3.1 Calculation of lifecycle impacts**

A generic model is applied to illustrate the calculation of energy and environmental impacts. This model is applied for all indicators investigated in this study based on the primal rule as shown in Eq. (3.1) [160]:

$$EP = Q \times IC \tag{3.1}$$

where EP, Q, and IC represents the energy or environmental impacts, activity quantity and impact coefficient, respectively. Eq. (3.2) is then expounded to suit different lifecycle phases in the following sections.

$$EP = EI + OI \quad (3.2)$$

where EP is the total lifecycle impacts, EI is the embodied impacts and OI is the operational impacts.

### (1) Embodied impacts

The embodied impacts are defined to include energy uses and carbon emissions from the material production, transportation, construction, building maintenance and end-of-life cycle phases. Thus, the total embodied impacts (EI) are given by Eq. (3.3):

$$EI = EI_m + EI_t + EI_c + EI_{bm} + EI_e \quad (3.3)$$

where,  $EI_m$ ,  $EI_t$ ,  $EI_c$ ,  $EI_{bm}$  and  $EI_e$  represent the impacts from material production, transportation, construction, building maintenance and end-of-lifecycle phases, respectively.

### Material production phase

The impacts from the material production phase include: (i) in-situ and (ii) prefabricated components. In situ components relate to the raw material production only, whereas precast components include the impacts from transporting and manufacturing of precast components in the prefabrication factory.

$EI_m$  from the material production phase is given by Eq. (3.4):

$$EI_m = EI_{mc} + EI_{mp} \quad (3.4)$$

where  $EI_{mc}$  is the impact from the production of in situ elements; and  $EI_{mp}$  is the impact from precast elements.  $EI_{mc}$  from the production of in situ materials is given by Eq. (3.5):

$$EI_{mc} = \sum_{i=1}^n Q_p (1 + w_f) \times IC_p \quad (3.5)$$

where  $n$  is the number of different building materials  $i$ ;  $Q_p$  is the quantity of materials;  $W_f$  is the wastage factor and  $IC_p$  is the impact coefficient.  $EI_{mp}$  from the production of prefabricated components is given by Eq. (3.6) :

$$EI_{mp} = EI_{mp1} + EI_{mp2} + EI_{mp3} \quad (3.6)$$

where  $EI_{mp1}$ ,  $EI_{mp2}$ , and  $EI_{mp3}$  represent the impacts generated from material production, transportation to factory and manufacturing of prefabricated components, respectively.  $EI_{mp1}$  from the material production of prefabricated components is expressed by Eq. (3.7):

$$EI_{mp1} = \sum_{c=1}^m \sum_{i=1}^n Q_t \times IC_p \quad (3.7)$$

where  $Q_t$  is the quantity of each material  $i$  used in precast component  $c$ ;  $m$  and  $n$  are the total number of precast components and materials, respectively;  $IC_p$  is the impact coefficient for material  $i$ .  $EI_{mp2}$  from the transportation of materials to the prefabrication factory is expressed by Eq. (3.8):

$$EI_{mp2} = \sum_{i=1}^n Q_t \times IC_t \quad (3.8)$$

where  $Q_t$  is the quantity of material  $i$  (ton.kilometer) to be transported to a prefabrication factory;  $IC_t$  is the impact coefficient for the transport mode.

$EI_{mp3}$  from manufacturing of prefabricated components is expressed by Eq. (3.9):

$$EI_{mp3} = \sum_{e=1}^f \sum_{c=1}^m Q_{p,c} \times E_{p,e} \times IC_{p,e} \quad (3.9)$$

where  $Q_{p,c}$  is the production volume of prefabricated component  $c$ , which requires energy type  $e$ ;  $E_{p,e}$  is the mass of energy for the production of the unit volume of  $c$ ;  $IC_{p,e}$  is the impact coefficient of the energy type  $c$ ;  $f$  and  $m$  represent the total number of energy types and precast components respectively.

### **Transportation phase**

The impacts generated from transportation consist of the total energy use and emission incurred from delivering insitu materials and prefabricated components via different modes of transportation.  $EI_t$  from transportation is given by Eq. (3.10):

$$EI_t = \sum_{p=1}^x \sum_{o=1}^y Q_t \times IC_{t,m} \times l_f \quad (3.10)$$

where  $Q_t$  is the quantity of material/element/assembly  $o$  (ton.kilometer) to be transported by method  $p$ ;  $IC_t$  is the impact coefficient for transportation mode  $p$ ;  $l_f$  is the load factor;  $x$  and  $y$  are the total transportation modes and materials/components, respectively.

### **Building construction phase**

The impacts from the building construction phase consist of energy use and emissions from onsite construction equipment. Major on-site construction equipment includes the tower crane, truck-mounted crane, truck-mounted concrete pump, hoist, and forklift.  $EI_c$  from construction is given by Eq. (3.11):

$$EI_c = \sum_{q=1}^z \sum_{w=1}^v Q_c \times E_{p,e} \times IC_{c,e} \quad (3.11)$$

where  $Q_c$  is the amount of work  $w$  which uses equipment type  $q$ ;  $E_{p,e}$  is the mass of energy used by equipment type  $q$  for work  $Q_c$ ;  $IC_{p,e}$  is the impact coefficient of energy type  $E_{p,e}$ ; and  $z$  is the total number of equipment for work type  $w$ . The building construction data are sourced from relevant research studies and a consultancy study on building LCA by the Electrical and Mechanical Service Department in Hong Kong [44,161].

### **Building maintenance phase**

The energy uses and emissions from maintenance are estimated according to the reference service life of building materials and components. It is assumed that periodic maintenance activities including painting, rendering, replacement of windows are performed as the service building life exceeds those of some materials. In such scenarios, the differences are

addressed as recurrent materials using replacement factors sourced from relevant literatures [162–164].

$EI_{bm}$  from the building maintenance phase is given by Eq. (3.12):

$$EI_{bm} = \sum_{i=1}^n [(Q_p \times R_f) \times (1 + W_f)] \times IC_p \quad (3.12)$$

where  $n$  is the number of different building materials or prefabricated component  $i$  used for repairs or replacement;  $Q_p$  is the quantity of materials or prefabricated components;  $R_f$  is the replacement factor;  $W_f$  is the wastage factor and  $IC_p$  is the impact coefficient.

### **End-of-life phase**

The end-of-life phase includes energy and emissions related to building demolition and transportation for landfills or recycling. It is assumed that an excavator, a wheel loader and trucks are used for demolishing and transportation. Each material is considered for recycling or landfills and the net impact is estimated based on whether it joins other processes or exits the material flow completely. Based on the practice in Hong Kong [165], it is assumed that steel is recycled while concrete and other non-inert materials such as wood, glass and plastics are sent to public landfills. It is assumed that only half of steel used in the building is recovered. Thus, after demolition, half of steel used in the building is recovered while all other materials are landfilled. The impact of the end-of-life phase ( $EI_e$ ) is given by Eq. (3.13):

$$EI_e = \sum_{i=1}^g Q_r \times (E_{ee} - E_{re} - E_t) \quad (3.13)$$

where  $Q_r$  represents the percentage of total material  $i$  to be recycled or landfilled;  $E_{ee}$  represents the impact coefficient of the material  $i$ ,  $E_{re}$  represents the impact incurred in demolishing process;  $E_t$  is the impact incurred from transporting materials from the demolishing site to the landfill or recycling plant; and  $g$  is the total number of materials to be demolished.

### **(2) Building operation phase**

The operational impact consists of energy and emissions from building operation (i.e. cooling, cooking, daily hot water, lighting, and other appliances) for a 50 year reference study period which is equal to the service life of the case building. Building system and occupancy schedules are used to calculate occupational heat gains and operational energy demands. Emission factors are then applied to calculate the total emission during the operation phase. The impacts from building operation (OI) are given by Eq. (3.14):

$$OI = \sum_{e=1}^f \sum_{l=1}^u Q_{bo} \times IC_{c,e} \quad (3.14)$$

where  $Q_{bo}$  is the quantity of activity  $l$  which requires the energy type  $e$ ; and  $u$  is the total number of activities during the operation phase of the building.

### **3.2 Evaluating uncertainties in the life cycle of buildings**

A tier-hybrid approach is developed to stochastically evaluate and quantify parameter uncertainties in the lifecycle assessment of buildings while scenarios are used to evaluate model and scenario uncertainties in the lifecycle of buildings. The uncertainty analysis focuses on embodied impacts and excludes those from the operation phase such as lighting and air-conditioning, which have been widely addressed in existing literature. Figs. 3.4 and 3.5 illustrate the framework and flow chart of the uncertainty analysis, respectively.

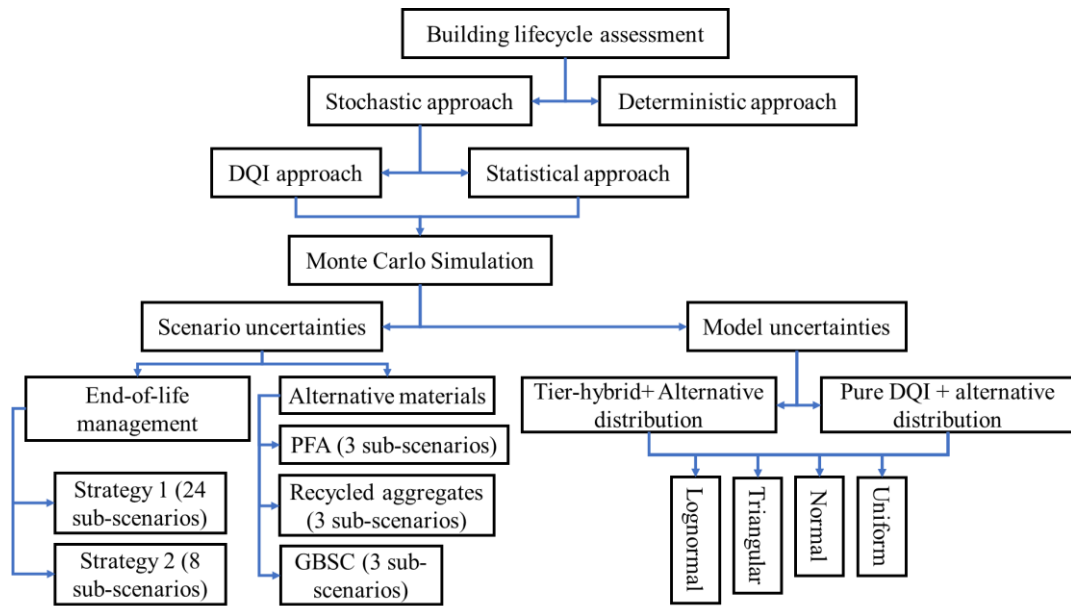


Fig. 3. 4 Methodological framework for uncertainty analysis

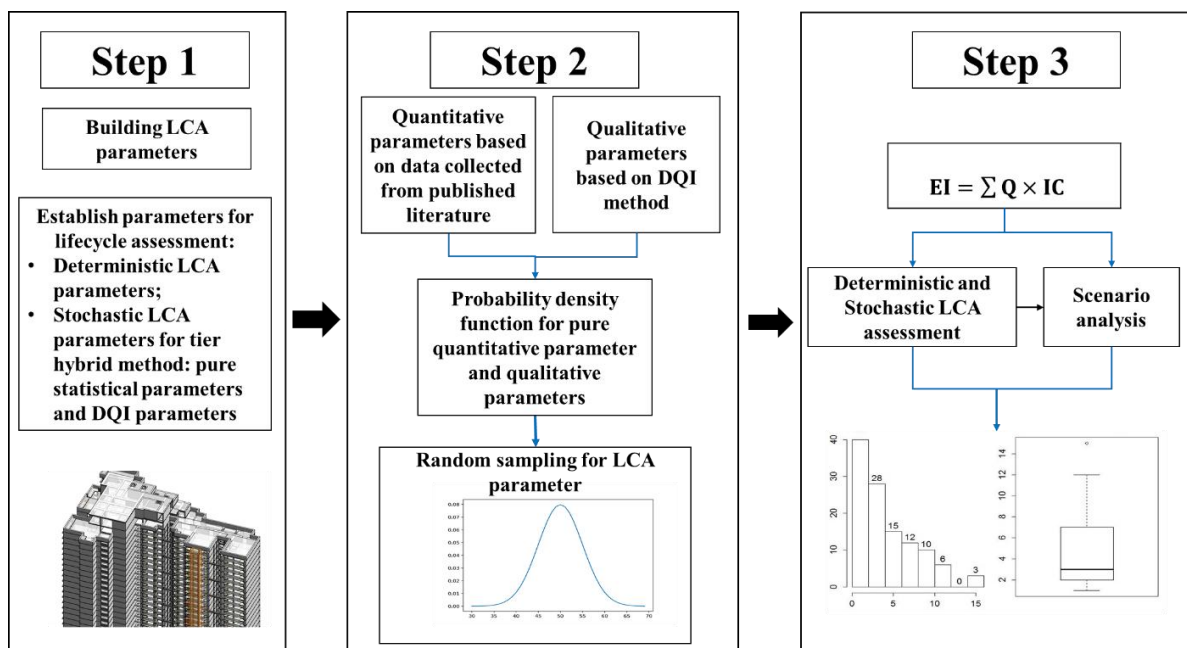


Fig. 3. 5 Flow chart for uncertainty analysis

### 3.2.1 Tier-hybrid stochastic analysis

Uncertainties occur due to the lack of knowledge on the true value of a parameter. Normally, statistical approaches are used to determine a likely value when there is a sufficient

amount of data points/observations. However, the nature of building LCA decreases the feasibility of collecting many observations. This is the results of a limited number of LCA databases coupled with a lack of data on the embodied coefficients of some materials within these databases. To address this limitation, Weidema et al. [166] proposed a DQI-based method which applies expert judgement to appraise the probable distribution of uncertainty parameters. However, subjective evaluation can reduce the validity of a pure DQI-based assessment. This research therefore proposes a tier-hybrid approach to improve the comprehensiveness and reliability of evaluating uncertainties in building LCA. The proposed approach follows a two-stage process: uncertainty characterization and uncertainty propagation.

### **3.2.1.1 Uncertainty characterization**

Uncertainty characterization is implemented to determine the probability distribution of uncertainties in a parameter. The developed tier-hybrid approach is based on the integration of: (i) a pure statistical method and (ii) a DQI method prior to uncertainty propagation. Table 3.1 illustrates the sources of parameter uncertainties and the characterization approach used. The pure statistical approach is applied when a sufficient number of datapoints could be retrieved to determine the probability distribution of the parameter. In the case where sufficient amount of data could not be collected, the DQI approach is implemented. For the statistical approach, data such as material densities and waste rates are retrieved from literature, websites and reports of manufacturers. Statistical methods are then applied to determine parameters such as the mean and standard deviation (SD) which are applied to characterize uncertainties of the retrieved data. The results of uncertainty characterization for pure statistics parameters are summarized in Appendix 2.

The DQI approach used is based on the method of Ecoinvent which categorize parameter uncertainties into basic and additional uncertainties expressed in terms of variance (Weidema et al. [166]). Basic uncertainties reflect the lack of knowledge on the exact value of

a parameter (i.e. inconsistency in measurements) and additional uncertainties express imperfections in data (e.g. geographical and temporal variations). The total uncertainty is derived as a sum of basic and additional uncertainties. Ecoinvent provides a default variance ( $\sigma_b^2$ ) for basic uncertainties based on expert judgement. Contrarily, additional uncertainties ( $\sigma_{a,i}^2$ ) is estimated using a semi-qualitative approach incorporating a pedigree matrix with representative variances specified by Data quality guideline for Ecoinvent. [166]. As shown in Table 3.2, this pedigree matrix includes five data quality indicators. For each indicator, a score between 1 (highest quality data) and 5 (lowest quality data) is assigned. After determining the scores of an uncertainty parameter, representative variances with lognormal distributions are defined using Table 3.3. The results of DQI analysis are presented in Appendix 1.

The total variance for the parameter is then estimated using Eq. (3.15):

$$\sigma_t^2 = \sigma_b^2 + \sum_{i=1}^5 \sigma_{a,i}^2 \quad (3.15)$$

To extend the transformational relationship to other probabilistic distributions, the variance is converted to coefficient of variation (CV) using Eq. (3.16):

$$CV = \sqrt{\exp(\sigma^2) - 1} \quad (3.16)$$

Table 3. 1 Uncertainty parameters and assessment methods

<b>Parameter</b>	<b>Classification of uncertainty</b>	<b>Assessment method</b>
Material quantities	Parameter uncertainty	DQI and Monte Carlo simulation
Material densities	Parameter uncertainty	Statistical and Monte Carlo simulation
Onsite construction processes	Parameter uncertainty	DQI and Monte Carlo simulation
Building maintenance schedule	Parameter uncertainty	DQI and Monte Carlo simulation
Material waste rate	Parameter uncertainty	Statistical and Monte Carlo simulation

<b>Parameter</b>	<b>Classification of uncertainty</b>	<b>Assessment method</b>
Transportation distances	Parameter uncertainty	Statistical and Monte Carlo simulation
Energy and emission factors	Parameter uncertainty	DQI and Monte Carlo simulation
Uncertainty model	Model uncertainty	Statistical and Monte Carlo simulation

Table 3. 2 Data quality pedigree matrix

<b>Score</b>	<b>Data quality indicators</b>				
	<b>Reliability</b>	<b>Completeness</b>	<b>Temporal correlation</b>	<b>Geographical correlation</b>	<b>Further technological correlation</b>
<b>1</b>	Verified data based on measurements	Representative data from relevant parties over an adequate period	< 3 years	Field data	Data from enterprises, processes and materials under study
<b>2</b>	Verified data partly based on assumptions	Representative data from >50% of relevant parties over an adequate period	< 6 years	Data from similar area	Data from processes and materials under study
<b>3</b>	Unverified data partly based on	Representative data from <50% of relevant parties	< 10 years	Regional data	Data from processes and materials under study but from different technology

Score	Data quality indicators				
	Reliability	Completeness	Temporal correlation	Geographical correlation	Further technological correlation
	qualified estimates	or >50% but from shorter periods			
<b>4</b>	Qualified estimate	Representative data from only one site relevant party	< 15 years	National data	Data on related processes or materials
<b>5</b>	Unqualified estimate	Unknown representativeness	≥ 15 years	Data from unknown <i>or</i> distinctly different area	Data on related processes or materials but different technology

Table 3. 3 Variance of additional uncertainties

Data quality indicator	Score				
	1	2	3	4	5
Reliability	0.000	0.0006	0.002	0.008	0.04
Completeness	0.000	0.0001	0.0006	0.002	0.008
Temporal correlation	0.000	0.0002	0.002	0.008	0.04
Geographical correlation	0.000	$2.5 \times 10^{-5}$	0.0001	0.0006	0.002
Further technological correlation	0.000	0.0006	0.008	0.04	0.12

### 3.2.1.2 Uncertainty propagation

Uncertainty propagation involves propagating input uncertainties to calculate the overall uncertainty in the LCA result. Uncertainty propagation can be performed with an analytical method or a sampling method. The former produces limited results and is thus impractical for this study. On the contrary, the latter is more common and requires lesser computational resources. Accordingly, the Monte Carlo simulation, a sampling method, is chosen to generate sample data from non-linear input uncertainties based on the pure statistical and DQI-based uncertainty characterization.

The Monte Carlo simulation is performed based on the algorithm developed by [167]. Equations 3 to 5 show the parameters and variables used to perform the Monte Carlo simulation in this study. Equation 3 is a vector  $V$  which represents the parameters for the evaluation of each lifecycle phase:

$$V = \{T_1 \dots T_h \dots T_i\} \quad (3.17)$$

where  $i$  represents the total number of processes  $T$  for a given lifecycle phase;  $h$  represents a vector  $F$  with a complete dataset for the stochastic evaluation of the embodied energy  $e$  in the process  $T$ .

For each process  $T$ , random variables can be chosen from the vector  $F$  for the Monte Carlo simulation in accordance with a given probability distribution. Vector  $F$  is given by Eq. (3.18):

$$F_h = \{f_{h,1} \dots T_{h,l} \dots T_{h,i}\} \quad (3.18)$$

The vector  $F$  represents two inputs as the outcome of the uncertainty characterization for the (i) pure statistical approach and (ii) DQI approach.

The two-input data are illustrated by the vector  $Q$  which contains a pair of inputs  $V_h$  and  $U_h$  as shown in Eq. (3.19):

$$Q = \{(V_1, U_1) \dots (V_h, U_h) \dots (V_i, U_i)\} \quad (3.19)$$

In the case of pure statistical parameters,  $V_h$ , and  $U_h$  represent the mean and standard deviation of a normal distribution, whereas they represent the activity quantity and covariance for a lognormal distribution in a DQI-based case.

Different sets of Monte Carlo simulations are performed for different lifecycle stages and scenario analyses. For each simulation, 10,000 samples are generated. Each output generated represents the energy use or carbon emission associated with a lifecycle phase or scenario evaluated with randomly selected input variables.

### **3.2.2 Scenario and model analysis**

Reasonable scenarios and models are utilized to individually appraise decision variables for clearly depicting changes in possible outcomes, while parameter uncertainties are evaluated simultaneously through Monte Carlo simulations. Four scenarios with seven sub-scenarios are defined to explore end-of-life strategies, alternative materials and analytical model assumptions as summarized in Table 3.4.

End-of-life scenarios explore the impact of end-of-life management strategies on the overall lifecycle impacts of buildings. Different combinations of demolishing practices, offsite/onsite waste sorting, recycling and landfilling can significantly vary the contribution of the end-of-life phase to the overall lifecycle impacts. Two strategies are therefore defined: EoL1 and EoL2. EoL1 considers an all-inclusive offsite sorting for demolishing wastes. After sorting, cementitious wastes and non-inert wastes (e.g. wood and paper waste) are disposed at public filling areas and landfills respectively, while steel scrap is recycled. Totally, 24 sub-scenarios are designed using alternative sorting, landfill and public filling areas to explore the impact of

transportation. EoL2 considers a selective demolishing strategy in which wood wastes and aluminum in windows are sorted onsite. The remaining demolishing wastes are sorted offsite. This scenario also considers an extensive recycling approach in which timber and all metals including reinforcement steel, iron and aluminum are recycled. A recovery rate of 90% is applied to recycling materials. Cementitious wastes are however disposed at public filling areas. Totally, 8 sub-scenarios are designed to explore the impacts of transportation.

The use of alternative materials is considered an effective approach to reduce the embodied impacts of buildings as material production, especially concrete, contributes significantly to the lifecycle impact of buildings. Three scenarios are designed to replace virgin aggregates with recycled aggregates and Ordinary Portland Cement (OPC) with Granulated Blast furnace Slag (GBFS) or Pulverized Fly Ash (PFA). S1 explores the impacts of using recycled aggregates in both in-situ and precast concrete. Two sub-scenarios are also defined: sub-scenario 1 assumes that aggregates are recycled at a site with an equal transportation distance to the source of virgin materials whereas sub-scenario 2 assumes a recycling site 15 km away from the production site of concrete. Replacement rates of 50%, 70% and 100% are also explored for S1. S2 and S3 explores impact reduction from the use of GBFS and PFA respectively. Similarly, replacement rates of 50%, 70% and 80% are explored for both GBFS and PFA.

Assumptions about the analytical model is a crucial factor which may significantly change the results. Scenarios M1 and M2 are defined to explore model uncertainties. M1 investigates the impact of the probability distribution assumption on the proposed tier-hybrid method. In the base case (B2), a lognormal distribution is applied to the DQI components. Because other distributions such as normal, triangular and uniform could vary the results significantly, M1 explores the impacts of these distributions within the context of the tier-hybrid approach. M2 however is designed to compare the results of a pure DQI approach to the

proposed tier-hybrid approach. To increase the comprehensiveness of assessments, all four probability distributions are considered in the pure DQI approach as well.

Table 3. 4 Summary of scenarios analysis

Goal	Sub-type	Scenario code	Description
Basic case	Deterministic case	B1	Complete LCA based on primary data collected
	Stochastic case	B2	Complete LCA based on tier-hybrid method
Scenario analysis	End of life Scenario	EoL1	Off-site sorting; non-inert waste disposed at landfills; concrete disposed at public filling areas; scrap recycled ( <i>generating 24 sub-scenarios</i> )
		EoL2	Onsite (waste wood) and offsite waste sorting (concrete and steel, waterproofing, etc.); maximum materials recycling ( <i>generating 8 sub-scenarios</i> )
	Alternative materials	SC1	Use recycled aggregates ( <i>generating 6 sub-scenarios</i> )
		SC2	Replace ordinary Portland cement with blast furnace slag cement ( <i>generating 3 sub-scenarios</i> )
		SC3	Replace ordinary Portland cement with pulverized fly ash ( <i>generating 3 sub-scenarios</i> )

<b>Goal</b>	<b>Sub-type</b>	<b>Scenario code</b>	<b>Description</b>
Model uncertainties	Distribution selection	M1	Normal, triangular and uniform distribution applied to B2
	Pure DQI + distribution selection	M2	DQI only approach with Normal, lognormal, triangular and uniform distribution applied to B2

### **3.3 Multi-objective lifecycle optimization of building**

The developed BIM-based LCA framework is adapted with a multi-objective optimization framework which is based on the premise of jointly exploring the energy, environmental and economic implications of the embodied and operational impacts of buildings. An LCA and LCCA framework is presented which includes, energy use, carbon emission and cost modules. Thereafter, the optimization framework incorporating objective functions, decision variable and optimization algorithm is presented.

The optimization framework is designed to optimize the environmental performance of building design strategies in a cost-effective approach. System boundaries include direct and indirect emissions from material production, maintenance, and operational phases. The transportation, construction and end-of-life phases are excluded from the multi-objective optimization due to the complexities of integrating into the optimization process. Moreover, general strategies like recycling, improved construction processes and shorter haulage distances can be implemented to reduce the impacts of these phases regardless of the type of constructions. Life cycle inventory is performed using a bottom-up approach to quantify the input and output for the range of building constructions and PV installations. Thereafter, the LCA is performed to translate the life cycle inventory to energy and carbon emissions. The

Cumulative energy demand (CED) and Global warming potential (GWP) are selected as the main environmental indicators. The GWP is based on the CML 2001 midpoint method. Other primary data from Ecoinvent are used to supplement the database.

### 3.3.1 Energy evaluation

The CED is formulated as a sum of the operational energy (OE) and the embodied energy (EE) as shown in Eq. (3.20):

$$CED = OE + EE \quad (3.20)$$

Operational energy use is expressed in Eq. (3.21):

$$OE = EUI_{ao} \times L_s \quad (3.21)$$

where  $EUI_{ao}$  is the annual energy use intensity; and  $L_s$  is the building lifespan. The embodied energy (EE) is evaluated using Eq. (3.22):

$$EE = EE_a + EE_z \quad (3.22)$$

where  $EE_a$  and  $EE_z$  represent the initial and recurring embodied energy, respectively.

### 3.3.2 Environment evaluation

The environmental impact is estimated in terms of GWP which represents the amount of carbon emission from the combination of different design strategies. GWP is estimated in Eq. (3.23):

$$GWP = OC + EC \quad (3.23)$$

where OC is the operational carbon emission; and EC is the embodied carbon emission.

Operational carbon emission is expressed in Eq. (3.24):

$$OC = OC_a \times L_s \quad (3.24)$$

where  $OC_{ao}$  is the annual energy use intensity; and  $L_s$  is the building lifespan.

Embodied carbon emission (EC) is expressed using Eq. (3.25):

$$EC = EC_a + EC_z \quad (3.25)$$

where  $EC_a$  and  $EC_z$  represent the initial and recurring embodied carbon, respectively.

### 3.3.3 Economic evaluation

The total life cycle cost of the building is formulated to evaluate the economic implication of the design strategies. The fundamental principle underlying this assessment approach is that a higher initial cost in terms of envelope construction and PV installation can reduce the overall lifecycle cost. The total LCC is illustrated by Eq. (3.26):

$$LCC = IC + d.PC \quad (3.26)$$

where IC is the initial investment cost of the building including building and PV materials, as well as equipment and installation; and d.PC is the net present value of periodic costs which include annual electricity consumption and periodic maintenance.

The net present value of periodic cost is evaluated using Eq. (3.27):

$$d.PC = \left( OP \times \frac{(1+r)^n - 1}{r(1+r)^n} \right) + \sum_k \left( MC \times \left( \frac{1}{(1+r)^k} \right) \right) \quad (3.27)$$

where  $OP$  is the annual energy cost during the operational phases;  $MC$  is the periodic maintenance cost of building and PV installation  $k$ ;  $r$  is the interest rate (9.6%); and  $n$  is the year. The cost of building constructions and PV installation are provided in Tables 3 to 7 of the appendix. The cost of electricity per kWh is \$0.046.

### 3.3.4 Multi-objective optimization

The multi-objective optimization is formulated considering the objective functions, design variables and optimization algorithm. The objective functions are developed in line with the main objective of the study which is to reduce energy use and carbon emission in a cost-effective approach, hence three objective functions are considered in the study. The objective functions are illustrated by Eq. (3.28):

$$\min\{f_1(\partial)\} \{f_2(\partial)\} \{f_3(\partial)\} = [x_1, x_2, \dots x_m] \quad (3.28)$$

where  $f_1$ ,  $f_2$ , and  $f_3$  represents the three objective functions to be minimized (total energy use, carbon emission and cost); and  $x_1$ ,  $x_2$ , and  $x_m$  represents the design optimization variables.

The final optimal solution is selected by normalizing and weighting the Pareto front using Eq. (3.29):

$$NV = \frac{(Z-Z_{min})}{Z_{max}-Z_{min}} \quad (3.29)$$

where NV is the normalized values of CED, GWP or cost of the Pareto front; Z is a value of CED, GWP, or cost in the Pareto front to be normalized,  $Z_{min}$  is the minimum value of CED, GWP or cost of the Pareto front; and  $Z_{max}$  is the maximum value of CED, GWP or cost of the Pareto front.

### 3.3.5 Optimization algorithm

NSGA-II is a metaheuristic genetic algorithm based on natural selection for solving the optimization problem in this study. NSGA-II is selected because of its enhanced computational efficiency, crowding distance method to maintain population diversity and enhanced probability to create better solutions based on elitism which maintains the best solutions for the next generation [168–170]. The optimization problem is solved with Wallacei, an evolutionary engine used to run simulation in parametric design tool Grasshopper 3D. The parameters for

setting up NSGA-II are defined in accordance with the number of variables as illustrated in [170]. Table 3 shows the NSGA-II parameters for the optimization problem. The maximum number of generations is often used as a termination criterion. However, it has to be large enough to ensure convergence but not excessive to prolong computational time. Therefore, the influence of optimization settings is examined to ensure convergence within a reasonable computational time.

Table 3. 5 Optimization settings

<b>Parameter (NSGA-II)</b>	<b>Value</b>
Population size	50
Maximum number of generations	100
Crossover	0.9
Mutation probability	0.1

**3.3.6 Scenario analysis for confounding factors and climate change**

Scenario analyses are used to model the impact of confounding factor and climate change on the overall performance of the building. The climate change scenario analysis is grounded on the premise that the four representative concentration pathways (RCPs) require different mitigation efforts from the built environment whose energy use is influence by increasing temperatures. Particularly, the scenarios integrate reduction in embodied impacts through increased construction process efficiency in the future as a core component towards achievement of carbon neutrality. Therefore, the scenarios explore the whole lifecycle impacts of buildings constructed after each decade in order to visualise the relationship between future embodied energy reduction and carbon neutrality of buildings.

### 3.3.6.1 Confounding factors

Confounding factors can be defined as variables with potential influence on the performance of buildings but outside the scope of designers [171,172]. Previous studies investigated the impacts of design variable without considerations for confounding factors. However, wide variation of confounding factors can lead to significantly higher or lower performances [173]. Hence, it is necessary to investigate the impacts of confounding factors. Few studies have identified confounding factors such as the building age, building size, building system loads, urban context, occupancy rate and energy efficiency upgrades [171,174–176]. These factors induce high levels of uncertainty and can increase the uncertainty in evaluating building energy use and carbon emissions. Two changes are applied to perform scenario analyses: (i) low case and (ii) high case. In the low case, lighting density, equipment load, occupancy load, ventilation rate and occupancy activity levels are reduced by 50% off the baseline case whereas in the high case they are increased by 50%. The scenario analysis is summarized in Table 3.6.

Table 3. 6 Scenarios for confounding factors

<b>Item</b>	<b>Low level</b>	<b>Medium level</b>	<b>High level</b>
Lighting density	7.5 W/m <sup>2</sup>	15 W/m <sup>2</sup>	22.5 W/m <sup>2</sup>
Equipment Load	5 W/m <sup>2</sup>	10 W/m <sup>2</sup>	15 W/m <sup>2</sup>
Ventilation rate	0.001	0.0035	0.006
Occupancy gain	80 W/person	160 W/person	240 W/person
Occupancy density	0.02 m <sup>2</sup> /person	0.04 m <sup>2</sup> /person	0.06 m <sup>2</sup> /person

### 3.3.6.2 Climate change

Climate change is a widely recognized global issue which requires immediate mitigation strategies in order to safeguard the ecosystem and built environment. In attempts to limit the

emission of anthropogenic greenhouse gases, Intergovernmental Panel on Climate Change (IPCC) adopted RCPs as a greenhouse concentration trajectory used for climate modelling in the IPCC fifth Assessment Report (AR5) (IPCC, 2014). These RCPs represent different time-dependent trajectories dependent on the level of greenhouse gas emissions. RCPs include a rigorous mitigation scenario (RCP 2.6), two intermediate scenarios (RCP 4.5 and RCP 6.0) and a scenario with extremely high GHG emissions (RCP 8.5). RCP 2.6 represents a scenario with the goal to maintain the global average temperature within 2° of preindustrial levels. In order to keep global temperatures within habitable levels, mitigation strategies geared towards the reduction of carbon emissions should be implemented in the built environment, whose energy and carbon performances are also influenced by increasing temperatures. Hence it is necessary to investigate the impact of climate change on building design optimizations and the possible trajectories of building energy use and carbon emissions.

Four scenarios, each with four sub scenarios, are applied to model the impact of climate change on building performances: RCP 2.6, RCP 4.5, RCP 6.0, and RCP 8.5. Under each scenario: (i) weather data is modified to reflect changes in projected outdoor air temperatures and (ii) representative mitigation strategies are implemented. Stringent to moderate strategies are applied to RCP 2.6, RCP 4.5, and RCP 6.0 whereas no strategy is applied to RCP 8.5. Modifications to weather data are based on a study which modelled mean temperature anomalies based on RCP scenarios [177]. Four weather files are generated for each RCP scenario to model operational impacts of buildings construct after each decade within 2030 to 2070. Temperature within 2020 and 2029 are applied as the baseline model. Two mitigation strategies are applied to perform the climate change scenario analysis: (i) improved efficiency of construction process and (ii) use of renewable energy sources. According to the 2020 global status report for building and construction, about 6% reduction in building sector emission is required each decade to meet net-zero carbon emission target by 2050 [178]. In line with this,

RCP2.6 is defined to implement 6% improvement in construction process efficiency each decade and complete transition of grid electricity to renewable energy sources for operational energy use. RCP 4.5 represents a scenario with 2% improvement in construction process efficiency each decade and 40% renewable energy. RCP 6.0 represent a scenario with 4% improvement in construction process efficiency and 50% renewable energy. RCP 8.0 mirrors a scenario no improvement in construction process and no renewable energy application. The scenario analysis is summarized in Table 3.7.

Table 3. 7 Scenarios for climate change

<b>Scenario</b>		<b>2030- 2039</b>	<b>2040-249</b>	<b>2050- 2059</b>	<b>2060- 2069</b>	<b>Renewable energy</b>
RCP 2.6	Mean temperature increase	1.04	1.24	1.32	1.35	100%
	Construction efficiency	6%	12%	18%	24%	
RCP 4.5	Mean temperature increase	1.1	1.36	0.162	0.182	40%
	Construction efficiency	2%	4%	6%	8%	
RCP 6.0	Mean temperature increase	0.74	1.01	1.2	1.46	50%
	Construction efficiency	4%	8%	12%	16%	
RCP 8.5	Mean temperature increase	1.17	1.58	2.11	2.57	0%

<b>Scenario</b>		<b>2030- 2039</b>	<b>2040-249</b>	<b>2050- 2059</b>	<b>2060- 2069</b>	<b>Renewable energy</b>
	Construction efficiency	0%	0%	0%	0%	

### 3.4 Summary

This chapter presented the research methodology for developing a BIM-based LCA Approach for Cost-effective Lifecycle Optimization. The design methodology incorporates a BIM-based LCA model, uncertainty assessment model and design optimization framework. The developed through LCA framework conceptualization, mathematical model formulation, and BIM-based simulation to support an automated LCA of buildings. The methodology design focuses on both conceptualizing and operationalizing the BIM-based method for a systematic whole life cycle which is applicable to a wide range of building architypes. In addition, a tier-hybrid uncertainty assessment approach is proposed which leverages both quantitative and qualitative uncertainty to quantify uncertainties in building improve the comprehensiveness and reliability of evaluating uncertainties in building LCA. The developed tier-hybrid approach is based on the integration of a pure statistical method and a DQI method prior to uncertainty propagation through Monte Carlo simulations to stochastically evaluate uncertainties in building LCA. Following, the uncertainty evaluation model, multi-objective optimizations methods are presented which include a staged optimization and a wholistic optimization framework. The staged optimization centers on the different lifecycle stages to explore the tradeoff between embodied and operational impacts whereas the wholistic optimization framework focus on the whole lifecycle to improve energy and carbon performance in a cost-effective approach.

## **CHAPTER 4 SYSTEMATIC BIM-BASED LCA OF A TYPICAL PREFABRICATED HIGH-RISE BUILDING**

LCA is automated to provide deep insights of the life cycle energy and environmental performances of a case study building under the subtropical climate of Hong Kong. This chapter highlights results of an inventory of materials/components and the lifecycle impacts through the studied indicators. Important findings are presented and analysed at different levels of assessments with unique functional units and system boundaries.

### **4.1 Modelling the embodied impacts of a prefabricated high-rise building**

The developed BIM-based LCA method is applied to a prefabricated residential building in Hong Kong. The selected case study can represent the general characteristics of most newly constructed public rental housing. The case building has 40 floors with a single floor height of 2.75 m. It features a reinforced concrete structure with 40% precast elements including precast façades, slabs, connecting slabs, kitchen/bathroom pods, stairs and refuse chutes. The building is modularly designed and contains standardized assemblies and 24 standardized flats (i.e., 7 two-person-three-person flat (2P3P), 12 one-bedroom flat (1B) and 5 two-bedroom flat (2B)) on each typical floor. Fig. 4.1 illustrates the standardized flats and some precast components used in the building. The floor plan and BIM model are shown in Fig. 4.2 while the main characteristics are provided in Table 4.1. The gross floor area (GFA) and total building height are 52685.50 m<sup>2</sup> and 130 m, respectively. A 50-year lifespan is uniformly specified for all assessments while system boundaries and functional units vary with assessment/prefabrication levels as per Table 4.2. The BIM model of the case building is developed in Autodesk Revit. After creating necessary parameters and applying zoning techniques, the rest of the assessment process is automated in Dynamo player. Subsequent runs after initializing the model take three minutes on average, indicating a high computational efficiency.

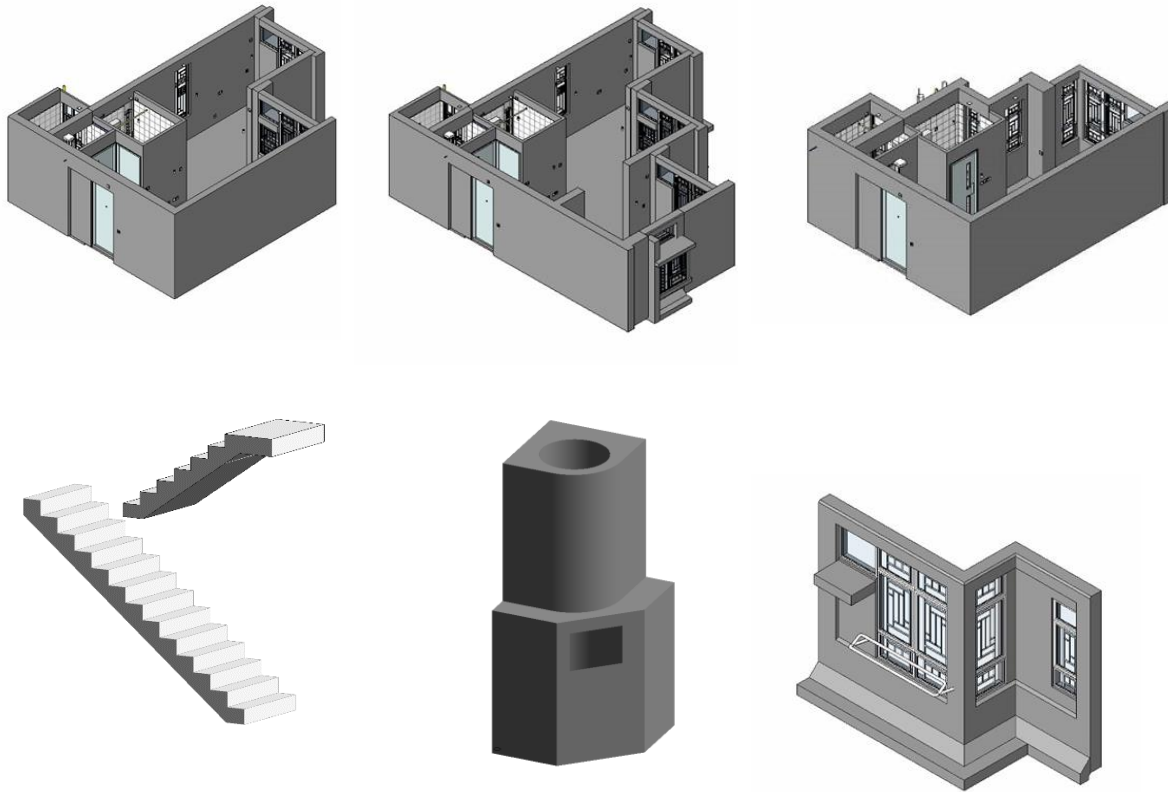


Fig. 4.1 Modular flats and samples of prefabricated components used in Hong Kong public residential buildings

Table 4.1 Characteristics of case building

<b>Building parameter</b>	<b>Specification</b>
Floor height	2750 mm
GFA	52685.50 m <sup>2</sup>
Number of floors	40
Number of units	960
Structure	Reinforced concrete, precast units
Level of prefabrication	40%

<b>Building parameter</b>	<b>Specification</b>
Walls	200 mm or 250 mm Structural cast-insitu concrete walls with steel reinforcement, cement sand plaster, paint finish  Precast façades
Upper floor slabs	70 mm precast slabs, 90 mm cast-in-situ concrete
Openings (Doors and Windows)	Hollow core hardwood doors with hardwood frame and metal fixtures  Aluminum framed windows with 6 mm clear float glazing
Lifespan	50 years

Table 4. 2 Assessment level, system boundary and functional units used in this study

<b>Assessment level</b>	<b>System boundary</b>	<b>Functional equivalent</b>
Whole building level	Cradle to end-of-life phase	Gross Floor Area · year (m <sup>2</sup> ·y)
Flat levels	Cradle to end of construction phase	Gross Floor Area · year (m <sup>2</sup> ·y)
Assembly level (bathroom pods; façades; kitchen pods; refuse chutes)	Cradle to gate	Unit · year (u·y)
Component level (Beams; Columns; Doors; Floors; Stairs; Refuse chutes; Roof; Walls; Windows)	Cradle to end-of-life phases	Unit · year (u·y)

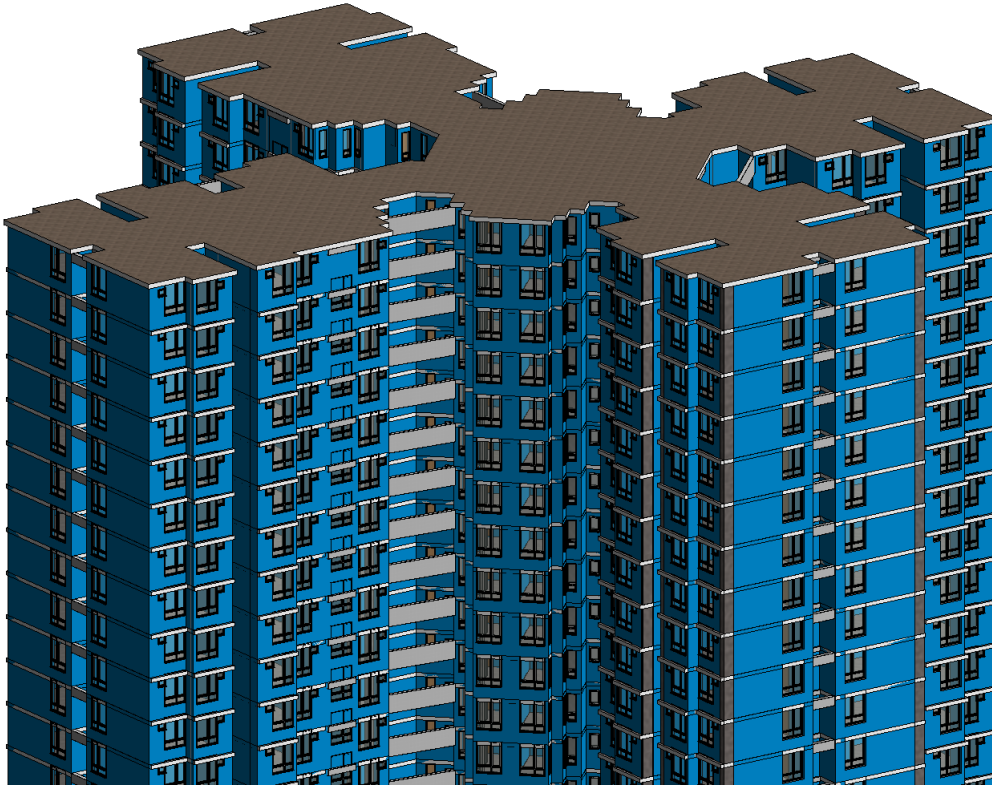


Figure 4.2a BIM Model

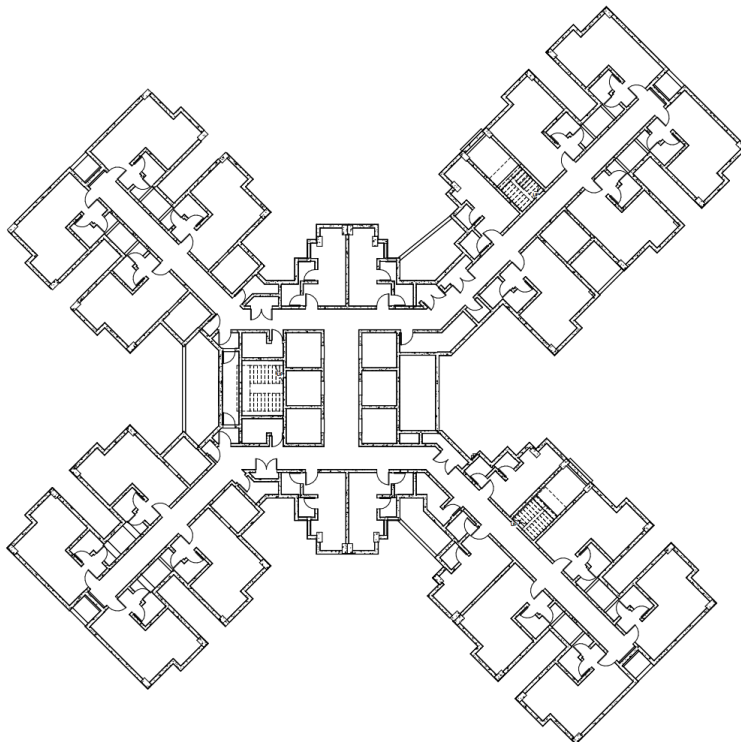


Figure 4.2b Floor plan

Fig. 4. 2 Floor plan and 3D BIM Model of case building

## 4.2 Profile of inventory

The developed BIM-based LCA method produced a profile of materials/components used in the case building. Table 4.3 summarizes the inventory of precast elements and in situ materials by weights. The inventory of materials and precast elements includes waste generation using waste factors of materials and components sourced from literature [179–182]. Cementitious materials and steel dominate the material inventory which is a common trend for buildings in China [183]. The total weight of building materials is 78,102,203.00 kg or 1,482.41 kg/m<sup>2</sup>, where precast components and materials used on site contribute 40.27% (558.05 kg/m<sup>2</sup>) and 59.73% (885.52 kg/m<sup>2</sup>), respectively. Splitting between materials used on site, in-situ concrete contributes 48.59% (702 kg/m<sup>2</sup>) followed by cement plaster 4.38% (64.92 kg/m<sup>2</sup>), steel reinforcement in in-situ concrete 2.95% (43.70 kg/m<sup>2</sup>), timber 2.38% (35.32 kg/m<sup>2</sup>), ceramic tiles 0.98% (14.47 kg/m<sup>2</sup>), glass 0.23% (3.36 kg/m<sup>2</sup>), stainless-steel and others 0.19% (2.86 kg/m<sup>2</sup>), paint 0.04% (0.53 kg/m<sup>2</sup>), and asphalt 0.01% (0.05 kg/m<sup>2</sup>).

Table 4. 3 Inventory of materials/elements

<b>Material</b>	<b>Element/Component/Assembly</b>	<b>Quantity (tons)</b>	<b>Waste factor</b>
Aluminum	Windows frames	22.125	1.05
Asphalt	Damp-proof; roof covering	2.7	1.05
Cement plaster	Beams; columns; facades; bathroom/kitchen pods; structural walls; floors; ceiling	3420.177	1.10
Ceramic tiles	Walls; slabs	762.375	1.10
Glass	Windows	177	1.025

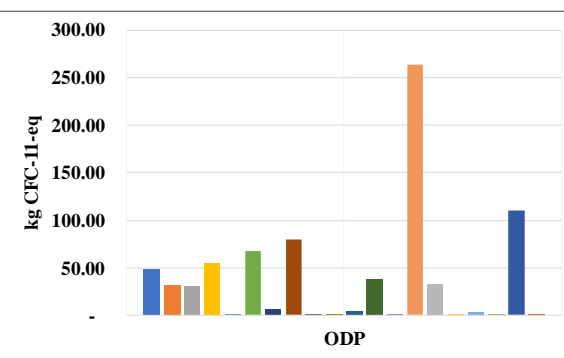
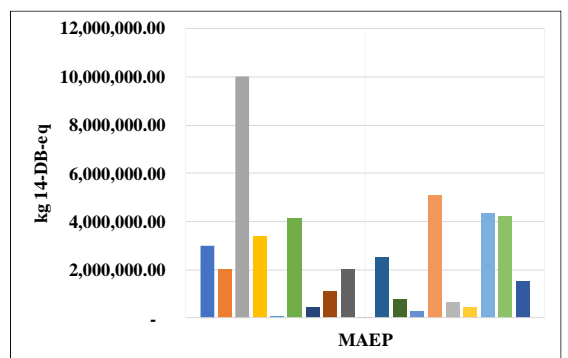
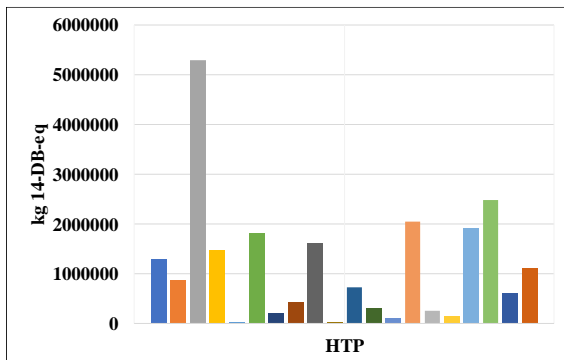
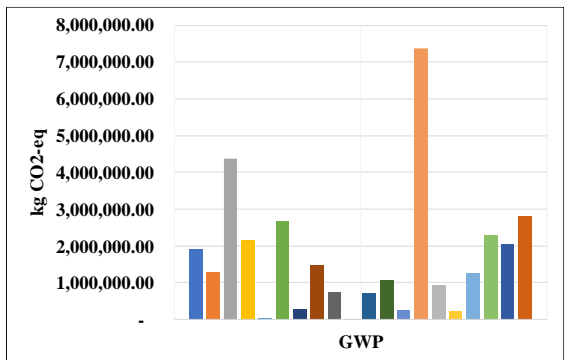
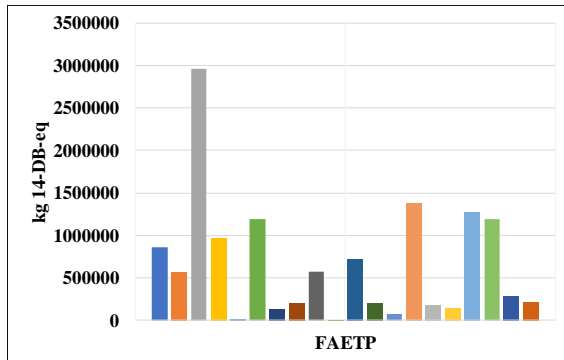
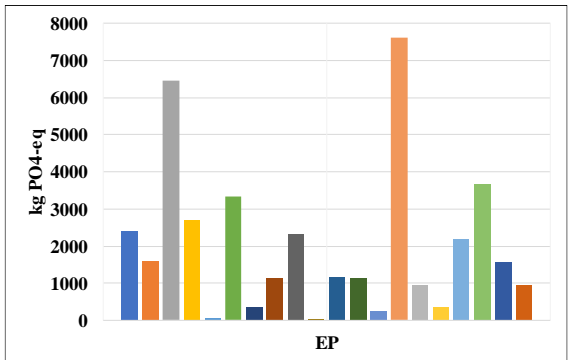
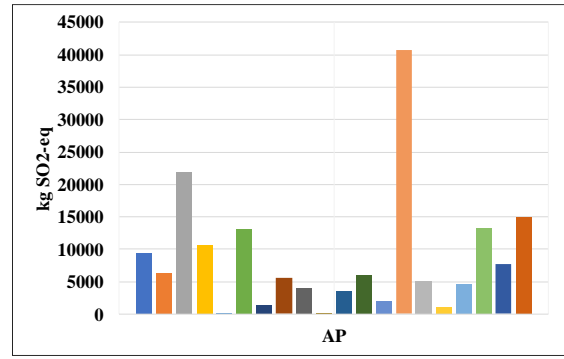
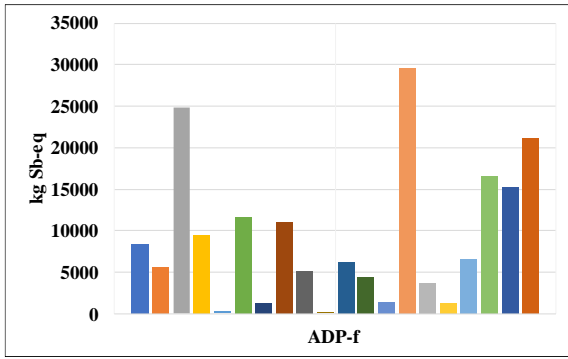
<b>Material</b>	<b>Element/Component/Assembly</b>	<b>Quantity (tons)</b>	<b>Waste factor</b>
In-situ concrete	Beams; columns; structural walls; slabs; roof	35,949.98	1.05
Paint	Beams; columns; facades; bathroom/kitchen pods; structural walls; floors; ceiling	28.08	1.05
Steel reinforcement in in-situ elements	Beams; Columns; Structural walls, roofs	2302.256	1.03
Steel reinforcement in precast elements	Façades; staircases; refuse chute; kitchen/bathroom pods; slabs; connecting slabs; beams	2024.75	1.01
Stainless-steel	Metal doors; windows; metal grills etc.	150.76	1.03
Timber	Doors; formwork	1860.75	1.07
Precast concrete	Façades; staircases; refuse chute; kitchen/bathroom pods; slabs; connecting slabs; beams	28,701.25	1.01

### 4.3 Embodied impacts at the whole building level

The overall embodied impacts in GWP and CED are 12.85 kg CO<sub>2</sub> eq/m<sup>2</sup>·year and 0.16 GJ/m<sup>2</sup>·year. This estimate includes all impacts from material extraction, transportation to site/factory-to-site, onsite construction processes and end-of-lifecycle. For clarity and

comparison with previous studies, GWP and CED are highlighted in the analysis and discussion. Considering different lifecycle phases, material and component production contributes the highest impact in both GWP and CED (76.98% and 80.22%), followed by transportation (10.01% and 9.07%), onsite construction (7.96% and 7.19%) and finally the end-of-life phase (5.05% and 4.58%). Transportation of precast components contributes up to 50% of the transportation impact due to partial loads and long hauling distances [184,185]. This validates the need to establish prefabricated factories in closer proximity to construction sites.

Fig. 4.3 depicts the contribution of each material and precast component to the embodied impacts of the case building. For prefabricated components, façades generate the highest impact on both GWP and CED (7.77% and 8.09%), followed by kitchen pods (5.62% and 5.86%), bathroom pods (4.93% and 5.14%), slabs (4.06% and 4.23%), connecting slab (2.16% and 2.25%), stairs (0.79% and 0.82%) and refuse chute (0.14% and 0.14%). For materials used on site, cast-in-situ concrete contributes the highest GWP and CED (27.98% and 29.16%), followed by steel reinforcement (8.98% and 9.39%), timber (6.46% and 6.73%), plaster (2.59% and 2.69%), aluminum (2.08% and 2.17%), ceramic tiles (2.05% and 2.14%), glass (0.68% and 0.71%), paint (0.64% and 0.67%) and asphalt (0.04% and 0.04%). Varying trends are observed when comparing the impacts of materials/components across different indicators. Taking insitu concrete as an example, although it has the highest impact on ADP-f, AP, EP, GWP and CED, its impact on HTP, FAETP and TETP is relatively low because of the higher impact factors of other materials and components. Therefore, it is necessary to report different impact categories for a comprehensive LCA.



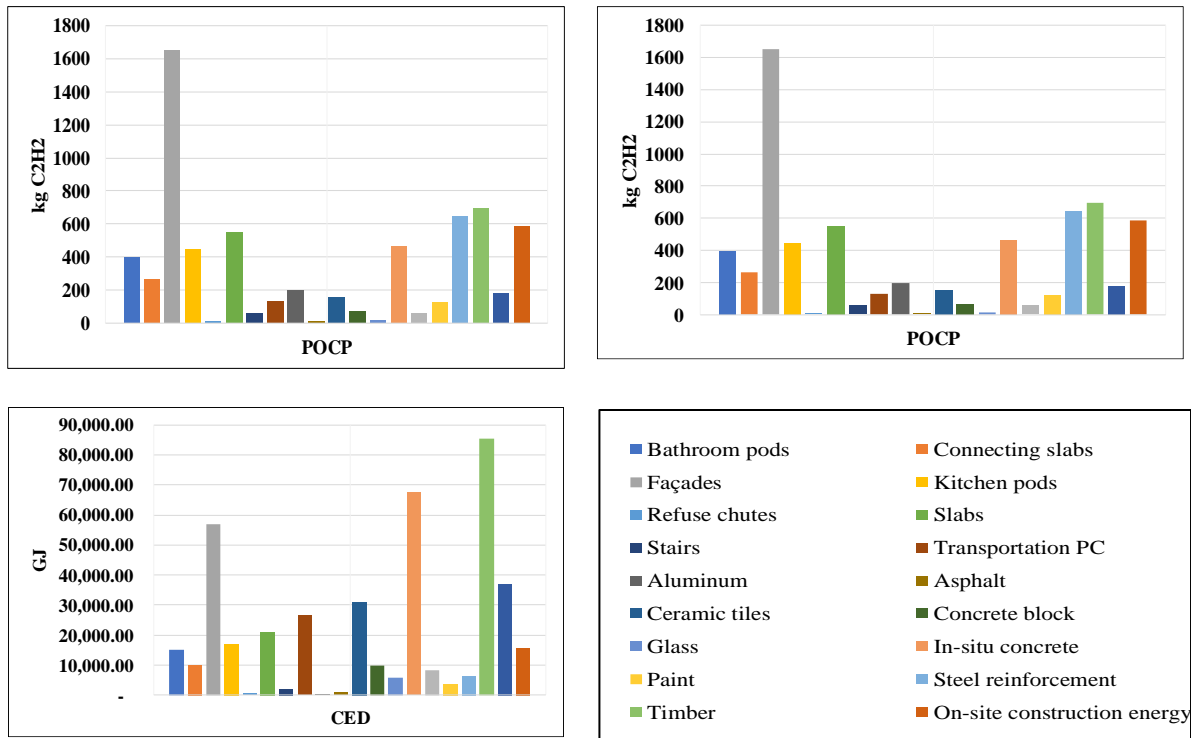


Fig. 4.3 Life cycle impacts at the whole building level

#### 4.4 Embodied impacts at flat level

Public rental buildings in Hong Kong adopt modularly designed standardized flats so that it is useful to evaluate and compare the performance of different flat types as a guide for the design of future buildings. By adopting the types with lower energy and environmental impacts per unit area, the overall impacts of the building can be further reduced. Fig. 4.4 compares embodied impacts of three standard flats (2P3P, 1B and 2B) used in the case building. The results at flat level consist of impacts from material consumption, transportation, and energy use on site. Consistent trends are observed in the contribution of each material across the studied impact categories except ODP. The mean CED and GWP per flat are 134,984.17 MJ and 14,935.95 kg CO<sub>2</sub>, 193,204.56 MJ and 21,190.32 kg CO<sub>2</sub> as well as 252194.74 MJ and 27,818.07 kg CO<sub>2</sub> for Flat 2P3P, Flat 1B and Flat 2B respectively. If Flat 2P3P is used as baseline, an increase of 53% and 87% is observed for Flat 1B and 2B respectively. However,

when compared per floor area, Flat 1B has 3% and 10% less impact than Flat 2P3P and 2B and is therefore validated as the most favorable flat design [112]. The contribution of each component or material in CED, GWP and other studied indicators is also presented in Fig. 4.4.

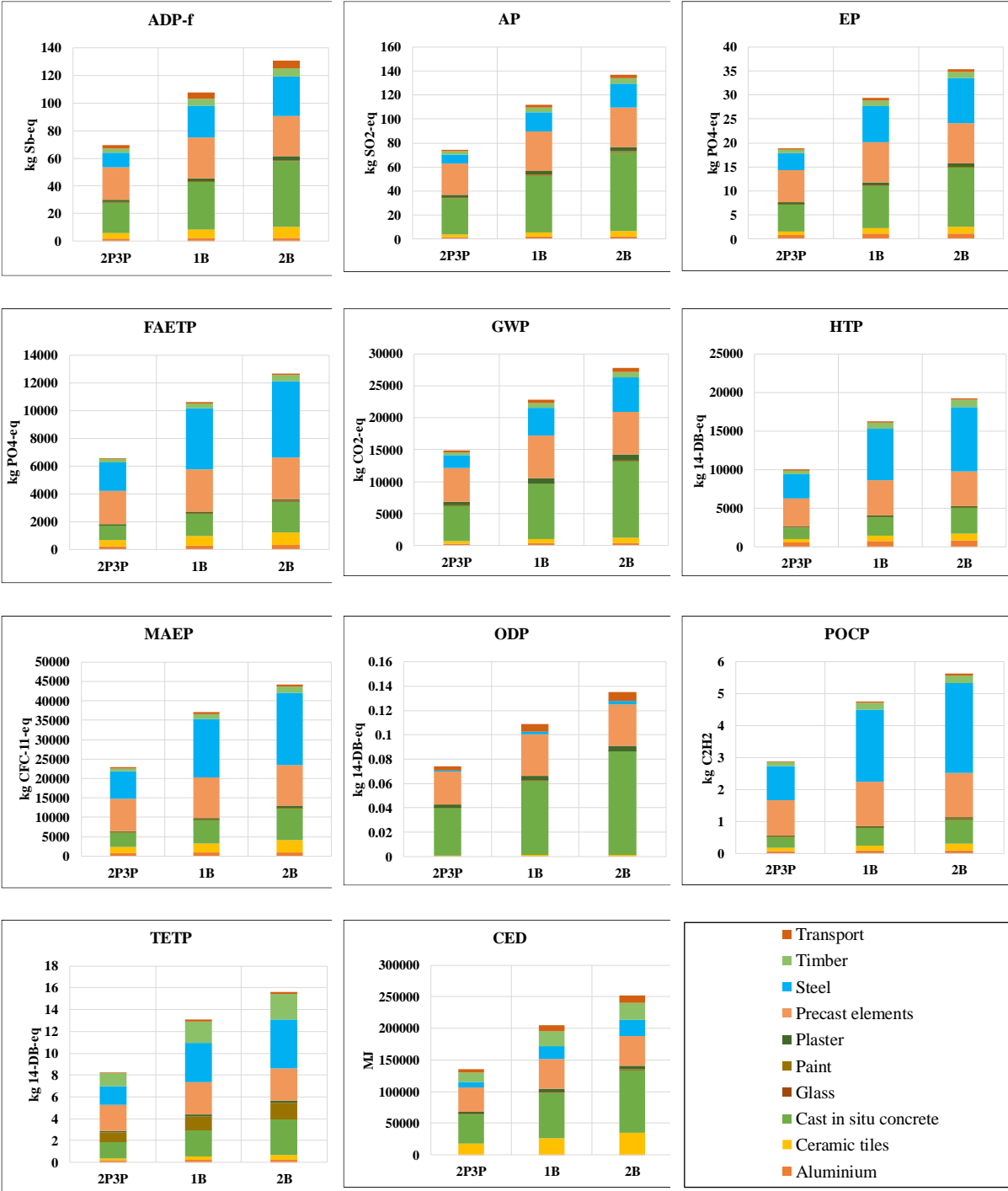


Fig. 4.4 Embodied impacts at flat levels

### 4.5 Embodied impacts at assembly levels

Public residential buildings in Hong Kong use precast assemblies including façades, bathroom pods, kitchen pods, refuse chutes and water tanks. Therefore, the developed method automates embodied impact at these levels as well. Fig. 4.5 shows the embodied impacts of four assemblies which is evaluated per unit of each assembly for standardized bathroom pods, kitchen pods, and refuse chutes, whereas that for the façade is an average value as more than one façade type is used in the case building. Refuse chute has the lowest impact on GWP and CED (1179.94 kg CO<sub>2</sub> and 13.39 GJ), followed by façades (1408.58 kg CO<sub>2</sub> and 14.96GJ), bathroom pods (1735.44 kg CO<sub>2</sub> and 17.67 GJ) and kitchen pods (3653.55 kg CO<sub>2</sub> and 37.21). The results for other impact categories are also illustrated in Fig. 4.4. In addition, impacts per material are evaluated to elucidate main contributors to production and transportation phases. Concrete, steel, and aluminum (façade only) are identified as hotspots which totally contribute from 84% to 89% in all assemblies. The remaining 11% to 16% is attributed to manufacturing and transportation.

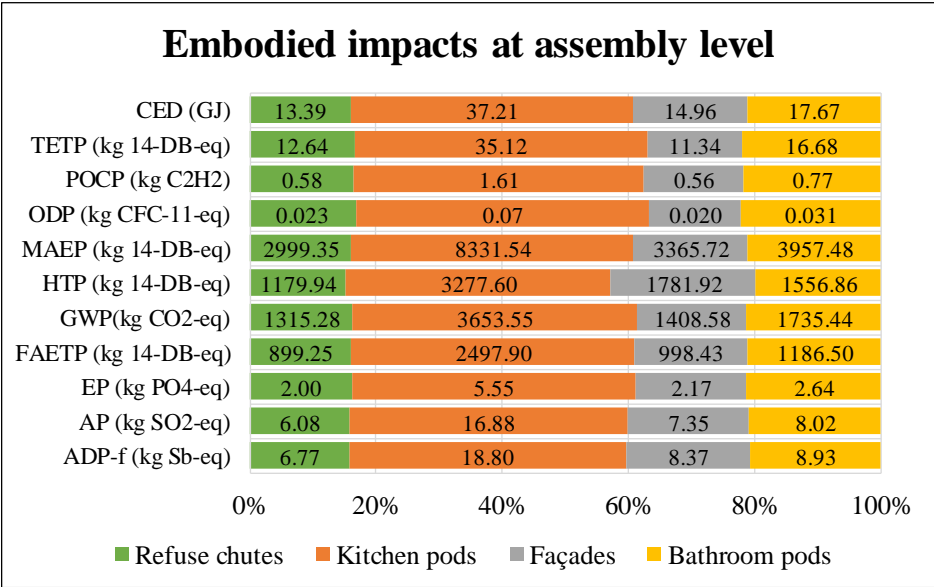


Fig. 4.5 Embodied impacts at assembly levels

#### 4.6 Embodied impacts at component level

Fig. 4.6. illustrates the contribution of each building element to the life cycle impact of the case building. A cradle to end-of-life analysis is performed in this level for the studied impact categories. Similar trends of contributions from different components are observed for all impact categories except HTP, OPD and TETP. The contribution of walls prevails in all impact categories (ranging from 18.40% to 38.87%) except in TETP where the contribution of doors dominates (36.47%). Next to walls, floor slabs contribute significantly to all impact categories ranging from 22.36% to 37.48%. Contributions of other structural framing components such as beams, and columns are between 7.43% and 12.14% and 9.36% and 16.78%, respectively. Openings including doors and windows also make significant contributions ranging from 0.62% to 36.47% and 0.12% to 9.40% respectively due to the use of timber and aluminum. These results are consistent with the component contribution ranges reported in [186]. For the purpose of comparison between components, the contribution to GWP and CED from different components is presented as: walls (36.34% and 35.89%), floor (23.96% and 24.25%), columns (16.20% and 15.90%), beams (11.15% and 10.84%), doors (7.58% and 7.84%), windows (3.24% and 3.36%), stairs (0.81% and 0.83%), roof (0.84% and 0.92%) and refuse chute (0.14% and 0.15%).

A comparative analysis of residential buildings in Hong Kong is presented in terms of GWP as most existing studies use this indicator. The assessment results, scopes and deviations are presented in Table 4.4. Significant deviations are observed among studies due to variations in system boundaries and LCIA data. For instance, the results of [187] indicate an underestimation of 22.59% in GHG emissions as only principal structural material were considered in their study. Although the study is consistent with the finding in [112], the overall LCA impacts is found to be higher due to the expanded system boundaries. Thus, if the system boundaries are adjusted the results are likely to very similar to the present study.

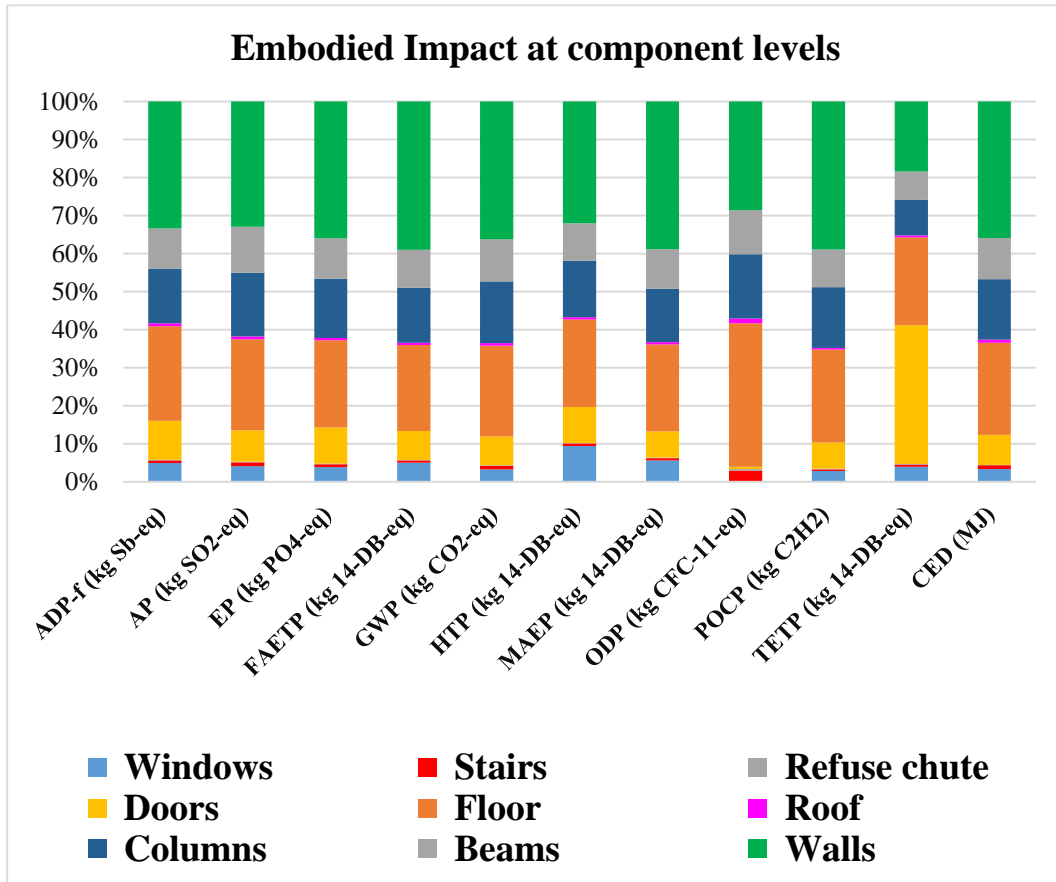


Fig. 4.6 Embodied impacts at component levels

General assumptions from existing literatures and Ecoinvent have been adopted for developing the database. However, evolving construction processes and technologies could result in different impact levels which can be resolved through primary data collections from experts. Particularly, the collection of real operational data such as used equipment, fuel consumption and operation times during the construction of a typical prefabricated project could improve the evaluation accuracy of the construction phase. For the end-of-life phase, diverse management strategies can be explored for a more comprehensive assessment subject to the inclusion of more strategies in the database and enhancing the developed method for such applications. Presently, only recycling benefits of reinforcement bars are considered. If

recycling is excluded from the tool, the embodied impacts of the end-of-life phases could be much higher as steel is one of the most influential materials.

Table 4.4 Comparative analysis of residential buildings in Hong Kong

<b>Study</b>	<b>System boundary</b>	<b>kg CO<sub>2</sub> eq/m<sup>2</sup>·y</b>	<b>LCIA data</b>	<b>Deviation</b>
Present study	Cradle to end-of-life	12.84	Localized	-
[98]	Cradle to end-of-life	13.82	Localized	7.63%
		11.86	Generic	-7.63%
[112]	Cradle to end of construction	11.22	Localized	-12.62%
[187]	Cradle to site	9.94	Localized	-22.59%
[184]	Cradle to end of construction	12.74	Generic	-0.78%
[188]	cradle-to-end of construction	13.38	Generic	4.21%

Furthermore, investigating a broader scope of lifecycle phases leads to a more comprehensive lifecycle profile which has not been achieved in previous BIM-based LCA studies. Particularly, improvements in the evaluation of transportation, construction and end-of-life phases have been achieved with an enhanced database and its integration with BIM to allocate transport modes, load factors, construction, and demolition equipment. Although transportation distances are currently included in the database, map applications can be integrated into the process with prospects of optimizing transportation distances. In addition, the developed method includes equipment uses in the construction phase and can therefore

enhance the estimation of construction impact which has been a major blind spot in previous studies. Limitations are identified in bridging gaps between structural and architectural domains of the model. For elements such as columns, significant challenges are identified in coordinating structural elements in reinforcement and finishes (e.g. plaster and paints). Although their impacts could be easily eliminated in a one-off modeling, it could be a significant challenge during repeated design iterations. Another significant challenge exists in applying the developed method to building service components. Most components such as ducts are treated as solids instead of hollow units which could result in large errors. Two potential solutions are proposed in such situations: estimating an average value based on a parameter of ducts or assessing impacts at aggregated levels (components) rather than specific materials.

#### **4.7 Summary**

This chapter presents a BIM-based LCA method to evaluate the life cycle energy and environmental impacts of prefabricated buildings. This approach is based on a more standardized levels of assessments, a broader scope of lifecycle phases, and more comprehensive functional units and system boundaries. The unique characteristics of prefabricated including transportation and construction modalities have also been addressed to automate the lifecycle process with high accuracy. A more detailed, and comparable LCA results are automatically produced allowing for deep analyses and identifications of hotspots including the best combination of components such as façades, bathroom/kitchen pods or even flats in modular designs. For instance, through this method, the one-bedroom flat is identified as the best performing flat type in comparison with other flats in the case building. Such characterization provides insight to design optimization of prefabricated buildings.

The method has been successfully tested on a typical prefabricated high-rise building in Hong Kong and proven to produce accurate results with a higher computational efficiency for

different levels of assessments, system boundaries and functional units comparable with previous studies. It is achieved through an automated process of systematic zoning and set up after creating parameters and populating BIM with LCA data. The total CED and GWP of the case building are estimated to be 30.22 GJ/m<sup>2</sup> and 4141.70 kgCO<sub>2</sub>eq, respectively. Also, the operational CED and GWP are estimated to be 22.24 GJ/m<sup>2</sup> and 3499.30 kgCO<sub>2</sub>eq respectively while embodied CED and GWP are 7.99 GJ and 642.40 kg CO<sub>2</sub> eq respectively. Embodied impacts at flat levels are estimated to be 134,984.17 MJ and 14,935.95 kg CO<sub>2</sub> for Flat 2P3P, 193,204.56 MJ and 21,190.32 kg CO<sub>2</sub> for Flat 1B and 252,194.74 MJ and 27,818.07 kg CO<sub>2</sub> for Flat 2B. Therefore, Flat 1B is proved to be the most sustainable design given its lowest lifecycle impact. In addition, kitchen pods and walls are found with the highest impact in their corresponding assessment levels.

The detailed levels of assessments addressed as well as automation and computational efficiency achieved will provide an enhanced mechanism to iterate design options at materials, element, assembly, or flat levels to evaluate energy and environmental management opportunities in future studies. Moreover, the designed assessment levels can be easily manipulated to reflect other geographical or prefabrication systems. The method is particularly useful for building practitioners to swiftly evaluate the lifecycle impact of prefabricated buildings with deep insights. Also, the research finding can guide design optimizations of low-carbon building constructions and renovations.

At this stage, additional efforts are needed for a complete representation of the lifecycle profile. The study has considered varying system boundaries from cradle to end-of-life phases, however a wider range of end-of-life management strategies could be integrated for more comprehensive assessments. Also, the method did not include the embodied impacts of building service systems as significant challenges are faced in the extraction and processing of materials used in some of these components. In future studies, these limitations can be addressed. The

method will be further incorporated into extensive uncertainty analyses for a robust life-cycle design optimization.

## **CHAPTER 5 A COMPARATIVE INTEGRATED LIFE CYCLE ASSESSMENT OF DIFFERENT FAÇADE SYSTEMS FOR A TYPICAL LOW-RISE RESIDENTIAL BUILDING**

Based on the implementation of the BIM-based LCA method in Chapter 4, this chapter aims to study the energy and environmental performance of novel façade systems for a low-rise residential building under the subtropical climate of Ghana. A BIM model is developed based on a case study incorporating the conventional building façade system to perform energy and environmental impact assessments. Three alternative façade systems are then explored to investigate opportunities to improve the performance of the building. The system boundary is expanded to include operational impacts to evaluate the impacts of the alternative façade systems on both embodied and operational performance of the building. The results are then subject to an in-depth comparative analysis of different life cycle phases followed by an economic evaluation.

### **5.1 Case descriptions**

The goal of this LCA is to compare the environmental and economic impacts of G. Steel ICF, Shotcrete ICF, SEBF with the conventional CBMF used in Ghana. The functional unit is set to 180.50 m<sup>2</sup> gross floor area (GFA) for a lifespan of 50 years. Therefore, all results presented are for 180.50 m<sup>2</sup>·50years. The impact of windows is included as it significantly affects the operational energy use.

LCA covers processes of the material extraction, product manufacturing, transportation, onsite construction and building operation but end-of-life phase due to the lack of reliable data for buildings in Ghana. Also, only the impact of cooling is considered for the operational phase. Single storey buildings are common archetypes in the Ghanaian residential sector. The case building, located in Amasaman, Accra is selected because the location is representative of the

typical Ghanaian climate. The building is on a site with an altitude of 23m, longitude of 0.3019° W, latitude of 5.7062° N, a Tropical Savanna Climate (Aw) under the Koppen-Geiger climate classification, 761 heating degree days (HDD) and 3793.8 cooling degree days (CDD). The average annual temperature fluctuates between 23.0° and 30.0°, with a dominant cooling load. The building is compartmentalized into six zones: three bedrooms, a living room, a kitchen, two washrooms, a corridor and a porch. It has dimensions close to 12m (length) by 15m (width) and a height of 7m (from the apex of the roof to the ground plane). The floor plan and 3D model are shown in Fig. 5.1, while the main differences in the four façades are described below.

### **5.1.1 Concrete block and mortar façade**

The case building's façade (CBMF) is composed of 150mm thick concrete blocks and 15mm thick mortar on both sides. Concrete blocks are manufactured from locally available cement, river sand and water in the ratio of 2:7:1. Cement and sand are manually mixed while adding water steadily until a homogenous mixture is reached. The mixture is then poured into moulds and compressed manually. They are subject to air-drying and curing before laid with mortar bonds. The structure is plastered with mortar after drying. The main supporting components are reinforced concrete beams and columns. Based on the information provided by the construction team, it is assumed that a concrete mixer is used to prepare concrete. In the same regard, blocks are manufactured 200 metres from the site while aggregates and cement are manufactured 10.7 km and 43.1 km from the construction site respectively.

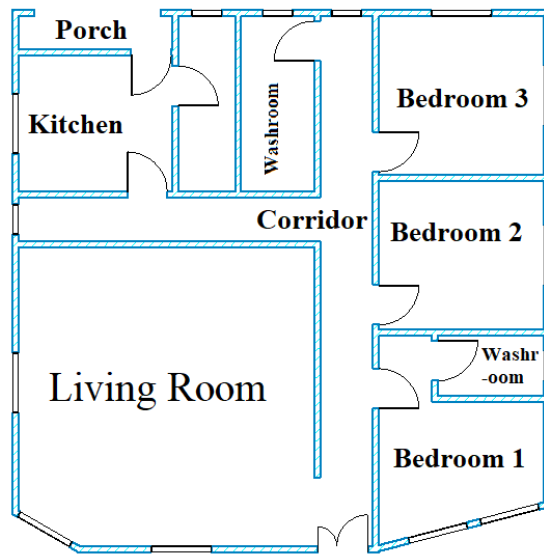


Fig. 5.1a Floor Plan

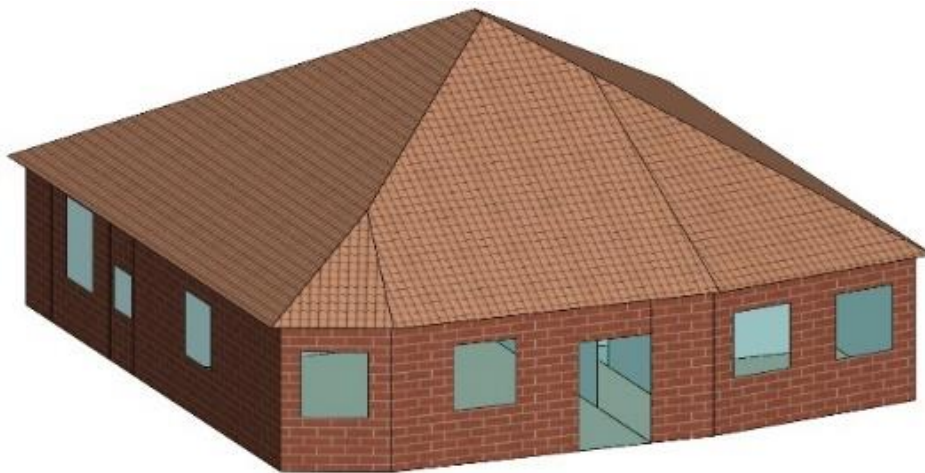


Figure 5.1b 3D BIM Model

Fig. 5.1 Floor plan and 3D BIM simulation model

### 5.1.2 Stabilized earth block façade

The SEBF is made from locally sourced laterite and 8% cement as described in [189–192]. It is usually 180mm thick and requires no finishing as its natural surface is desirable. Laterite usually consisting of 10% to 20% clay, 10% to 20% silt and 50% to 70% coarser soil is first air-dried, grinded manually, sieved to attain uniform size particles after which the

stabilizer (cement) is added. Water is added steadily while manually mixing until a homogenous mixture is attained. The mixture is poured in the mould and compressed manually to increase its density and strength. After demoulding, blocks are air-dried under shades pending use. The shape of blocks is altered using mould inserts so that corner sets and hollow cores for reinforcement can be manufactured. These blocks are interlocking and are therefore directly stacked on-top of each other except for a few portions where thin layers of cement-sand mortar are applied as jointing or for airtightness. These special portions include the first course of blocks, window levels and corners of wall. The same transportation distances used for the case building façade is assumed for this alternative design.

### **5.1.3 Galvanised steel insulated composite façade**

G. Steel ICF is factory made in China and exported to Ghana. This façade consists of panels made up of a 50mm EPS core with 0.5mm galvanised steel sheets on both sides. The panels span a length of 3m and a width of 0.9m. In addition, cold-drawn light weight steel sections, and steel ties are used as the support frame for panels. It is assumed that small construction equipment for cutting, welding, riveting and finishing wall assemblies is powered by a diesel generator. Materials such as EPS, paints, steel bars and steel sections are all imported from China and both domestic and oversea transportations are considered. Distances are established from Google Map and Sea Distance respectively. Transoceanic vessels and trucks are used for oversea and domestic transport respectively. A direct transportation route from Tema harbour to the construction site is assumed as the material supplier is located on the same route.

### **5.1.4 Shotcrete insulated composite façade**

Shotcrete ICF consists of a 70 mm thick expanded polystyrene core sandwiched between two 40mm thick reinforced shotcretes. The main reinforcement is a welded wire mesh, while vertical and diagonal steel bars at 8 mm diameters and at 100 mm intervals are provided

for structural support. The EPS core is first placed and fixed by reinforcement bars extending from the concrete slab. The welded wire mesh, vertical steel and diagonal steel bars are then erected on the EPS core, after which the shotcrete is sprayed. Two diesel powered plants, a concrete mixer and a wet shotcrete spraying machine, are used for building this façade. EPS and the welded wire mesh for this façade are imported as individual units to be assembled on site. It is assumed EPS and steel reinforcement are imported from China whereas the raw materials for shotcrete are sourced locally.

All façades incorporate a double-slide single-pane window with aluminium frames. Windows are manufactured in a factory and transported to the site for assembly, so that it is possible to retrieve monthly electricity bills from the manufacturer. Energy demands for fabricating the windows are prorated over the number of windows used. Materials such as aluminium and glass are imported from China. The construction details of the analysed façade alternatives are illustrated in Fig. 5.2.

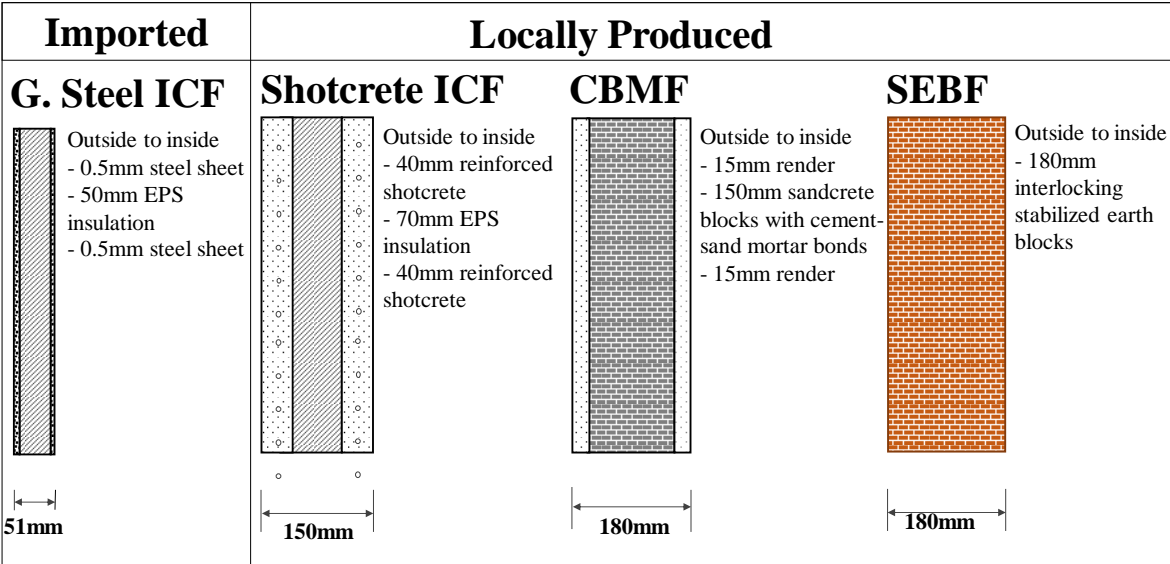
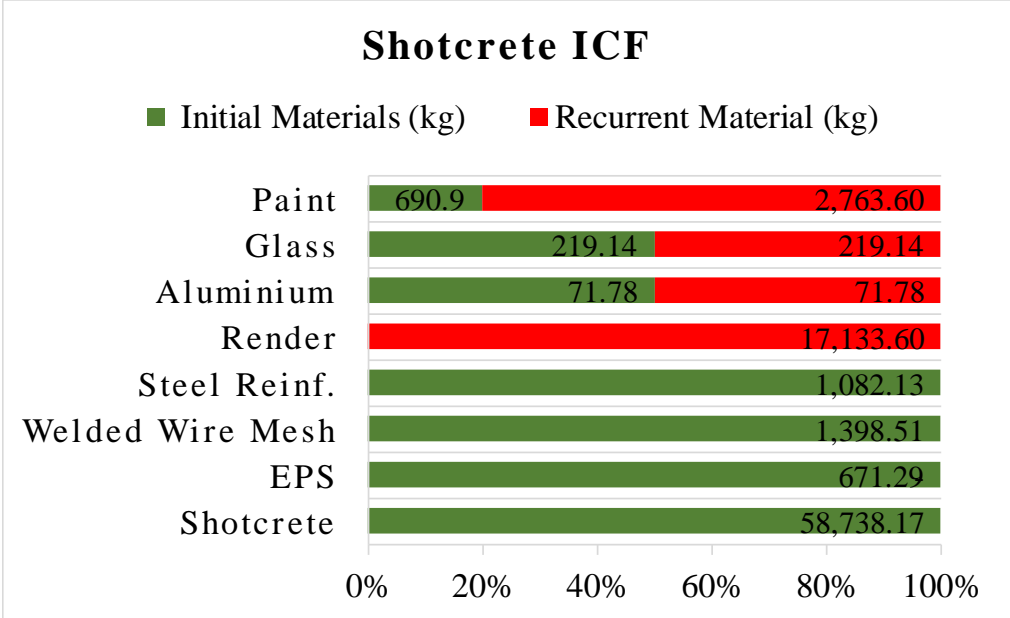


Fig. 5.2 Schematic diagrams of the four façades

### 5.2 Life cycle inventory

A bottom-up approach is adopted to generate a detailed BIM models which includes all data requirement for the automated BIM-based LCA process for the four different façade systems. For the reference façades, primary data including building drawings, material specifications, sources of materials, transportation modes, method statements, electricity and fuel consumption for plants and equipment were retrieved from the owner and contractor. Drawings and materials specifications for alternative façades were sourced from multiple contractors to reach a convergence in designing the alternative models. Other data such as method statements and equipment use were retrieved through short interviews with the experts.

The detailed models are designed in Revit using a parametric process to define specific layers of various construction materials. Thereafter, the automated assessment process is performed to generate a detailed materials inventory, energy, and environmental impact assessment.



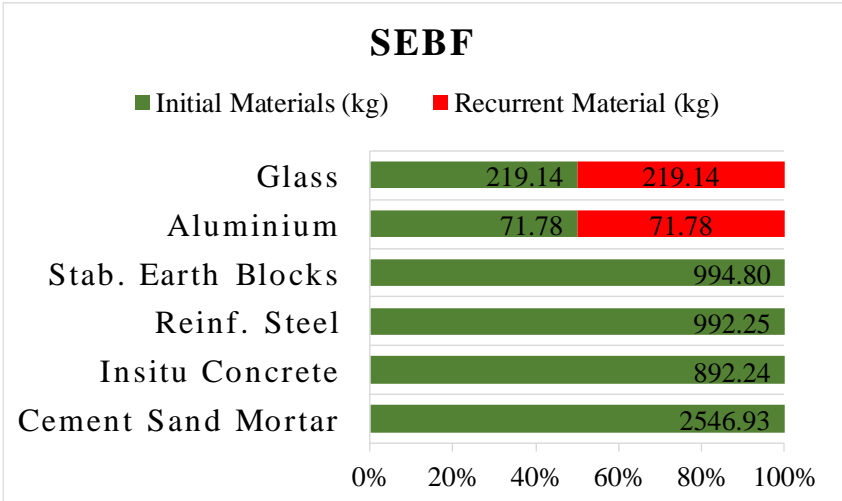
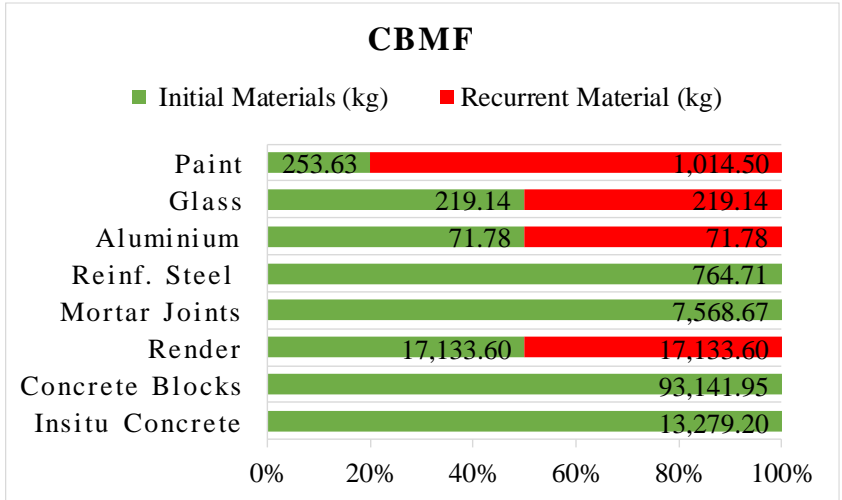
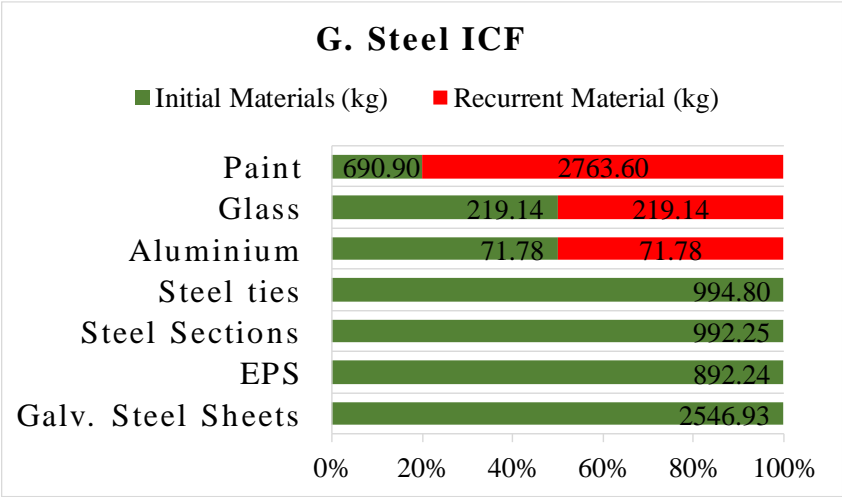


Fig. 5.3 Materials inventory of four façades

Fig. 5.3 illustrates the inventory of materials categorised into initial and recurrent for all cases presented. The initial materials represent materials used at the construction stage. It is assumed that maintenance activities including painting, rendering and window replacement are required as the building's lifespan exceeds the service life of some materials. In such scenarios, the differences are credited as recurrent materials per the replacement factors provided in Table 1. The net quantity of materials is adjusted to account for waste during the construction based on the recommendation of local contractors and existing literatures as summarised in Table 5.1.

Table 5.1 Material replacement and waste factors

<b>Material</b>	<b>Materials' Service Life (yrs.)</b>	<b>Material Durability (yrs.) (a)</b>	<b>Replacement Factors</b>	<b>Wastage (%)</b>
Aluminium	50	45	1.11	5
Cement Sand Mortar	50	50	1.00	5
Concrete Blocks	50	50	1.00	10
Expanded Polystyrene	50	50	1.00	10
Galvanised steel plates	50	50	1.00	5
Glass	50	36	1.39	5
Insitu Concrete	50	50	1.00	10
Paint	50	10	5.00	10
Render	50	20	2.50	10
Steel Reinforcement	50	50	1.00	10
Steel Sections	50	50	1.00	5

<sup>a</sup> [193–196]

### 5.3 Life cycle impact assessment

Life cycle impact assessment translates the results of the inventory analysis to corresponding environmental impacts [197]. The Inventory of Carbon and Energy (ICE) database V2.0 developed by the University of Bath is selected for this impact assessment as it is applicable to regions which lack impact assessment data [198]. Moreover, it is based on aggregated global values and therefore is appropriate for the study. The database is an excel document with energy and carbon coefficients of most used building materials. It is also selected because its inventory data are based on a cradle-to-gate boundary and are estimated from many LCA studies with high credibility. For ICE V2.0, products are assessed by their energy use intensity (MJ/kg) and Global Warming Potential (GWP) (kg CO<sub>2</sub>eq/kg), which are the most commonly used LCA indicators for buildings [199]. Also, CO<sub>2</sub>eq/kg accounts for other greenhouse gases (GHG) as the carbon equivalent. Metered data in kWh of electricity or litres of fuel are retrieved from the contractor where possible to estimate the construction impact. Since no appropriate energy/carbon conversion factor was found for Ghana, their energy and carbon contents are estimated with reference to UK Greenhouse Gas Reporting: Conversion Factors 2018 [200]. The comparative analysis of façades remains valid as the same conversion factor is maintained for all façades. A similar approach is applied to local transportation. Also, the energy use and emission factors for cross continent transport are provided in Table 5.2 [201].

Table 5.2 The energy use, emission factor and transportation distance for the transport mode

<b>Transport mode</b>	<b>Energy use (MJ/ton.km)</b>	<b>Emission factor (g/ton.km)</b>	<b>Transportation distance (km)</b>
Cross continent transport	0.216	15.98	26211.36
Road Freight (local transport)	2.275	168.35	43.1

Furthermore, references are made to [202,203] as shown in Table 5.3 to complement equipment workload and rated power retrieved from the contractor. With these data, the direct and indirect energy consumption and environmental impacts are estimated.

Table 5.3 Equipment energy use and emission factors for the construction stage

<b>Equipment</b>	<b>Workload per Machine per day (m<sup>3</sup>)</b>	<b>Rated Power (kW)</b>	<b>kWh to MJ conversion factor</b>	<b>kWh to kgCO<sup>2</sup>eq conversion factor</b>
Concrete mixer	50	4.4	3.6	0.26910
Shotcrete pump	24	3	3.6	0.26910

The actual energy use during the operational phase of the case building is retrieved from monthly electricity bills for the year 2017. While the retrieved data cover energy demands for cooling, lighting and household appliances, the main interest lies in the cooling energy demand. Moreover, the energy use with alternative facade systems also needs to be predicted, so that IES-VE is used to predict operational energy uses. IES-VE is a platform for modelling the energy, daylight, renewable energy system, airflow performance related to buildings. The weather data used to assess the annual operational performance is generated from the ASHRAE database using IES-VE. For all models, U-values of walls are varied while all other assumptions (e.g. the floor properties, roof properties, occupancy and internal gains) are referenced to the case building. Table 5.4 shows main input settings for the building energy simulation.

Table 5.4 Input parameter for building energy simulations

<b>Parameter</b>	<b>Value</b>
Indoor cooling setpoint	23°C
Air change rate	1.2m/s
Equipment gain	10W/m <sup>2</sup>
Illuminance setpoint	150 Lux
Lighting gains	15 W/m <sup>2</sup>
Occupancy	4 persons
Occupancy gains	100 W/person
Operation schedule	Weekdays (18:30 - 07:30), Weekends (00:00 - 24:00)

The life cycle cost is calculated for both initial and recurrent investments, including the cost of all materials, plants and labours used for façade construction. The rates used are weighted averages from several contractors to avoid biases. Total amounts are calculated as a product of quantities and rates.

#### **5.4 Scenario analysis for each façade**

Scenario analyses have been increasingly applied in LCA studies [204–207]. To identify strategies for further improving the performance of each façade, scenario analyses are conducted to assess the variation induced in CED and GWP. At least two scenarios are defined stepwise for each façade combining design and material source variations. The ratio of the change in results to the variation of a parameter (i.e. Sensitivity Ratio) is expressed by Eq. (5.1).

$$\text{Sensitivity Ratio} = \frac{\text{Change in results}/\text{initial results}}{\text{change in parameter}/\text{initial parameter}} \quad (5.1)$$

The first two scenarios are defined for materials that are locally available although mainly imported. Scenario 1 considers modifying the sources of EPS and the paint, thus addressing the impact of transportation. It is assumed that importing EPS and paints increases the impact of transportation, as these materials are available in Ghana (i.e. a scenario is considered where they are locally supplied). Similarly, the energy embedded in transporting steel is also found to be significant. Besides importing steel from countries like China and Ukraine, Ghana produces some amount of steel from scrap sourced within the country and nearby regions like Kenya. Therefore, Scenario 2 is proposed to explore the impact of locally manufactured steel given that Ghana recycles some quantities of steel.

The third scenario is defined by varying the facade design. For SEBF, blocks account for a large portion of the material embodied energy considering its mass. Therefore, the impact induced by reducing the thickness of blocks and replacing reinforced concrete lintels with reinforced compressed-mud blocks are explored. Similarly, the mass of CBMF can be reduced using hollow blocks so that a scenario is set to explore its effect. Information retrieved from experts indicates the thickness of Shotcrete can be reduced from 40mm to 30mm so that its impact is also explored. All assumptions for the scenario analysis are summarized in Table 5.5.

## 5.5 Model validation

For validation purpose, the simulated energy use for baseline model is compared with energy end-use data retrieved from the case building. Based on monthly electricity bills for the year 2017, the total energy use for HVAC, equipment and lighting is estimated as 25.60kWh/m<sup>2</sup>/y. On the other hand, the baseline model is estimated to be 24.15 kWh/m<sup>2</sup>/y. From Fig. 5.4, the simulated data is shown to be consistent with the end-use data with a minor

difference of 5.65%. In this regard, the baseline model can sufficiently represent an average residential building in Ghana. A breakdown of annual energy consumption for all four façade designs is presented in Table 5.6.

Table 5.5 Main assumptions for scenario analysis

Scenario	Shotcrete ICF	G. Steel ICF	CBMF	SEBF
Paint and EPS Source	Accra, Ghana	Accra, Ghana	Accra, Ghana	Accra, Ghana
Steel Source	Accra, Ghana	Accra, Ghana	Accra, Ghana	Accra, Ghana
Wall design	With 30mm shotcrete thickness	-	With hollow concrete blocks	With reinforced mud block lintels, 300mm thick blocks

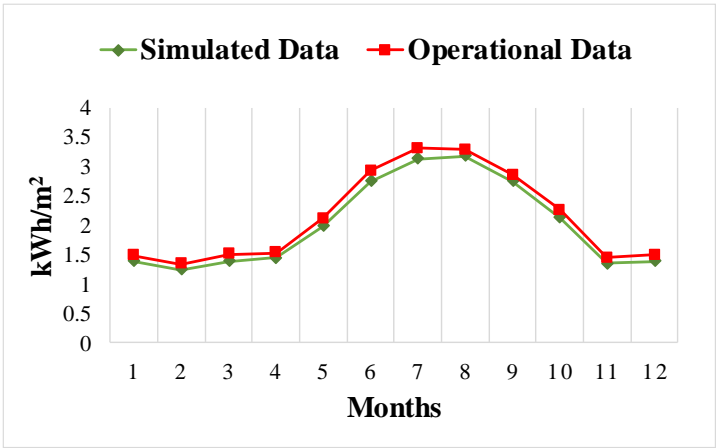


Fig. 5.4 Comparison of energy end-use data and simulation data of case building

Table 5.6 Breakdown of simulated annual energy demands during use phase of buildings

<b>Energy use breakdown</b>	<b>Shotcrete ICF (kWh)</b>	<b>G. Steel ICF (kWh)</b>	<b>CBMF (kWh)</b>	<b>SEBF (kWh)</b>
Chillers	14.88	14.96	16.33	14.87
Heat rejection fans	1.75	1.78	1.82	2.04
Total equipment	5.60	5.60	5.60	5.60
Total lights	1.85	1.85	1.85	1.85
Total electricity	24.07	24.18	25.60	24.36

## 5.6 Comparative analysis of façade types

### 5.6.1 Concrete Block and Mortar Façade

The baseline model (CBMF) is evaluated with a CED of 100.04 MJ/m<sup>2</sup>/y. The contribution of various LCA phases is presented in Fig. 5.5 while a detailed breakdown is provided in Table 5.7. OE and EE contribute 65.10% and 34.90% of CED while GWP<sub>OE</sub> and GWP<sub>EE</sub> contributes 79.09% and 21.91% respectively. Material production contributes 93.60% of EE and 95.38% of GWP<sub>EE</sub>. Most of these impacts are associated with the paint, sandcrete block, and cement plaster. The high impact of paints is explained by its high energy intensity and frequent replacement. Similarly, cement in concrete blocks and render is energy intensive in addition to the large quantities used [208]. This finding echoes with [209] where coatings and masonry are found to make the large contribution to EE of single-family dwellings. Furthermore, EE<sub>t</sub> is proved to be mainly associated with the importation of window, paint, and steel reinforcement materials, which is also indicated in an existing study that using local materials can significantly optimize the impact of transportation [194]. Like EE<sub>t</sub>, majority of GWP<sub>t</sub> originates from paint, steel reinforcement rods and sandcrete blocks. The contribution of the construction phase is however less important with close to zero EE and GWP [210]. The

small amount of  $EE_c$  is mainly attributed to concrete and windows with 29.79% and 70.21% respectively.

Table 5.7 Embodied energy and global warming potential of concrete block and mortar façade

<b>Materials</b>	<b>EE (MJ)</b>	<b>GWP (kg CO<sub>2</sub>e)</b>
<b>Materials Production Phase</b>		
Concrete Blocks	69,856.46	12,036.22
Insitu Concrete	10,623.36	1,713.02
Mortar Joints	7,224.70	1,244.81
Paint	109,740.00	5,196.84
Reinforcement Steel	16,517.81	1,422.37
Render	49,064.81	8,453.83
Windows	30,115.53	1,759.81
<b>Transportation Phase</b>		
Concrete Blocks	2,411.71	179.36
Insitu Concrete	347.71	25.86
Mortar Joints	239.34	17.80
Paint	7,360.53	544.61
Reinforcement Steel	4,369.30	323.26
Render	1,625.42	120.88
Windows	3,335.10	284.50
<b>Construction Phase</b>		
Insitu Concrete	99.98	7.44
Windows	235.58	12.04

Materials	EE (MJ)	GWP (kg CO <sub>2</sub> e)
Total	313,167.34	33,342.65

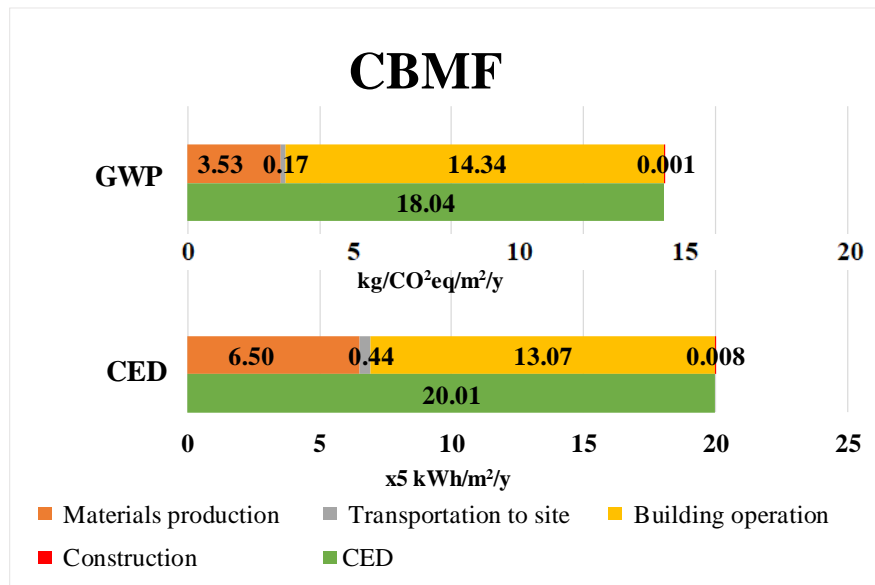


Fig. 5.5 CED and GWP for CBFM per unit GFA and across the building lifespan

### 5.6.2 Stabilized Earth Block Façade

SEBF is proved as the most sustainable façade. Its contributions to CED and GWP for different life cycle stages are shown in Fig. 5.6 while a detailed breakdown of EE and GWP<sub>EE</sub> is summarized in Table 5.8. SEBF does not alter the ranking of lifecycle phases however, the difference in impacts of life cycle phases fluctuates within a range from 6.85% to 63.18% significantly influencing total CED. From Fig. 5.6, CED decreases from 100.4 MJm<sup>2</sup>/y to 75 MJm<sup>2</sup>/y which represents 39.13% CED saving. EE<sub>c</sub> is increased by 25% but still approaching zero with a relatively less importance [211,212]. EE<sub>t</sub> is increased by 14.68% which can be explained by the larger mass of soil materials for SEBF, which also leads to the decrease in EE<sub>m</sub>. SEBF is characterised by higher soil contents with a low EE coefficient and lower cement contents with a high EE coefficient whereas this relationship between soil and cement is reverse

for CMBF. Furthermore, SEBF is constructed with interlocking joints which reduce the mortar joint extensively used in CBMF.

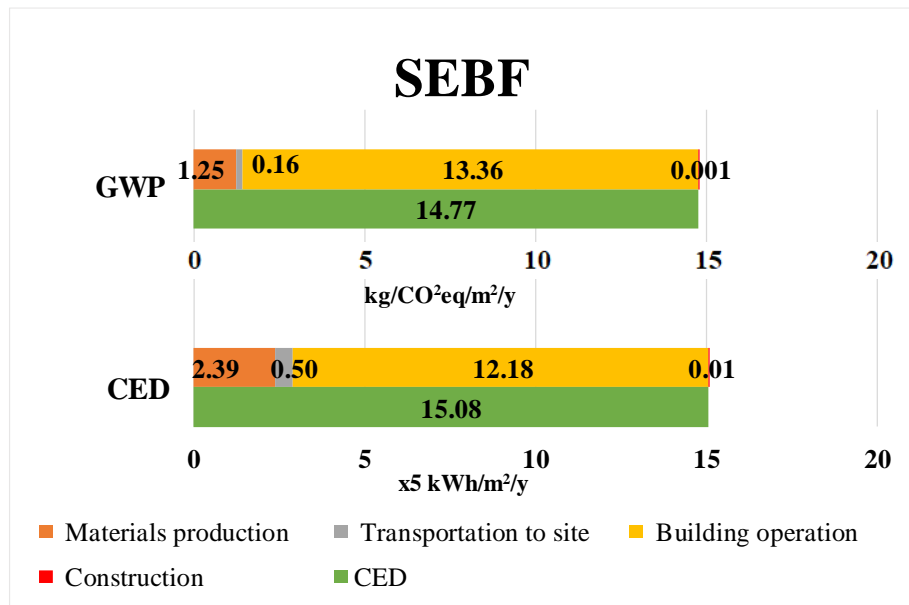


Fig. 5.6 CED and GWP for SEBF per unit GFA and across the building lifespan

Table 5.8 Embodied energy and global warming potential of stabilised earth block façade

Materials	EE (MJ)	GWP (kg CO <sub>2e</sub> )
<b>Material Production Phase</b>		
Cement Sand Mortar	6849.81	1,123.02
Insitu Concrete	7,054.36	1,066.76
Stabilised Earth Blocks	5,3526.73	8,223.68
Steel Reinforcement	10,374.612	893.37
Windows	30,115.53	1,759.81
<b>Transportation Phase</b>		
Cement Sand Mortar	98.7173	7.34

<b>Materials</b>	<b>EE (MJ)</b>	<b>GWP (kg CO<sub>2</sub>e)</b>
Insitu Concrete	195.60	14.55
Stabilised Earth Blocks	16,185.34	1,225.825
Steel Reinforcement	2,755.46	203.87
Windows	3,335.10	284.50
<b>Construction Phase</b>		
Insitu Concrete	66.39	4.94
Windows	235.58	12.04
<b>Total</b>	<b>130,793.23</b>	<b>14,819.71</b>

SEBF is also characterised by a lower GWP of about 14.77 kgCO<sub>2</sub>eq compared with 18.04 kgCO<sub>2</sub>eq of CBMF, leading to a savings of approximately 18.07% in GWP. The main difference in GWP originates from the material manufacturing and operational phase. A change in façades from CBMF to SEBF decreases GWP<sub>m</sub> by 64.59%. Given the same source of operational energy, GWP<sub>EO</sub> covariates with EO in similar trends. The change in GWP<sub>c</sub> and GWP<sub>t</sub> is however relatively less significant especially as GWP<sub>t</sub> approaches zero. Although not directly comparable, these findings are consistent with previous studies on small houses [211,212]. However, they contradict with one study which reported that concrete blocks performed better than stabilised earth blocks [213]. In summary, 39.13% and 18.07% savings in CED and GWP are achieved for adopting SEBF.

### **5.6.3 Galvanised Steel Insulted Composite Façade**

As shown in Fig. 5.7, G. Steel ICF has no influence over the ranking of life cycle phases. However, an 8.32% increase is observed in total CED. The exact contribution of each life cycle phase also fluctuates but within a larger range of 7.81% to 100%. It is noteworthy that EE<sub>m</sub> increases by 34.55% because of the extensive use of energy intensive materials in G. Steel ICF.

This may be associated with the massive use of EPS, galvanised steel sheets, sections and ties which are energy intensive materials [148]. Due to the importation of these three materials,  $EE_t$  is also doubled from 2.18 MJ/m<sup>2</sup>/y to 4.36 MJ/m<sup>2</sup>/y. Although, the impact of  $EE_c$  on the total CED is not significant, a 50% increase is observed due to the use of welding and revetting equipment.

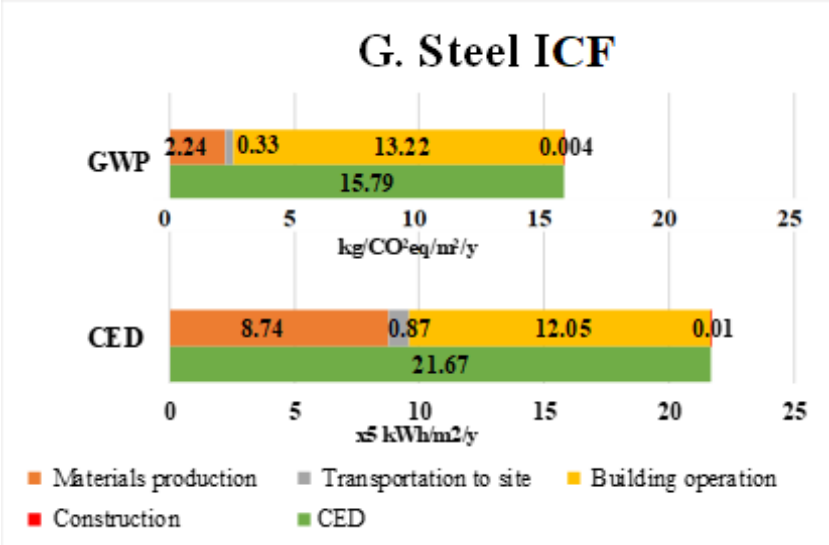


Fig. 5.7 CED and GWP for per unit GFA and across the building lifespan

Fig. 5.7 also illustrates the GWP. A decrease from 18.04 kgCO<sub>2</sub>eq to 15.79 kgCO<sub>2</sub>eq approximates to 12.47% is observed. The unique influence of each material explains the higher ratio of  $EE_m$  to  $GWP_m$  [199]. For CBMF, 32.48 MJ/m<sup>2</sup>/y of  $EE_m$  yields 3.53 kgCO<sub>2</sub>eq of  $GWP_{EEM}$  whereas 43.70 MJ/m<sup>2</sup>/y yields 2.24 kgCO<sub>2</sub>eq. Like  $EE_t$ ,  $GWP_t$  is significantly decreased by 234% although the absolute value is negligible. The results is not directly comparable with the existing studies as the impact of supporting frame is considered, nonetheless the main sources of CED and GWP are identified the same as [148]. A breakdown of EE and  $GWP_{EE}$  is provided in Table 5.9.

Table 5.9 Embodied energy and global warming potential of Galvanised Steel Insulated Composite Façade

<b>Materials</b>	<b>EE (MJ)</b>	<b>GWP (kgCO<sub>2</sub>e)</b>
<b>Materials Production Phase</b>		
EPS	39,526.12	1,467.73
Galvanized Steel Sheet	81,501.84	5,628.72
Paint	189,441.00	7,343.28
Steel Sections	26,889.98	2,014.27
Steel ties	26,959.18	2,019.45
Window	30,115.53	1,759.81
<b>Transportation Phase</b>		
EPS	2,561.91	189.55
Paint	7,960.53	584.27
Steel Panel	15,173.31	1,122.56
Steel Section (Studs)	4,374.37	323.63
Steel ties	5,926.53	438.46
Window	3,335.10	284.5
<b>Construction Phase</b>		
Structure	534.87	39.78
Windows	235.58	12.04
<b>Total</b>	<b>434,535.84</b>	<b>23,228.04</b>

#### 5.6.4 Shotcrete Insulated Composite Façade

Fig. 5.8 illustrates that Shotcrete ICF does not affect the lifecycle phase ranking. However, total CED and contributions of all life cycle phases are increased significantly. The

contributions of each material to life cycle phases are presented in Table 5.10. The operational energy is predicted as 59.86 MJ/m<sup>2</sup>/y corresponding to 8.39% decrease in EE<sub>o</sub>. On the other hand, EE<sub>m</sub> and EE<sub>t</sub> are increased by 11.95% and 404.59% respectively. The cumulative impact of these increment significantly affects total CED. The total CED is increased by 7.32% (7.32 MJ/m<sup>2</sup>/y) with the largest increase in EE<sub>c</sub> for Shotcrete ICF. EE<sub>c</sub> is increased by 250% although the absolute value remains comparatively less significant. In terms of GWP, Shotcrete ICF contributes the second highest impact. GWP is increased by 6.88%, equivalent to 1.24 kgCO<sub>2</sub>eq/m<sup>2</sup>/y. The contribution of construction and transportation phases to total GWP are increased while those of the material production and operational phases are decreased. It is observed that GWP<sub>EEc</sub> is scaled up over 7 times while GWP<sub>EEt</sub> is scaled up over 4 times of CBMF. On the contrary, GWP<sub>EEm</sub> and GWP<sub>OE</sub> are decreased by 22.38% and 8.37% respectively.

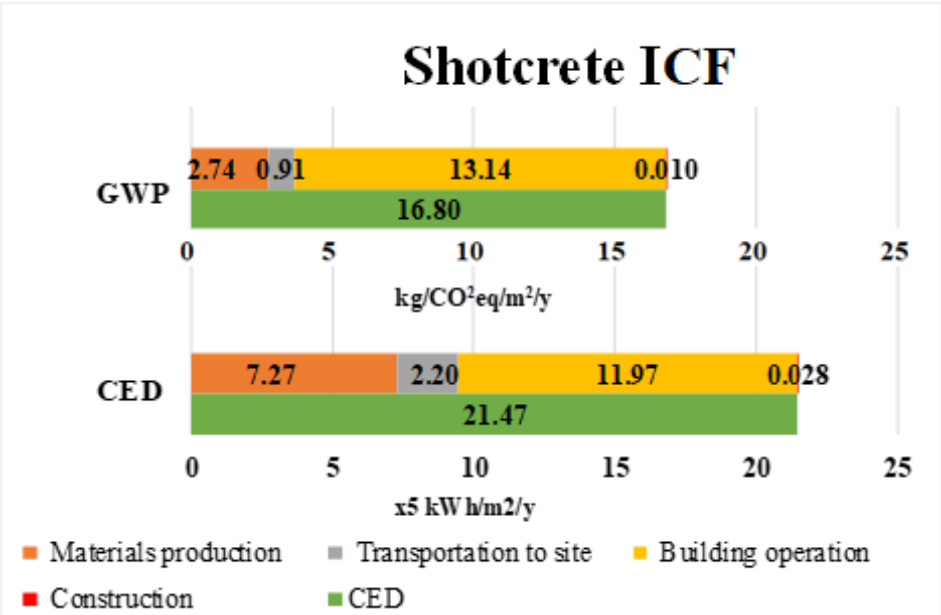


Fig. 5.8 CED and GWP per unit GFA and across the building lifespan

Table 5.10 Embodied energy and global warming potential of Shotcrete Insulated Composite Façade

<b>Materials</b>	<b>EE (MJ)</b>	<b>GWP (kg CO2e)</b>
<b>Materials Production Phase</b>		
EPS	59,476.59	2,208.56
Paint	109,740.00	5,196.84
Render	16,354.94	2,817.94
Shotcrete	58,150.79	9,104.42
Steel Reinforcement	23,373.92	2,012.75
Welded Mesh Fabric	30,907.12	1,636.26
Windows	30,115.53	1,759.81
<b>Transportation Phase</b>		
EPS	18,336.61	1,532.46
Paint	7,360.53	544.61
Render	541.81	40.29
Shotcrete	1,980.64	147.30
Steel Reinforcement	29,536.79	2,468.71
Welded Mesh Fabric	38,161.83	3,189.69
Windows	3,335.10	284.50
<b>Construction Phase</b>		
Shotcrete	1,061.40	78.94
Windows	235.58	12.04
<b>Total</b>	<b>428,669.18</b>	<b>33,035.12</b>

### 5.6.5 Life Cycle Cost

The life cycle cost for all façade systems are presented in Fig. 5.9. CBMF is proved as the most expensive among the assessed façades. Because of the higher replacement factor of

materials used in Shotcrete ICF, G. Steel ICF and CBMF, their recurrent costs contribute up to 40% of the total cost. However, the recurrent cost of SEBF is much lower and constitutes to 21% of the total life cycle cost. The lower cost of SEBF can be associated with the lower cost of stabilised earth blocks as well as the relatively less amount of material used in this façade. The cost of Shotcrete ICF, G. Steel ICF and SEBF is 4.56%, 22.44% and 47.87% lower than that of CBMF.

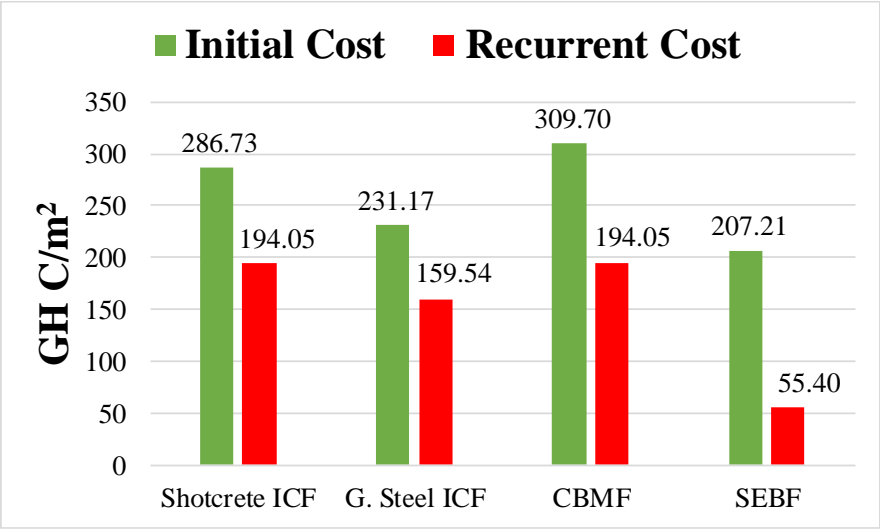


Fig. 5.9 Life Cycle Cost for all façades per floor area

**5.7 Scenario analysis**

The scenario analysis indicates that EE and  $GWP_{EE}$  of Shotcrete ICF are scaled down by 6.32% and 6.46% respectively when paints and EPS are sourced locally. By sourcing steel locally, EE and  $GWP_{EE}$  is reduced by 12.81% and 13.89% respectively. A reduction of the thickness of shotcretes by 10mm can lower EE and  $GWP_{EE}$  by 3.51% and 7.06%. Cumulatively, 22.64% and 27.41% reduction of EE and  $GWP_{EE}$  is attained. For G. Steel ICF, 2.36% of EE and 2.48% of  $GWP_{EE}$  is reduced by sourcing paints and EPS locally. Likewise, sourcing steel locally, reduces EE and  $GWP_{EE}$  by 4.80% and 6.32% respectively. Both scenarios reduce EE and  $GWP_{EE}$  by 7.16% and 8.80%. For CBMF, the hollow block scenario reduces EE and

GWP<sub>EE</sub> by 9.6% and 11.12%, while 2.29% of EE and 1.48% of GWP<sub>EE</sub> reductions are attained by sourcing paints and EPS locally. Furthermore, the use of locally manufactured steel reduces EE and GWP<sub>EE</sub> by 1.13% and 0.85% respectively. Thus, a total reduction of 13.02% of EE and 13.45% of GWP<sub>EE</sub> are attained by applying all three scenarios. After replacing reinforced concrete lintels in SEBF with reinforced stabilized earth blocks, the total EE and GWP<sub>EE</sub> is reduced by 11.68% and 15.58%. By sourcing steel locally, an additional 0.19% of EE and 0.29% of GWP<sub>EE</sub> reduction are attained. Cumulatively the total EE and GWP<sub>EE</sub> is reduced by 11.87% and 15.87% respectively. Table 5.11 provides the percentage reduction in EE and GWP from the scenarios identified in Table 5.5. Also, ranking of the façades in accordance with CED, GWP and cost before and after the scenario analysis are provided in Table 5.12. It is observed that SEBF outperforms all alternatives except for GWP, in which CBMF ranks first after the scenario analysis.

Table 5.11 Percentage reductions after scenario analysis

Scenario	Shotcrete ICF		G. Steel ICF		CBMF		SEBF	
	CED	GWP	CED	GWP	CED	GWP	CED	GWP
Paint and EPS	6.32%	6.46%	2.36%	2.48%	2.29%	1.48%	-	-
Steel bars, plate, and ties	12.81%	13.89%	4.80%	6.32%	1.13%	0.85%	0.19%	0.29%
Wall design	3.51%	7.06%	-	-	9.60%	11.12%	11.68%	15.58%

Table 5. 12 Ranking of four façade before and after scenario analysis

<b>Rank</b>		<b>Shotcrete ICF</b>	<b>G. Steel ICF</b>	<b>CBMF</b>	<b>SEBF</b>
By CED	Before scenario analysis	3	4	2	1
	After scenario analysis	3	4	2	1
By GWP	Before scenario analysis	3	2	4	1
	After scenario analysis	4	3	1	2
By cost		3	2	4	1

Overall, this study indicates that the operational phase makes the greatest environmental impact across all façade systems, followed by the material production phase, transportation phase and construction phase. In comparison with the reference façade (CBMF), total CED of SEBF is decreased by 39.13% while CED of Shotcrete ICF and G. Steel ICF is increased by 8.32% and 7.32% respectively. On the other hand, GWP is decreased by 18.07%, 12.47% and 6.88% for SEBF, G. Steel ICF and Shotcrete ICF respectively. The scenario analysis reduces CED and GWP of all façades with a major impact on Shotcrete ICF. The economic assessment showed that the reference façade (CBMF) has the highest cost. In comparison, the cost of SEBF, G. Steel ICF and Shotcrete ICF is reduced by 47.87%, 22.44% and 4.59% respectively.

## 5.8 Summary

This chapter presents a comparative assessment of three façades systems with a conventional façade system used in Ghana. A sustainable design process is modelled to guide stakeholders involved in the decision-making process to select façades with lower environmental impacts. In this approach, the developed BIM-based LCA method is applied to swiftly evaluate the lifecycle impacts of the different façade systems.

A detailed comparative assessment of G. Steel ICF, Shotcrete ICF and SEBF with the conventional CBMF is performed for a low-income Ghanaian residential building. Given the expected increase in housing developments, findings of this study are useful for selecting sustainable façades to lower their environmental impacts. An important contribution is therefore the detailed life cycle assessment of Shotcrete IFC, G. Steel IFC in each stage and a deliberate consideration of the construction industry in Ghana. Also, the assessment serves as pioneer research for more comprehensive life cycle assessments in future.

This study covers the entire life cycle of all four façade except the end-of-life stage where reliable data are not available for Ghana. The comparative assessment revealed that SEBF can save up to 39.13% of CED, 18.07% of GWP and 47.87% of the cost. Also, for all facades, the operational stage accounts for the largest life cycle impact whereas material production accounts for most of the embodied impact. Scenario analyses indicate that the impact of transportation is significant, as sourcing materials locally can reduce CED and GWP of Shotcrete IFC by over 18%.

The developed framework is also suitable for assessing buildings in similar regions with immature LCA applications given the adoption of the ICE database. The exact transportation, construction, operation and end-of-life situation can then be evaluated and combined with the material production stage to provide the total environmental impact of a building. The approach can also be applied to different building elements/components as well as archetypes.

Although the framework is applicable to the entire building, it is demonstrated for the façade system. Furthermore, design optimizations and decision-making strategies would be incorporated into the framework to investigate diverse building archetypes, multiple geographical regions and include the end-of-life stage in the following chapters.

## CHAPTER 6 TIER-HYBRID UNCERTAINTY ANALYSIS APPROACH FOR LIFECYCLE IMPACT ASSESSMENT

This chapter aims to study the uncertainties in the lifecycle assessment of buildings in order to improve the accuracy and precision of LCA results. A novel tier-hybrid method which integrate quantitative and qualitative uncertainty characterization is applied to evaluate the impacts of parameter uncertainties while proper assumptions are adopted to explore scenario and model uncertainties.

A second typical public rental housing block in Hong Kong is selected as a case study. The building is characterized by a reinforced concrete structure with prefabricated components. The gross floor area and total height are 12488 m<sup>2</sup> and 107 m, respectively. There are 36 habitable floors with 10 standardized flats on each. The ground floor and roof house electro-mechanical equipment. The design information and material specifications are acquired from a BIM model of the building as illustrated in Fig. 6.1.

### 6.1 Assessment of embodied impacts

Deterministic and stochastic analyses are performed for each building material or process which is summed up for comparison in Tables 6.1 and 6.2. The mean overall lifecycle impacts (B2) are estimated as 6.86 GJ/m<sup>2</sup> and 638.28 kgCO<sub>2</sub>/m<sup>2</sup>, which are consistent with the deterministic results (B1). The minimum and maximum lifecycle impacts are 67.69% and 137.42% of the mean CED while 68.79% and 134.83% of the mean GWP. SDs of the overall CED and GWP are determined to be 0.76 GJ/m<sup>2</sup> and 71.75 kgCO<sub>2</sub>/m<sup>2</sup> with corresponding CVs of about 11.79%.

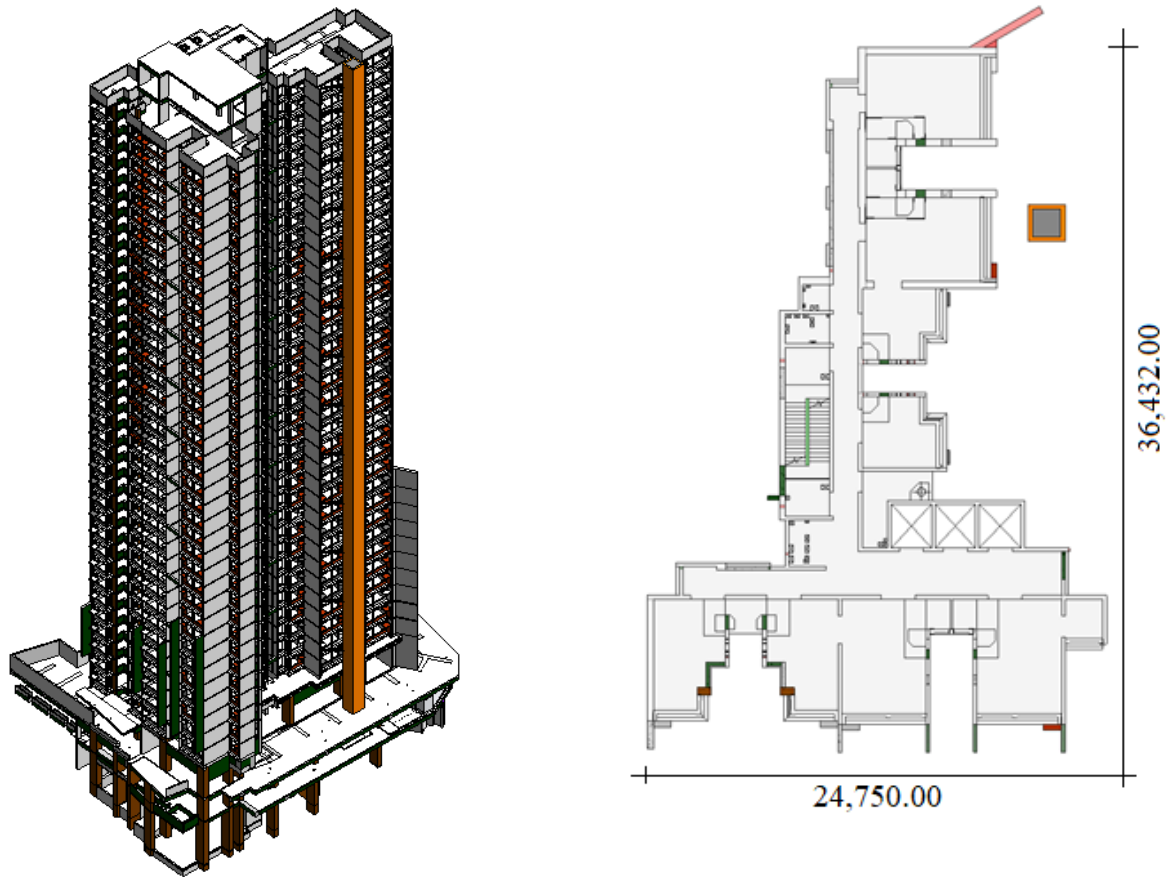


Fig. 6.1 BIM model and a typical floor plan of the case building

Table 6.1 Comparison of the stochastic and deterministic cumulative energy demands

Lifecycle phase	Cumulative energy demand (GJ/m <sup>2</sup> )			
	Deterministic (B1)	Stochastic (B2)		
		Mean	Minimum	Maximum
Material production	4.99	4.99	3.62	6.67
Building maintenance	1.34	1.34	0.79	1.95
Transportation	0.30	0.29	0.09	0.80
Construction	0.23	0.23	0.15	0.23
Total lifecycle impacts	6.86	6.86	4.65	9.43

Table 6.2 Comparison of the stochastic and deterministic global warming potential.

Life Cycle Phase	Global Warming Potential (kgCO <sub>2</sub> -eq./m <sup>2</sup> )			
	Deterministic	Stochastic		
		Mean	Minimum	Maximum
Material Production	494.91	495.78	357.84	647.16
Building Maintenance	87.56	87.52	53.12	124.57
Transportation	22.09	22.16	6.83	44.51
Construction	32.99	32.82	21.27	44.36
Total life cycle phase	637.56	638.28	439.05	860.60

Contribution analyses in terms of CED and GWP are presented in Figs. 6.2 and 6.3, respectively. It is observed that over 54% of CED and 66% of GWP are generated from the use of concrete and steel. Other materials also contributed significantly higher to both CED and GWP than reported in previous literature [98,112,187]. Particularly, windows, doors, composite mortar and ceramic tiles together contribute over 19% of both GWP and CED because of their high impact coefficient despite the low usage rate. From the perspective of uncertainties in material production, CV of each material ranges from 8.9 to 15.95 indicating a low dispersion around the mean. Materials yielding the highest uncertainties include windows, doors, aluminum, paint and formwork.

Fig. 6.4 illustrates a contribution analysis of the maintenance stage. It is assumed that public rental residential buildings have very limited opportunities of major renovations, so that building occupants have less influences over building maintenance. All maintenance activities throughout the lifecycle of the building is only to keep the required basic performance.

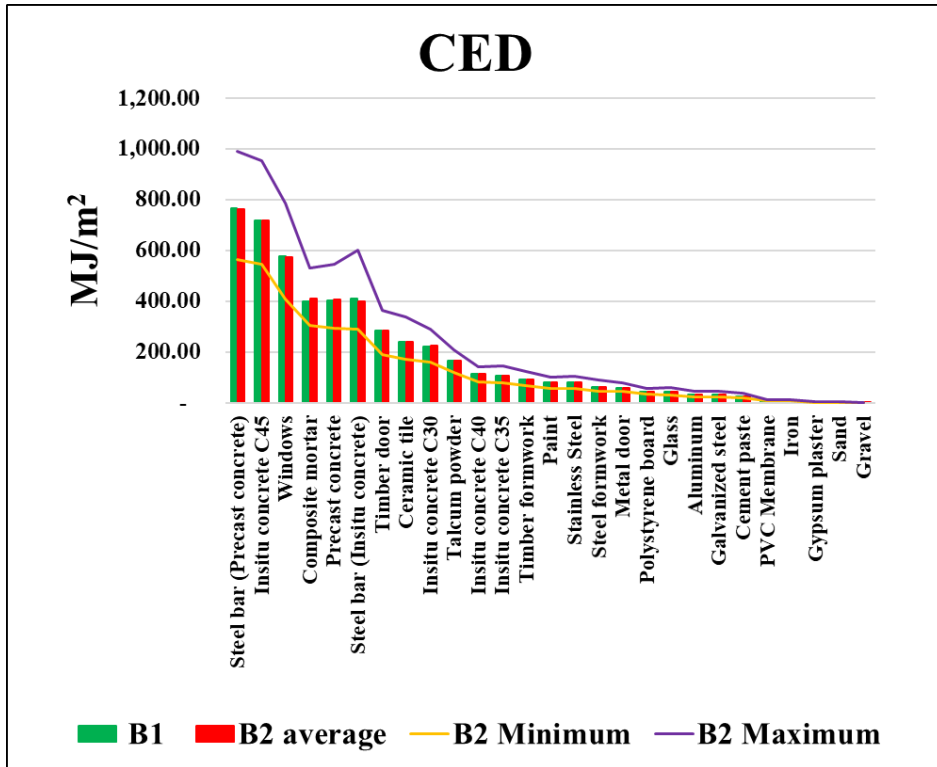


Fig. 6.2 Contribution analysis of material production phase (CED)

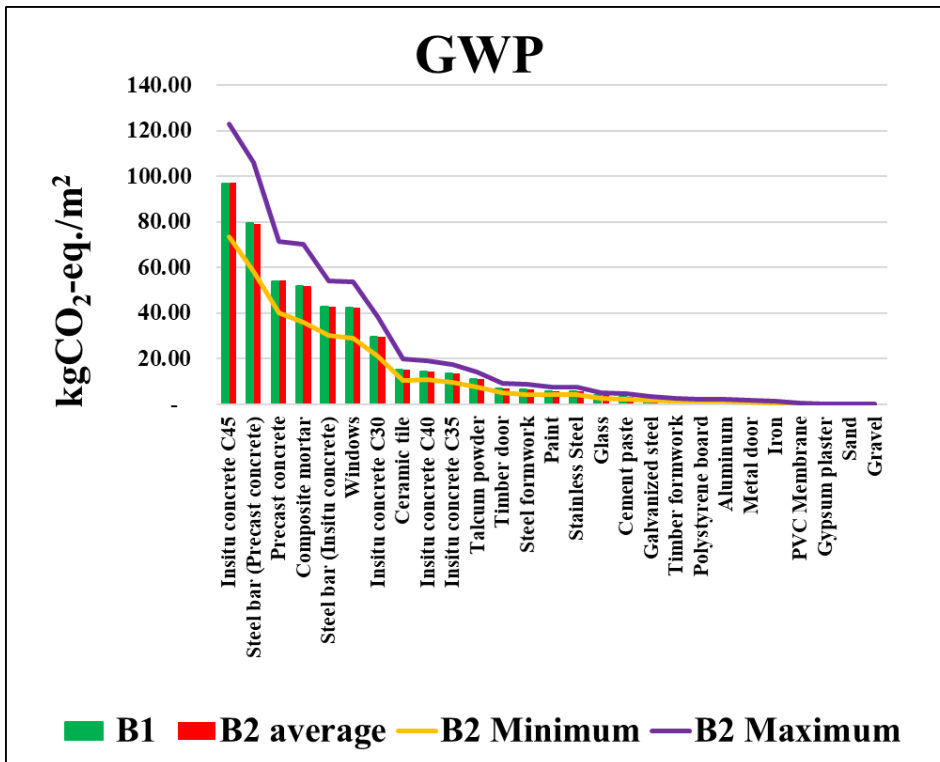


Fig. 6.3 Contribution analysis of material production phase (GWP)

Due to the complexities in modelling the actual degradation of components in high-rise buildings (e.g. challenges in visual inspection and lack of maintenance data), this study employs fixed cycles of replacement as applied in previous studies. The variations in the service life of building components and materials are counted as uncertainties in this lifecycle phase. From Fig. 6.4, it is observed that the majority of the impacts is from windows, doors and paint contributing 87.75% of CED and 82.28% of GWP. Composite mortar, glass, aluminum, PVC membrane and gypsum plaster correspondingly constituted 12.25% of CED and 17.69% of GWP. Although the latter contributed less, larger uncertainties are observed due to great variation in their maintenance schedules. The overall CV for the maintenance phase is found to be 24.59%. Given the contribution of these materials to both material production and maintenance, the comprehensiveness of system boundaries is critical for LCA results and therefore requires necessary adjustments especially when only primary materials are considered.

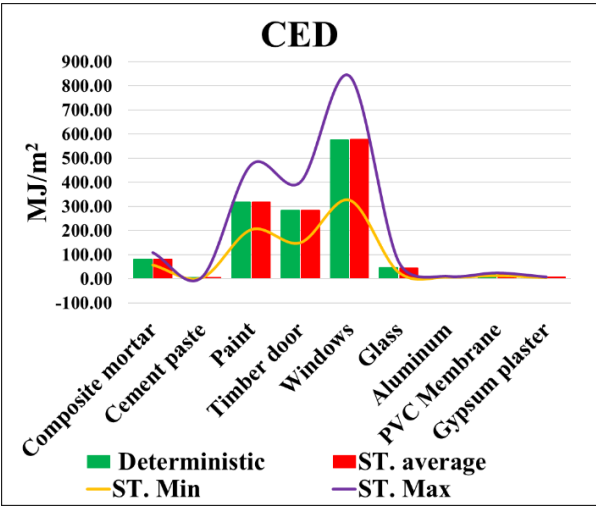


Fig. 6.4a Cumulative energy demand

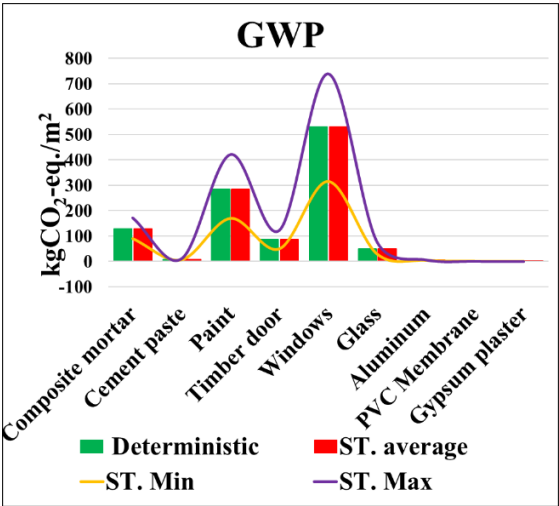


Fig. 6.4b Global warming potential

Fig. 6.4 Contribution analysis of building maintenance phase

CVs of the transportation and construction phases are comparatively higher although their contributions to the total lifecycle impact are very low. Specifically, the overall CV of transportation is 29.73% due to the wide variation in the transportation distance of materials other than precast and insitu concrete. Similarly, the CV of construction phase is 19.47% owing to the assumption that construction process details are estimated based on previous literature. Nonetheless, the findings are coherent with Teng and Pan (2020) which recorded much higher uncertainties in the transportation and construction phases.

## **6.2 Scenario uncertainties**

### **6.2.1 End-of-life cycle strategies**

Currently, recycling of demolished materials at the end of a building's life cycle is promoted in circular economy literature [214]. In this context, end-of-life management strategies such as selective demolishing, onsite or offsite sorting and recycling may increase the contribution of the end-of-life phase. Scenarios EoL1 and EoL2 consider two end-of-life management strategies.

In EoL1, demolished materials are transported to an offsite sorting yard, non-inert materials (e.g. wood and paper wastes) are landfilled and concrete is disposed at public filling areas, whereas steel is recycled. Embodied impacts from recycling are estimated using the impact coefficients of materials with an assumption of 100% recycled contents. As indicated in Fig. 6.5, the mean value for recycling alone results in a saving of 0.69 GJ/m<sup>2</sup> in CED and 33.10 kgCO<sub>2</sub>/m<sup>2</sup> in GWP. Demolition, sorting and transportation jointly increase CED by 0.24 GJ/m<sup>2</sup> and GWP by 34.91 kgCO<sub>2</sub>/m<sup>2</sup>. In total, EoL1 results in a net CED saving of 0.45 GJ/m<sup>2</sup> but net GWP increase of 1.80 kgCO<sub>2</sub>/m<sup>2</sup>. The foregoing scenario assumes the shortest transportation distance for all activities. To further explore the impact of transportation, 24 other possible sub-scenarios generated by combining different sorting and public disposal/landfill sites in Hong

Kong are presented in Fig. 6.6. The impact of transportation is highlighted as a combination of the longest transportation distances can increase CED by 2.7 times and GWP by 13.7 times.

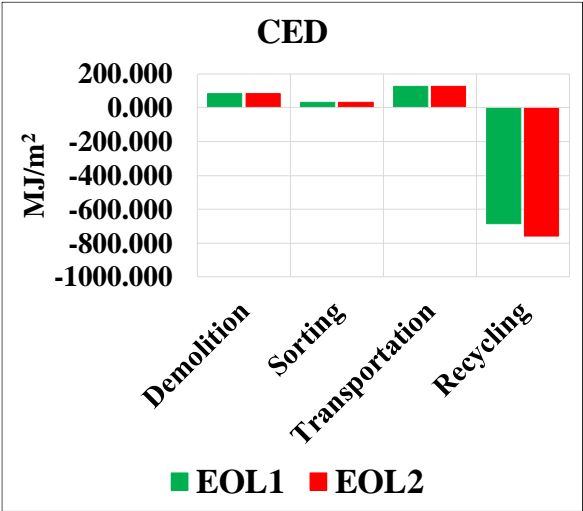


Fig. 6.5a Cumulative energy demand.

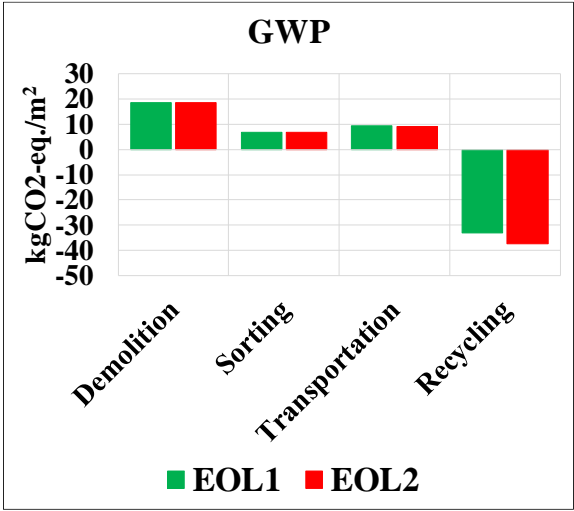


Fig. 6.5b Global warming potential.

Fig. 6.5 Comparison of end-of-life management strategy 1 and 2

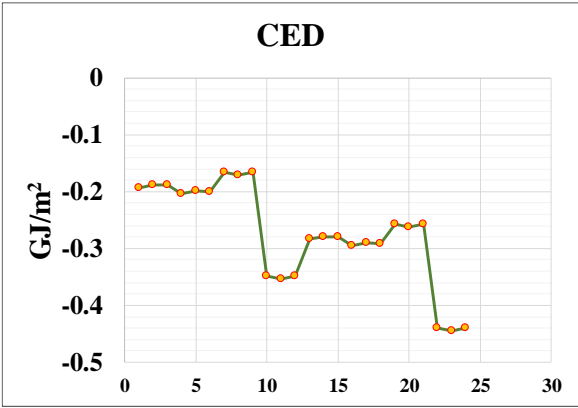


Fig. 6.6a Cumulative energy demand

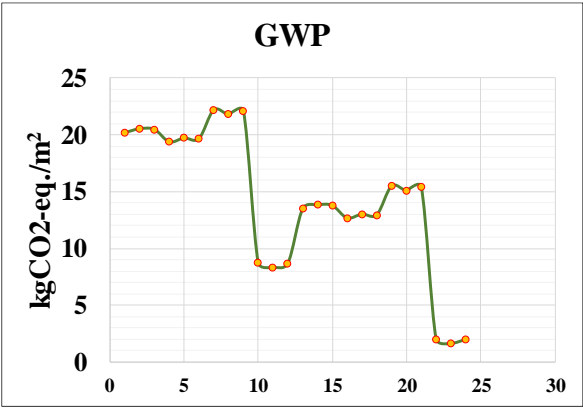


Fig. 6.6b Global warming potential

Fig. 6.6 Scenario analysis of end-of-life management strategy 1

EoL2 considers a selective demolishing strategy in which wood wastes and aluminum in windows are sorted on-site while all other demolished materials are sorted offsite. This strategy is designed to include an extensive recycling of materials including aluminum, galvanized steel, iron steel and timber. Other materials such as concrete are disposed at public

filling areas. The mean value for the recycling scenario indicates savings of 0.76 GJ/m<sup>2</sup> in CED and 37.34 kgCO<sub>2</sub>/m<sup>2</sup> in GWP. The total mean values for demolition, sorting and transportation increase CED by 0.24 GJ/m<sup>2</sup> and GWP by 34.57 kgCO<sub>2</sub>/m<sup>2</sup>. Cumulatively, net savings of 0.52 GJ/m<sup>2</sup> in CED and 2.78 kgCO<sub>2</sub>/m<sup>2</sup> in GWP are achieved. Also, the results from 8 sub-scenarios are shown in Fig. 6.7. It can be observed that the mean values of the base scenario EoL2 could be increased by 2.1 and 6.2 times for CED and GWP respectively given that the farthest sorting, landfill or public filling areas are used.

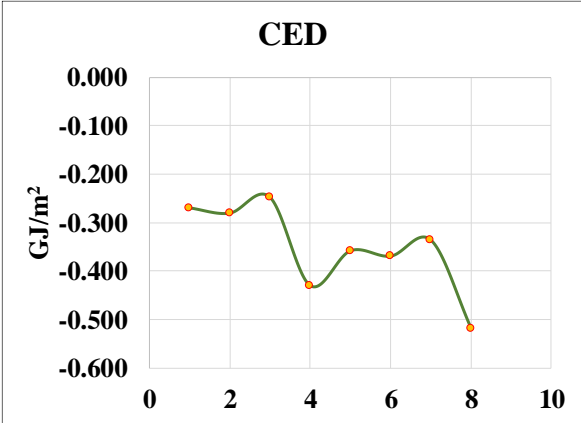


Fig. 6.7a. Cumulative energy demand.

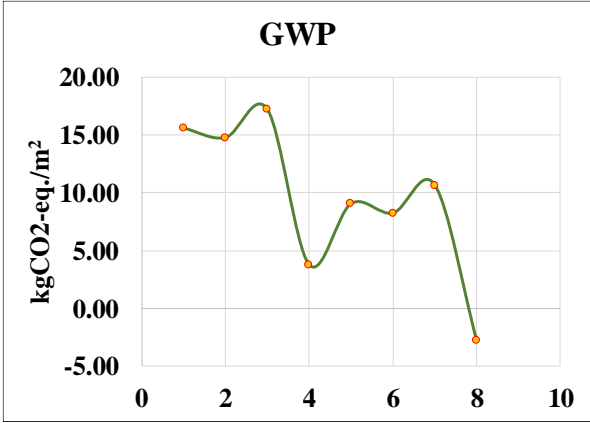


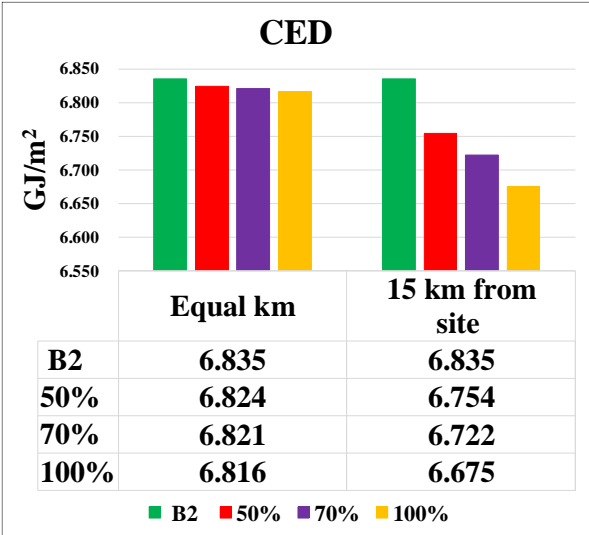
Fig. 6.7b Global warming potential.

Fig. 6.7 Scenario analysis of end-of-life management strategy 2

**6.2.2 Alternative materials**

The use of recycled aggregates is considered a strategy to reduce the energy use and carbon emission, so that SC1 is defined to evaluate the impact of recycled aggregates for concrete production. Furthermore, two sub-scenarios are defined to explore the impact of transportation within this context. The first sub-scenario assumes that aggregates are recycled at a site with an equal transportation distance to the production site of virgin aggregates. The second sub-scenario on the other hand considers a recycling site 15 km away from the insitu or precast concrete production site. For each sub-scenario, usage rates of 50%, 70% and 100% are

considered for recycled aggregates. Fig. 6.8 presents a comparison between the two sub-scenarios and with B2. Considering an equal transportation distance, a very minor reduction in the total lifecycle CED is observed across the three usage rates (less than 1% for CED and 1.2% for GWP). Thus, increasing the usage rate of recycled aggregates yields insignificant impact on LCA results. For a recycling plant 10 km away from the concrete production site, a slightly higher impact is observed. The CED is reduced by 1.19%, 1.65%, 2.34% for 50%, 70% and 100% usage rates respectively. Similarly, the GWP is reduced by 0.92%, 1.35%, and 1.91%. It can be observed that LCA results are more sensitive to increases in the usage rate which can decrease transportation distances. Such observations echo with [215], which explored the lifecycle impacts of recycled aggregates for concrete production in China.



**Fig. 6.8a** Cumulative energy demand.

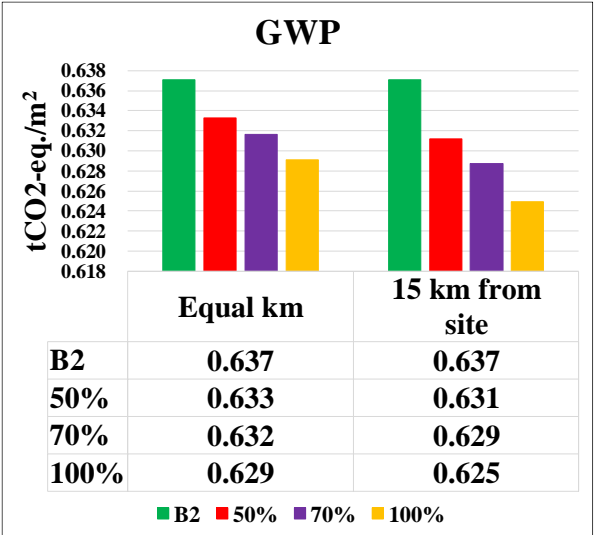


**Fig. 6.8b** Global warming potential.

**Fig. 6.8** Impact reduction from the use of recycled aggregates.

The use of cementitious materials is a major source of the energy use and carbon emissions, so that SC2 and SC3 are defined to replace OPC with GBFS and PFA respectively. Furthermore, replacement rates of 50%, 70%, and 80% are defined for both materials as sub-scenarios. Replacement of OPC is performed for three materials namely concrete, composite

mortar and cement paste. Fig. 6.9 illustrates the reduction in CED and GWP for both GBFS and PFA in comparison to B2. It can be observed that the use of GBFS reduces the overall average CED by 8.11%, 11.34% and 12.95% for 50%, 70% and 80% replacement rates respectively. Comparatively, higher GWP reductions of 11.8%, 15.95% and 18.24% are achieved for the same replacement rates. With the use of PFA, 6.13%, 8.57% and 9.79% reductions in CED are achieved for 50%, 70%, 80% replacement rates respectively, while 8.65%, 12.13% and 13.88% reductions are achieved in GWP for the same replacement rates.

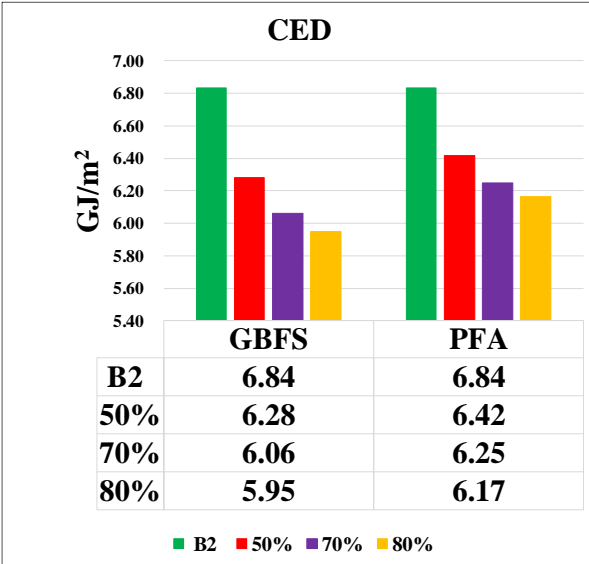


**Fig. 6.9a** Cumulative energy demand.

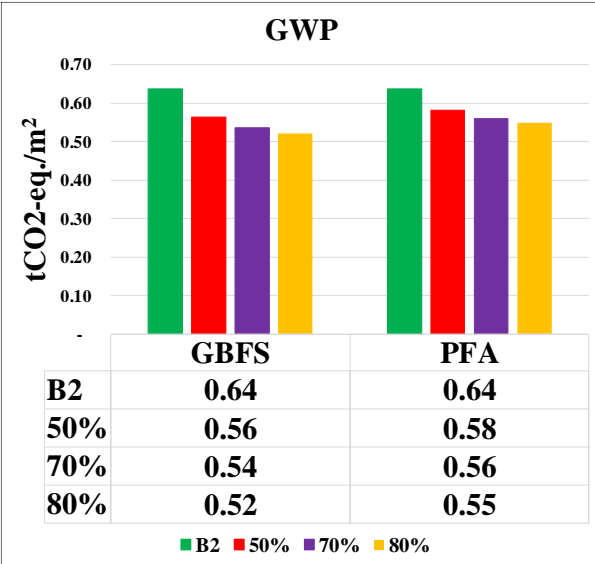


**Fig. 6.9b** Global warming potential.

Fig. 6.9 Impact reduction from the use of alternative cementitious materials.

**6.3 Model uncertainties**

Scenarios M1 and M2 examine the effect of analytical model uncertainties for LCA results. For the baseline stochastic assessment (B2), a tier-hybrid approach is applied by incorporating a lognormal distribution for DQI components and normal distribution for statistical components. Alternative distributions such as triangular, uniform and normal are

further coupled with the proposed hybrid method or a pure DQI approach to study their potential impact on LCA results. Table 6.3 presents a comparison of the overall mean impact of alternative distributions on the proposed tier-hybrid approach and pure DQI approach.

For scenario M1, it should be noted that only probability distributions of DQI-based parameters are modified whereas statistical parameters are held constant. In comparison to the lognormal distribution, the overall sample mean of uniform, normal and triangular distributions is about 6% lower with similar implication in their standard deviations. Moreover, the CV for each distribution does not vary significantly (about 11%).

In the case of M2, it can be observed that the mean overall lifecycle impact with lognormal distribution is slightly higher (1.6% for CED and 1.56% for GWP) than the base scenario (B2). Comparing the uniform, normal and triangular distributions to the lognormal distribution, decrements of about 3.5% are observed for both CED and GWP. From the perspective of CVs, the pure DQI approach yields a slightly lower value across all distributions (approximately 9%).

In general, few studies have evaluated uncertainties in building LCA. Among these studies, a semi-quantitative approach incorporating the DQI-based assessment and stochastic simulation is commonly used. A pure statistical distribution of uncertainty parameters could increase the reliability of DQI based assessments but has scarcely been applied in literature. This research therefore applied a tier-hybrid approach integrating pure statistical distributions and DQI-based methods to evaluate uncertainties in the lifecycle CED and GWP of a case building in Hong Kong.

Table 6.3 Comparison of overall mean lifecycle impacts, standard deviation and coefficient of variation from different probability distributions.

Approach	Distribution	CED			GWP		
		$\mu'$ (GJ/m <sup>2</sup> )	$\sigma$	CV	$\mu'$ (kgCO <sub>2</sub> -eq./m <sup>2</sup> )	$\sigma$	CV
Tier-hybrid (M1)	Lognormal	6.86	0.76	11.74	638.28	71.75	11.79
	Uniform	6.46	0.72	11.68	602.20	67.15	11.68
	Normal	6.47	0.72	11.53	601.52	67.10	11.68
	Triangular	6.46	0.72	11.64	602.00	67.39	11.73
Pure DQI (M2)	Lognormal	6.97	0.63	9.62	647.50	59.99	9.84
	Uniform	6.71	0.62	9.84	624.88	56.30	9.47
	Normal	6.70	0.62	9.73	624.17	57.45	9.75
	Triangular	6.68	0.61	9.32	623.99	57.37	9.73

The reliability of the tier-hybrid approach is validated as the mean CED and GWP at different levels of assessments (e.g. individual materials and processes, lifecycle phases and overall impacts) are consistent with the deterministic results. Thus, it is validated for further discussion of the afore-described analysis. Considering the deterministic results alone could lead to misinterpretation of LCA results as it does not reflect potential variations in input parameters. From the perspective of lifecycle phases, the material production phase contributes

the largest impact but the least uncertainty. On the contrary, transportation, construction and end-of-life phases with relatively lower impacts are embedded with very large uncertainties. High uncertainties in the transportation phase can be explained by the large variation in transport distances of modeled materials. High uncertainties in the construction phase can be attributed to poor quality input data based on assumptions and estimations from previous studies. Similarly, the rarity of end-of-life cycle modelling implies the use of unverified or unrepresentative input data. This study further explores the contribution of each material to the impact of the material production stage. As commonly reported, concrete and steel contribute the majority of building impacts, although lower than reported in previous studies. The contribution of other materials such as windows and doors is significant with even higher uncertainties than primary materials like steel and concrete. Wide variations are observed in the impact coefficient of the former group in comparison to the later.

Based on the scenario analysis, essential approaches to reducing lifecycle impacts are identified. For the end-of-life management strategies, the demolishing, transportation and sorting process increases the overall lifecycle impact, but recycling strategies can reduce such impact especially when extensively adopted. As a proof, EoL2 reduces CED and GWP by 7.78% and 0.43% respectively, while much a higher GWP saving can be achieved with a cleaner fuel mix. Key attention must be given to transportation as the impact of end-of-life activities is highly sensitive to alternative sorting, landfill and public filling areas. From the perspective of alternative materials, maximum carbon savings are achieved by using GBFS and PFA to replace OPC with significantly higher energy and carbon coefficients. Specifically, up to 12.9% (CED) and 18.2% (GWP) savings can be achieved with GBFS while 9.8% (CED) and 13.79% (GWP) with PFA. On the contrary, using recycled aggregates yields very limited impact reductions of about 0.28% and 1.25% in CED and GWP respectively. By decreasing the transportation distance to the recycling site, the maximum CED and GWP savings can be increased to 2.34%

and 1.91%, respectively. Totally, up to 19.91% of the overall CED and 15.23% of the overall GWP can be saved through a combination of alternative materials and end-of-life management strategies.

The results of the model/analytical uncertainty imply that the final output uncertainty is highly correlated with defined probability distributions rather than the uncertainty characterization method. Hence integrating the pure statistical approach based on adequate data with the DQI method can reflect uncertainties more precisely. However, the proposed tier-hybrid approach can increase dispersion of LCA results as pure statistical distributions are collected from a wide range of sources. Finally, the selection of probability distributions can significantly vary statistical modelling outcomes, so that particular attention must be paid to the tier-hybrid approach when combining different probability distributions.

## **6.4 Summary**

This chapter evaluated the uncertainties in the lifecycle assessment of buildings using a reliable tier-hybrid approach. The pure statistical and DQI approaches are integrated to increase the comprehensiveness and accuracy of uncertainty evaluations. A case study was performed on a typical public rental housing block in Hong Kong using both deterministic and stochastic approaches, where lifecycle impacts are expressed in terms of CED and GWP. The stochastic approach exemplifies the proposed tier-hybrid approach which can be adopted by LCA modelers in future. In this approach, pure statistical distributions are applied when rich information is available and complemented with expert judgement (DQI) where information is insufficient. Insights from the study provide a basis to interpret future LCA results in which multiple probability distributions are jointly applied in an analytical model. Hence the impact of arbitrarily assigning probability distributions due to data deficiency can be appropriately quantified.

The results of this study validate the initial hypothesis that a tier-hybrid method can improve the efficiency and accuracy of the uncertainty evaluation in building LCAs. Firstly, the results of this approach are proven valid because the mean stochastic outputs are almost the same as the deterministic results. It can be therefore concluded that the statistical characterization of uncertainties coupled with the DQI approach is an accurate method to characterize and propagate building LCA uncertainties. Secondly, the study further strengthens this approach by illustrating the effects of different probability distributions for the exploration of analytical uncertainties. It should be noted that the results vary slightly when the tier-hybrid approach is compared with the pure DQI approach. Lastly, the study illustrates the impacts of different probability distributions on the tier-hybrid approach in tandem with the impact of probability distribution on the pure DQI approach.

The main findings from evaluating scenario and model uncertainties can be summarized as follows:

- The material production stage yields the least uncertainties although it contributes the most to the overall lifecycle impact.
- The overall uncertainties in other phases are significantly higher than the material production stage, and decrease in the order of transportation, maintenance, to construction.
- An extensive end-of-life management strategy can produce significant CED savings which will be translated into a lower GWP using a cleaner fuel mix.
- Replacing virgin aggregates with recycled aggregates yields minor impact reduction, whereas replacing OPC with GBFS or PFA produces large CED and GWP savings.

Overall, this study provided deep insight into applying a tier-hybrid approach to evaluate the uncertainties in the lifecycle of buildings. In future research, the collection of data

for pure statistical methods could be stratified to facilitate a more detailed estimation of uncertainties. Basic uncertainties can be processed as a function of pure measurement errors, while additional uncertainties can be processed as a function of geographical, temporal or technological differences.

## **CHAPTER 7 STAGED WHOLE LIFECYCLE ENERGY OPTIMIZATION ALTERNATIVE COMPOSITE FAÇADE SYSTEMS FOR MID-RISE RESIDENTIAL BUILDINGS**

Following the comparative study in Chapter 5, this chapter aims to optimize the performance of a mid-rise residential building using the developed method. Multi-objective optimizations are performed considering the four façade systems, other passive design parameters and renewable energy systems. The optimization is executed in a stepwise approach while considering the trade-off between embodied and operational impacts of the building. The systematic approach followed for this two-staged approach is illustrated in Fig. 7.1. First a base model is designed parametrically with reference to local data on residential buildings followed by an optimization of the building geometry and renewable energy system. The result of the first stage optimization is then processed for a second optimization of the trade-off between the embodied and operational impacts.

### **7.1 Case study building model**

The case study model is a mid-rise residential building located in Accra, Ghana. Such buildings are classified as mid-income dwellings. The building was designed with reference to as-built drawings retrieved from the owner and a field survey and is representative of a typical residential building in sub-Saharan Africa. The building is a 10-floor apartment block with a total area and height of 30 m. The floor plan and 3D model are shown in Figure 7.2. Each floor has 4 units, a stair, an elevator, and a corridor which leads to the four units. Also, each unit consists of a living room, kitchen, washroom, storeroom and three bedrooms with a total surface area of 480 sq.m. The envelope of the base case consists of a 150 mm sandcrete block wall with a 15 mm thick cement sand render on both sides, a 100 mm reinforced concrete floor, with 25 mm thick cement sand mortar and ceramic tiles, an Aluzinc metal roofing sheet with timber carcassing, and 6 mm clear single glazed aluminum windows. A parametric model of the case

building is built in McNeel Rhinoceros/Grasshopper which is a valid modelling platform with plugins for numerous analyses including the energy simulation using Ladybug and Honeybee [37].

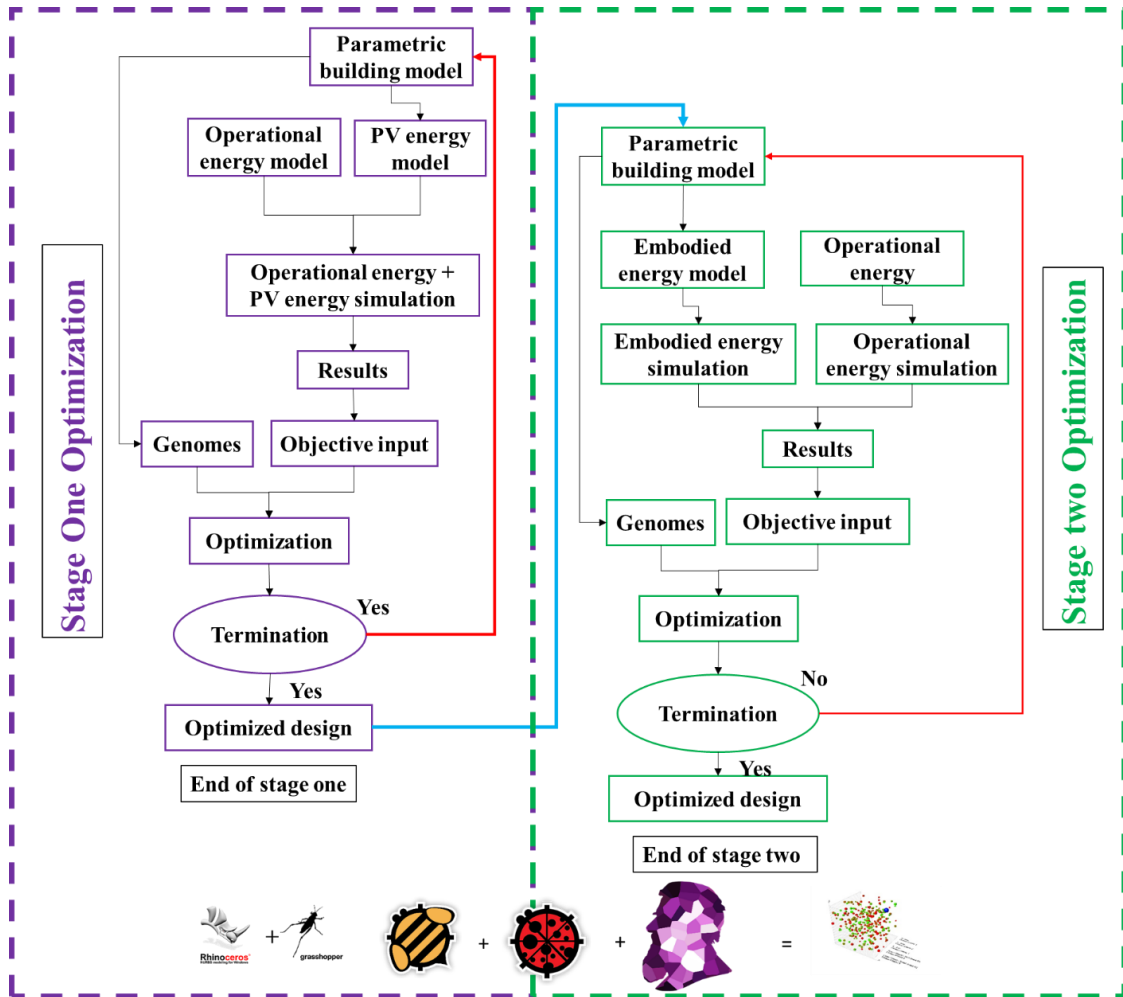


Fig. 7.1 Framework for two-stage optimization of residential building

Regarding the thermal zones, each space within the units, the connecting corridor and stairs are considered as separate thermal zones. The building schedules illustrated in Figures. 7.3 and 7.4 were defined through a survey with the building occupants. The figures illustrate a daily profile which is composed of hourly values. Each hourly value represents a fraction of the occupancy, HVAC, lighting, or equipment uses in relation to the peak values (i.e. 1.0). All living spaces are occupied during non-working hours whereas corridors and stairs are occupied

before and after non-working hours. All spaces are equipped with a split-type air conditioner (COP of 2.6) except the connecting corridors, stair, storerooms, and washrooms which are naturally ventilated. The building requires only cooling and a cooling setpoint of 24 °C is defined.

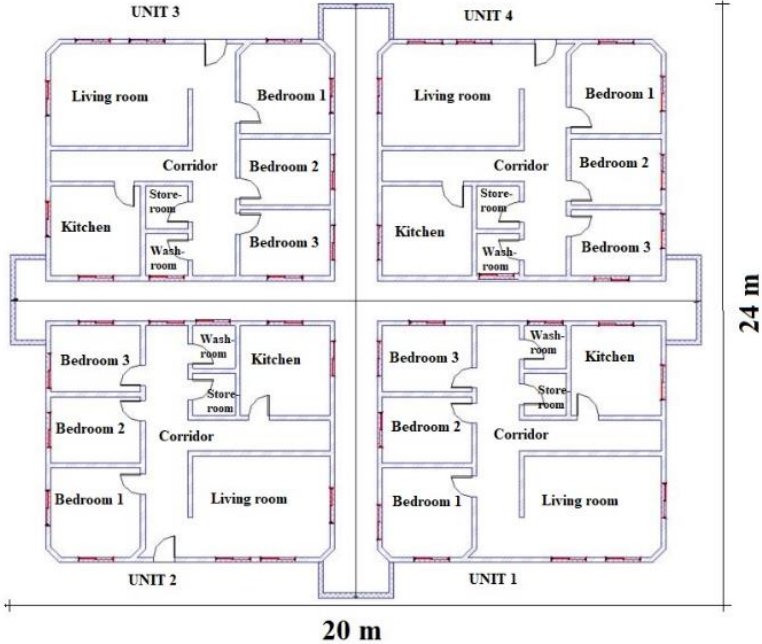


Figure 7.2a Floor plan

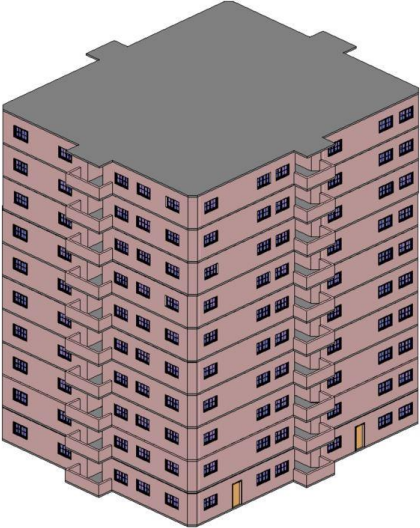


Figure 7.2b Floor plan

Fig. 7.2 Floor plan and 3D BIM model of the case study building

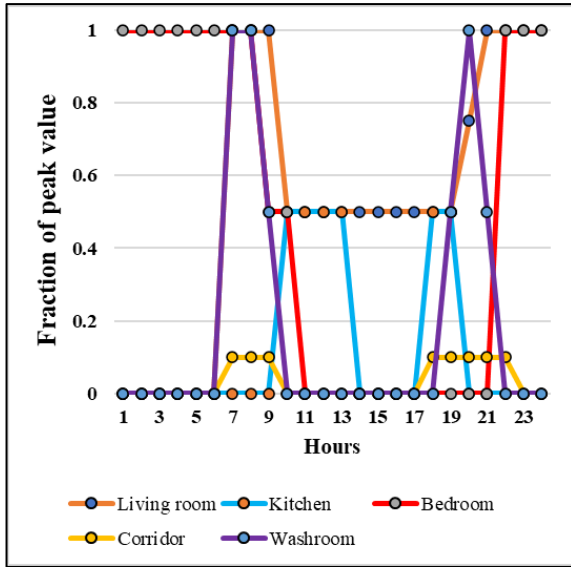


Figure 7.3a Occupancy schedule

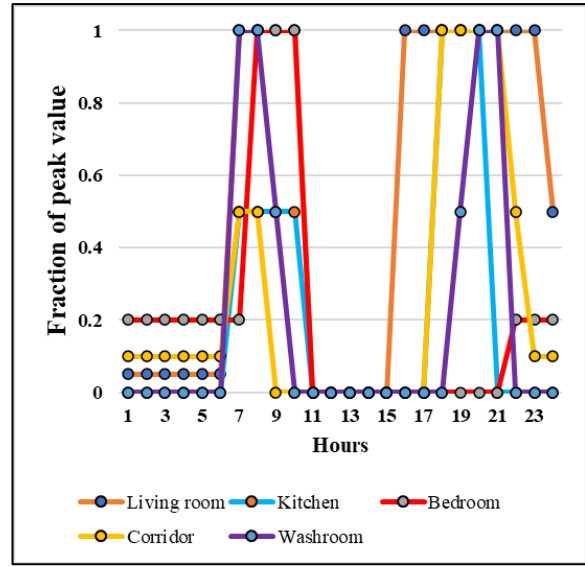


Figure 7.3b Lighting schedule

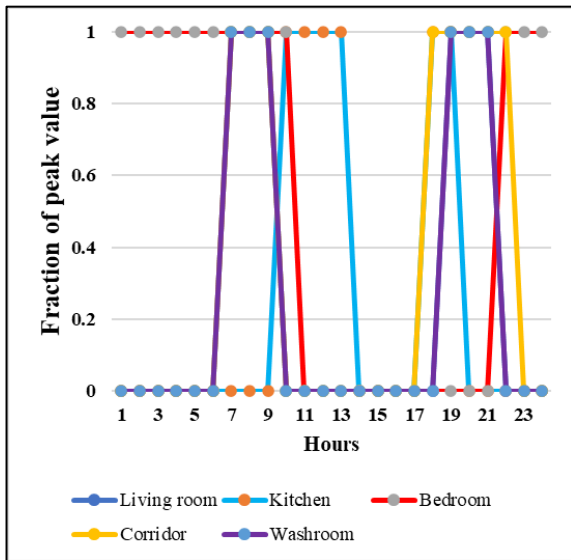


Figure 7.3c HVAC schedule

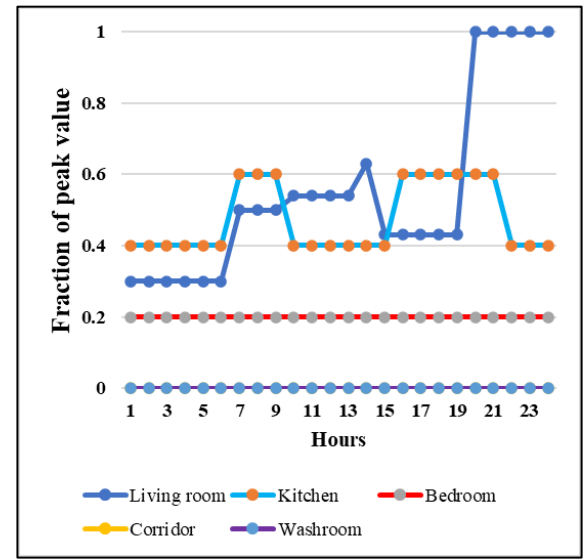


Figure 7.3d Equipment schedule

Fig. 7.3 Weekday building schedules

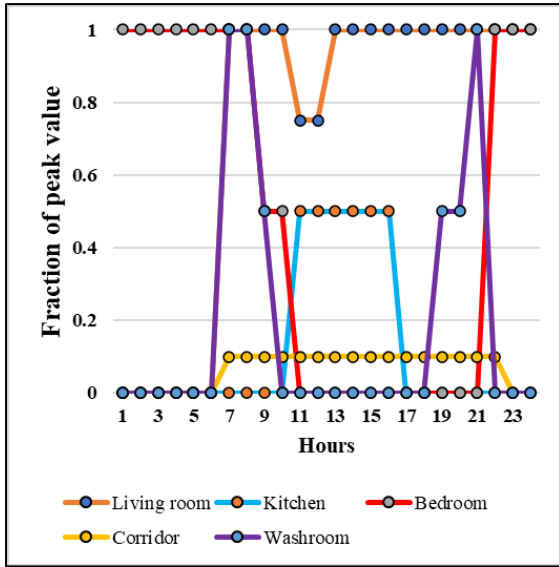


Figure 7.4a Occupancy schedule

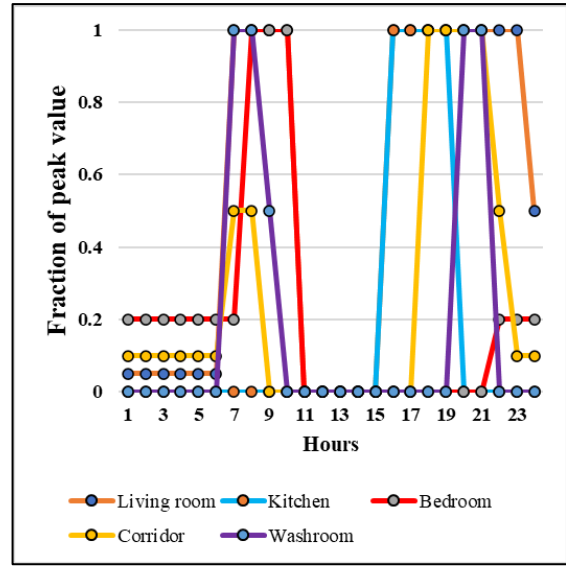


Figure 7.4b Lighting schedule

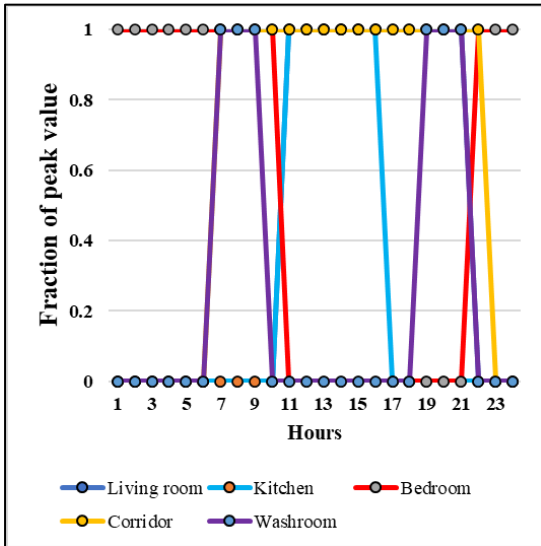


Figure 7.4c HVAC schedule

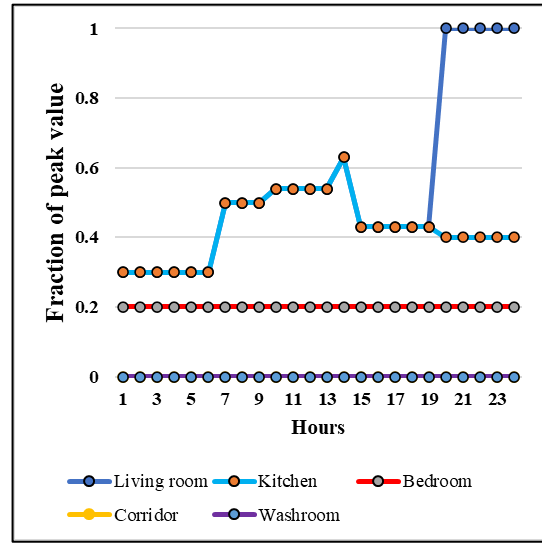


Figure 7.4d Equipment schedule

Fig. 7.4 Weekend building schedules

The study explores a number of passive and active design strategies related to building geometry, renewable energy application and the thermophysical properties of façades used within the region of the case study building [216]. The strategies related to building geometry and renewable energy systems were selected with reference to the reviewed studies and summarized in Figure 5. For the thermophysical properties of the façades, a field survey was

conducted to identify different local façade types and materials used within the region. Detailed descriptions of the survey on different local façade types are provided in Chapter 5 [217]. Through the survey, four local façades including that of the base case model were identified. In addition, a BIPV window is also investigated in this study. The passive strategies and active strategies investigated include window-to-wall ratio, building orientation, external wall material type and external wall materials thickness, HVAC system, rooftop photovoltaic system and the BIPV window. Particularly, the façade materials are defined according to commercially available prototypes in order to provide a realistic result which is practically applicable to the region. Opaque mono-crystalline silicon modules with an average conversion efficiency of 15% are used for the rooftop PV whereas semi-transparent amorphous silicon modules with a conversion efficiency of 6.3% are used in the windows of the BIPV window [171]. The rooftop PV is assumed to cover 90% of the roof space in order to ensure roof accessibility. Various orientations of the solar panel were investigated to maximize the PV electricity generation. The range of the design parameters investigated, and the construction detail of the studied façades are illustrated in Table 7.1.

The case study building is located in Accra with a Tropical Savanna Climate (Aw) under the Koppen-Geiger climate classification. The dominant characteristics are prolonged hot summers with moderate rainfalls from March to mid-November. The monthly average outdoor temperature range between 23 °C and 34 °C whereas the daily outdoor average temperature ranges from 24 °C during the night to 30 °C during the day. According to the climatic data, the climatic condition in the northern areas of Ghana and other regions of sub-Saharan Africa vary significantly. Bearing in mind that climate is a critical determinant of building energy consumption, two other zones/countries are selected across sub-Saharan Africa to explore the impact of climate on the building cooling load. In particular, a capital city is identified in each zone/country to set a specific weather file: Nigeria (Abuja) and Burkina Faso (Ouagadougou).

An hourly weather file for each city is retrieved for the energy simulation model. The weather file for each city is retrieved from Climate Analytics in the EPW format for Energy Plus which is a widely used energy simulation program. These weather files are typical meteorological year (TMY) weather data which represent the long term mean weather conditions of the selected locations.

## **7.2 Energy analysis**

First the energy analysis is implemented in two stages simultaneously: operational energy analysis; and the embodied energy analysis. The operational energy simulation includes the net impact of building energy use (annual cooling, lighting, and equipment load) and PV energy generation. The parametric building model is connected to Honeybee plugin components which provide the function of energy simulation. Honeybee is utilized to assign constructions, internal loads, lighting, HVAC (ideal load) and occupancy schedules, and weather files. Hereafter, an IDF file is generated and run in EnergyPlus which produces the simulation output. The values for infiltration rate are preset in the Honeybee plugin which represent Passive house, tight building, ASHRAE 90. 1-2013, average building and Leaky building. The simulation output includes annual cooling, lighting, occupancy, and equipment loads. Similarly, Honeybee is used to parametrically define PV surfaces (including rooftop PV and semi-transparent vertical BIPV façades) which are coupled with a generator module. Weather data are then assigned to simulate the PV electricity generation. The total building energy use and PV electricity generation are both expressed in kWh/m<sup>2</sup>/yr. The building space load and physical characteristics are illustrated in Table 7.2.

Embodied energy is defined as the energy required for the material manufacturing, transportation, construction, maintenance and repairs, and the end-of-life cycle processes of the building. LCA is performed in this study to measure the embodied energy of different construction set and also to evaluate the trade-off between operational and embodied energy.

The LCA is performed with Grasshopper modelling tools. After assigning constructions to the building model, additional parameters are created using the native Grasshopper components to define the needed input parameters. The quantity of materials is extracted from the model and matched with embodied coefficient in Grasshopper. The embodied energy is then evaluated by multiplying the material quantities by their embodied coefficient. The system boundary is set for the material production stage to construction stage and the building lifespan is defined as 60 years. The impact of PV is calculated is also estimated per unit area and with a lifespan of 25 years so that the PV modules are replaced once in their lifetime. The embodied coefficient is sourced from Bath ICE since no country in sub-Saharan Africa has an LCA database. Similarly, the embodied energy of the building is expressed in terms of kWh/m<sup>2</sup>/yr.

### **7.3 Optimization settings**

A staged multi-objective optimization is performed by incorporating energy simulation and embodied impacts assessments tools with a multi-objective optimization algorithm to find the optimal building design from a lifecycle perspective. This approach allows the iteration of design parameters in search for a solution that correspond with the optimal design goals. The optimization is performed in Wallacei, an optimization plugin for Rhino/Grasshopper. Wallacei plugin is driven by a genetic algorithm and allows users to define iteration loops for different applications. Its analytical tools also allow different evaluations and visualizations of the optimization results. The workflow of Wallacei involved optimization design by defining inputs and output, setting (genetic algorithm parameters) and analytics (evaluation of results). The main inputs include genes (design parameters) and the design objectives (building energy demand, PV energy generation and embodied energy).

Table 7.1 Variable for the two-staged optimizations [8,217–219]

Variable		Values (unit)	Range (unit)	Notes
Building orientation		0 (°)	0 (°) - 180 (°).	15 ° interval
Window-to-wall ratio		0.35	0.15 - 0.80	0.05 interval
Façade infiltration rate		0.0003 (m <sup>3</sup> /s/m <sup>2</sup> )	0.0001, 0.000071 , 0.000285, 0.0003, 0.0006 (m <sup>3</sup> /s/m <sup>2</sup> )	Represent tight building, passive house, ASHRAE 90.1-2013, Average leaky building and leaky building, respectively.
Rooftop PV		90 (% of roof area)		Mono-Si cells with 15% conversion efficiency
BIPV Windows		90 (% window area)		Driven by WWR variable; a-Si cells with 6.3% conversion efficiency
Block wall and Mortar façade (BWMF)	Ext. render	12 (mm)	10 (mm), 12 (mm), 15 (mm)	
	Block wall	150 (mm)	100 (mm), 150 (mm), 200 (mm)	
	Internal render	12 (mm)	10 (mm), 12 (mm), 15 (mm)	
Shotcrete Insulated	Ext. shotcrete	15 (mm)	10 (mm), 12 (mm), 15 (mm)	

composite façade (SICF)	Mesh reinforcement	-	-	
	EPS insulation	78 (mm)	50 (mm), 78 (mm), 100 (mm)	
	Mesh reinforcement	-	-	
	Int. shotcrete	15 (mm)	10 (mm), 12 (mm), 15 (mm)	
Galvanized steel Insulated composite façade (GS. ICF)	Int. galvanized steel plate	0.6 (mm)	-	
	EPS insulation	78 (mm)	50 (mm), 78 (mm), 100 (mm)	
	Ext. galvanized steel plate	0.6 (mm)	-	
Compressed mud block façade (CMBF)	200 (mm)	150 (mm), 200 (mm), 250 (mm)		

The layers of façade are presented from the outer to inner layer

Table 7. 2 Building parameter settings

Variable	Value (unit)
Occupancy Activity level	2 (person/room) 120 (W/person)
Lighting gain	12 (W/m <sup>2</sup> )
Equipment gain	10 (W/m <sup>2</sup> )

Variable	Value (unit)
HVAC system	IdeaLoadAirSystem
Cooling setpoint	24 (°C)
Roof U-value	0.35 (W/m <sup>2</sup> °C)
Floor U-value	1.5 (W/m <sup>2</sup> °C)
Window U-value	5.69W/m <sup>2</sup> k)

Likewise, the corresponding output include genomes (combination of input parameters for each simulation run) and fitness values (design objectives). Furthermore, other data and phenotypes may be included as inputs and outputs of Wallacei. In this study the optimization is performed in two stages. In order to design the optimization problem, the dependent and independent variables are identified for each stage. The main goal of the first stage is to optimize PV power generation. The independent parameters for the first stage of the optimization include PV (rooftop and BIPV windows), window to wall ratio, building orientation and window types. Two dependent variables are defined to determine the optimal configuration for the independent variables:

- Energy use intensity (kWh/m<sup>2</sup>/yr): the annual energy demand for cooling, lighting and equipment for all conditioned areas of the building.
- PV energy supply (kWh/m<sup>2</sup>/yr): the total power generated from roof top PV and BIPV windows.

Since the goal of this stage was to optimize the PV power generation, the inclusion of alternative façades was less significant at this stage as it does not influence the PV energy supply. The rooftop PV is designed to cover 90% of the rooftop area whereas the window BIPV capacity is driven by the window to wall ratio parameter. Furthermore, operable windows account for

10% of the window to wall ratio. Considering the above independent and dependent parameters the optimization problem for stage 1 is designed to maximize PV energy supply and minimize building energy use in Eq. (7.1) with reference to [24] as follows :

$$\min\{f_1(\partial)\} \max\{f_2(\partial)\}, \partial = [x_1, x_2, x_m] \quad (7.1)$$

where  $f_1$  is the first objective function which minimizes the operational energy use;  $f_2$  is the second objective function which maximizes PV energy supply; and  $\partial$  is a combination of any design variables  $x_1, x_2, x_m$ .

The second stage is performed to explore façade types and strategies towards a low whole lifecycle energy use which includes both the embodied and operational energy. Thus, this stage is performed to jointly minimize both the embodied energy and operational energy. The building model is set up using optimal configuration from the first stage of the optimization. The independent variables for this stage include four façades (including the base model) used within the sub-Saharan Africa region. The description of various layers and characteristics of these facades are presented in Table 7.1. Likewise, the dependent variables include:

- Operational energy use (kWh/m<sup>2</sup>/yr): the annual energy demand for cooling, lighting and equipment for all conditioned areas of the building
- Embodied energy use (kWh/m<sup>2</sup>/yr): the total energy for manufacturing of building materials, transportation, construction, and maintenance during the service life of the building. Considering the above dependent and independent variables, the optimization problem for stage two which minimizes both embodied and operational energy is defined in Eq. (7.2) with reference to [29] as follows:

$$\min\{f_1(\partial), f_2(\partial)\}, \partial = [x_1, x_2, x_m] \quad (7.2)$$

where  $f_1$  is the first objective function which minimizes the operational energy use;  $f_2$  is the second objective function which minimizes the embodied energy; and  $\partial$  is a combination of any design variables  $x_1, x_2, x_m$ .

Since the aim of this stage is minimize the whole lifecycle energy use of the building, the joint optimization of both operational energy and embodied energy will ensure realistic design solutions that optimally reduce both objectives. Thus, the trade-off between the conflicting embodied and operational aspects are explored.

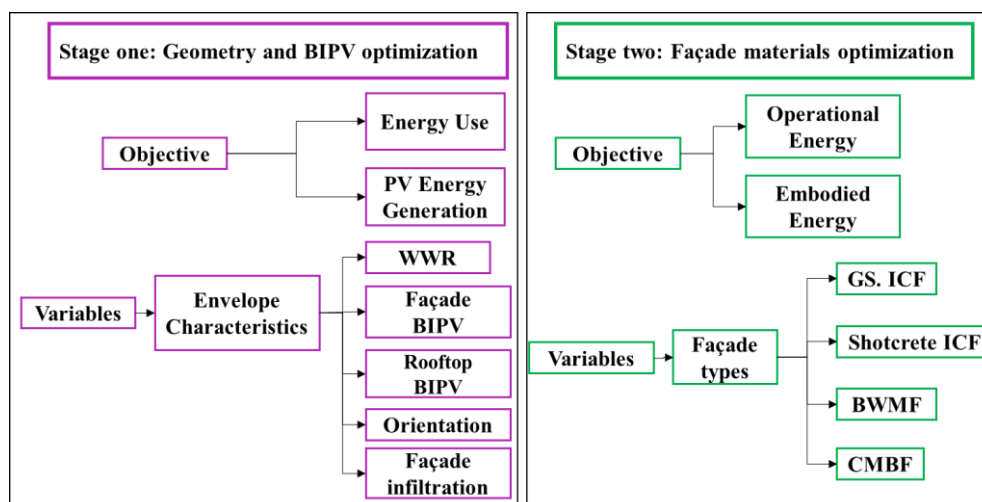


Fig. 7.5 Illustration of passive and active parameters two-stage optimization [217]

The optimization is driven by NSGA-2 algorithm as the primary evolutionary algorithm and was run on an intel core i7 desktop with 16gb of RAM. The average evaluation time for each design simulation was 39” and 18” for stage one and two respectively. The genetic algorithm parameters were set as follows: population size: 50; generation: 100; crossover probability: 0.8; mutation probability: 0.1; crossover distribution index: 20; and mutation distribution index: 20 [168]. The termination criterion used for this study is the maximum generation since a test indicated convergence after the 90<sup>th</sup> generations. In this case, each optimization ends with the 99<sup>th</sup> generation since the first generation is counted as 0. The Pareto

front with the non-dominated solutions (i.e. no single objective can be improved without sacrificing another one) is used to select the optimal design solutions).

#### 7.4 Validation

For validation purposes the simulation model is calibrated by varying certain parameters for the simulation model to fit metered data retrieved from the building management. The American Society of Heating, Refrigerating and Air Conditioning Engineers (ASHRAE) specify a method for validating the whole building energy simulation by evaluating the error between real metered data and simulated results. For energy use, the ASHRAE guideline specifies thresholds for the Coefficient of Variation of Root Mean Square Error (CV(RMSE)) and Normalized Mean Bias Error (NMBE) as 15% and  $\pm 5\%$ , respectively. It is recommended that the base model is calibrated with a minimum of continuous annual metered data. The calibration follows the process of designing the baseline model, analysis of primary results, calibration against monthly metered data and validation using the CV(RMSE) and NMBE.

CV(RMSE) is illustrated in Eq. (7.3) as follows:

$$CV(RMSE) = \frac{1}{m} \sqrt{\frac{\sum_i^n (m_i - s_i)^2}{n-p}} \times 100 (\%) \quad (7.3)$$

NMBE is illustrated in Eq. (4) as shown below:

$$NMBE = \frac{1}{m} \cdot \frac{\sum_{i=1}^n (m_i - s_i)}{n-p} \times 100 (\%) \quad (7.4)$$

where  $m$  is the mean of measured values;  $p$  is the number of adjustable parameters;  $n$  is the number of measured data plot;  $m_i$  is the measured values; and  $s_i$  is the simulated values.

The main parameters for calibrating the building model include the building plan and zone layout, utility data and operation schedules. For the building plan and zone layout,

contextual details are evaluated to identify the real condition of the various zones including storerooms, bathrooms, living rooms, bedrooms, and corridors. Hence, the simulation is performed on a zone-to-zone basis rather than aggregating all zones. Furthermore, the as-built properties of windows and glazing are also taken into consideration in order to improve the simulation results. Lighting and equipment density and schedules are calibrated by varying the number of lamps and equipment as well as their schedules. In terms of occupancy, density is calibrated by modulating the ratio of working to non-working occupants. The usage of equipment is also calibrated in relation to the occupancy density.

Table 7.6 shows the results of the calibration process in comparison to the threshold specified by ASHRAE 14. It can be observed that the model accuracy in terms monthly CV(RMSE) and NMBE are consistency with criteria of ASHRAE 14 guideline.

Fig. 7.6 Estimated CV(RMSE) and NMBE of calibrated simulation model for operational energy uses

<b>Index</b>	<b>ASHRAE Criteria</b>	<b>Baseline Model</b>	<b>Calibrated Model</b>
CV(RMSE)	15	32.58%	14.56%
NMBE	±5%	24.43%	-4.79%

Figure 7.7 shows the monthly energy use of the building including lighting, cooling, equipment, and occupancy gains plotted against the metered data retrieved. It can be observed that the monthly variation between the simulated data and the actual building energy use is less than 5%. Cumulatively, the simulated annual energy use intensity is expressed as 135 kWh/m<sup>2</sup>/yr while the actual value is 128.76 kWh/m<sup>2</sup>/yr. This is relatively high when compared

with the energy use intensity of a low-income dwelling house evaluated by [217]. The main reason for this high deviation is the different energy use profile between the different two groups of income earners. From the field survey, it was observed that the equipment density per building area of the mid- income earners (present study) is much higher compared to the low-income earners in the previous study. Also, the low-income earners mainly adopt heat extraction fans whereas the mid-income earners largely rely on mechanical cooling. As observed the lighting energy use is also much higher due to use of efficient lighting system and design in the mid-income dwelling in this study. From Figure 6, it can be observed that the cooling energy required is much lower in the months of June to September which due to lower outdoor temperatures during this period. The lower temperature can be attributed to higher rainfalls during this period. Given the minimal difference between the simulated and metered data, the building energy model is suitable for subsequent optimization process.

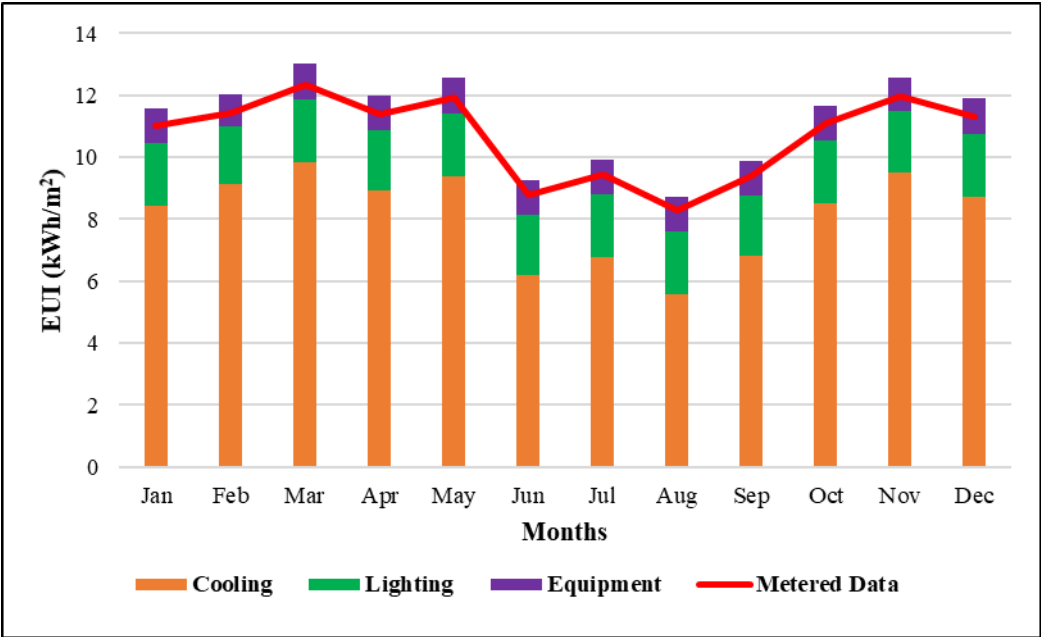


Fig. 7.7 Validation of base model building loads

## 7.5 Stage one optimization results

The results of the first-stage optimization is used to develop scatterplots as expressed in Fig. 7.7. This plot shows the relationship between the building energy use and the PV power supply using the results of 5000 simulations. Fig. 7.7a illustrates the entire solution space whereas Fig. 7.7b shows the Pareto front. In the figure, each dot corresponds to a set of variables (WWR, rooftop PV, BIPV window, infiltration rate and orientation) selected by the optimization algorithm for each simulation run. The results of the design solutions that cannot be improved without compromising the other objective are Pareto front solutions. In this study the solutions that minimize the operational energy use but maximize the PV energy supply are selected as the Pareto solution. Specifically, the optimal solution corresponds to a South oriented building ( $180^\circ$ ). The window to wall ratio and PV window to wall ratio are 0.55 and 0.495, respectively. Also, the infiltration is  $0.000071 \text{ m}^3/\text{s}/\text{m}^2$  which underscores the essence of an airtight façade. This optimal solution results reduces the operational energy use by 26.78% when compared with the energy of the base case model. Fig. 7.9 illustrates the monthly energy consumption and PV power supply of the optimal solution. It can be observed that except March, April, May, September and October, the PV power supply exceed the energy use requirement throughout the year. Nonetheless the energy deficit is less than 10% in these periods. About 80% of the PV energy supply is generated by the rooftop PV while the remaining 20% is generated by the BIPV window.

Table 7.3 provides a detailed configuration of the Pareto optimal for the first stage optimization. The table shows the list of Pareto front, the specific design parameters, PV power generation, operational energy uses and the frequency of occurrence in a design solution in series. The variables (genomes) for the Pareto front are summarized. It can be observed that all solutions are characterized by a south facing building and almost all by an orientation of  $180^\circ$ .

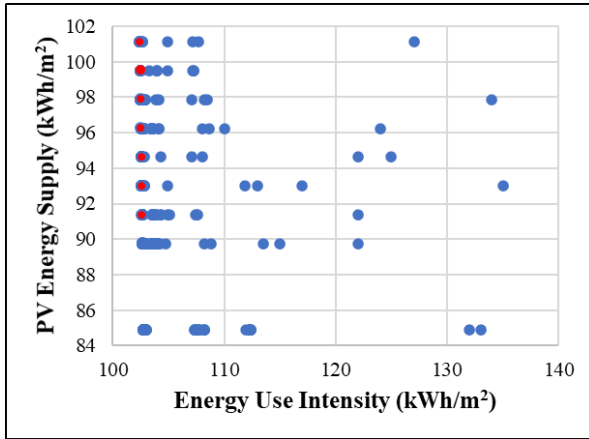


Figure 7.7a Entire solution space

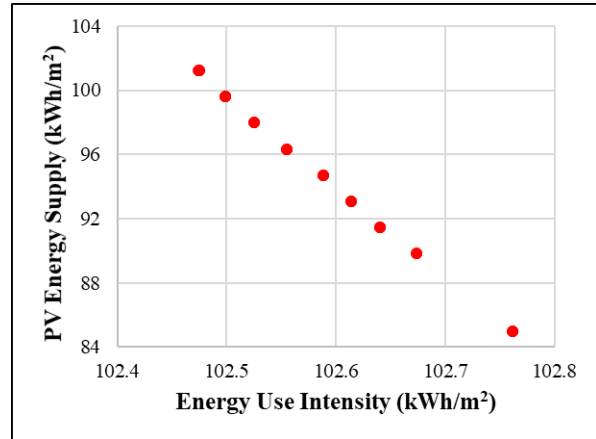


Figure 7.7b Pareto optimal solutions

Fig. 7.8 Scatterplot of Energy use intensity against PV energy supply

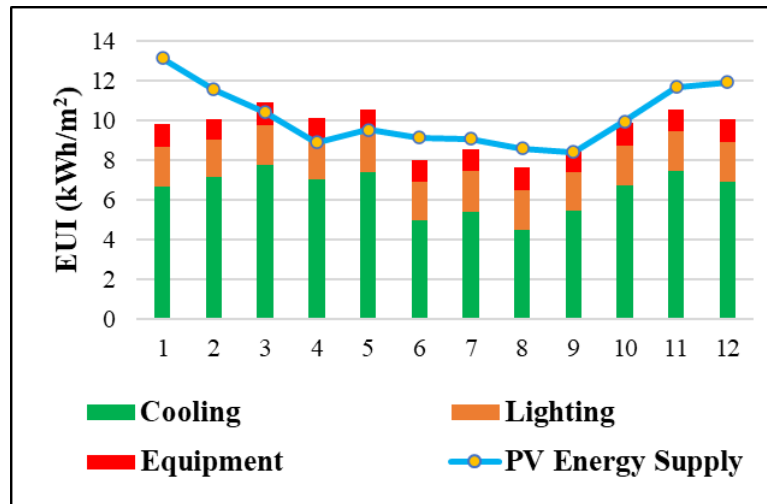


Fig. 7.9 Total operational energy use against PV energy supply

Furthermore, it is observed that the optimal solutions are spread uniformly across the WWR ratio. Since 90% of the windows are replaced with BIPV, the variation in WWR results in less significant changes in the operational energy use. It can be observed that the choice of the best performing design solution is highly related to the WWR rather than the orientation and infiltration rate. The results favor the exploitation of window and BIPV design in other to

select design solutions that best fit. Figure 7.10 further illustrates the performance of design variables against the energy use intensity for the optimized solution.

Table 7. 3 Configuration of Pareto optimal solutions of stage one

<b>BO (°)</b>	<b>WWR</b>	<b>Façade infiltration rate (m<sup>3</sup>/s/m<sup>2</sup>)</b>	<b>Roof top PV (% of roof area)</b>	<b>BIPV WWR</b>	<b>EUI (kWh/m<sup>2</sup>/yr)</b>	<b>PV Energy Supply (kWh/m<sup>2</sup>/yr)</b>	<b>No. of Pareto solution in series</b>
165	0.15	0.000071	90	0.135	102.7616	84.97314	115
165	0.3	0.000071	90	0.27	102.6732	89.84629	92
180	0.45	0.000071	90	0.405	102.6403	91.47067	161
180	0.35	0.000071	90	0.315	102.6139	93.09505	115
180	0.55	0.000071	90	0.495	102.5882	94.71943	138
180	0.5	0.000071	90	0.45	102.5545	96.34381	161
180	0.4	0.000071	90	0.36	102.5248	97.96819	115
180	0.65	0.000071	90	0.585	102.4983	99.59257	115
180	0.7	0.000071	90	0.63	102.4748	101.217	138

## 7.6 Stage two optimization results

The results of the first stage of the optimization forms the basis for stage two of the optimization process. In order to incorporate the optimal design solution from the first stage to the second stage of the optimization, parameters (genomes) of the optimal solution are used to remodel the base case design. The remodeled case building is a south oriented building with a 0.55 and 0.495 of WWR ratio and BIPV window ratio, respectively, has 90% rooftop PV coverage and

a façade infiltration rate of  $0.000071 \text{ m}^3/\text{h}/\text{m}^2$ . Furthermore, the same solar cells and conversion efficiencies are maintained for the rooftop PV and BIPV windows. The second stage of the optimization is performed to demonstrate the trade-off between embodied and operational energy of the building.

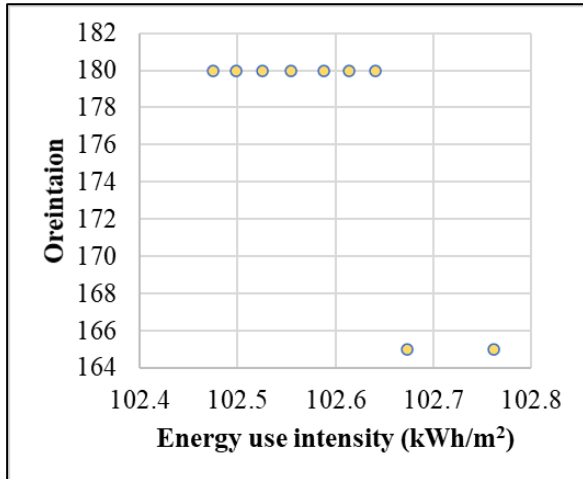


Figure 7.10a. Orientation vs. energy use intensity

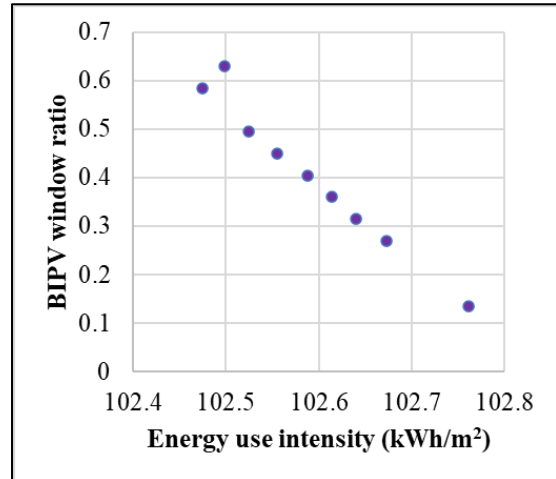


Figure 7.10b. BIPV windows ratio vs. energy use intensity

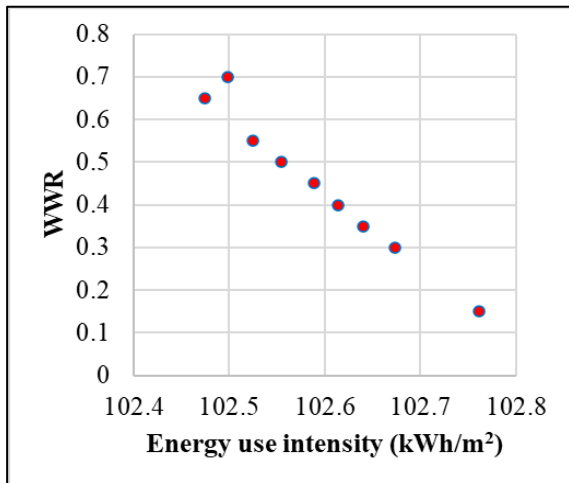


Figure 7.10c WWR vs. energy use intensity

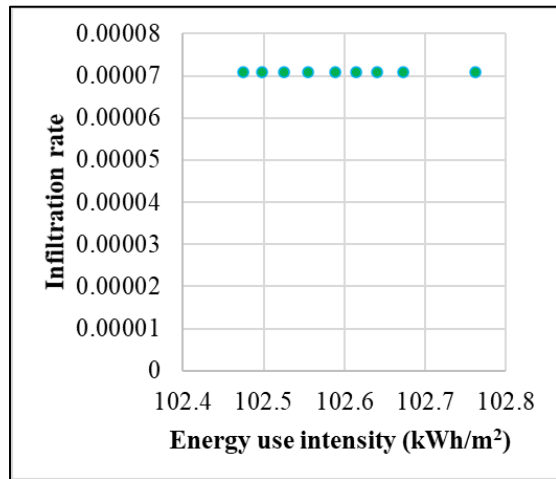
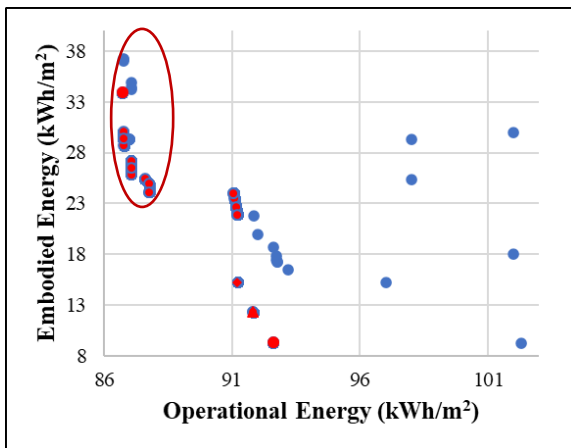


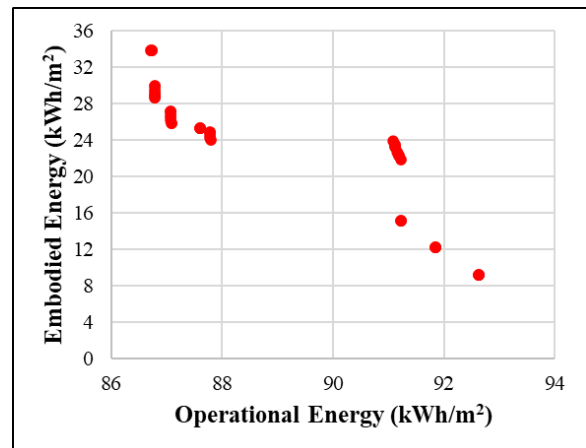
Figure 7.10d Infiltration rate vs. energy use intensity

Fig. 7. 10 Scatterplot of WWR, infiltration rate, oreintation and BIPV window ratio against energy use intensity

The different layers of four façade type are varied to explore their performance on both embodied energy and operational energy. In order to extend the boundaries of the study beyond Ghana, the optimization is performed for two other regions, Abuja, Nigeria and Ouagadougou, Burkina Faso. The results from the second stage of the optimization are presented in Figs. 7.11 to 7.13. The figures show the variations in operational and embodied energy and each dot in the scatter plot represent a unique combination of different variables that control the types and thickness of materials for a façade type. Here, the goal is to minimize the whole lifecycle energy use of the building (both embodied and operational energy) therefore the Pareto front are those solutions that minimize both objectives in a manner that there is no possibility of decreasing one objective without compromising another objective.



**Figure 7.11a** Entire solution space



**Figure 7.11b** Pareto optimal solutions

Fig. 7.11 Scatterplot of operational energy use against embodied energy use (Accra, Ghana)

From Figure 7.11, it can be observed that the design solutions for Ghana are clustered around almost horizontally. This indicated that around these points, the operational energy is relatively steady whereas the embodied energy fluctuates significantly. Particularly it is observed that around the operational energy value of 87-89 kWh/m<sup>2</sup>/yr, the embodied energy fluctuates with a difference as high as 15 kWh/m<sup>2</sup>/yr. This indicates that any further decrease in the operational energy will results in an exponential increase in the embodied energy. A more precise representation of the Pareto front is illustrated in Fig. 7.11b. Similarly, it is observed that minimal reduction in the operational energy use leads to an exponential increase in the embodied energy use. It is revealed that the distribution of the Pareto optimal solutions are more concentrated and less distributed which confirm that significant embodied energy saving can be around similar levels of operational energy. The configuration of the Pareto optimal solutions are presented in Table 7.4. Considering the optimal design solution for the BWMF façade, the selected genes center around 150 mm thick block wall and a 10 mm thick render. Although some optimal solutions increase the thickness of the render to 12 mm, the corresponding increase in embodied energy is much higher than the decrease in operational energy. Therefore, the net benefits from this solution is less desirable. All three thicknesses of the CMBF resulted in similar operational energy, however the embodied energy increased significantly with the increase in thickness. For the Shotcrete ICF, an insulation thickness of 78mm is most representative of the optimal solutions and the most desirable shotcrete thickness is 12 or 15mm. An increase of the insulation thickness to 100 mm leads to an increase in the embodied energy which is not proportional to the decrease in the operational energy. Unlike the foregoing, the thickness of the insulation layer for the optimal GS. ICF has a uniformly spread insulation thickness which proportional reductions in the operational energy use. However, an increase of the insulation thickness to 100 mm yields an exponential increase in the embodied energy.

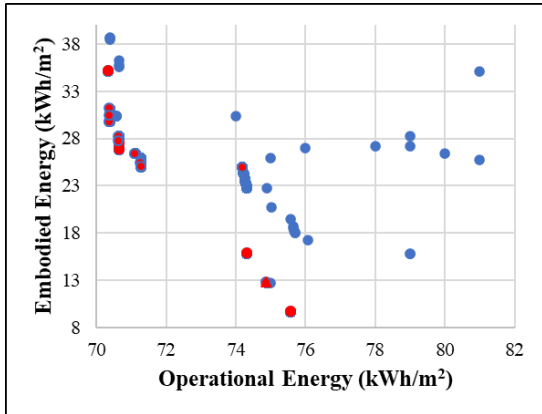
Cumulatively, the net energy use of the optimal solution reduces yields an energy reduction of about 24.59% in comparison with the initial base case model.

The optimization is performed for two other regions in sub-Saharan Africa: Abuja, Nigeria and Ouagadougou, Burkina Faso, and the results are detailed in Figure 7.11 and 7.13, respectively. It can be observed that the distribution of the entire solution are similar. However, operational energy was much lower in these two regions compared to Ghana. This is mainly attributed to the weather data thus the prevailing climatic conditions in the area. Likewise, slight variations are observed in the embodied energy values due to the differences in transportation distances and materials manufacturing processes. For instance, Nigeria is a major manufacturer and distributor of cement in Africa, hence the impacts of transportation are slightly lower in Nigeria when compared with Ghana. Specifically, the optimal solution for Abuja Nigeria and Ouagadougou, Burkina Faso after the second stage of the optimization reduces the energy use by 36.93% and 33.33%, respectively.

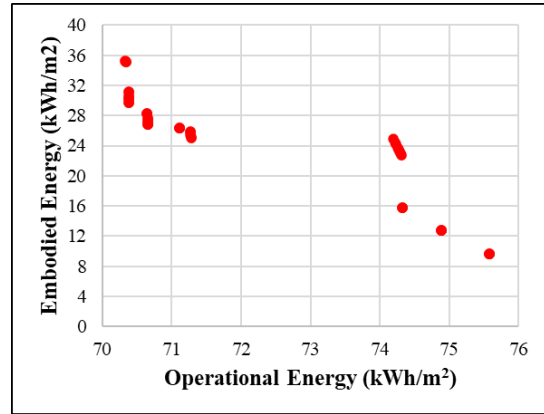
Table 7.4 provides a detailed configuration of the Pareto optimal for the second stage optimization. The table shows the list of Pareto front, the specific design parameters, embodied energy, operational energy uses and the frequency of occurrence in a design solution in series.

Table 7. 4 Configuration of Pareto optimal solutions of stage two

Materials thickness (mm)								Pareto solutions		
CM BF	BWMF			Shotcrete ICF			GS. ICF	Operatio n energy (kWh/m <sup>2</sup> /yr)	Embodie d energy (kWh/m <sup>2</sup> /yr)	Numb er of Paret o soluti ons in series
	Ext. rend er	Bloc k- wall	Int. rend er	Ext. shotcr ete	EPS Insulat ion	Int. shotcr ete	EPS insulat ion			
150								92.63	9.24	92
200								91.85	12.22	115
250								91.23	15.18	138
	10	100	10					91.22	21.86	92
	10	150	10					91.08	23.96	161
	12	150	12					91.11	24.36	69
				15	78	12		87.80	24.06	115
				15	78	15		87.79	24.45	92
							50	87.61	25.38	69
							50	87.09	25.82	92
	15	200	15					87.80	25.06	115
				15	100	15		86.59	29.33	69
				12	78	12		87.80	24.33	115
	12	200	12					87.80	24.36	69
	15	200	12					87.80	24.98	115
							100	86.78	30.00	161
				12	100	10		86.59	28.93	138
				12	100	12		86.59	29.33	69



**Figure 7.12a** Entire solution space



**Figure 7.12b** Pareto optimal solutions

Fig. 7. 12 Scatterplot of operational energy use against embodied energy use (Abuja, Nigeria)

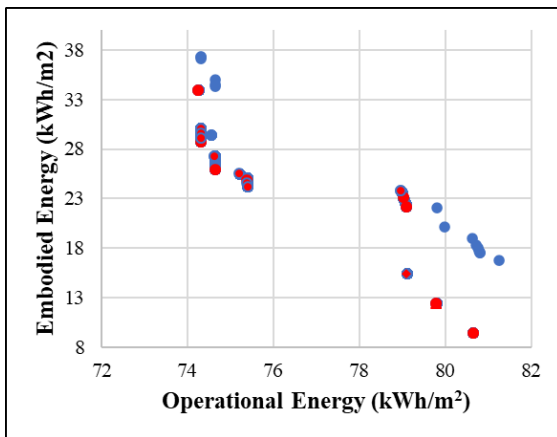


**Figure 7.13a** Entire solution space

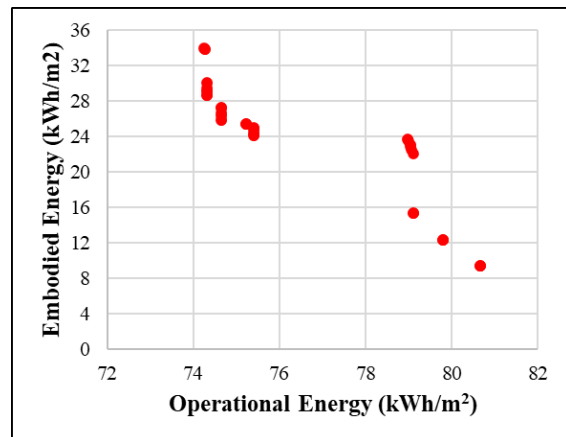


**Figure 7.13b** Pareto optimal solutions

Fig. 7. 13 Scatterplot of operational energy use against embodied energy use (Ouagadougou, Burkina Faso)

## 7.7 Summary

This study evaluated the optimal configuration of different building envelopes with local materials representative of climatic conditions in the sub-Saharan region of Africa. An evolutionary algorithm is coupled with the building energy simulation and LCA to explore the optimal energy performance of different building envelopes and design variable under different climatic conditions. A case study was performed on a typical residential building in Ghana using a two-stage optimization approach which can be adopted by designers in similar regions. In this approach, the building geometry and renewable energy is first optimized and adopted as the basis to configure the building model for evaluating the trade-off between embodied and operational energy with alternative façades in the second stage. Consequently, the arbitrary selection of optimal building designs solely from the perspective of operational energy can be avoided.

It has been proved that the proposed joint optimization approach considering the whole lifecycle of buildings (including both operation and embodied energy) can improve the modelling accuracy and reduce the lifecycle energy use. Such an approach is more favorable as the optimization of operational energy alone may lead to a sub-optimal design from a lifecycle perspective. Furthermore, the study illustrates the trade-off between embodied and the operational energy through the multi-objective optimization approach.

The main findings from the two-staged optimizations are summarized as follows:

- Based on the stage-one optimization, the optimal design solution which maximizes PV energy generation and minimizes operational energy use is mainly south orientated. The coupling of WWR and prefabricated BIPV window is identified to have a much higher influence on the power supply than operational energy. The increase in the BIPV

window area leads to a corresponding increase in the PV power supply but a low window u-value which increases the cooling load in return. Notwithstanding, the rooftop PV alone contributes to nearly 80% of the PV energy supply while the Prefabricated BIPV window contributes to about 20% of the PV power supply.

- The joint optimization operational and embodied energy is proven a more efficient method to reduce the whole lifecycle energy use. Specifically, the different façade types with a wide range of embodied energy values are capable of achieving very similar optimal operational energy. Therefore, a sub-optimal design solution may be selected if not considering from a lifecycle perspective. From the perspective of the different façades explored, it is realized that a slight reduction in the thickness of cementitious materials can reduce the embodied energy without significantly affecting the thermal mass and therefore operational energy. Similarly, an increase in the thicknesses does not necessarily guarantee a decrease in operational energy but increases the embodied energy. Regarding the composite facades with insulation materials, an increase in the insulation thickness significantly reduces operational energy. However, this could also have a counteracting impact on the whole lifecycle energy due to the exponential increase in the embodied energy.
- The lifecycle energy performance of the explored façade is found to vary significantly among the three regions explored with an increasing performance in the order of Ghana, Burkina Faso and Nigeria. Particularly their performance at the operational stage vary significantly due to the variation in weather conditions. Also, the different modes of materials production, transportation, and construction processes impact embodied energy. Hence it is necessary to pay attention to the specificities of the evaluated region. Overall, the first stage of the optimization reduced the total lifecycle building energy

use by 26.78%. Cumulatively, over 24.59%, 33.33%, and 36.93% energy reduction are achieved for Ghana, Burkina Faso and Nigeria respectively.

In summary, this study has provided insights into the optimal configuration of building envelopes with different façade materials representative of the sub-Saharan Africa region from a whole lifecycle perspective using a multi-objective optimization approach. In the future, the range of design variable will be expanded and coupled with economic and environmental indicators. Also, other envelope elements than façades and building architypes will be explored in detail.

## **CHAPTER 8 HOLISTIC ENVIRONMENTAL AND ECONOMIC DESIGN OPTIMIZATION TOWARDS LOW CARBON BUILDINGS CONSIDERING CLIMATE CHANGE AND CONFOUNDING FACTORS**

Following the developed BIM-based LCA method and optimization in the previous chapters, this Chapter further formulates a robust computational multi-objective optimization to identify cost effective building design solutions to mitigate environmental impact and climate change. Lifecycle energy and environmental impact analyses are integrated with a comprehensive cost analysis, and multi-objective optimization to explore potential design solutions based on passive design parameters and renewable energy systems. The optimization problems are formulated robustly to accounts for confounding factors such as difference in internal loads due to occupancy behaviours, improvement in construction efficiency, and future climate change scenarios.

The overall optimization framework is summarized in Fig. 8.1. The figure illustrates that the multi-objective optimization process of the energy, carbon and cost follows the design of a baseline model with reference to a typical mid-rise residential building in Ghana. Passive design strategies and PV installations are identified as design parameters to perform the lifecycle environmental and economic performance analyses including energy use, carbon emission and cost indicators. Thereafter, the optimization framework incorporating objective functions, decision variables and the optimization algorithm is subject to a comprehensive scenario analysis to explore the influence of confounding factors and climate change.

### **8.1 Case study description**

The case study building is representative of a mid-rise residential building located in Accra, Ghana. Information concerning its design, construction and operation was retrieved from the owner and occupants. Construction of mid-rise residential buildings is expected to surge due to the growth in housing demand. Hence, it is critical to investigate measures to reduce their

environmental impacts towards carbon neutrality. The building has a gross floor area (GFA) of 7500 m<sup>2</sup> and each floor is divided into 4 apartments. The estimated lifespan of the building is 50 years.

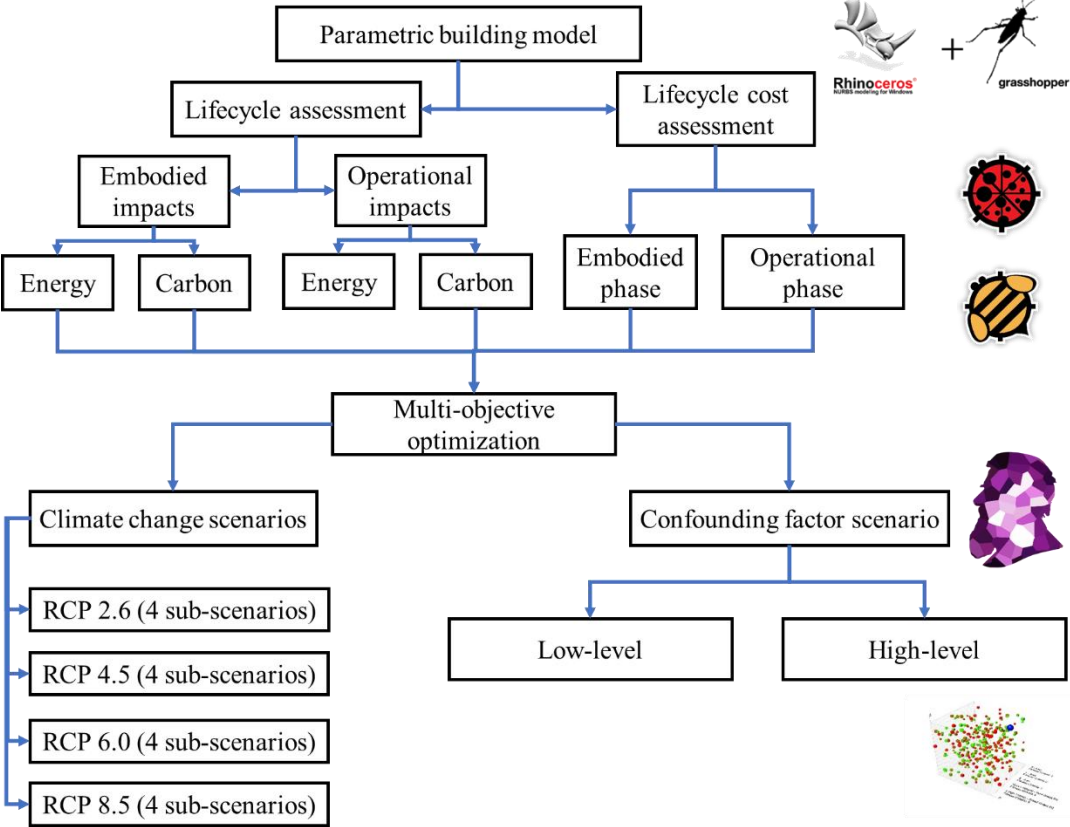


Fig. 8. 1 Framework for cost effective optimization of energy and carbon of residential building

The main energy use includes cooking, cooling, lighting, and household equipment, but cooking is excluded from this study as it is fueled by natural gas. The building energy use is fully supplied by grid electricity. The case building is located in a tropical savanna climate (Aw) under the Koppen-Geiger climate classification. The weather data is retrieved from Energyplus website in the format of epw to evaluate the annual operational energy performance. The baseline model is constructed parametrically in Grasshopper Rhinoceros which is a robust building information modelling and simulation platform for building performance assessment.

Its visual programming nodes and wide range of plugins allow various assessment including energy, carbon emission, and cost analyses. Ladybug and Honeybee plugins are used to couple EnergyPlus to evaluate the operational energy use and photovoltaic electricity generation while Grasshopper's native nodes are used to evaluate the embodied energy, carbon, and cost. The impact assessment data are integrated within nodes in Grasshopper to facilitate the LCA and LCCA process. Table 8.1 outlines the settings for the baseline case. The case building is illustrated in Fig. 8.2.

Table 8. 1 Setting for the baseline model

Item	Setting
Floor area	25m × 30m
Floor height	2.7m
No of floors	10
Lighting load	15 W/m <sup>2</sup>
Occupancy load	160 W/person
Equipment load	10 W/m <sup>2</sup>
Window U-value	5.69 W/m <sup>2</sup> K
Floor U-value	0.48 W/m <sup>2</sup> K
Wall U-value	2.74 W/m <sup>2</sup> K
Window to wall ration	0.4

## 8.2 Multi-objective optimization

The multi-objective optimization is formulated considering the objective functions, design variables and optimization algorithm. The objective functions are developed in line with the main objective of the study which is to reduce energy use and carbon emission in a cost-

effective approach, hence three objective functions are considered in the study. The objective functions are illustrated by Eq. (8.1):

$$\min\{f_1(\theta)\} \{f_2(\theta)\} \{f_3(\theta)\} = [x_1, x_2, \dots x_m] \quad (8.1)$$

where  $f_1$ ,  $f_2$ , and  $f_3$  minimizes the total energy use, carbon emission and cost with a combination of any design variables  $x_1$ ,  $x_2$ , and  $x_m$ .

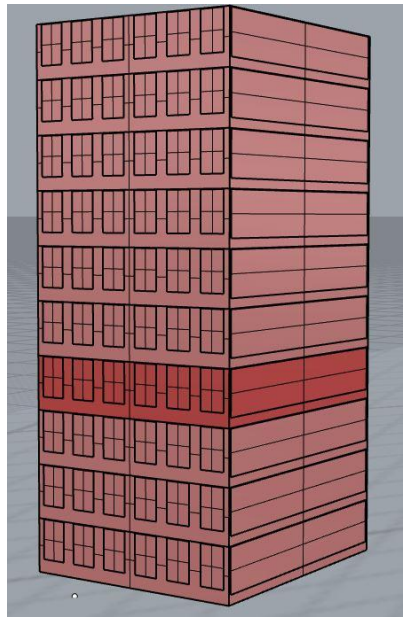


Fig. 8. 2 Parametric model of case study building

The final optimal solution is selected by normalizing and weighting the Pareto front using Eq. (8.2):

$$NV = \frac{(X - X_{min})}{X_{max} - X_{min}} \quad (8.2)$$

where NV is the normalized values of CED, GWP or cost of the Pareto front;  $X$  is a value of CED, GWP, or cost in the Pareto front to be normalized,  $X_{min}$  is the minimum value of CED,

GWP or cost of the Pareto front; and  $X_{max}$  is the maximum value of CED, GWP or cost of the Pareto front.

A total of 18 design variables are selected to optimize the lifecycle performance of the building. To ensure the optimization results are realistic and in compliance with feasible engineering solutions and occupant satisfaction, the distribution range of variables are determined based on local engineering practices in Table 8.2. For instance, envelope constructions are specified within the limits of materials available in the market while building geometries are defined as per building codes (Ghana Standards Authority, 2018).

Table 8. 2 Design optimization variables

<b>Design variable</b>		<b>Range</b>
Building orientation		0° - 360°
Shape coefficient		0.5 – 1
Window to wall ratio	North façade	0.2 - 0.8
	South façade	0.2 - 0.8
	West façade	0.2 - 0.8
	East façade	0.2 - 0.8
Window construction		A
Wall construction		B
Roof construction		C
Floor construction		D
PV installation (15% efficiency mono-crystalline PV modules)	Roof top PV	10% - 80% roof area
	North façade	10% - 90% façade area
	South façade	10% - 90% façade area
	West façade	10% - 90% façade area

Design variable		Range
	East façade	10% - 90% façade area
Rooftop PV orientation		South, North, East, West
Rooftop PV tilt		5° - 15°
Façade infiltration rate		0.0001 m <sup>3</sup> /s/m <sup>2</sup> , 0.000071 m <sup>3</sup> /s/m <sup>2</sup> , 0.000285 m <sup>3</sup> /s/m <sup>2</sup> , 0.0003 m <sup>3</sup> /s/m <sup>2</sup> , 0.0006 m <sup>3</sup> /s/m <sup>2</sup> .

**a, b, c** and **d** are listed in Tables 3 to 7 of the appendix.

Although initial optimization settings are specified as Table 3.5, such configuration resulted in prolonged computational time without significant improvement in the optimization objective. To identify the best settings to achieve convergence within the minimal time, the 20<sup>th</sup> to 50<sup>th</sup> generation is analyzed. Fig. 8.3 illustrates the changes in optimization results for single and multi-objective optimization of the CED, GWP and cost. It is observed that convergence is achieved for all three single objective optimizations after the 15<sup>th</sup> generation. However the minimum CED, GWP and cost is only achieved for the multi-objective optimization after the 20<sup>th</sup> generation. Since no significant improvements in the three objectives can be achieved after the 25<sup>th</sup> generation, the optimization process is performed with a generation size of 25 instead of 50.

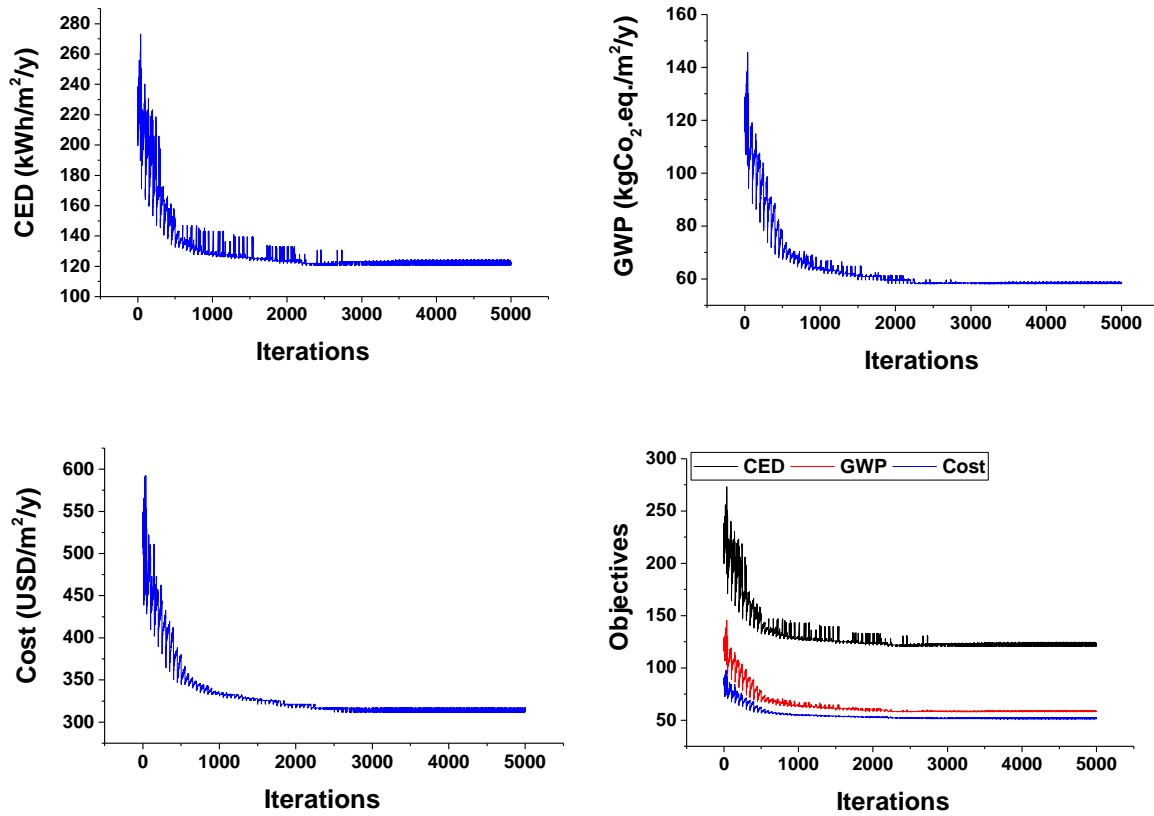


Fig. 8.3 Single and multiobjective convergence over generations

The result of the developed simulation model is compared with operational data of the building in order to validate its accuracy in terms of the operational energy use. The operational energy use data was collected through an onsite survey which includes cooling, lighting and plug loads over a period of one year. Fig. 8.4 shows a comparison between the simulated results and the actual operational data. It is observed that the monthly variations in energy use are less than 5%. The simulated results are slightly higher than the real data retrieved except in the months of January, June and July where a notable variation is observed. A brief survey with the building occupants indicated an increase of occupancy during these periods which explains the slightly higher energy use in the real operation data. The total annual energy use intensity is 175 kWh/m<sup>2</sup>/y which includes 57.77% cooling, 20.57% lighting and 21.75% plug loads. In comparison, the annual energy from the operational data is 173.74 kWh/m<sup>2</sup>/y, and the

simulation model is validated for the subsequent optimization process. The total CED, GWP and cost representing both embodied and operational impacts are evaluated to be 210 kWh/m<sup>2</sup>/y, 138 kgCO<sub>2</sub>.eq./m<sup>2</sup>/y and USD 76.68/m<sup>2</sup>/y respectively for the initial design.

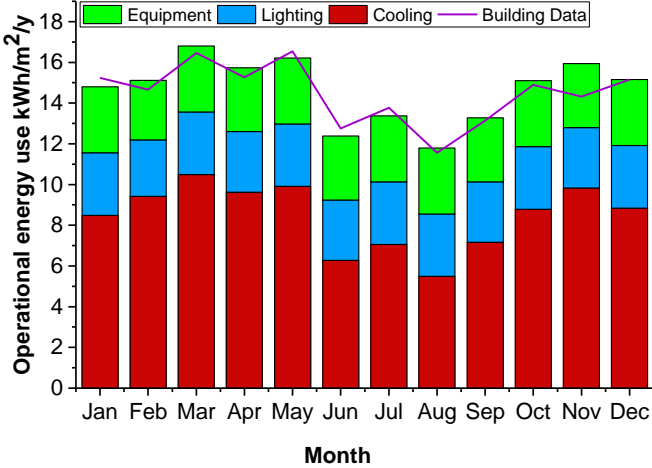


Fig. 8. 4 Validating the developed model

A multi-objective optimization is performed to explore the range of selected passive design strategies and renewable energy system. The results of the optimal solution is compared to the initial design in order to evaluate the corresponding improvement in the CED, GWP and cost. Fig. 8.5 shows the results of the optimization process in a 3D scatter plot. The Pareto front indicating the best solutions are highlighted blue and illustrated in the box plot. The normalization and weighting criteria is applied to select the best result from the Pareto front. The optimal result includes both embodied and operational impacts for all three performance indicators. Precisely, the CED, GWP and cost of the optimal design model are 121.43 kWh/m<sup>2</sup>/y, 58.56 kgCO<sub>2</sub>.eq./m<sup>2</sup>/y, and USD 51.92/m<sup>2</sup>/y which indicate an improved performance of about 42.01%, 57.67% and 32.28% respectively in comparison with the initial design model. The optimal solution corresponds to building designs with a shape coefficient of 0.5 which is the lower limit of the building width to length ratio. Similarly, a low WWR ratio of 0.2 is selected

for the north, east, west and south facades with a very low infiltration rate per m<sup>2</sup> of the façade. The orientation of the optimal solution is 150° with respect to the north. With regards to the window construction, the optimal design is characterised by a wooden-framed tripple glazed window. The same floor construction in the baseline model is maintained in the optimal design solutions as a reinforced concrete floor with screed and fired clay tiles. The optimal roof design is characterised by a reinforced concrete, Polyurethane rigid (PUR) foam insulation and ethylene propylene diene terpolymer (EPDM) membrane. For the PV system, the optimal solution is characterised by the maximum PV area configuration (80% of roof and 90% external wall area). The roof PV are south facing with a tilt angle of 8°. The configuration of design parameters for the optimal solutions are illustrated in Table 8.3.

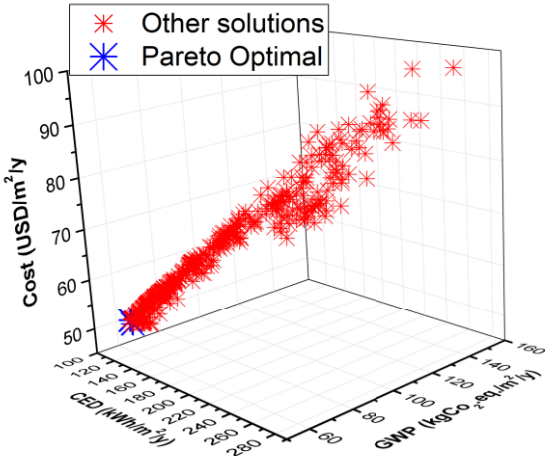


Fig. 8.5a 3D Scatter plot of the optimized solutions

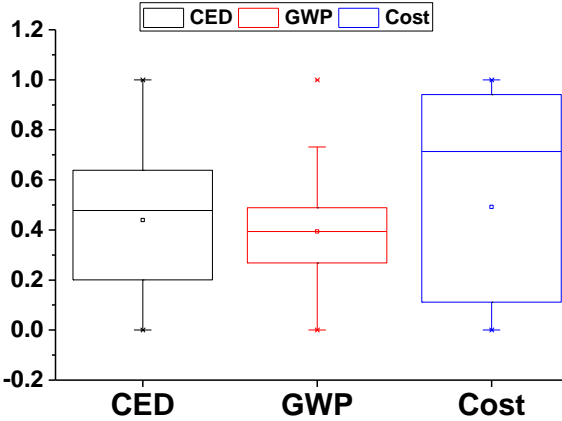


Fig. 8.5b Box plot of Pareto optimal solutions

Fig. 8. 5 3D Scatter plot of CED, GWP and Cost of the optimized base model

Table 8. 2 Configuration of the optimal design model

<b>Design variable</b>		<b>Range</b>
Building orientation		150°
Shape coefficient		0.5
Window to wall ratio	North façade	0.2
	South façade	0.2
	West façade	0.2
	East façade	0.2
Window construction		Tropical hardwood-framed triple- glazing
Wall construction		FJI-cellulose-roughcast gypsum blocks
Roof construction		Gypsum plaster-concrete-PUR-EPDM2
Floor construction		Concrete-Screed mix-fired clay tiles
PV installation (15% efficiency mono-crystalline PV modules)	Roof top PV	80% roof area
	North façade	90% façade area
	South façade	90% façade area
	West façade	90% façade area
	East façade	90% façade area
Rooftop PV orientation		South
Rooftop PV tilt		8°
Façade infiltration rate		0.000071 m <sup>3</sup> /s/m <sup>2</sup>

Similarly, a comparison between the embodied and operational GWP of the optimised and baseline model is illustrated in Fig. 8.6. The embodied impacts contributes to 13.03% of the total GWP whereas the operational impacts contributes to 86.96%. Considering the impacts of PV generated electricity, the operational GWP is further decreased which changes the contribution of embodied and operational GWP to 25.46% and 74.53%. By increasing the

renewable energy supply the operational GWP can be reduced drastically. This scenario is illustrated in section 4.4.1. In comparison to the baseline model, the operational GWP is decreased by 65.00% whereas the embodied GWP is increased by 9.47%. Cumulatively, GWP of the optimised model is decreased by 57.67%.

The total cost of building materials, PV and installations account for 41.83% whereas cost from energy use at the operational phases account for 58.16% in the optimised design model. For the baseline model, materials and installation cost account for 22.49% whereas operation related cost contribute to 77.51%. The cost of materials, PV and installation is increased by 25.6%, however the operation related cost is decreased by 49.19% leading to a net cost reduction of about 32.28%.

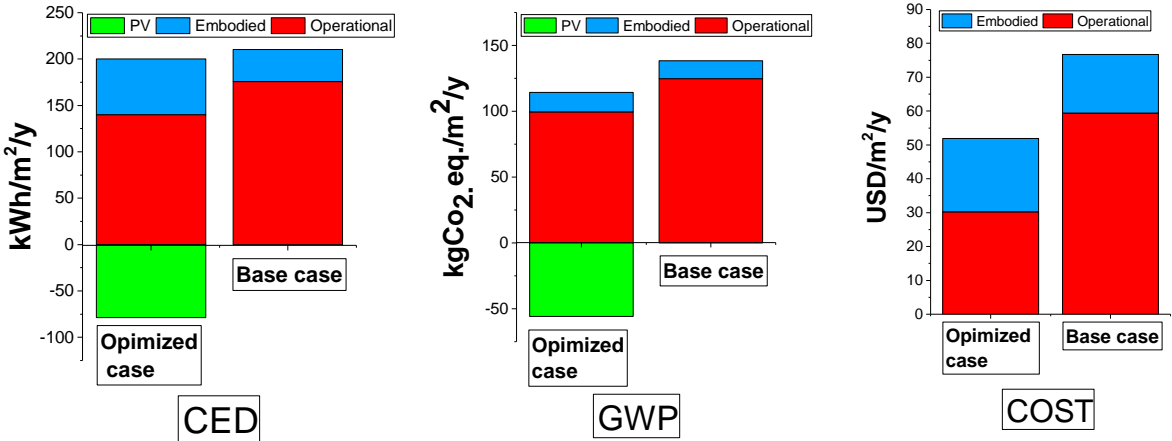


Fig. 8. 6 Contribution of embodied and operational impacts of the baseline and optimized solutions

In addition to the share of embodied and operational impacts, contributions of different building elements to the embodied impacts and the monthly profile of operational impacts are also illustrated. Fig. 8.7 shows the results of the optimized solution in terms of monthly cooling, lighting, equipment loads, PV generation and the net operational EUI. In comparison with the baseline model, it is observed that majority of energy reductions are due to the reduced cooling

load, while lighting and equipment loads contributed very little to the operational energy reduction. Also, it is realised that the PV power generation can cover 49% to 60% of the monthly operational energy use. Fig. 8.8 illustrate the distribution of embodied energy by building elements. In the baseline model, it is observed that walls, windows, roof and floors account for 41.44%, 16.19%, 3.37% and 38.99% of the embodied energy respectively. However, these elements account for only 18.03%, 10.37%, 4.23%, 24.036% in the optimized model. The PV installation accounts for the remaining 43.33% of the embodied energy. In terms of GWP, the contribution of walls, windows, roof and floors are 30.55%, 18.14%, 2.67% and 48.62% for the baseline model whereas these elements account for only 19.65%, 9.76%, 2.89% and 29.49%, respectively in the optimized model. PV installation accounts for the largest portion of GWP of 38.19%. The contribution of materials and installation cost for the baseline model are 37.94%, 23.47%, 3.82% and 34.76% for walls, windows, roof and floors, respectively. In the optimized model, walls, windows, roof, floors and PV contribute 3.31%, 1.62%, 0.26%, 1.82% and 92.99% to the total cost respectively. Despite the high cost of PV installation, its net benefits are realised at the operational phases of the building which reduces the total cost of the optimised building by 32.28% in comparison to the baseline model.

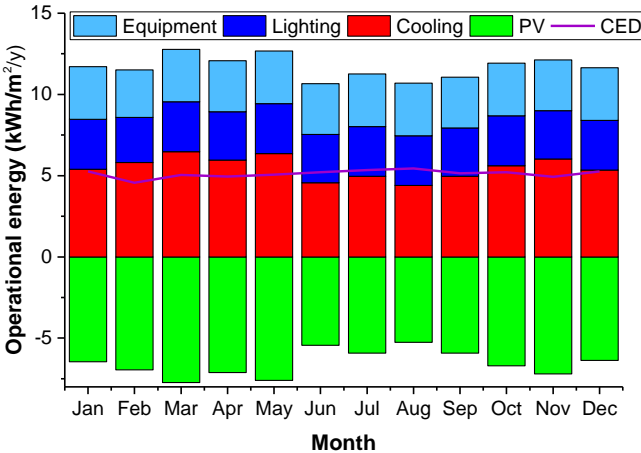


Fig. 8. 7 Monthly profile of operational energy use of the optimized solution

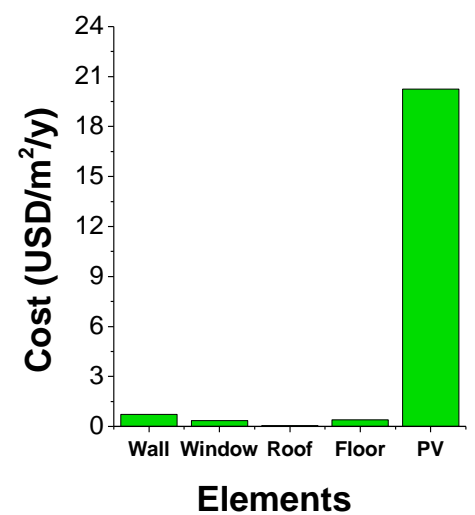
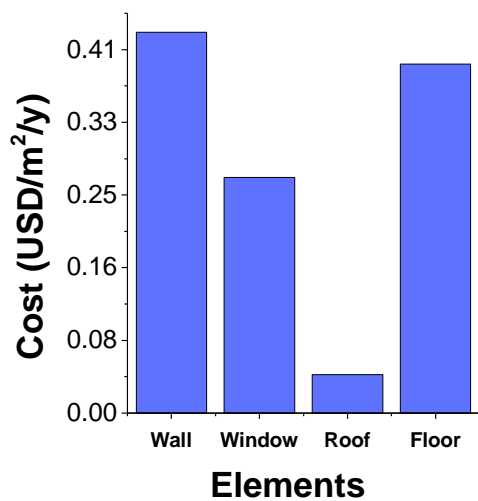
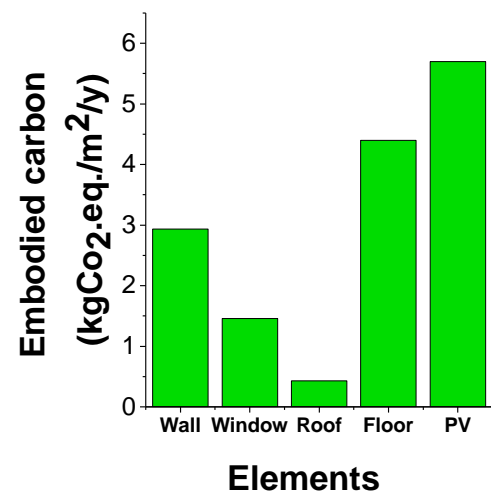
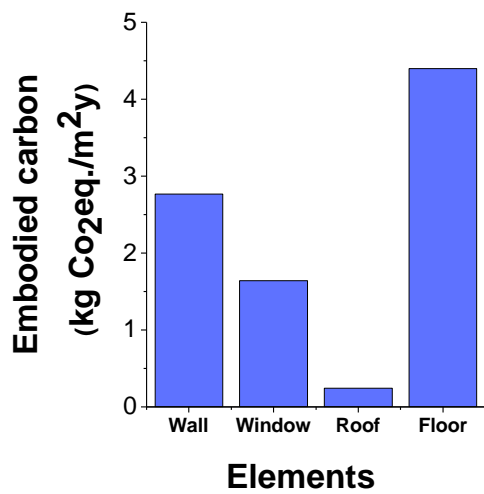
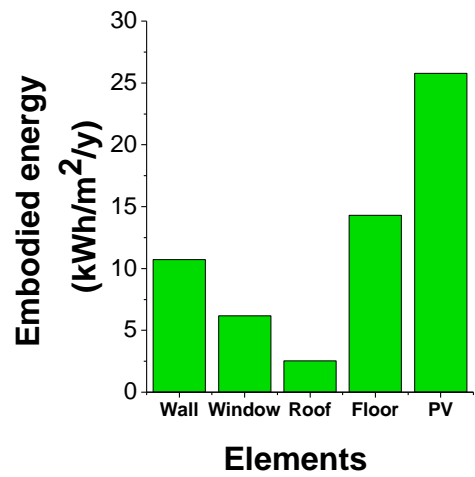
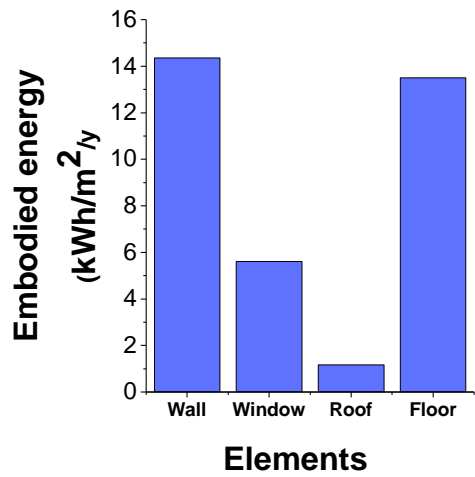


Fig. 8. 8 Contribution of building elements to the total CED, GWP and Cost

### 8.3 Impacts of confounding factors

Building energy use, carbon emissions and cost are affected by confounding factors whose impacts are unclear. Two scenarios are defined alongside the optimised scenario to investigate the impacts of confounding factors. Scenarios 1 and 2 represent a low and high level of confounding factors respectively. Scenario 1 characterizes a condition where the equipment loads, lighting, occupancy, ventilation rate and occupancy activity level are reduced by 50% off the baseline model. The result of the optimization process is illustrated on a 3D scatter plot in Fig. 8.9a.

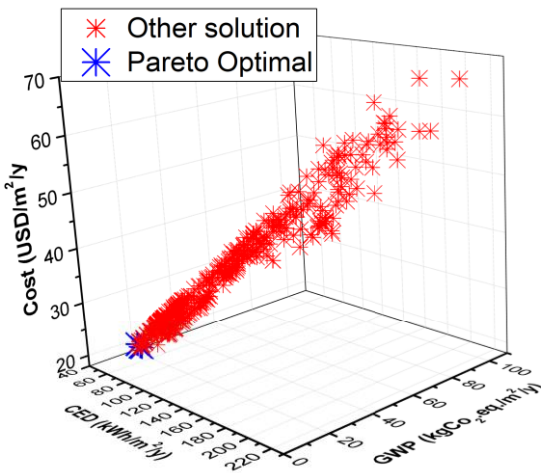


Fig. 8.9a Low level

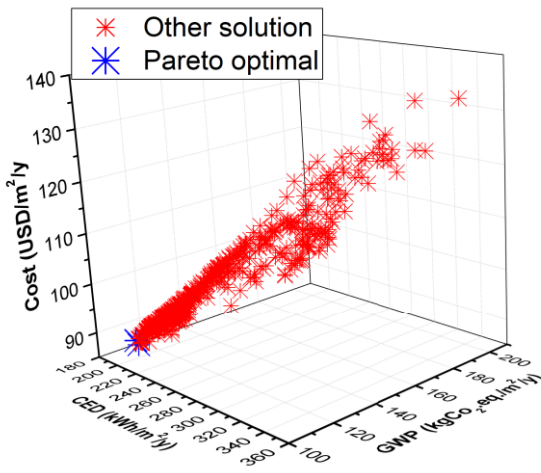


Fig. 8.9b High level

Fig. 8.9 3D Scatter plot of CED, GWP and Cost for optimization under confounding factors

An evaluation of the optimal solution from this scenario shows a CED, GWP and cost of 58.60 kWh/m<sup>2</sup>/y, 14.86 kgCO<sub>2</sub>eq./m<sup>2</sup>/y, and USD 21.31/m<sup>2</sup>/y respectively, indicating unproportionate reduction in all three indicators. Further evaluation of the optimal solution reveals that the CED and cost are reduced by 52.65% and 58.95% from the optimized baseline scenario. On the other hand, GWP is reduced by 74.62%. The drastic reduction in GWP can be attributed to the reduction in CED. As a result, the PV power generation covers the operational

CED making the building near carbon neutral. The GWP is therefore mainly generated from the embodied impacts. The reduction in cost can also be attributed to the reduced operational cost and lower initial investment on PV power generation with downsized capacity. With regards to the design parameters, the same geometries and thermo-physical properties are maintained in comparison to the initial optimised design solution.

The second scenario is representative of a condition where the confounding factors are increased by 50% off the baseline model. The result of the optimization process is illustrated in Fig. 8.9b. Unlike scenario 1, the CED, GWP and cost are increased by 197.03 kWh/m<sup>2</sup>/y, 111.66735 kgCO<sub>2</sub>.eq./m<sup>2</sup>/y and USD 87.06/m<sup>2</sup>/y for 62.26%, 90.68% and 67.70%, respectively. The significant increase in GWP and cost is attributed to the high carbon coefficient and cost of grid electricity. The building geometries and thermo-physical properties of the optimized solutions in this scenario remained the same as the optimised baseline scenario with a preference of the lowest WWR, shape coefficient and high levels of insulations in the external envelope.

## **8.4 Impacts of climate change**

The IPCC defined four RCPs which show different future climates depending on the level of greenhouse gas emissions. These RCPs also serve as a guide for the implementation of strategies to reduce greenhouse emissions. Four sets of scenarios are defined to explore the impacts of each concentration pathway on future building performances. Each scenario includes simulation with a modified weather data, improvement in electricity mix, and increased efficiency in construction processes for a projection of 4 decades (2030-2070). Hence four sub-scenarios are explored for each RCP.

### **8.4.1 RCP 2.6**

RCP 2.6 represents a scenario where the mean dry bulb temperatures are modified to reflect mean increments in future climatic temperature. Also, the efficiency of building

construction processes is increased by 6% every 10 years while the operational energy use is fully met with renewable sources. As shown in Fig. 8.10, the total CED for the four sub scenarios were found to be 125.66kWh/m<sup>2</sup>/y, 123.46 kWh/m<sup>2</sup>/y, 117.03 kWh/m<sup>2</sup>/y and 112.95 kWh/m<sup>2</sup>/y. These values show a projection of energy use for buildings constructed in 2030-2039, 2040-2049, 2050-2059 and 2060-2069, respectively. Further breakdown into operational and embodied impacts indicate an increase in the operational energy use by 4.87%, 5.86%, 6.41% and 6.92% which can be attributed to the average increase in temperature through the four decades. However, the results show a decrease in embodied impacts due to the cumulative increase in construction efficiency. Overall, the total CED is increased by 3.49% and 1.67% in the first and second decade whereas it is decreased by 3.63% and 6.99% in the third and fourth decade. Thus, the cumulative improvement in the efficiency of construction processes can yield an overall decrease in the total CED of buildings.

In terms of carbon emissions, the total GWP is reduced to 13.69 kgCO<sub>2</sub>.eq./m<sup>2</sup>/y, 12.79 kgCO<sub>2</sub>.eq./m<sup>2</sup>/y, 11.93 kgCO<sub>2</sub>.eq./m<sup>2</sup>/y and 11.05 kgCO<sub>2</sub>.eq./m<sup>2</sup>/y for 2030-2039, 2040-2049, 2050-2059 and 2060-2069, respectively. The overall drastic decrease in GWP can be attributed to the application of renewable energy sources and increased efficiency in building construction processes. Through the application of renewable energy during building construction, further carbon reduction can be achieved.

The increase in energy use results in a proportionate increase in the total cost, thus the figures also illustrate an increase in the total cost to USD 55.54/m<sup>2</sup>/y, USD 56.22/m<sup>2</sup>/y, USD 56.60/m<sup>2</sup>/y and USD 56.96/m<sup>2</sup>/y for buildings constructed in the first to fourth decade respectively. This increase in total cost is solely attributed to the increase in operational CED.

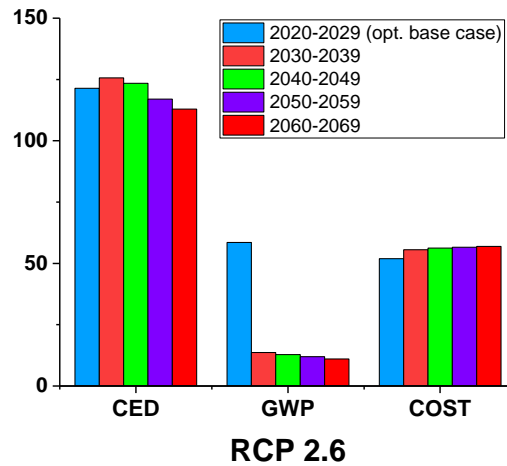


Fig. 8.10 Trajectory of CED, GWP and cost under RCP 2.6

#### 8.4.2 RCP 4.5

RCP 4.5 is defined to explore a trajectory with modest strategies measures towards climate change. The modified weather data reflect slightly higher temperatures. Similarly, the production efficiency of construction processes is improved by 2% every decade while the electricity mix is improved by 40%.

The building optimization results for the four decades are indicated in Fig. 8.11. It is observed that the total CED is increased to 128.67 kWh/m<sup>2</sup>/y, 129.76 kWh/m<sup>2</sup>/y, 130.14 kWh/m<sup>2</sup>/y, 130.47 kWh/m<sup>2</sup>/y through the four decades respectively. This represents 5.96%, 6.85%, 7.17% and 7.44% increase in total CED respectively. Further analyses of the results show an increase in the operational CED by 5.29%, 6.92% 8.05% and 9.15%. This far outweighs the reduction in embodied CED which therefore results in an increased total CED.

Similar reductions are realised for the embodied GWP due to the increased construction process efficiency. However, much larger reductions are achieved due to the improved electricity mix. Specifically, the operational GWP is reduced by about 34% which leads to an overall reduction in the total GWP by 23.74%, 22.46%, 21.91% and 21.31% through the first

to fourth decade. The total cost is also increased to USD 55.83/m<sup>2</sup>/y, USD 56.96/m<sup>2</sup>/y, USD 57.74/m<sup>2</sup>/y and USD 58.49/m<sup>2</sup>/y because of the increase in operational energy use.

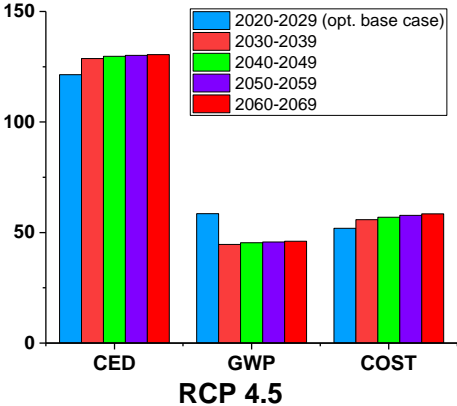


Fig. 8.11 Trajectory of CED, GWP and cost under RCP 4.5

### 8.4.3 RCP 6.0

RCP 6.0 represents another scenario with moderate interventions to limit carbon emissions. Fig. 8.12 illustrates the results of the optimization process using the modified weather data, improved electricity mix by 50% and improved construction process efficiency by 4%. An increase in operational CED by 3.35%, 4.78%, 5.84% and 7.49% is shown for the four subscenarios due to the increase in temperatures. The increased construction process efficiency also reduces the embodied CED, which is however outweighed by the increase in operational CED, leading to a net increase in the total CED by 2.72%, 2.39%, 1.65% and 1.57% respectively. In terms of carbon emissions, the improved electricity mix reduces GWP by 34.77%, 34.64%, 34.78% and 34.38% for the four subscenarios respectively. Due to the increase in operational energy use, the overall cost of these scenarios is also increased to USD 54.50/m<sup>2</sup>/y, USD 55.48/m<sup>2</sup>/y, USD 56.20/m<sup>2</sup>/y and USD 57.35/m<sup>2</sup>/y, respectively.

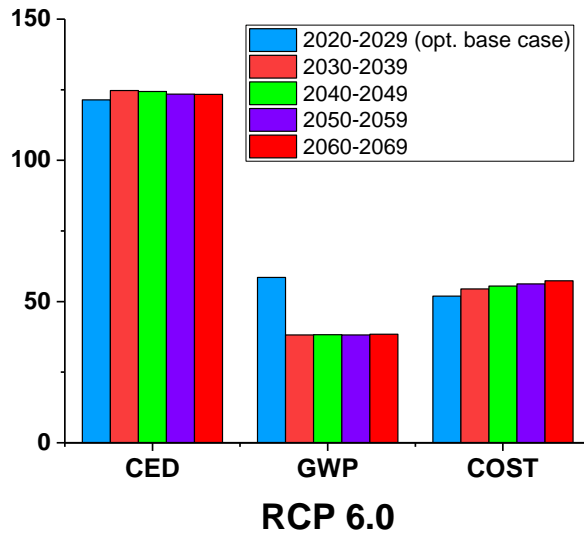


Fig. 8.12 Trajectory of CED, GWP and cost under RCP 6.0

#### 8.4.4 RCP 8.5

RCP 8.5 represents a scenario with no intervention to limit carbon emissions and global temperatures. Hence this scenario is the worst case without improvement in the energy mix and construction process efficiency subject to the highest temperature rise. The results of the optimization process is illustrated in Fig. 8.13. It is observed that the operational CED is increased by 5.83%, 8.04%, 10.79% and 13.40% for the four subscenarios. Moreover, no reduction is achieved in the embodied CED which leads to an increase in the total CED by 7.56%, 10.11%, 13.28% and 16.30%, respectively. Proportional increases in GWP and cost are also noted due to the increase in the operational energy use. Specifically, the total cost through the four decades is increased to USD 56.20/m<sup>2</sup>/y, USD 57.72/m<sup>2</sup>/y, USD 59.62/m<sup>2</sup>/y and USD 61.42/m<sup>2</sup>/y, respectively.

In summary, the trajectory of CED and GWP are plotted in Fig. 8.14. A very high energy use and carbon emission through decades is observed for buildings in the worst scenario RCP 8.5. Among the two moderate scenarios, it is observed that RCP 6.0 results in lower energy use

and carbon emissions. The best scenario RCP 2.6 though leads to slightly high emissions in the first two decades while a reduction of the GWP and CED in subsequent decades.

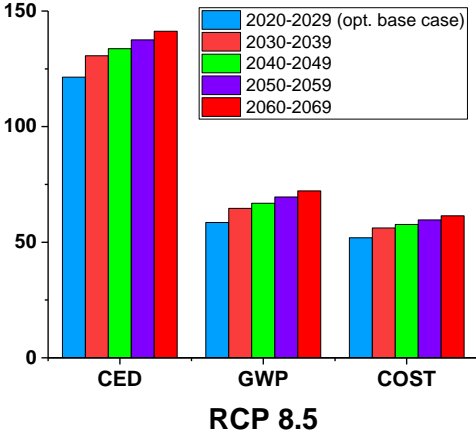


Fig. 8.13 Trajectory of CED, GWP and cost under RCP 8.5

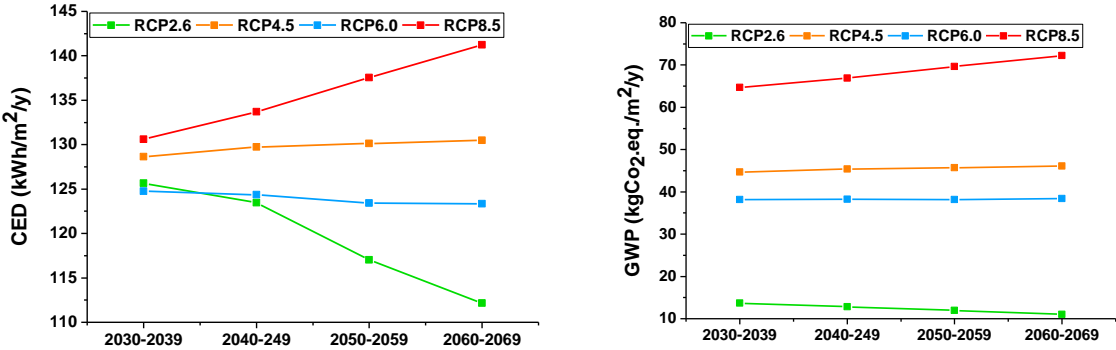


Fig. 8.14 Trajectory of CED and GWP for RCPs from 2030 to 2069

Multi-objective optimization can resolve complex environmental design problems in buildings, which determines the best design variables that will reduce the total energy use and carbon emissions in a cost-effective approach. However, the system boundary, assumptions and scenarios affect the results of environmental and cost assessment, therefore a joint optimization of the embodied and operational impacts can increase the reliability of design solutions to

improve the overall environmental performance of buildings. Also, low energy building designs do not necessarily translate to low carbon emissions, and hence the optimization of energy and carbon emission through all phases of the building lifecycle is critical. This study therefore applied a parametric multi-objective optimization approach integrating both embodied and operational impacts to evaluate the total energy use, carbon emissions and cost of a mid-rise residential building. The reliability of the developed model is validated as the operational CED is consistent with real operational data retrieved from the building. Accordingly, it is validated for further modelling analyses. Considering the operational impacts alone can lead to sub-optimal results as it does not account for the trade-off between the operational and embodied impacts. From a general perspective, the operational carbon and cost are proportional to operational energy use due to the fixed cost and carbon emission coefficient of energy use (i.e. electricity consumption). Since the operational impacts often outweigh embodied impacts, a reduction in the operational impacts may strongly influence the total lifecycle impacts. However, this is not the case for low carbon buildings in which embodied impacts contribute as much as operational impacts especially with the use of renewable energy sources. Different materials and constructions can yield unique carbon emissions and costs. For instance, a single optimization of the operational energy use may yield significant reductions in operational energy with proportional reductions in the carbon emission and cost. However, such reductions may translate to high embodied impacts and costs if they are not included in the design process. It is therefore important to explore the intrinsic trade-offs between the operational and embodied performance of different materials and constructions in terms of the energy use, carbon emission and cost. The multi-objective optimization serves an important role especially for the embodied phase since many trade-offs are found between the energy use, carbon emission and cost of different building constructions and materials. In this light, the study provides an integrated framework which allows the joint optimization of both operational and

embodied impacts to explore design alternatives that reduce both operational and embodied impacts. By exploring building design variables under this optimization framework, materials and constructions balancing the embodied and operational impacts can be determined.

From the perspective of lifecycle phase, the contribution of embodied impacts is increased to about 50% of the total life cycle impacts which increases the significance of reducing embodied impacts using low energy and low carbon materials. Therefore, a joint optimization of all phases in the lifecycle provides better opportunities to reduce the overall environmental impacts of buildings. This study has demonstrated that low carbon materials that also reduce embodied impacts and cost while attaining similar levels of operational efficiency can be identified in the design optimization approach. For instance, the findings guide the selection of high-performance materials with lower embodied impacts for constructions. The findings also highlight the need to prioritize renewable energy sources since it drastically reduces carbon emissions and costs. Although PV installation increases the initial embodied impacts and costs, its operational benefits outweigh the initial embodied impacts leading to drastic reduction of the total energy use, carbon emission and cost of the building. The optimal configuration of the PV system is influenced by factors such as the orientation of the PV, tilt, and peripheral shading. Especially, the tilt angle for roof top installation is selected per local latitude (Yang and Lu, 2005). Although the maximized PV coverage often yields the maximum power generation, the installation of PV on fully or partially shaded façades may lead to poor energy conversion efficiency and cost effectiveness. Thus, it is important to explore the façade areas that receive the most solar radiance. By exploring different roof PV orientations, tilt angles and installations of PV on facades, the framework can identify the optimal design case for the PV envelope. Considerations of different PV coverage areas on east, north, south and west façades also enable the allocation of PV facades for a cost-optimal low carbon design solution.

Confounding factors affect the energy use, carbon emission and economic assessments by varying the levels of internal loads. The finding underscores the role of confounding factors in achieving carbon neutrality. By moderating internal loads using energy efficient equipment, low levels of operational CED can be achieved with onsite PV generated electricity to reduce the overall carbon and cost of the building. In the case of higher internal loads, the choice of off grid electricity must be renewable sources in order to limit the overall carbon emissions. Hence the feasibility of achieving carbon neutrality is largely dependent on the electricity mix.

The scenario analysis of climate change reveals the sensitivity of building performance to the representative concentration pathways and vice versa. Increasing temperatures exacerbates the building energy use, carbon emission and cost which also aggregates climate change in the long run. As a proof, scenario RCP 8.5 illustrates how no intervention leads to extremely high carbon emissions which are progressive over the decades. Contrarily, RCP 2.6 illustrates a progressive reduction in the energy use, carbon emission and cost. As the efficiency of building construction processes are improved, the overall impacts of the built environment are moderated which decrease global temperature and building energy use in return. Applying moderate scenarios also demonstrate the impacts of constrained climate action on the overall performance of buildings. Although these moderate mitigation strategies reduce carbon emissions, they are not sufficient to reduce carbon emissions to limit the temperature within habitable levels.

The results demonstrate that stringent climate mitigation strategies are feasible without large investments. The findings indicate a lower life cycle cost in comparison with the base case model. The study's optimization approach leads to a positive linear relationship between the three studied objectives. Thus, the solutions identified can reduce the energy use, carbon and cost significantly. Nevertheless, a significant amount of initial investment is required for the installation of renewable energy systems.

This research covers the life cycle of the building except transportation, construction, and end-of-life phases. The integration of these lifecycle phases could lead to further improvement in the overall performance of the building with beneficial implications on mitigating climate change. For instance, recycling of materials and using renewable energy sources during the construction phase can further reduce environmental impacts. The design optimization method can be applied to other building archetypes and regions by modifying the configuration of building envelope constructions and the LCA database.

## **8.5 Summary**

This chapter presented a parametric multi-objective optimization method that integrates LCA and LCCA to evaluate the energy use, carbon emission and cost of buildings. The joint optimization of embodied and operational impacts allows a comprehensive assessment of the whole lifecycle impacts to select a cost effective and climate responsive building design. This multi-objective optimization approach can solve the trade-off between conflicting design variables and guides the identification of design solutions with a positive linear relationship between the CED, GWP and cost.

The main findings from the study are summarised as follows:

- A parametric optimization approach is applied to design a low carbon mid-rise building by coupling energy efficient building envelope designs with building integrated PV through a joint optimization of the embodied and operational impacts. The reference model was validated with operational data which showed a deviation within 5%. Based on the multi-objective optimization, the CED, GWP and cost are improved by 42.01%, 57.67% and 32.28%, respectively. PV generated electricity covers up to 57% of the

annual operational energy use which reduces the carbon and cost burden of grid imported electricity.

- The optimal building design shows a WWR of 0.2, shape coefficient of 0.5, BO of 150° from the north, wooden-framed tripple glazed windows, very low infiltration rate, highly insulated facade and roof, non-insulated floors and south facing rooftop PV systems. Specifically, the optimal roof design is characterised by a reinforced concrete, PUR foam insulation and EPDM membrane. The optimal design scenarios also show a preference for maximised PV coverage on the roof and façade.
- Confounding factors can greatly influence the total energy use, carbon emission and cost performance of buildings. By reducing the internal loads of the building, the CED, GWP and cost can be further reduced by 52.65%, 74.62% and 58.95%. On the contrary a high level of internal loads can lead to 62.26%, 90.68 and 67.70% increase in the CED, GWP and cost.
- All scenarios to explore the impact of climate change on buildings indicate a continuous increase in building energy use in the future, however a drastic mitigation strategy with renewable energy applications and improved efficiency in building construction processes can reduce the building energy use and carbon emission after the next two decades.

Overall, the study provides valuable insight into coupling passive design strategies with PV to achieve low carbon building design under the impacts of confounding factors and climate change. In future studies, the construction and end-of-life phases can be integrated into the optimization process when exploring other renewable energy sources and recycling strategies.

## **CHAPTER 9 CONCLUSION AND RECOMMENDATION FOR FUTURE WORK**

Building lifecycle assessment is spotlighted given its potential to improve the overall performance of buildings towards carbon neutrality. Hence, the integration of BIM and LCA is underscored as an effective approach to implement LCA during the design of buildings. In this thesis, a comprehensive literature review was conducted to identify research gaps in BIM-based LCA. Based on the deficiencies of existing research methods, a comprehensive BIM-based LCA method was developed to evaluate the embodied impacts of buildings. A systematic LCA integrating different assessment levels, lifecycle stages and impact assessment methods was conducted to evaluate the lifecycle performance of a building's representative of a residential archetype in Hong Kong and Ghana. Furthermore, a detailed tier-hybrid uncertainty assessment method integrating qualitative and quantitative approaches was applied to evaluate parameter, model and scenario uncertainties induced in the embodied impact assessment. The developed BIM-based LCA method is incorporated into a whole building lifecycle optimization process integrating passive design strategies, renewable energy systems, technical and economic indicators, and multi-objective optimization. An integrated design optimization is performed on design decisions to identify the optimal trade-off between the embodied and operational impacts of buildings. Also, a comprehensive technical and economic optimization of passive design strategies and renewable energy systems to determine optimal building design with reference to energy, environmental and economic performance is performed. The developed integrated BIM-based LCA optimization method and research finding will guide the implementation of BIM-based LCA during the design and construction of low carbon building with renewable energy applications in order to achieve carbon neutrality. The main research finding and recommendations for future works are summarised as follows.

## **9.1 Development of the BIM-based LCA method for the embodied phases of buildings**

The automated modelling and systematic evaluation for the BIM-based LCA method has been developed for application in both prefabricated and conventional buildings. A comprehensive assessment method is specified involving database repository, BIM module, and impact estimation module. A systematic result at different levels of assessments is automatically produced allowing for deep analyses and identifications of hotspots at elementary, component and unit levels. Different impact assessment methods are implemented to enhance decision making based on various assessment criteria while assessment is formulated to include key embodied impacts (materials production, transportation, maintenance, and end-of-life phases). Improvements in the evaluation of transportation, construction and end-of-life phases is achieved with an enhanced database and its integration with BIM to allocate transport modes, load factors, construction, and demolition equipment. Modelling assessments are conducted on a high-rise residential building in Hong Kong to explore the operational performance of developed method and validate its accuracy. The systematic results at different levels of assessment is found to be consistent with conventional LCA research. Given an adjusted system boundary, the results are highly probable to be the same as conventional LCA. The developed method is proven to produce accurate results with a higher computational efficiency for different levels of assessments, system boundaries and functional units comparable with previous studies. It is achieved through an automated process of systematic zoning and set up after creating parameters and populating BIM with LCA data which can provide an enhanced mechanism to iterate design options at materials, element or assembly to further whole lifecycle design optimization of buildings.

## **9.2 Comparative assessment of the energy and carbon performance of alternative façade systems**

Following the study on the lifecycle performance of a residential building in Hong Kong, a comparative study was performed on a residential building model in Ghana to investigate the energy and environmental performance of novel façades in comparison to the conventional façades used in the Ghanaian residential sector. Three novel façades including G. Steel ICF, Shotcrete ICF and SEBF were compared with the conventional CBMF. The results revealed that in comparison with the reference façade (CBMF), total CED of SEBF is decreased by 39.13% while CED of Shotcrete ICF and G. Steel ICF is increased by 8.32% and 7.32% respectively. On the other hand, GWP is decreased by 18.07%, 12.47% and 6.88% for SEBF, G. Steel ICF and Shotcrete ICF respectively. Scenarios are developed to investigate the potential to reduce energy use and carbon impacts by moderating the source of materials and design of façades. By using hollow CBMF and sourcing insulation, finishes and reinforcement locally, the embodied energy use and carbon emissions can be reduced by 13.02% and 13.45%, respectively. By replacing reinforced concrete lintels in SEBF with reinforced stabilized earth blocks, and sourcing steel locally, the embodied energy use and carbon emissions can be reduced by 11.87% and 15.87%, respectively. Similarly, a reduction of 22.64% and 27.41% in the embodied energy use and carbon emission is achieved for Shotcrete ICF by reducing the thickness of shotcrete and sourcing steel locally. The embodied energy use and carbon emission of G. Steel ICF can also be reduced by 7.16% and 8.80%, respectively using locally manufactured finishes, insulation, and reinforcement. The scenario analysis reduces CED and GWP of all façades with particularly profound impact on Shotcrete ICF. An economic assessment also indicated that the reference façade (CBMF) has a higher cost in comparison with SEBF, G. Steel ICF and Shotcrete ICF cost 47.87%, 22.44% and 4.59% less, respectively. Such detailed technical and economic assessment of conventional and new façade systems

using the designed BIM-LCA method provide useful reference and guidance to stakeholders in designing sustainable buildings for the Ghanaian residential sector.

### **9.3 Uncertainty in the embodied impacts of buildings**

On top of the BIM-based LCA, a tier-hybrid uncertainty analysis was developed to investigate the impacts of parameter, model, and scenario uncertainties in the embodied impacts of buildings. The developed uncertainty analysis approach is composed of a DQI method to characterize uncertainty parameters without sufficient data qualitatively and a statistical method to qualify parameters with sufficient data quantitatively. A large sample of LCA parameters were retrieved to obtain the statistical distribution in the case of the former whereas a data quality pedigree matrix was applied to derive the covariance in the case of the latter. Monte Carlo simulation is applied to generate a large sample size of 10,000 per parameter to obtain the statistical estimations of parameter, scenario, and model uncertainties. These are expressed in terms of the coefficient of variation according to material types, life cycle phases and the impact assessment method. The tier-hybrid method is applied to quantify uncertainties in life cycle of actual case study building in Hong Kong. The coefficient of variation with regards to CED and GWP was found to range between 8.9% to 15.9% and materials with the highest uncertainties are windows, doors, aluminum, paints and formwork. The analysis of each lifecycle phase indicates that the material production phase contributes the largest impact but the least uncertainty while transportation, construction and maintenance phases with relatively lower impacts are embedded with very large uncertainties. The overall coefficient of variation for materials production, construction, transportation and maintenance phases were 11.79%, 24.59%, 29.73% and 19.47%. High uncertainties in the construction, transportation and maintenance phases can be attributed to poor quality input data based on assumptions and estimations from previous studies, large variation in transport distances of modeled materials, variations in the service life of building components and materials. Similarly, the rarity of end-

of-life cycle modelling implies the use of unverified or unrepresentative input data. Hence proper modelling of the degradation of materials and components, enhancement in LCA data quality through proper measurement can reduce parameter uncertainties. Two approaches are modelled to investigate the impacts of model uncertainties. The first scenario in which the probability distributions are modified indicates that overall mean of the uniform, normal and triangular distribution was 6% lower in comparison with the initial lognormal distribution and has similar implication in their standard deviation. The second scenario which compares a pure DQI approach to the tier-hybrid approach shows about 3.5% decrements in the overall means of uniform, normal and triangular distribution. The analysis helps to precisely quantify the uncertainties through the integration of statistical and DQI approach which reflects the dispersion in the results. The choice and integration of probability distribution can also vary the results of uncertainty analysis even with a DQI approach only. This comprehensive uncertainty analysis study can guide stakeholders in decision making with regards to the embodied impacts of buildings.

#### **9.4 Staged optimization of mid-rise residential buildings with alternative composite façade systems**

In addition to the BIM-based LCA study on novel facades for Ghanaian residential buildings, an optimization of the embodied and operational impacts has also been studied. An actual case study on a mid-rise residential building integrating passive design strategies, four façade systems and integrated renewable system is investigated to optimize the trade-off between embodied and operational impacts. The multi-objective optimization is performed in two stages to first optimize building energy use and renewable energy generation followed by an optimization of the trade-off between embodied and operational impacts based on the façade systems. The first stage of the optimization includes parameters such as building orientation, window to wall ratio, façade infiltration and BIPV window to wall ratio. The optimal solutions

showed preference for a south facing building with an orientation of 180°. Furthermore, the results also favor the exploitation of windows and BIPV design as they have more influence to improve the performance of the building. The second stage optimization indicated that similar levels of operational energy can be achieved with wide variations in the embodied impacts. Slight increment in the thickness of BWMF façade leads to a much higher increase in its embodied impacts without a significant decrease in the operational impact, thus leading to higher net impacts. Also, the variations in the thickness of CMBF yielded similar operational impacts but large difference in embodied impacts thus the least acceptable thickness represents its most sustainable solution. For shotcrete ICF and GS. ICF, an increment in the thickness of insulation leads to exponential increase without significant decrease in the operational energy. Overall, the optimal solution can reduce total life cycle energy use by up to 24.59% in comparison to the baseline building and PV energy generation can cover up to 90% of the total building energy demand. The optimization results were also validated as applicable in Burkina Faso and Nigeria with similar archetypes and climatic conditions which showed up to 33.33% and 36.93% energy savings respectively. Such a whole lifecycle optimization of buildings in developing regions will provide a valuable reference for stakeholders to develop sustainable housing projects amidst the increasing demands for social housing.

### **9.5 Holistic environmental and economic design optimization of buildings**

Finally, a comprehensive parametric BIM-based LCA optimization as an alternative to conventional LCA analysis was performed. The developed approach integrates building energy simulation with LCA to perform rigorous assessment and optimization of energy use and carbon emission in a cost-effective approach. Extensive analyses are conducted with a wide range of passive design strategies, building envelope material passport and renewable energy systems. Assessment criteria were defined to include dynamic prospects such as confounding factors like building occupancy and performance variations due to climate change. Sub-scenarios were

adjusted, and post-optimization assessment revealed an influence of these confounding factors. The comprehensive parametric BIM-based LCA design optimization method was applied to a mid-rise residential building in Ghana. Eighteen design variables including building orientation, shape coefficient, window to wall ratio (north façade, south façade, west façade, east façade), window construction, wall construction, roof construction, floor construction, PV installation (roof top PV, north, south, west, east façade BIPV), rooftop PV orientation, rooftop PV tilt, façade infiltration rate variables were included in the comprehensive assessment method. In comparison to the benchmark model, the optimized model improved CED, GWP and cost by 42%, 58% and 32%. With an upper and lower limit determined through variations of confounding factors, the variations in the optimized results were illustrated. Confounding factors can greatly increase or decrease the optimal results. In case of a high confounding factor level CED, GWP and cost can be increased by 63%, 91% and 68%, respectively. On the contrary, CED, GWP and cost can be decreased by 53%, 75% and 59%, respectively. Post exploration of optimization results indicate feasibility to reduce optimization time by 50%. The exploration of representative concentration pathways indicates a continuous increase in energy use with similar implications for carbon emission and cost. However, stringent application of sustainable design measures and renewable energy systems can reverse trends in the future. This new parametric BIM-based LCA design assessment method provides a comprehensive approach for stakeholders to make informed design decision based on optimized energy and carbon performance of the whole lifecycle of buildings in a cost-effective method. The systematic approach detailed in this study can also guide the development of similar methodologies for varying design or geographical contexts. The results detailed in the study can also provide guidance to stakeholders and policy makers towards designing for whole lifecycle carbon neutrality.

## 9.6 Recommendations for future research

This thesis presents a systematic study on a robust BIM-based LCA design approach which integrates LCA, building energy simulation, parametric design optimization, passive design and renewable energy integration for a comprehensively optimized energy and carbon performance in a cost-effective approach. However, there are scopes which need to be subject to further detailed investigation in future works due to limited time and data unavailability.

Firstly, the optimization algorithm adopted for the multi-objective optimization requires huge computational resources and long periods of computation due to the large number of parameters involved in building LCA. In future studies comprehensive sensitivity analysis will be integrated into the optimization process to investigate the most relevant parameters to whole lifecycle building performance. Also, machine learning techniques will be implemented to reduce the time and computational resources required for the whole lifecycle performance.

Secondly, the uncertainty analysis of the embodied impacts was not included into the optimization process due to complexities of integrating the quantitative approach into the BIM-based LCA approach. Likewise, the transportation phase, construction and end-of-life cycle phases were excluded in the optimization process due to rarity of data and lack of uniformity in available LCIA data. In the future more complicated models will be examined to streamline uncertainties in other investigate the influence of lack of data and these lifecycle phases on the whole life cycle optimization of buildings.

Lastly, a dynamic modelling of carbon emissions during the operational phase of building needs to be studied, considering the hourly variation in carbon emissions due to imports and export of renewable energy to and from the grid. The resultant variations in hourly carbon emissions can profoundly impact joint optimization of energy use and carbon emissions which needs to be explored in a comprehensive optimization process.

## REFERENCES

- [1] M.K. Dixit, C.H. Culp, J.L. Fernández-Solís, System boundary for embodied energy in buildings: A conceptual model for definition, *Renewable and Sustainable Energy Reviews*. 21 (2013) 153–164. <https://doi.org/10.1016/J.RSER.2012.12.037>.
- [2] A. Acquaye, S. Taylor, L. Ozawa-Meida, R. Greenough, T. Ibn-Mohammed, Operational vs. embodied emissions in buildings—A review of current trends, *Energy and Buildings*. 66 (2013) 232–245. <https://doi.org/10.1016/j.enbuild.2013.07.026>.
- [3] M. Najjar, K. Figueiredo, M. Palumbo, A. Haddad, Integration of BIM and LCA: Evaluating the environmental impacts of building materials at an early stage of designing a typical office building, *Journal of Building Engineering*. 14 (2017) 115–126. <https://doi.org/10.1016/J.JOBE.2017.10.005>.
- [4] B. Soust-Verdaguer, C. Llatas, A. García-Martínez, Critical review of bim-based LCA method to buildings, *Energy and Buildings*. 136 (2017) 110–120. <https://doi.org/10.1016/J.ENBUILD.2016.12.009>.
- [5] X. Chen, H. Yang, L. Lu, A comprehensive review on passive design approaches in green building rating tools, *Renewable and Sustainable Energy Reviews*. 50 (2015) 1425–1436. <https://doi.org/10.1016/j.rser.2015.06.003>.
- [6] X. Chen, H. Yang, A multi-stage optimization of passively designed high-rise residential buildings in multiple building operation scenarios, *Applied Energy*. 206 (2017) 541–557. <https://doi.org/10.1016/j.apenergy.2017.08.204>.
- [7] X. Chen, H. Yang, Integrated energy performance optimization of a passively designed high-rise residential building in different climatic zones of China, *Applied Energy*. 215 (2018) 145–158. <https://doi.org/10.1016/j.apenergy.2018.01.099>.

- [8] I. Oropeza-Perez, P.A. Østergaard, Active and passive cooling methods for dwellings: A review, *Renewable and Sustainable Energy Reviews*. 82 (2018) 531–544.  
<https://doi.org/10.1016/j.rser.2017.09.059>.
- [9] F. Harkouss, F. Fardoun, P.H. Biwole, Passive design optimization of low energy buildings in different climates, *Energy*. 165 (2018) 591–613.  
<https://doi.org/10.1016/j.energy.2018.09.019>.
- [10] K. Konis, A. Gamas, K. Kensek, Passive performance and building form: An optimization framework for early-stage design support, *Solar Energy*. 125 (2016) 161–179. <https://doi.org/10.1016/j.solener.2015.12.020>.
- [11] A. Balali, A. Valipour, Prioritization of passive measures for energy optimization designing of sustainable hospitals and health centres, *Journal of Building Engineering*. 35 (2021) 101992. <https://doi.org/10.1016/j.jobe.2020.101992>.
- [12] X. Su, S. Tian, X. Shao, X. Zhao, Embodied and operational energy and carbon emissions of passive building in HSCW zone in China: A case study, *Energy and Buildings*. 222 (2020) 110090.  
<https://doi.org/https://doi.org/10.1016/j.enbuild.2020.110090>.
- [13] V. Venkatraj, M.K. Dixit, W. Yan, S. Lavy, Evaluating the impact of operating energy reduction measures on embodied energy, *Energy and Buildings*. 226 (2020) 110340.  
<https://doi.org/https://doi.org/10.1016/j.enbuild.2020.110340>.
- [14] F. Shadram, J. Mukkavaara, An integrated BIM-based framework for the optimization of the trade-off between embodied and operational energy, *Energy and Buildings*. 158 (2018) 1189–1205. <https://doi.org/10.1016/J.ENBUILD.2017.11.017>.

- [15] F. Shadram, J. Mukkavaara, Exploring the effects of several energy efficiency measures on the embodied/operational energy trade-off: A case study of swedish residential buildings, *Energy and Buildings*. 183 (2019) 283–296.  
<https://doi.org/10.1016/j.enbuild.2018.11.026>.
- [16] M.A. Adabre, A.P.C. Chan, Critical success factors (CSFs) for sustainable affordable housing, *Building and Environment*. 156 (2019) 203–214.  
<https://doi.org/10.1016/J.BUILDENV.2019.04.030>.
- [17] A. Owusu-Ansah, K.W. Soyeh, P.K. Asabere, Developer constraints on housing supply in urban Ghana, *International Journal of Housing Markets and Analysis*. 12 (2019) 59–73. <https://doi.org/10.1108/IJHMA-07-2018-0052>.
- [18] International Energy Agency, *Buildings – A source of enormous untapped efficiency potential*, (2021). <https://www.iea.org/topics/buildings> (accessed June 1, 2021).
- [19] A. Sharma, A. Saxena, M. Sethi, V. Shree, Varun, Life cycle assessment of buildings: A review, *Renewable and Sustainable Energy Reviews*. 15 (2011) 871–875.  
<https://doi.org/10.1016/J.RSER.2010.09.008>.
- [20] M. Kamali, K. Hewage, Life cycle performance of modular buildings: A critical review, *Renewable and Sustainable Energy Reviews*. 62 (2016) 1171–1183.  
<https://doi.org/10.1016/J.RSER.2016.05.031>.
- [21] M.K. Dixit, J.L. Fernández-Solís, S. Lavy, C.H. Culp, Need for an embodied energy measurement protocol for buildings: A review paper, *Renewable and Sustainable Energy Reviews*. 16 (2012) 3730–3743. <https://doi.org/10.1016/j.rser.2012.03.021>.

- [22] F. Shadram, S. Bhattacharjee, S. Lidelöw, J. Mukkavaara, T. Olofsson, Exploring the trade-off in life cycle energy of building retrofit through optimization, *Applied Energy*. 269 (2020) 115083. <https://doi.org/https://doi.org/10.1016/j.apenergy.2020.115083>.
- [23] M.K. Ansah, X. Chen, H. Yang, L. Lu, P.T.I. Lam, A review and outlook for integrated BIM application in green building assessment, *Sustainable Cities and Society*. 48 (2019). <https://doi.org/10.1016/j.scs.2019.101576>.
- [24] J.K.-W. Wong, K.-L. Kuan, Implementing “BEAM Plus” for BIM-based sustainability analysis, *Automation in Construction*. 44 (2014) 163–175. <https://doi.org/10.1016/j.autcon.2014.04.003>.
- [25] R. Santos, A.A. Costa, J.D. Silvestre, L. Pyl, Informetric analysis and review of literature on the role of BIM in sustainable construction, *Automation in Construction*. 103 (2019) 221–234. <https://doi.org/https://doi.org/10.1016/j.autcon.2019.02.022>.
- [26] Z. Pezeshki, A. Soleimani, A. Darabi, Application of BEM and using BIM database for BEM: A review, *Journal of Building Engineering*. 23 (2019) 1–17. <https://doi.org/https://doi.org/10.1016/j.jobe.2019.01.021>.
- [27] A. Andriamamonjy, D. Saelens, R. Klein, A combined scientometric and conventional literature review to grasp the entire BIM knowledge and its integration with energy simulation, *Journal of Building Engineering*. 22 (2019) 513–527. <https://doi.org/https://doi.org/10.1016/j.jobe.2018.12.021>.
- [28] M. Röck, A. Hollberg, G. Habert, A. Passer, LCA and BIM: Visualization of environmental potentials in building construction at early design stages, *Building and Environment*. 140 (2018) 153–161. <https://doi.org/10.1016/J.BUILDENV.2018.05.006>.

- [29] M. Park, N. Kwon, J. Lee, S. Lee, Y. Ahn, Probabilistic maintenance cost analysis for aged Multi-Family housing, *Sustainability*. 11 (2019) 1843.
- [30] B. Meacham, R. Bowen, J. Traw, A. Moore, Performance-based building regulation: current situation and future needs, *Building Research & Information*. 33 (2005) 91–106.
- [31] M.U. Hossain, C.S. Poon, Global warming potential and energy consumption of temporary works in building construction: A case study in Hong Kong, *Building and Environment*. 142 (2018) 171–179. <https://doi.org/10.1016/j.buildenv.2018.06.026>.
- [32] H. Yan, Q. Shen, L.C.H. Fan, Y. Wang, L. Zhang, Greenhouse gas emissions in building construction: A case study of One Peking in Hong Kong, *Building and Environment*. 45 (2010) 949–955. <https://doi.org/10.1016/J.BUILDENV.2009.09.014>.
- [33] K. Goulouti, P. Padey, A. Galimshina, G. Habert, S. Lasvaux, Uncertainty of building elements' service lives in building LCA & LCC: What matters?, *Building and Environment*. (2020) 106904. <https://doi.org/https://doi.org/10.1016/j.buildenv.2020.106904>.
- [34] S. Fufa, R. Schlanbusch, K. Sørnes, M. Inman, A Norwegian ZEB definition guideline, (2016). [https://brage.bibsys.no/xmlui/bitstream/handle/11250/2406473/ZEB\\_pr\\_report\\_no29.pdf?sequence=3](https://brage.bibsys.no/xmlui/bitstream/handle/11250/2406473/ZEB_pr_report_no29.pdf?sequence=3) (accessed April 25, 2019).
- [35] B. Soust-Verdaguer, C. Llatas, A. García-Martínez, Critical review of bim-based LCA method to buildings, *Energy and Buildings*. 136 (2017) 110–120. <https://doi.org/10.1016/J.ENBUILD.2016.12.009>.

- [36] M. Röck, A. Hollberg, G. Habert, A. Passer, LCA and BIM: Visualization of environmental potentials in building construction at early design stages, *Building and Environment*. 140 (2018) 153–161. <https://doi.org/10.1016/J.BUILDENV.2018.05.006>.
- [37] J. Basbagill, F. Flager, M. Lepech, M. Fischer, Application of life-cycle assessment to early stage building design for reduced embodied environmental impacts, *Building and Environment*. 60 (2013) 81–92. <https://doi.org/10.1016/J.BUILDENV.2012.11.009>.
- [38] L. Georges, M. Haase, A. Houlihan Wiberg, T. Kristjansdottir, B. Risholt, Life cycle emissions analysis of two nZEB concepts, *Building Research and Information*. 43 (2015) 82–93. <https://doi.org/10.1080/09613218.2015.955755>.
- [39] J.L. Hao, B. Cheng, W. Lu, J. Xu, J. Wang, W. Bu, Z. Guo, Carbon emission reduction in prefabrication construction during materialization stage: A BIM-based life-cycle assessment approach, *Science of The Total Environment*. 723 (2020) 137870. <https://doi.org/https://doi.org/10.1016/j.scitotenv.2020.137870>.
- [40] C. Peng, Calculation of a building's life cycle carbon emissions based on Ecotect and building information modeling, *Journal of Cleaner Production*. 112 (2016) 453–465. <https://doi.org/10.1016/J.JCLEPRO.2015.08.078>.
- [41] Y.S. Shin, K. Cho, BIM application to select appropriate design alternative with consideration of LCA and LCCA, *Mathematical Problems in Engineering*. 2015 (2015). <https://doi.org/10.1155/2015/281640>.
- [42] M. Najjar, K. Figueiredo, A.W.A. Hammad, A. Haddad, Integrated optimization with building information modeling and life cycle assessment for generating energy efficient buildings, *Applied Energy*. 250 (2019) 1366–1382. <https://doi.org/10.1016/J.APENERGY.2019.05.101>.

- [43] R.S. Nizam, C. Zhang, L. Tian, A BIM based tool for assessing embodied energy for buildings, *Energy and Buildings*. 170 (2018) 1–14.  
<https://doi.org/10.1016/j.enbuild.2018.03.067>.
- [44] F. Rezaei, C. Bulle, P. Lesage, Integrating building information modeling and life cycle assessment in the early and detailed building design stages, *Building and Environment*. 153 (2019) 158–167. <https://doi.org/10.1016/J.BUILDENV.2019.01.034>.
- [45] X. Yang, M. Hu, J. Wu, B. Zhao, Building-information-modeling enabled life cycle assessment, a case study on carbon footprint accounting for a residential building in China, *Journal of Cleaner Production*. 183 (2018) 729–743.  
<https://doi.org/10.1016/J.JCLEPRO.2018.02.070>.
- [46] C. Zhang, R.S. Nizam, L. Tian, BIM-based investigation of total energy consumption in delivering building products, *Advanced Engineering Informatics*. 38 (2018) 370–380. <https://doi.org/10.1016/J.AEI.2018.08.009>.
- [47] C. Cavalliere, G.R. Dell’Osso, A. Pierucci, F. Iannone, Life cycle assessment data structure for building information modelling, *Journal of Cleaner Production*. 199 (2018) 193–204. <https://doi.org/10.1016/j.jclepro.2018.07.149>.
- [48] A. Hollberg, G. Genova, G. Habert, Evaluation of BIM-based LCA results for building design, *Automation in Construction*. 109 (2020) 102972.  
<https://doi.org/10.1016/J.AUTCON.2019.102972>.
- [49] R. Santos, A.A. Costa, J.D. Silvestre, L. Pyl, Integration of LCA and LCC analysis within a BIM-based environment, *Automation in Construction*. 103 (2019) 127–149.  
<https://doi.org/10.1016/J.AUTCON.2019.02.011>.

- [50] F. Shadram, J. Mukkavaara, An integrated BIM-based framework for the optimization of the trade-off between embodied and operational energy, *Energy and Buildings*. 158 (2018) 1189–1205. <https://doi.org/10.1016/j.enbuild.2017.11.017>.
- [51] X. Chen, H. Yang, Combined thermal and daylight analysis of a typical public rental housing development to fulfil green building guidance in Hong Kong, *Energy and Buildings*. 108 (2015) 420–432. <https://doi.org/10.1016/j.enbuild.2015.09.032>.
- [52] Y. Sun, Sensitivity analysis of macro-parameters in the system design of net zero energy building, *Energy and Buildings*. 86 (2015) 464–477. <https://doi.org/10.1016/j.enbuild.2014.10.031>.
- [53] I. Oropeza-Perez, P.A. Østergaard, Active and passive cooling methods for dwellings: A review, *Renewable and Sustainable Energy Reviews*. 82 (2018) 531–544. <https://doi.org/10.1016/j.rser.2017.09.059>.
- [54] Y. Jung, Y. Heo, H. Lee, Multi-objective optimization of the multi-story residential building with passive design strategy in South Korea, *Building and Environment*. 203 (2021) 108061. <https://doi.org/10.1016/j.buildenv.2021.108061>.
- [55] C. Lamnatou, M. Smyth, D. Chemisana, Building-Integrated Photovoltaic/Thermal (BIPVT): LCA of a façade-integrated prototype and issues about human health, ecosystems, resources, *Science of the Total Environment*. 660 (2019) 1576–1592. <https://doi.org/10.1016/j.scitotenv.2018.12.461>.
- [56] F. Rossi, M. Heleno, R. Basosi, A. Sinicropi, Environmental and economic optima of solar home systems design: A combined LCA and LCC approach, *Science of the Total Environment*. 744 (2020) 140569. <https://doi.org/10.1016/j.scitotenv.2020.140569>.

- [57] C. Lamnatou, G. Notton, D. Chemisana, C. Cristofari, Storage systems for building-integrated photovoltaic (BIPV) and building-integrated photovoltaic/thermal (BIPVT) installations: Environmental profile and other aspects, *Science of the Total Environment*. 699 (2020) 134269. <https://doi.org/10.1016/j.scitotenv.2019.134269>.
- [58] X. Chen, H. Yang, L. Lu, A comprehensive review on passive design approaches in green building rating tools, *Renewable and Sustainable Energy Reviews*. 50 (2015) 1425–1436. <https://doi.org/10.1016/j.rser.2015.06.003>.
- [59] F. Shadram, S. Bhattacharjee, S. Lidelöw, J. Mikkavaara, T. Olofsson, Exploring the trade-off in life cycle energy of building retrofit through optimization, *Applied Energy*. 269 (2020) 115083. <https://doi.org/https://doi.org/10.1016/j.apenergy.2020.115083>.
- [60] E. Hoxha, T. Jusselme, On the necessity of improving the environmental impacts of furniture and appliances in net-zero energy buildings, *Science of the Total Environment*. 596–597 (2017) 405–416. <https://doi.org/10.1016/j.scitotenv.2017.03.107>.
- [61] J. Choi, M.G. Lee, H.S. Oh, S.G. Bae, J.H. An, D.Y. Yun, H.S. Park, Multi-objective green design model to mitigate environmental impact of construction of mega columns for super-tall buildings, *Science of the Total Environment*. 674 (2019) 580–591. <https://doi.org/10.1016/j.scitotenv.2019.04.152>.
- [62] N. Abdou, Y. EL Mghouchi, S. Hamdaoui, N. EL Asri, M. Mouqallid, Multi-objective optimization of passive energy efficiency measures for net-zero energy building in Morocco, *Building and Environment*. 204 (2021) 108141. <https://doi.org/10.1016/j.buildenv.2021.108141>.

- [63] K. Lakhdari, L. Sriti, B. Painter, Parametric optimization of daylight, thermal and energy performance of middle school classrooms, case of hot and dry regions, *Building and Environment*. 204 (2021) 108173. <https://doi.org/10.1016/j.buildenv.2021.108173>.
- [64] E. Vettorazzi, A. Figueiredo, F. Rebelo, R. Vicente, E. Grala da Cunha, Optimization of the passive house concept for residential buildings in the South-Brazilian region, *Energy and Buildings*. 240 (2021) 110871. <https://doi.org/10.1016/j.enbuild.2021.110871>.
- [65] R. Wang, S. Lu, W. Feng, A three-stage optimization methodology for envelope design of passive house considering energy demand, thermal comfort and cost, *Energy*. 192 (2020) 116723. <https://doi.org/10.1016/j.energy.2019.116723>.
- [66] X. Chen, H. Yang, K. Sun, A holistic passive design approach to optimize indoor environmental quality of a typical residential building in Hong Kong, *Energy*. 113 (2016) 267–281. <https://doi.org/10.1016/j.energy.2016.07.058>.
- [67] R. Lapisa, E. Bozonnet, P. Salagnac, M.O. Abadie, Optimized design of low-rise commercial buildings under various climates – Energy performance and passive cooling strategies, *Building and Environment*. 132 (2018) 83–95. <https://doi.org/10.1016/j.buildenv.2018.01.029>.
- [68] A. Vukadinović, J. Radosavljević, A. Đorđević, M. Protić, N. Petrović, Multi-objective optimization of energy performance for a detached residential building with a sunspace using the NSGA-II genetic algorithm, *Solar Energy*. 224 (2021) 1426–1444. <https://doi.org/10.1016/j.solener.2021.06.082>.
- [69] D. D’Agostino, P. D’Agostino, F. Minelli, F. Minichiello, Proposal of a new automated workflow for the computational performance-driven design optimization of building

- energy need and construction cost, *Energy and Buildings*. 239 (2021) 110857.  
<https://doi.org/10.1016/j.enbuild.2021.110857>.
- [70] P.E. Camporeale, P. Mercader-Moyano, Towards nearly Zero Energy Buildings: Shape optimization of typical housing typologies in Ibero-American temperate climate cities from a holistic perspective, *Solar Energy*. 193 (2019) 738–765.  
<https://doi.org/10.1016/j.solener.2019.09.091>.
- [71] X. Chen, H. Yang, J. Peng, Energy optimization of high-rise commercial buildings integrated with photovoltaic facades in urban context, *Energy*. 172 (2019) 1–17.  
<https://doi.org/10.1016/J.ENERGY.2019.01.112>.
- [72] L. Zhu, B. Wang, Y. Sun, Multi-objective optimization for energy consumption, daylighting and thermal comfort performance of rural tourism buildings in north China, *Building and Environment*. 176 (2020) 106841.  
<https://doi.org/https://doi.org/10.1016/j.buildenv.2020.106841>.
- [73] T. Hong, J. Kim, M. Lee, A multi-objective optimization model for determining the building design and occupant behaviors based on energy, economic, and environmental performance, *Energy*. 174 (2019) 823–834.  
<https://doi.org/10.1016/j.energy.2019.02.035>.
- [74] B. Kiss, Z. Szalay, Modular approach to multi-objective environmental optimization of buildings, *Automation in Construction*. 111 (2020) 103044.  
<https://doi.org/https://doi.org/10.1016/j.autcon.2019.103044>.
- [75] A. Ciardiello, F. Rosso, J. Dell’Olmo, V. Ciancio, M. Ferrero, F. Salata, Multi-objective approach to the optimization of shape and envelope in building energy design, *Applied Energy*. 280 (2020) 115984.  
<https://doi.org/10.1016/j.apenergy.2020.115984>.

- [76] Y. Xu, G. Zhang, C. Yan, G. Wang, Y. Jiang, K. Zhao, A two-stage multi-objective optimization method for envelope and energy generation systems of primary and secondary school teaching buildings in China, *Building and Environment*. 204 (2021) 108142. <https://doi.org/10.1016/j.buildenv.2021.108142>.
- [77] E. Hoxha, G. Habert, S. Lasvaux, J. Chevalier, R. Le Roy, Influence of construction material uncertainties on residential building LCA reliability, *Journal of Cleaner Production*. 144 (2017) 33–47. <https://doi.org/10.1016/j.jclepro.2016.12.068>.
- [78] M.K. Ansah, X. Chen, H. Yang, L. Lu, P.T.I. Lam, An integrated life cycle assessment of different façade systems for a typical residential building in Ghana, *Sustainable Cities and Society*. 53 (2020). <https://doi.org/10.1016/j.scs.2019.101974>.
- [79] X. Zhang, R. Zheng, Reducing building embodied emissions in the design phase: A comparative study on structural alternatives, *Journal of Cleaner Production*. 243 (2020) 118656. <https://doi.org/10.1016/J.JCLEPRO.2019.118656>.
- [80] X. Zhang, R. Zheng, F. Wang, Uncertainty in the life cycle assessment of building emissions: A comparative case study of stochastic approaches, *Building and Environment*. 147 (2019) 121–131. <https://doi.org/10.1016/J.BUILDENV.2018.10.016>.
- [81] X. Zhang, F. Wang, Stochastic analysis of embodied emissions of building construction: A comparative case study in China, *Energy and Buildings*. 151 (2017) 574–584. <https://doi.org/10.1016/j.enbuild.2017.07.012>.
- [82] Y. Teng, W. Pan, Estimating and minimizing embodied carbon of prefabricated high-rise residential buildings considering parameter, scenario and model uncertainties, *Building and Environment*. 180 (2020) 106951. <https://doi.org/10.1016/j.buildenv.2020.106951>.

- [83] M. Robati, D. Daly, G. Kokogiannakis, A method of uncertainty analysis for whole-life embodied carbon emissions (CO<sub>2</sub>-e) of building materials of a net-zero energy building in Australia, *Journal of Cleaner Production*. 225 (2019) 541–553.  
<https://doi.org/10.1016/J.JCLEPRO.2019.03.339>.
- [84] X. Su, X. Zhang, A detailed analysis of the embodied energy and carbon emissions of steel-construction residential buildings in China, *Energy and Buildings*. 119 (2016) 323–330. <https://doi.org/10.1016/J.ENBUILD.2016.03.070>.
- [85] T. Opher, M. Duhamel, I.D. Posen, D.K. Panesar, R. Brugmann, A. Roy, R. Zizzo, L. Sequeira, A. Anvari, H.L. MacLean, Life cycle GHG assessment of a building restoration: Case study of a heritage industrial building in Toronto, Canada, *Journal of Cleaner Production*. 279 (2021) 123819.  
<https://doi.org/https://doi.org/10.1016/j.jclepro.2020.123819>.
- [86] N. Kwon, K. Song, Y. Ahn, M. Park, Y. Jang, Maintenance cost prediction for aging residential buildings based on case-based reasoning and genetic algorithm, *Journal of Building Engineering*. 28 (2020) 101006. <https://doi.org/10.1016/j.jobe.2019.101006>.
- [87] M.F.D. Morales, N. Reguly, A.P. Kirchheim, A. Passuello, Uncertainties related to the replacement stage in LCA of buildings: A case study of a structural masonry clay hollow brick wall, *Journal of Cleaner Production*. 251 (2020) 119649.  
<https://doi.org/https://doi.org/10.1016/j.jclepro.2019.119649>.
- [88] A. Grant, R. Ries, Impact of building service life models on life cycle assessment, *Building Research and Information*. 41 (2013) 168–186.  
<https://doi.org/10.1080/09613218.2012.730735>.
- [89] C. Ferreira, A. Silva, J. de Brito, I.S. Dias, I. Flores-Colen, The impact of imperfect maintenance actions on the degradation of buildings' envelope components, *Journal of*

Building Engineering. 33 (2021) 101571.

<https://doi.org/https://doi.org/10.1016/j.jobe.2020.101571>.

- [90] C. Marques, J. de Brito, A. Silva, Application of the factor method to the service life prediction of etics, *International Journal of Strategic Property Management*. 22 (2018) 204–222. <https://doi.org/10.3846/ijspm.2018.1546>.
- [91] I.M. Shohet, L. Nobili, Performance-Based Maintenance of Public Facilities: Principles and Implementation in Courthouses, *Journal of Performance of Constructed Facilities*. 30 (2016) 04015086. [https://doi.org/10.1061/\(asce\)cf.1943-5509.0000835](https://doi.org/10.1061/(asce)cf.1943-5509.0000835).
- [92] S.H. Mousavi, A. Silva, J. de Brito, A. Ekhlassi, S.B. Hosseini, Service Life Prediction of Natural Stone Claddings with an Indirect Fastening System, *Journal of Performance of Constructed Facilities*. 31 (2017) 04017014. [https://doi.org/10.1061/\(asce\)cf.1943-5509.0001007](https://doi.org/10.1061/(asce)cf.1943-5509.0001007).
- [93] A.J. Prieto, J.M. Macías-Bernal, M.-J. Chávez, F.J. Alejandro, Fuzzy Modeling of the Functional Service Life of Architectural Heritage Buildings, *Journal of Performance of Constructed Facilities*. 31 (2017) 04017041. [https://doi.org/10.1061/\(asce\)cf.1943-5509.0001021](https://doi.org/10.1061/(asce)cf.1943-5509.0001021).
- [94] M.K. Dixit, Life cycle embodied energy analysis of residential buildings: A review of literature to investigate embodied energy parameters, *Renewable and Sustainable Energy Reviews*. 79 (2017) 390–413. <https://doi.org/10.1016/J.RSER.2017.05.051>.
- [95] Y. Zhang, D. Yan, S. Hu, S. Guo, Modelling of energy consumption and carbon emission from the building construction sector in China, a process-based LCA approach, *Energy Policy*. 134 (2019) 110949. <https://doi.org/https://doi.org/10.1016/j.enpol.2019.110949>.

- [96] C.K. Chau, J.M. Xu, T.M. Leung, W.Y. Ng, Evaluation of the impacts of end-of-life management strategies for deconstruction of a high-rise concrete framed office building, *Applied Energy*. 185 (2017) 1595–1603.  
<https://doi.org/10.1016/j.apenergy.2016.01.019>.
- [97] Md.U. Hossain, S.T. Ng, Strategies for enhancing the accuracy of evaluation and sustainability performance of building, *Journal of Environmental Management*. 261 (2020) 110230. <https://doi.org/10.1016/J.JENVMAN.2020.110230>.
- [98] A. Mendoza Beltran, V. Prado, D. Font Vivanco, P.J.G. Henriksson, J.B. Guinée, R. Heijungs, Quantified Uncertainties in Comparative Life Cycle Assessment: What Can Be Concluded?, *Environmental Science & Technology*. 52 (2018) 2152–2161.  
<https://doi.org/10.1021/acs.est.7b06365>.
- [99] E. Igos, E. Benetto, R. Meyer, P. Baustert, B. Othoniel, How to treat uncertainties in life cycle assessment studies?, *The International Journal of Life Cycle Assessment*. 24 (2019) 794–807. <https://doi.org/10.1007/s11367-018-1477-1>.
- [100] S.M. Lloyd, R. Ries, Characterizing, Propagating, and Analyzing Uncertainty in Life-Cycle Assessment: A Survey of Quantitative Approaches, *Journal of Industrial Ecology*. 11 (2007) 161–179. <https://doi.org/10.1162/jiec.2007.1136>.
- [101] A.E. Björklund, Survey of approaches to improve reliability in lca, *The International Journal of Life Cycle Assessment*. 7 (2002) 64. <https://doi.org/10.1007/BF02978849>.
- [102] J. Clavreul, D. Guyonnet, T.H. Christensen, Quantifying uncertainty in LCA-modelling of waste management systems, *Waste Management*. 32 (2012) 2482–2495.  
<https://doi.org/10.1016/j.wasman.2012.07.008>.

- [103] L. Jim, G. Guill, Combined use of life cycle assessment , data envelopment analysis and Monte Carlo simulation for quantifying environmental efficiencies under uncertainty, *Journal of Cleaner Production*. 166 (2017).  
<https://doi.org/10.1016/j.jclepro.2017.07.215>.
- [104] Y. Teng, W. Pan, Estimating and minimizing embodied carbon of prefabricated high-rise residential buildings considering parameter, scenario and model uncertainties, *Building and Environment*. 180 (2020) 106951.  
<https://doi.org/https://doi.org/10.1016/j.buildenv.2020.106951>.
- [105] E. Di Giuseppe, M. D’Orazio, G. Du, C. Favi, S. Lasvaux, G. Maracchini, P. Padey, A Stochastic Approach to LCA of Internal Insulation Solutions for Historic Buildings, *Sustainability*. 12 (2020) 1535. <https://doi.org/10.3390/su12041535>.
- [106] X. Su, Z. Luo, Y. Li, C. Huang, Life cycle inventory comparison of different building insulation materials and uncertainty analysis, *Journal of Cleaner Production*. 112 (2016) 275–281. <https://doi.org/10.1016/J.JCLEPRO.2015.08.113>.
- [107] M. Robati, D. Daly, G. Kokogiannakis, A method of uncertainty analysis for whole-life embodied carbon emissions (CO<sub>2</sub>-e) of building materials of a net-zero energy building in Australia, *Journal of Cleaner Production*. 225 (2019) 541–553.  
<https://doi.org/10.1016/J.JCLEPRO.2019.03.339>.
- [108] R. Heijungs, M. Lenzen, Error propagation methods for LCA - A comparison, *International Journal of Life Cycle Assessment*. 19 (2014) 1445–1461.  
<https://doi.org/10.1007/s11367-014-0751-0>.
- [109] F. Orsini, P. Marrone, Approaches for a low-carbon production of building materials : A review, *Journal of Cleaner Production*. 241 (2019) 118380.  
<https://doi.org/10.1016/j.jclepro.2019.118380>.

- [110] Y. Teng, W. Pan, Systematic embodied carbon assessment and reduction of prefabricated high-rise public residential buildings in Hong Kong, *Journal of Cleaner Production*. 238 (2019) 117791. <https://doi.org/10.1016/J.JCLEPRO.2019.117791>.
- [111] Y. Teng, W. Pan, Systematic embodied carbon assessment and reduction of prefabricated high-rise public residential buildings in Hong Kong, *Journal of Cleaner Production*. 238 (2019) 117791. <https://doi.org/10.1016/J.JCLEPRO.2019.117791>.
- [112] V.J.L. Gan, J.C.P. Cheng, I.M.C. Lo, C.M. Chan, Developing a CO<sub>2</sub>-e accounting method for quantification and analysis of embodied carbon in high-rise buildings, *Journal of Cleaner Production*. 141 (2017) 825–836. <https://doi.org/https://doi.org/10.1016/j.jclepro.2016.09.126>.
- [113] J. Xiao, C. Wang, T. Ding, A. Akbarnezhad, A recycled aggregate concrete high-rise building: Structural performance and embodied carbon footprint, *Journal of Cleaner Production*. 199 (2018) 868–881. <https://doi.org/https://doi.org/10.1016/j.jclepro.2018.07.210>.
- [114] H. AzariJafari, M.J. Taheri Amiri, A. Ashrafiyan, H. Rasekh, M.J. Barforooshi, J. Berenjia, Ternary blended cement: An eco-friendly alternative to improve resistivity of high-performance self-consolidating concrete against elevated temperature, *Journal of Cleaner Production*. 223 (2019) 575–586. <https://doi.org/https://doi.org/10.1016/j.jclepro.2019.03.054>.
- [115] R. Kurda, J. de Brito, J.D. Silvestre, CONCRET<sub>op</sub> method: Optimization of concrete with various incorporation ratios of fly ash and recycled aggregates in terms of quality performance and life-cycle cost and environmental impacts, *Journal of Cleaner Production*. 226 (2019) 642–657. <https://doi.org/https://doi.org/10.1016/j.jclepro.2019.04.070>.

- [116] D. Mavrokapnidis, C.Ch. Mitropoulou, N.D. Lagaros, Environmental assessment of cost optimized structural systems in tall buildings, *Journal of Building Engineering*. 24 (2019) 100730. <https://doi.org/https://doi.org/10.1016/j.jobe.2019.100730>.
- [117] Md.U. Hossain, C.S. Poon, I.M.C. Lo, J.C.P. Cheng, Comparative LCA on using waste materials in the cement industry: A Hong Kong case study, *Resources, Conservation and Recycling*. 120 (2017) 199–208. <https://doi.org/https://doi.org/10.1016/j.resconrec.2016.12.012>.
- [118] Md.U. Hossain, C.S. Poon, I.M.C. Lo, J.C.P. Cheng, Comparative environmental evaluation of aggregate production from recycled waste materials and virgin sources by LCA, *Resources, Conservation and Recycling*. 109 (2016) 67–77. <https://doi.org/https://doi.org/10.1016/j.resconrec.2016.02.009>.
- [119] A.L. Kleijer, S. Lasvaux, S. Citherlet, M. Viviani, Product-specific Life Cycle Assessment of ready mix concrete: Comparison between a recycled and an ordinary concrete, *Resources, Conservation and Recycling*. 122 (2017) 210–218. <https://doi.org/https://doi.org/10.1016/j.resconrec.2017.02.004>.
- [120] Md.U. Hossain, Z. Wu, C.S. Poon, Comparative environmental evaluation of construction waste management through different waste sorting systems in Hong Kong, *Waste Management*. 69 (2017) 325–335. <https://doi.org/https://doi.org/10.1016/j.wasman.2017.07.043>.
- [121] L.F. Cabeza, C. Barreneche, L. Miró, J.M. Morera, E. Bartolí, A. Inés Fernández, Low carbon and low embodied energy materials in buildings: A review, *Renewable and Sustainable Energy Reviews*. 23 (2013) 536–542. <https://doi.org/10.1016/j.rser.2013.03.017>.

- [122] M.K. Ansah, X. Chen, H. Yang, L. Lu, P.T.I. Lam, An integrated life cycle assessment of different façade systems for a typical residential building in Ghana, *Sustainable Cities and Society*. 53 (2019) 101974. <https://doi.org/10.1016/j.scs.2019.101974>.
- [123] J. Xiao, C. Wang, T. Ding, A. Akbarnezhad, A recycled aggregate concrete high-rise building: Structural performance and embodied carbon footprint, *Journal of Cleaner Production*. 199 (2018) 868–881. <https://doi.org/10.1016/j.jclepro.2018.07.210>.
- [124] Md.U. Hossain, C.S. Poon, I.M.C. Lo, J.C.P. Cheng, Comparative environmental evaluation of aggregate production from recycled waste materials and virgin sources by LCA, *Resources, Conservation and Recycling*. 109 (2016) 67–77. <https://doi.org/https://doi.org/10.1016/j.resconrec.2016.02.009>.
- [125] M.K. Ansah, X. Chen, H. Yang, L. Lu, H. Li, Developing a tier-hybrid uncertainty analysis approach for lifecycle impact assessment of a typical high-rise residential building, *Resources, Conservation and Recycling*. 167 (2021) 105424. <https://doi.org/10.1016/j.resconrec.2021.105424>.
- [126] B. V Venkatarama Reddy, Sustainable materials for low carbon buildings, *International Journal of Low-Carbon Technologies*. 4 (2009) 175–181. <https://doi.org/10.1093/ijlct/ctp025>.
- [127] Z. Zhang, Y.C. Wong, A. Arulrajah, S. Horpibulsuk, A review of studies on bricks using alternative materials and approaches, *Construction and Building Materials*. 188 (2018) 1101–1118. <https://doi.org/10.1016/j.conbuildmat.2018.08.152>.
- [128] D.A. Salas, A.D. Ramirez, N. Ulloa, H. Baykara, A.J. Boero, Life cycle assessment of geopolymer concrete, *Construction and Building Materials*. 190 (2018) 170–177. <https://doi.org/10.1016/j.conbuildmat.2018.09.123>.

- [129] K.W. Corscadden, J.N. Biggs, D.K. Stiles, Sheep's wool insulation: A sustainable alternative use for a renewable resource?, *Resources, Conservation and Recycling*. 86 (2014) 9–15. <https://doi.org/10.1016/j.resconrec.2014.01.004>.
- [130] N. Ata-Ali, V. Penadés-Plà, D. Martínez-Muñoz, V. Yepes, Recycled versus non-recycled insulation alternatives: LCA analysis for different climatic conditions in Spain, *Resources, Conservation and Recycling*. 175 (2021). <https://doi.org/10.1016/j.resconrec.2021.105838>.
- [131] K. Konadu-Agyemang, A survey of housing conditions and characteristics in Accra, an African city, *Habitat International*. 25 (2001) 15–34. [https://doi.org/10.1016/S0197-3975\(00\)00016-3](https://doi.org/10.1016/S0197-3975(00)00016-3).
- [132] R. Oppong, E. Badu, Evaluation of Stabilised-Earth (Tek) Block for Housing Provision and Construction in Ghana, *Journal of Science and Technology (Ghana)*. 32 (2012) 104–118. <https://doi.org/10.4314/just.v32i2.12>.
- [133] R. Oppong, E. Badu, Evaluation of Stabilised-Earth (Tek) Block for Housing Provision and Construction in Ghana, *Journal of Science and Technology (Ghana)*. 32 (2012) 104–118. <https://doi.org/10.4314/just.v32i2.12>.
- [134] P. Chastas, T. Theodosiou, D. Bikas, Embodied energy in residential buildings-towards the nearly zero energy building: A literature review, *Building and Environment*. 105 (2016) 267–282. <https://doi.org/10.1016/J.BUILDENV.2016.05.040>.
- [135] E. Christoforou, A. Kylili, P.A. Fokaides, I. Ioannou, Cradle to site Life Cycle Assessment (LCA) of adobe bricks, *Journal of Cleaner Production*. 112 (2016) 443–452. <https://doi.org/10.1016/J.JCLEPRO.2015.09.016>.

- [136] C. Galán-Marín, C. Rivera-Gómez, A. García-Martínez, Embodied energy of conventional load-bearing walls versus natural stabilized earth blocks, *Energy and Buildings*. 97 (2015) 146–154. <https://doi.org/10.1016/J.ENBUILD.2015.03.054>.
- [137] S.N. Joglekar, R.A. Kharkar, S.A. Mandavgane, B.D. Kulkarni, Sustainability assessment of brick work for low-cost housing: A comparison between waste based bricks and burnt clay bricks, *Sustainable Cities and Society*. 37 (2018) 396–406. <https://doi.org/10.1016/J.SCS.2017.11.025>.
- [138] Z. Guo, A. Tu, C. Chen, D.E. Lehman, Mechanical properties, durability, and life-cycle assessment of concrete building blocks incorporating recycled concrete aggregates, *Journal of Cleaner Production*. 199 (2018) 136–149. <https://doi.org/10.1016/J.JCLEPRO.2018.07.069>.
- [139] L. Ben-Alon, V. Loftness, K.A. Harries, G. DiPietro, E.C. Hameen, Cradle to site Life Cycle Assessment (LCA) of natural vs conventional building materials: A case study on cob earthen material, *Building and Environment*. (2019). <https://doi.org/10.1016/J.BUILDENV.2019.05.028>.
- [140] B.V. Venkatarama Reddy, P. Prasanna Kumar, Embodied energy in cement stabilised rammed earth walls, *Energy and Buildings*. 42 (2010) 380–385. <https://doi.org/10.1016/J.ENBUILD.2009.10.005>.
- [141] B.V. Venkatarama Reddy, G. Leuzinger, V.S. Sreeram, Low embodied energy cement stabilised rammed earth building—A case study, *Energy and Buildings*. 68 (2014) 541–546. <https://doi.org/10.1016/J.ENBUILD.2013.09.051>.
- [142] M. Sandanayake, W. Lokuge, G. Zhang, S. Setunge, Q. Thushar, Greenhouse gas emissions during timber and concrete building construction —A scenario based

- comparative case study, *Sustainable Cities and Society*. 38 (2018) 91–97.  
<https://doi.org/10.1016/J.SCS.2017.12.017>.
- [143] R. Prateep Na Talang, S. Sirivithayapakorn, Comparing environmental burdens, economic costs and thermal resistance of different materials for exterior building walls, *Journal of Cleaner Production*. 197 (2018) 1508–1520.  
<https://doi.org/10.1016/J.JCLEPRO.2018.06.255>.
- [144] A. Arrigoni, R. Pelosato, P. Melià, G. Ruggieri, S. Sabbadini, G. Dotelli, Life cycle assessment of natural building materials: the role of carbonation, mixture components and transport in the environmental impacts of hempcrete blocks, *Journal of Cleaner Production*. 149 (2017) 1051–1061. <https://doi.org/10.1016/J.JCLEPRO.2017.02.161>.
- [145] J. Dahmen, J. Kim, C.M. Ouellet-Plamondon, Life cycle assessment of emergent masonry blocks, *Journal of Cleaner Production*. 171 (2018) 1622–1637.  
<https://doi.org/10.1016/J.JCLEPRO.2017.10.044>.
- [146] C. Udawattha, R. Halwatura, Embodied energy of mud concrete block (MCB) versus brick and cement blocks, *Energy and Buildings*. 126 (2016) 28–35.  
<https://doi.org/10.1016/J.ENBUILD.2016.04.059>.
- [147] E. Yılmaz, H. Arslan, A. Bideci, Environmental performance analysis of insulated composite facade panels using life cycle assessment (LCA), *Construction and Building Materials*. 202 (2019) 806–813.  
<https://doi.org/10.1016/J.CONBUILDMAT.2019.01.057>.
- [148] T. Potrč, K.M. Rebec, F. Knez, R. Kunič, A. Legat, Environmental Footprint of External Thermal Insulation Composite Systems with Different Insulation Types, *Energy Procedia*. 96 (2016) 312–322. <https://doi.org/10.1016/J.EGYPRO.2016.09.154>.

- [149] J. Sierra-Pérez, J. Boschmonart-Rives, X. Gabarrell, Environmental assessment of façade-building systems and thermal insulation materials for different climatic conditions, *Journal of Cleaner Production*. 113 (2016) 102–113.  
<https://doi.org/10.1016/J.JCLEPRO.2015.11.090>.
- [150] Z.S. Moussavi Nadoushani, A. Akbarnezhad, J. Ferre Jornet, J. Xiao, Multi-criteria selection of façade systems based on sustainability criteria, *Building and Environment*. 121 (2017) 67–78. <https://doi.org/10.1016/J.BUILDENV.2017.05.016>.
- [151] D. Densley Tingley, A. Hathway, B. Davison, An environmental impact comparison of external wall insulation types, *Building and Environment*. 85 (2015) 182–189.  
<https://doi.org/10.1016/J.BUILDENV.2014.11.021>.
- [152] A.C. Schmidt, A.A. Jensen, A.U. Clausen, O. Kamstrup, D. Postlethwaite, A comparative Life Cycle assessment of building insulation products made of stone wool, paper wool and flax, *The International Journal of Life Cycle Assessment*. 9 (2004) 53–66. <https://doi.org/10.1007/BF02978536>.
- [153] S. Schiavoni, F. D'Alessandro, F. Bianchi, F. Asdrubali, Insulation materials for the building sector: A review and comparative analysis, *Renewable and Sustainable Energy Reviews*. 62 (2016) 988–1011. <https://doi.org/10.1016/J.RSER.2016.05.045>.
- [154] C. Hill, A. Norton, J. Dibdiakova, A comparison of the environmental impacts of different categories of insulation materials, *Energy and Buildings*. 162 (2018) 12–20.  
<https://doi.org/10.1016/J.ENBUILD.2017.12.009>.
- [155] B. Weidema, C. Bauer, R. Hirsch, C. Mutel, Overview and methodology: Data quality guideline for the ecoinvent database version 3, (2013).

- [156] C.K. Chau, W.K. Hui, W.Y. Ng, G. Powell, Assessment of CO<sub>2</sub> emissions reduction in high-rise concrete office buildings using different material use options, *Resources, Conservation and Recycling*. 61 (2012) 22–34.  
<https://doi.org/10.1016/J.RESCONREC.2012.01.001>.
- [157] HKBD, CODE OF PRACTICE FOR DEMOLITION OF BUILDINGS, (2004).
- [158] V.J.L. Gan, M. Deng, K.T. Tse, C.M. Chan, I.M.C. Lo, J.C.P. Cheng, Holistic BIM framework for sustainable low carbon design of high-rise buildings, *Journal of Cleaner Production*. 195 (2018) 1091–1104. <https://doi.org/10.1016/J.JCLEPRO.2018.05.272>.
- [159] X. Zhang, R. Zheng, Reducing building embodied emissions in the design phase: A comparative study on structural alternatives, *Journal of Cleaner Production*. 243 (2020) 118656. <https://doi.org/10.1016/J.JCLEPRO.2019.118656>.
- [160] EMSD, Electrical and Mechanical Services Department Consultancy Agreement No . CAO L013 - Consultancy Study on Life Cycle Energy Analysis of Building Construction Final Report, (2006).
- [161] C.K. Chau, H.K. Yu, H.C. Liu, F.W.H. Yik, W.K. Hui, Environmental impacts of building materials and building services components for commercial buildings in Hong Kong, *Journal of Cleaner Production*. 15 (2006) 1840–1851.  
<https://doi.org/10.1016/j.jclepro.2006.10.004>.
- [162] C.K. Chau, F.W.H. Yik, W.K. Hui, H.C. Liu, H.K. Yu, Environmental impacts of building materials and building services components for commercial buildings in Hong Kong, *Journal of Cleaner Production*. 15 (2007) 1840–1851.  
<https://doi.org/10.1016/J.JCLEPRO.2006.10.004>.

- [163] M.K. Dixit, Life cycle recurrent embodied energy calculation of buildings: A review, *Journal of Cleaner Production*. 209 (2019) 731–754.  
<https://doi.org/10.1016/j.jclepro.2018.10.230>.
- [164] Md.U. Hossain, S. Thomas Ng, Influence of waste materials on buildings' life cycle environmental impacts: Adopting resource recovery principle, *Resources, Conservation and Recycling*. 142 (2019) 10–23.  
<https://doi.org/https://doi.org/10.1016/j.resconrec.2018.11.010>.
- [165] B. Weidema, C. Bauer, R. Hischier, C. Mutel, Overview and methodology: Data quality guideline for the ecoinvent database version 3, (2013).  
<https://www.forskningsdatabasen.dk/en/catalog/2389389526> (accessed March 17, 2020).
- [166] F. Pomponi, B. D'Amico, A. Moncaster, A Method to Facilitate Uncertainty Analysis in LCAs of Buildings, *Energies (Basel)*. 10 (2017) 524.  
<https://doi.org/10.3390/en10040524>.
- [167] K. Deb, A. Pratap, S. Agarwal, T. Meyarivan, A fast and elitist multiobjective genetic algorithm: NSGA-II, *IEEE Transactions on Evolutionary Computation*. 6 (2002) 182–197. <https://doi.org/10.1109/4235.996017>.
- [168] H. Piroozfard, K.Y. Wong, W.P. Wong, Minimizing total carbon footprint and total late work criterion in flexible job shop scheduling by using an improved multi-objective genetic algorithm, *Resources, Conservation and Recycling*. 128 (2018) 267–283. <https://doi.org/10.1016/j.resconrec.2016.12.001>.
- [169] A. Vukadinović, J. Radosavljević, A. Đorđević, M. Protić, N. Petrović, Multi-objective optimization of energy performance for a detached residential building with a sunspace

- using the NSGA-II genetic algorithm, *Solar Energy*. 224 (2021) 1426–1444.  
<https://doi.org/10.1016/j.solener.2021.06.082>.
- [170] X. Chen, H. Yang, J. Peng, Energy optimization of high-rise commercial buildings integrated with photovoltaic facades in urban context, *Energy*. 172 (2019) 1–17.  
<https://doi.org/10.1016/j.energy.2019.01.112>.
- [171] H. Samuelson, S. Claussnitzer, A. Goyal, Y. Chen, A. Romo-Castillo, Parametric energy simulation in early design: High-rise residential buildings in urban contexts, *Building and Environment*. 101 (2016) 19–31.  
<https://doi.org/10.1016/j.buildenv.2016.02.018>.
- [172] C. Turner, M. Frankel, U.G.B. Council, Energy performance of LEED for new construction buildings, *New Buildings Institute*. 4 (2008) 1–42.
- [173] H. Adan, F. Fuerst, Do energy efficiency measures really reduce household energy consumption? A difference-in-difference analysis, *Energy Efficiency*. 9 (2016) 1207–1219.
- [174] D. Chasar, J. McIlvaine, J. Blanchard, S.H. Widder, M.C. Baechler, *Building Energy Model Development for Retrofit Homes*, Pacific Northwest National Lab.(PNNL), Richland, WA (United States), 2012.
- [175] B. Güneralp, Y. Zhou, D. Ürge-Vorsatz, M. Gupta, S. Yu, P.L. Patel, M. Fragkias, X. Li, K.C. Seto, Global scenarios of urban density and its impacts on building energy use through 2050, *Proceedings of the National Academy of Sciences*. 114 (2017) 8945–8950.
- [176] S. Liu, Y.T. Kwok, K.K.-L. Lau, H.W. Tong, P.W. Chan, N.G. Edward, Development and application of future design weather data for evaluating the building thermal-

- energy performance in subtropical Hong Kong, *Energy and Buildings*. 209 (2020) 109696.
- [177] IEA, 2019 Global status report for buildings and construction, United Nations Environment Programme. (2019).
- [178] L. Jaillon, C.S. Poon, Y.H. Chiang, Quantifying the waste reduction potential of using prefabrication in building construction in Hong Kong, *Waste Management*. 29 (2009) 309–320. <https://doi.org/https://doi.org/10.1016/j.wasman.2008.02.015>.
- [179] L. Jaillon, C.S. Poon, Life cycle design and prefabrication in buildings: A review and case studies in Hong Kong, *Automation in Construction*. 39 (2014) 195–202. <https://doi.org/10.1016/j.autcon.2013.09.006>.
- [180] Y.H. Dong, L. Jaillon, P. Chu, C.S. Poon, Comparing carbon emissions of precast and cast-in-situ construction methods – A case study of high-rise private building, *Construction and Building Materials*. 99 (2015) 39–53. <https://doi.org/https://doi.org/10.1016/j.conbuildmat.2015.08.145>.
- [181] Y.H. Dong, L. Jaillon, P. Chu, C.S. Poon, Comparing carbon emissions of precast and cast-in-situ construction methods - A case study of high-rise private building, *Construction and Building Materials*. 99 (2015) 39–53. <https://doi.org/10.1016/j.conbuildmat.2015.08.145>.
- [182] B. Huang, Y. Chen, W. McDowall, S. Türkeli, R. Bleischwitz, Y. Geng, Embodied GHG emissions of building materials in Shanghai, *Journal of Cleaner Production*. 210 (2019) 777–785. <https://doi.org/10.1016/J.JCLEPRO.2018.11.030>.

- [183] Y.H. Dong, S.T. Ng, A life cycle assessment model for evaluating the environmental impacts of building construction in Hong Kong, *Building and Environment*. 89 (2015) 183–191. <https://doi.org/10.1016/j.buildenv.2015.02.020>.
- [184] Y.H. Dong, S.T. Ng, A modeling framework to evaluate sustainability of building construction based on LCSA, *International Journal of Life Cycle Assessment*. 21 (2016) 555–568. <https://doi.org/10.1007/s11367-016-1044-6>.
- [185] M. Morales, G. Moraga, A.P. Kirchheim, A. Passuello, Regionalized inventory data in LCA of public housing: A comparison between two conventional typologies in southern Brazil, *Journal of Cleaner Production*. 238 (2019) 117869. <https://doi.org/10.1016/J.JCLEPRO.2019.117869>.
- [186] V.J.L. Gan, J.C.P. Cheng, I.M.C. Lo, C.M. Chan, Developing a CO<sub>2</sub>-e accounting method for quantification and analysis of embodied carbon in high-rise buildings, *Journal of Cleaner Production*. 141 (2017) 825–836. <https://doi.org/10.1016/j.jclepro.2016.09.126>.
- [187] Y.H. Dong, S.T. Ng, A social life cycle assessment model for building construction in Hong Kong, *International Journal of Life Cycle Assessment*. 20 (2015) 1166–1180. <https://doi.org/10.1007/s11367-015-0908-5>.
- [188] J.R. González-López, C.A. Juárez-Alvarado, B. Ayub-Francis, J.M. Mendoza-Rangel, Compaction effect on the compressive strength and durability of stabilized earth blocks, *Construction and Building Materials*. 163 (2018) 179–188. <https://doi.org/10.1016/J.CONBUILDMAT.2017.12.074>.
- [189] L.Á. Antón, J. Díaz, Integration of Life Cycle Assessment in a BIM Environment, *Procedia Engineering*. 85 (2014) 26–32. <https://doi.org/10.1016/J.PROENG.2014.10.525>.

- [190] P.M. Touré, V. Sambou, M. Faye, A. Thiam, M. Adj, D. Azilanon, Mechanical and hygrothermal properties of compressed stabilized earth bricks (CSEB), *Journal of Building Engineering*. 13 (2017) 266–271.  
<https://doi.org/10.1016/J.JOBE.2017.08.012>.
- [191] H. van Damme, H. Houben, Earth concrete. Stabilization revisited, *Cement and Concrete Research*. 114 (2018) 90–102.  
<https://doi.org/10.1016/J.CEMCONRES.2017.02.035>.
- [192] C.K. Chau, F.W.H. Yik, W.K. Hui, H.C. Liu, H.K. Yu, Environmental impacts of building materials and building services components for commercial buildings in Hong Kong, *Journal of Cleaner Production*. 15 (2007) 1840–1851.  
<https://doi.org/10.1016/J.JCLEPRO.2006.10.004>.
- [193] M.K. Dixit, Life cycle recurrent embodied energy calculation of buildings: A review, *Journal of Cleaner Production*. 209 (2019) 731–754.  
<https://doi.org/10.1016/J.JCLEPRO.2018.10.230>.
- [194] M.K. Dixit, Life cycle embodied energy analysis of residential buildings: A review of literature to investigate embodied energy parameters, *Renewable and Sustainable Energy Reviews*. 79 (2017) 390–413. <https://doi.org/10.1016/J.RSER.2017.05.051>.
- [195] M.K. Dixit, C.H. Culp, J.L. Fernández-Solís, System boundary for embodied energy in buildings: A conceptual model for definition, *Renewable and Sustainable Energy Reviews*. 21 (2013) 153–164. <https://doi.org/10.1016/j.rser.2012.12.037>.
- [196] P. Li, T.M. Froese, B.T. Cavka, Life cycle assessment of magnesium oxide structural insulated panels for a smart home in Vancouver, *Energy and Buildings*. 175 (2018) 78–86. <https://doi.org/10.1016/J.ENBUILD.2018.07.016>.

- [197] G. Hammond, C. Jones, Inventory of Carbon and Energy (ICE) Version 2.0., Sustainable Energy Research Team, Dept. Of Mechanical Engineering, University of Bath, 2011. [www.bath.ac.uk/mech-eng/sert/embodied](http://www.bath.ac.uk/mech-eng/sert/embodied) (accessed September 4, 2018).
- [198] V. Tavares, N. Lacerda, F. Freire, Embodied energy and greenhouse gas emissions analysis of a prefabricated modular house: The “Moby” case study, *Journal of Cleaner Production*. 212 (2019) 1044–1053. <https://doi.org/10.1016/J.JCLEPRO.2018.12.028>.
- [199] U.G. Department for Business, Energy & Industrial Strategy, Greenhouse Gas Reporting: Conversion Factors 2018 - GOV.UK, (2018). [https://www.gov.uk/government/uploads/system/uploads/attachment\\_data/file/715426/Conversion\\_Factors\\_2018\\_-\\_Full\\_set\\_\\_for\\_advanced\\_users\\_\\_v01-01.xls](https://www.gov.uk/government/uploads/system/uploads/attachment_data/file/715426/Conversion_Factors_2018_-_Full_set__for_advanced_users__v01-01.xls) (accessed November 23, 2018).
- [200] X. Zhang, L. Shen, L. Zhang, Life cycle assessment of the air emissions during building construction process: A case study in Hong Kong, *Renewable and Sustainable Energy Reviews*. 17 (2013) 160–169. <https://doi.org/10.1016/J.RSER.2012.09.024>.
- [201] C. Zhang, R.S. Nizam, L. Tian, BIM-based investigation of total energy consumption in delivering building products, *Advanced Engineering Informatics*. 38 (2018) 370–380. <https://doi.org/10.1016/J.AEI.2018.08.009>.
- [202] R.S. Nizam, C. Zhang, L. Tian, A BIM based tool for assessing embodied energy for buildings, *Energy and Buildings*. 170 (2018) 1–14. <https://doi.org/10.1016/j.enbuild.2018.03.067>.
- [203] C. Dara, C. Hachem-Vermette, G. Assefa, Life cycle assessment and life cycle costing of container-based single-family housing in Canada: A case study, *Building and Environment*. 163 (2019) 106332. <https://doi.org/10.1016/J.BUILDENV.2019.106332>.

- [204] C.Z. Li, G. Liu, Z. Wu, G.Q. Shen, J. Hong, X. Zhong, An integrated framework for embodied energy quantification of buildings in China: A multi-regional perspective, *Resources, Conservation and Recycling*. 138 (2018) 183–193.  
<https://doi.org/10.1016/j.resconrec.2018.06.016>.
- [205] M.K. Nematchoua, S. Asadi, S. Reiter, A Study of Life Cycle Assessment in two Old Neighbourhoods in Belgium, *Sustainable Cities and Society*. (2019) 101744.  
<https://doi.org/10.1016/J.SCS.2019.101744>.
- [206] M.K. Nematchoua, J.A. Orosa, S. Reiter, Life cycle assessment of two sustainable and old neighbourhoods affected by climate change in one city in Belgium: A review, *Environmental Impact Assessment Review*. 78 (2019) 106282.  
<https://doi.org/https://doi.org/10.1016/j.eiar.2019.106282>.
- [207] J. Dahmen, J. Kim, C.M. Ouellet-Plamondon, Life cycle assessment of emergent masonry blocks, *Journal of Cleaner Production*. 171 (2018) 1622–1637.  
<https://doi.org/10.1016/J.JCLEPRO.2017.10.044>.
- [208] P.P.A. Evangelista, A. Kiperstok, E.A. Torres, J.P. Gonçalves, Environmental performance analysis of residential buildings in Brazil using life cycle assessment (LCA), *Construction and Building Materials*. 169 (2018) 748–761.  
<https://doi.org/10.1016/J.CONBUILDMAT.2018.02.045>.
- [209] P. Chastas, T. Theodosiou, D. Bikas, Embodied energy in residential buildings-towards the nearly zero energy building: A literature review, *Building and Environment*. 105 (2016) 267–282. <https://doi.org/10.1016/J.BUILDENV.2016.05.040>.
- [210] C. Udawattha, R. Halwatura, Embodied energy of mud concrete block (MCB) versus brick and cement blocks, *Energy and Buildings*. 126 (2016) 28–35.  
<https://doi.org/10.1016/J.ENBUILD.2016.04.059>.

- [211] C. Udawattha, R. Halwatura, Life cycle cost of different Walling material used for affordable housing in tropics, *Case Studies in Construction Materials*. 7 (2017) 15–29. <https://doi.org/10.1016/J.CSCM.2017.04.005>.
- [212] C. Galán-Marín, C. Rivera-Gómez, A. García-Martínez, Embodied energy of conventional load-bearing walls versus natural stabilized earth blocks, *Energy and Buildings*. 97 (2015) 146–154. <https://doi.org/10.1016/J.ENBUILD.2015.03.054>.
- [213] S.H. Ghaffar, M. Burman, N. Braimah, Pathways to circular construction: An integrated management of construction and demolition waste for resource recovery, *J Clean Prod*. 244 (2020) 118710.
- [214] T. Ding, J. Xiao, V.W.Y. Tam, A closed-loop life cycle assessment of recycled aggregate concrete utilization in China, *Waste Management*. 56 (2016) 367–375.
- [215] M.K. Ansah, X. Chen, H. Yang, L. Lu, P.T.I. Lam, An integrated life cycle assessment of different façade systems for a typical residential building in Ghana, *Sustainable Cities and Society*. 53 (2019) 101974. <https://doi.org/10.1016/j.scs.2019.101974>.
- [216] M.K. Ansah, X. Chen, H. Yang, L. Lu, P.T.I. Lam, An integrated life cycle assessment of different façade systems for a typical residential building in Ghana, *Sustainable Cities and Society*. 53 (2019) 101974. <https://doi.org/10.1016/j.scs.2019.101974>.
- [217] X. Chen, J. Huang, H. Yang, J. Peng, Approaching low-energy high-rise building by integrating passive architectural design with photovoltaic application, *Journal of Cleaner Production*. 220 (2019) 313–330. <https://doi.org/10.1016/J.JCLEPRO.2019.02.137>.
- [218] X. Chen, H. Yang, W. Zhang, Simulation-based approach to optimize passively designed buildings: A case study on a typical architectural form in hot and humid

climates, *Renewable and Sustainable Energy Reviews*. 82 (2018) 1712–1725.

<https://doi.org/10.1016/j.rser.2017.06.018>.

## APPENDIX

Appendix 1 Uncertainty characterization for DQI-based parameters

Activity/Material	Quantity	Unit	Data quality score		
			Material Quantity	Energy use coefficient	Carbon emission coefficient
<b>Material Production</b>					
Aluminum	2500.00	kg	3,2,1,1,1	4,4,5,3,4	4,4,5,3,4
Cement paste	160949.60	kg	3,2,1,1,1	2,2,1,4,2	2,2,1,4,2
Ceramic tile	232800.70	kg	3,2,1,1,1	3,3,1,4,1	3,3,1,4,1
Composite mortar	2431381.0 0	kg	3,2,1,1,1	3,2,2,4,2	3,2,2,4,2
Galvanized steel	9892.03	kg	4,2,1,1,1	3,2,2,4,1	3,2,2,4,1
Glass	44762.39	kg	3,2,1,1,1	3,4,3,3,2	4,4,3,3,2
Gravel	5966.79	kg	3,2,1,1,1	3,2,2,4,1	3,2,2,4,1
Gypsum plaster	30877.90	kg	3,2,1,1,1	2,2,1,4,2	2,2,1,4,2
Insitu concrete C30	1284.86	m <sup>3</sup>	3,2,1,1,1	3,3,2,4,2	3,3,2,4,2
Insitu concrete C35	637.49	m <sup>3</sup>	3,2,1,1,2	3,3,2,4,2	3,3,2,4,2
Insitu concrete C40	642.65	m <sup>3</sup>	3,2,1,1,3	3,3,2,4,2	3,3,2,4,2
Insitu concrete C45	3487.75	m <sup>3</sup>	3,2,1,1,4	3,3,2,4,2	3,3,2,4,2
Iron	6009.18	kg	4,2,1,1,1	3,2,2,4,1	3,2,2,4,1
Metal door	507.22	m <sup>2</sup>	4,2,1,1,1	3,2,3,4,5	3,2,3,4,5
Paint	9820.00	kg	3,2,1,1,1	4,4,5,3,4	4,4,5,3,4

Activity/Material	Quantity	Unit	Data quality score		
			Material Quantity	Energy use coefficient	Carbon emission coefficient
Polystyrene board	8917.62	kg	3,2,1,1,1	3,3,2,4,1	3,3,2,4,1
Precast concrete	2424.37	m <sup>3</sup>	3,2,1,1,1	3,3,2,4,1	3,3,2,4,1
PVC Membrane	1178.42	kg	3,2,1,1,1	3,3,2,4,1	3,3,2,4,1
Sand	440375.30	kg	3,2,1,1,1	3,2,2,4,1	3,2,2,4,1
Stainless Steel	14173.13	kg	3,2,1,1,1	3,2,2,4,2	3,2,2,4,2
Steel bar (Insitu concrete)	223378.60	kg	3,2,1,1,1	3,2,2,4,2	3,2,2,4,2
Steel bar (Precast concrete)	414845.90	kg	3,1,1,1,1	3,2,2,4,2	3,2,2,4,2
Steel formwork	31290.39	kg	3,2,1,1,1	3,3,1,4,2	3,3,1,4,2
Talcum powder	82265.29	kg	3,2,1,1,1	3,3,4,5,2	1,3,4,5,2
Timber door	2534.45	m <sup>2</sup>	3,2,1,1,1	4,4,5,3,4	4,4,5,3,4
Timber formwork	395.67	m <sup>3</sup>	3,2,1,1,1	4,4,5,3,4	4,4,5,3,4
Windows	3148.30	m <sup>2</sup>	3,2,1,1,1	4,4,5,3,4	4,4,5,3,4
<b>Onsite construction</b>					
Electricity for temporary offices and onsite equipment	776502.60	kWh	3,4,3,4,4	3,4,2,4,5	3,4,2,4,5
Diesel for onsite vehicles and onsite equipment	31542.00	kWh	3,4,3,4,4	3,4,2,4,5	3,4,2,4,5
<b>Building maintenance</b>					
Aluminum	625.00	kg	3,2,1,4,3	4,4,5,3,4	4,4,5,3,4

Activity/Material	Quantity	Unit	Data quality score		
			Material Quantity	Energy use coefficient	Carbon emission coefficient
Cement paste	32189.92	kg	3,2,1,4,3	2,2,1,4,2	2,2,1,4,2
Composite mortar	486276.20	kg	3,2,1,4,3	3,2,2,4,2	3,2,2,4,2
Glass	44762.39	kg	3,2,1,4,3	3,4,3,3,2	4,4,3,3,2
Paint	39280.00	kg	3,2,1,4,3	4,4,5,3,4	4,4,5,3,4
Windows	3148.30	m <sup>2</sup>	3,2,1,4,3	4,4,5,3,4	4,4,5,3,4
Timber door	2534.45	m <sup>2</sup>	3,2,1,4,3	4,4,5,3,4	4,4,5,3,4
PVC Membrane	2356.84	kg	3,2,1,1,1	3,3,2,4,1	3,3,2,4,1
Gypsum plaster	61,755.86	kg	3,2,1,1,1	2,2,1,4,2	2,2,1,4,2

Appendix 2 Uncertainty characterization for pure statistical parameters

Material	Transportation		Material waste		Material density	
	distance (km)		rate (%)		(kg/m <sup>3</sup> )	
	Mean	SD	Mean	SD	Mean	SD
Aluminum	200	18.49	5	0.51	2,710	142.06
Cement paste	25	1.06	10	0.93	1520	155.86
Ceramic tile	185	16.01	10	0.76	2200	117.13
Composite mortar	25	1.06	10	0.57	1650	87.85
Galvanized steel	200	18.49	5	0.56	7850	96.95
Glass	10	0.21	7	0.32	2450	56.97
Gravel	180	25.65	5	0.51	1520	155.86
Gypsum plaster	150	12.52	5	0.38	2320	74.47
Insitu concrete C30	25	3.81	5	0.51	2400	246.10
Insitu concrete C35	25	3.81	5	0.51	2400	246.10
Insitu concrete C40	25	3.81	5	0.51	2400	246.10
Insitu concrete C45	25	3.81	5	0.51	2400	246.10
Iron	250	28.14	5	0.51	6970	737.70
Metal door	200	16.96	2	0.05	-	
Paint	150	36.38	7	1.91	1350	106.46
Polystyrene board	150	15.00	3	0.30	28	2.80
Precast concrete	100	3.45	1	0.03	2400	138.84
PVC Membrane	100	13.24	5	0.66	1070	27.18
Sand	180	9.62	5	0.23	1680	183.05
Stainless Steel	120	11.08	10	1.06	7590	707.69

Material	Transportation		Material waste		Material density	
	distance (km)		rate (%)		(kg/m <sup>3</sup> )	
	Mean	SD	Mean	SD	Mean	SD
Steel bar (Insitu concrete)	150	11.79	7	0.15	7860	805.96
Steel bar (Precast concrete)	100	5.32	7	0.72	7860	805.96
Steel formwork	28	1.08	7	0.35	7860	418.55
Talcum powder	150	12.38	5	0.47	2650	271.73
Timber door	220	60.63	2	0.25	-	-
Timber formwork	250	58.85	5	0.51	875	116.01
Windows	100	3.45	2	0.11	-	-

### Appendix 3 Windows types, U-value, GWP, CED and Cost

Window type	U-value (W/m <sup>2</sup> K)	GWP (kgCO <sub>2</sub> . eq./m <sup>2</sup> )	CED (MJ)	Cost (USD/m <sup>2</sup> )
PVC-framed double-glazing	1.1	294.00	3870.00	32.95
Aluminium-framed double- glazing	1.1	394.00	4850.00	39.54
Tropical hardwood-framed double- glazing	1.1	202.00	2570.00	44.48
Standard wood-framed double- glazing	1.1	186.00	2460.00	46.13
Wood & aluminium-framed double- glazing	1.1	315.00	3940.00	41.19
PVC-framed acoustic double- glazing	1.1	375.00	4910.00	62.60
PVC-framed double- double wire glazing	1.1	501.00	6130.00	65.90
PVC-framed triple-glazing	0.65	292.00	3730.00	74.14

<b>Window type</b>	<b>U-value (W/m<sup>2</sup>K)</b>	<b>GWP (kgCO<sub>2</sub>. eq./m<sup>2</sup>)</b>	<b>CED (MJ)</b>	<b>Cost (USD/m<sup>2</sup>)</b>
Aluminium-framed triple- glazing	0.65	276.00	3620.00	77.43
Tropical hardwood-framed triple- glazing	0.65	318.00	4220.00	65.90
Standard wood-framed triple- glazing	0.65	303.00	3990.00	69.19

Appendix 4 Roof types, U-value, GWP, CED and Cost

<b>Roof</b>	<b>U-value</b>	<b>GWP (kgCO<sub>2</sub>. eq./m<sup>2</sup>)</b>	<b>CED (MJ)</b>	<b>Cost (USD/m<sup>2</sup>)</b>
Gypsum plaster-concrete-PUR-EPDM	0.24	259.00	3910.00	25.86
Gypsum plaster-concrete-PUR-EPDM2	0.15	216.00	3100.00	28.01
Gypsum plaster-concrete-PUR-bitumen	0.24	284.00	4810.00	24.22
Gypsum plaster-hollow core slab-PUR-EPDM	0.23	267.00	3930.00	23.06
Gypsum plaster-hollow hollow core slab-PUR-EPDM2	0.24	250.00	3730.00	21.42
Gypsum-concrete-PUR-EPDM3	0.28	272.00	4210.00	23.89
Gypsum plaster-concrete-RW-EPDM	0.29	262.00	4060.00	24.05
Gypsum plaster-clay bricks-concrete-PUR-EPDM	4.45	246.00	3790.00	24.71
Gypsum plaster-aircrete-PUR-EPDM	0.27	273.00	4170.00	23.06

Appendix 5 Windows types, U-value, GWP, CED and Cost

<b>Floor type</b>	<b>U-value</b>	<b>GWP (kgCO<sub>2</sub>. eq./m<sup>2</sup>)</b>	<b>CED (MJ)</b>	<b>Cost (USD/m<sup>2</sup>)</b>
Concrete-PUR-Screed mix-fired clay tiles	0.22	465.00	8240.00	21.42
Concrete-PUR-Screed mix-fired clay tiles <sup>2</sup>	0.12	334.00	5850.00	26.36
Concrete-XPS-Screed mix-fired clay tiles	0.21	475.00	8040.00	22.24
Recycled concrete-PUR-Screed mix-fired clay tiles	0.21	465.00	8240.00	26.03
Trass lime concrete-PUR-Screed mix-fired clay tiles	0.48	380.00	6590.00	19.77
Concrete-PUR-Insulating EPS Screed mix-fired clay tiles	0.16	718.00	10200.00	28.01
Concrete-PUR-anhydrite-fired clay tiles	0.22	464.00	8360.00	27.18
Concrete-PUR-Screed mix-parquet	0.20	378.00	5800.00	29.65
Concrete-PUR-Screed mix-parquet <sup>2</sup>	0.32	377.00	5770.00	29.98
Concrete-Cork-Screed mix-parquet	0.06	275.00	3740.00	26.36
Concrete-Screed mix-fired clay tiles	0.48	220	2431	19.77

Appendix 6 GWP, CED and Cost of PV modules

<b>PV module</b>	<b>GWP (kgCO<sub>2</sub>. eq./m<sup>2</sup>)</b>	<b>CED (MJ)</b>	<b>Cost (USD/m<sup>2</sup>)</b>
------------------	--	-----------------	-------------------------------------

Monocrystalline silicon PV modules (15% conversion efficiency)	82.59	1304	293.51
--	-------	------	--------

Appendix 7 Windows types, U-value, GWP, CED and Cost

Wall type	U-value	GWP (kgCO <sub>2</sub> . eq./m <sup>2</sup> )	CED (MJ)	Cost (USD/m <sup>2</sup> )
Timber frame-RW-facing brick	0.57	253.00	4030.00	39.54
Timber frame-RW-facing brick	0.43	210.00	3260.00	41.19
Timber frame-RW-fibre cement board	0.41	207.00	3220.00	44.48
Timberframe_RW14-fibre cement board	0.55	242.00	3940.00	37.89
FJI-cellulose-facing brick	0.42	170.00	2570.00	46.13
FJI-cellulose-facing brick2	0.31	147.00	2150.00	49.42
FJI-cellulose-roughcast gypsum blocks	0.31	160.00	1950.00	39.21
Timber frame-RW-planks	0.31	228.00	3870.00	32.95
Concrete stone-hollow RW7-facingbrick	0.29	336.00	2620.00	36.08
Concrete stone-hollow RW-facing brick2	0.15	207.00	4810.00	37.89
Concrete stone-hollow PUR-facing brick	0.35	336.00	2780.00	35.42
Concrete stone-hollow PUR-facing brick	0.14	223.00	4940.00	36.24
Concrete stone-full RW-facing brick	0.35	342.00	5030.00	37.07
Hollow brick-RW-facing brick	0.27	330.00	4730.00	39.21
Hollow brick- roughcast	0.25	314.00	4910.00	31.30
Hollow brick-EPS-roughcast	0.27	324.00	4690.00	36.24

<b>Wall type</b>	<b>U-value</b>	<b>GWP (kgCO<sub>2</sub>. eq./m<sup>2</sup>)</b>	<b>CED (MJ)</b>	<b>Cost (USD/m<sup>2</sup>)</b>
Hollow brick-RW-facing brick	0.25	315.00	4860.00	35.42
Hollow brick-RW-facing brick-loam plaster	0.28	316.00	4660.00	32.95
Concrete stone-hollow-PUR-concrete stone	0.30	327.00	4900.00	32.95
Aircrete-facing brick	1.27	358.00	4640.00	31.30
Aircrete-roughcast	2.38	349.00	2930.00	29.65
Aircrete-facing brick	0.14	245.00	5130.00	35.42
Concrete insitu-RW-concrete board	0.36	345.00	4785.00	38.71
Gypsum plater-block wall-gypsum plaster	2.74	256.00	4940.00	24.71